

# Modification and Validation of Conceptual Design Aerodynamic Prediction Method HASC95 With VTXCHN

---

*Alan E. Albright, Charles J. Dixon, and Martin C. Hegedus*

Contract NAS1-19000  
Prepared for Langley Research Center

---

March 1996

<b>7. Conclusions.....</b>	<b>207</b>
<b>8. Recommendations.....</b>	<b>208</b>
<b>References .....</b>	<b>210</b>
<b>Appendix</b>	
<b>A HASC Utility Program Description.....</b>	<b>A-1</b>
<b>B VTXCHN Input Listings.....</b>	<b>B-1</b>
<b>C Examples of HASC Input Files.....</b>	<b>C-1</b>
<b>D Examples of HASC Output Files.....</b>	<b>D-1</b>
<b>E Application of the HASC Code to Buffet Analysis.....</b>	<b>E-1</b>

## **SUMMARY**

This report was prepared for NASA Langley Research Center by Lockheed Martin Tactical Aircraft Systems as prime contractor, with Nielsen Engineering & Research, Inc. and Consulting Aviation Services as subcontractors. Mike J. Logan at NASA Langley was the contract monitor. Alan E. Albright at Lockheed Martin was the program manager. The work reported was performed during the period from April through November 1995 with funding from NASA Langley Research Center.

A conceptual/preliminary design level subsonic aerodynamic prediction code HASC (High Angle of Attack Stability and Control) has been improved in several areas, validated, and documented. The improved code includes improved methodologies for increased accuracy and robustness, and simplified input/output files. An engineering method called VTXCHN (Vortex Chine) for predicting nose vortex shedding from circular and non-circular forebodies with sharp chine edges has been improved and integrated into the HASC code.

This report contains an summary of the modifications, description of the code, user's guide, and validation of HASC. Appendices include discussion of a new HASC utility code, listings of sample input and output files, and a discussion of the application of HASC to buffet analysis.

## LIST OF FIGURES

<b>Figure</b>	<b>Description</b>	<b>Page</b>
3.0-1	Overview of the HASC Analysis Flow Path.....	14
3.1-1	HASC(less VTXCHN) Subroutine Calls .....	21
3.2-1	VTXCHN Subroutine Calls.....	31
4.1-1	Listing of HASC Source Directory.....	38
4.1-2	HASC Makefile used on a Silicon Graphics Indigo 2 Platform .....	39
4.2-1	HASC Input/Output Files.....	41
4.2-2	Surface Definitions and Solution Options.....	50
4.2-3	Panel Definitions and Input Order Requirements.....	51
4.2-4	Airfoil Decomposition for HASC Input.....	55
4.2-5	Definitions of Airfoil Leading Edge Parameters .....	61
4.2-6	Definitions of Airfoil Input File airfoil.inp Parameters.....	63
4.2-7	Illustration of Forebody Lengths .....	97
5.0-1	Cross Sections of Forebodies Used in VTXCHN Validation.....	108
5.1-1	Longitudinal Characteristics for Forebody A1, M=0.2.....	110
5.1-2	Lateral Characteristics for Forebody A1, AOA=10°, M=0.2.....	111
5.1-3	Lateral Characteristics for Forebody A1, AOA=20°, M=0.2.....	112
5.1-4	Lateral Characteristics for Forebody A1, AOA=30°, M=0.2.....	113
5.1-5	Lateral Characteristics for Forebody A1, AOA=40°, M=0.2.....	114
5.1-6	Pressure Coefficient for Forebody A1, M=0.2.....	115
5.2-1	Longitudinal Characteristics for Forebody A2, M=0.2.....	117
5.2-2	Lateral Characteristics for Forebody A2, AOA=10°, M=0.2.....	118
5.2-3	Lateral Characteristics for Forebody A2, AOA=20°, M=0.2.....	119
5.2-4	Lateral Characteristics for Forebody A2, AOA=30°, M=0.2.....	120
5.2-5	Lateral Characteristics for Forebody A2, AOA=40°, M=0.2.....	121
5.2-6	Pressure Coefficient for Forebody A2, M=0.2.....	122
5.3-1	Longitudinal Characteristics for Forebody B1, M=0.2.....	124
5.3-2	Lateral Characteristics for Forebody B1, AOA=10°, M=0.2.....	125
5.3-3	Lateral Characteristics for Forebody B1, AOA=20°, M=0.2.....	126
5.3-4	Lateral Characteristics for Forebody B1, AOA=30°, M=0.2.....	127
5.3-5	Lateral Characteristics for Forebody B1, AOA=40°, M=0.2.....	128
5.3-6	Pressure Coefficient for Forebody B1, M=0.2.....	129



5.4-1	Longitudinal Characteristics for Forebody C1, M=0.2 .....	131
5.4-2	Lateral Characteristics for Forebody C1, AOA=10°, M=0.2 .....	132
5.4-3	Lateral Characteristics for Forebody C1, AOA=20°, M=0.2 .....	133
5.4-4	Lateral Characteristics for Forebody C1, AOA=30°, M=0.2 .....	134
5.4-5	Lateral Characteristics for Forebody C1, AOA=40°, M=0.2 .....	135
5.4-6	Pressure Coefficient for Forebody C1, M=0.2 .....	136
5.4-7	Vortex Distribution for Forebody C1, X=7.06, Beta=0°, M=0.2.....	137
5.4-8	Vortex Distribution for Forebody C1, X=14.06, Beta=0°, M=0.2 .....	138
5.4-9	Vortex Distribution for Forebody C1, X=7.06, Beta=5°, M=0.2.....	139
5.4-10	Vortex Distribution for Forebody C1, X=14.06, Beta=5°, M=0.2 .....	140
6.0-1	Summary of HASC Validation Cases .....	143
6.1-1	63.03 Degree Wing Baseline Comparison.....	144
6.1-2	Hummel Wing Baseline Comparison.....	145
6.1-3	44 Degree Trapezoidal Wing and Canard Baseline Comparison...	146
6.1-4	Predicted Pitch Rate Derivatives for a 65 Degree Delta Wing .....	148
6.2-1	Tailless Fighter Configuration.....	150
6.2-2	Tailless Fighter Baseline Comparison, M=.3, Controls=0.....	153
6.2-3	Sensitivity to SPC Parameter on Tailless Fighter.....	154
6.2-4	Sensitivity to Chordwise Paneling on Tailless Fighter.....	155
6.2-5	Sensitivity to Spanwise Paneling on Tailless Fighter.....	156
6.2-6	Sensitivity to Wing Camber Definition on Tailless Fighter.....	157
6.2-7	Tailless Fighter 10 deg. RH Elevon Long. Comparison, VORLIF ....	159
6.2-8	Tailless Fighter 30 deg. RH Elevon Long. Comparison, VORLIF ....	160
6.2-9	Tailless Fighter 10 deg. RH Elevon Long. Comparison, VORLAX...	161
6.2-10	Tailless Fighter 30 deg. RH Elevon Long. Comparison, VORLAX...	162
6.2-11	Tailless Fighter 10 deg. RH Elevon L/D Comparison, VORLIF .....	163
6.2-12	Tailless Fighter 30 deg. RH Elevon L/D Comparison, VORLIF .....	164
6.2-13	Tailless Fighter 10 deg. RH Elevon L/D Comparison, VORLAX.....	165
6.2-14	Tailless Fighter 30 deg. RH Elevon L/D Comparison, VORLAX.....	166
6.3-1	Falcon 21 Configuration.....	167
6.3-2	Falcon 21 Baseline Comparison, M=.2, Controls=0 .....	169
6.3-3	Comparison of Forebody Calculation Methods on Falcon 21 .....	170
6.3-4	Falcon 21 15 deg. Leading Edge Flap Comparison .....	172
6.3-5	Falcon 21 Symmetric 10 deg. Trailing Edge Flap Comparison .....	173
6.3-6	Falcon 21 Symmetric 30 deg. Trailing Edge Flap Comparison .....	174

6.3-7	Falcon 21 Asymmetric 10 deg. Trailing Edge Flap Comparison .....	175
6.4-1	F-16XL Configuration .....	176
6.4-2	F-16XL Baseline Comparison, M=.2, Controls=0 .....	178
6.4-3	Comparison of Forebody Calculation Methods on F-16XL .....	179
6.4-4	Sensitivity to Wing Definition on F-16XL .....	180
6.4-5	F-16XL Sensitivity to Vortex Flag (IVTXFLG) .....	181
6.4-6	F-16XL Symmetric 10 deg. Elevon Comparison .....	183
6.4-7	F-16XL Symmetric 30 deg. Elevon Comparison .....	184
6.5-1	F-16 Configuration .....	185
6.5-2	F-16 Baseline Comparison, M=.6, Controls=0 .....	187
6.5-3	Comparison of Forebody Calculation Methods on F-16 .....	188
6.5-4	Comparison of Computation Methods on F-16 Horizontal Tail .....	191
6.5-5	F-16 Sensitivity to Vortex Flag (IVTXFLG) .....	192
6.5-6	F-16 15 deg. Leading Edge Flap Comparison .....	193
6.5-7	F-16 25 deg. Leading Edge Flap Comparison .....	194
6.5-8	F-16 10 deg. Horizontal Tail Comparison, VORLIF .....	195
6.5-9	F-16 10 deg. Horizontal Tail Comparison, VORLAX .....	196
6.5-10	F-16 Horizontal Tail Increment (on-off) Comparison .....	197
6.5-11	F-16 30 deg. Rudder Comparison .....	198
6.5-12	F-16 Comparison of Forebody Methods at 5 deg. Sideslip .....	200
6.5-13	F-16 Comparison of VORLAX and VORLIF at 5 deg. Sideslip .....	201
6.5-14	F-16 Steady-State Dynamic Derivatives Comparison .....	203
6.6-1	Convair Model 200 Baseline Comparison .....	204
A-1	Overview of HASCUTIL Program Options .....	A-2
A-2	HASCUTIL Options 4 and 5 for Modifying a Surface .....	A-8
D-1	Geometry Written to Output Files grid_.p3d for the F-16 .....	D-14
E-1	Analytical and Test Buffet Reduced Frequency .....	E-2

## LIST OF TABLES

<b>Table</b>	<b>Description</b>	<b>Page</b>
3.1-1	Listing of HASC Subroutine Descriptions.....	22
3.2-1	Listing of VTXCHN Subroutine Descriptions.....	32
4.2-1	Summary of Parameters in Input File hasc.inp .....	42
4.2-2	Description of hasc.inp Input Variables .....	43
4.2-3	Summary of HASC Runs Times on a SG Indigo 2.....	58
4.2-4	Description of Parameters in Input File airfoil.inp.....	64
4.2-5	Summary of Empirical Factor File emprcl.inp.....	66
4.2-6	Description of the Empirical Factors in emprcl.inp.....	67
4.2-7	Summary of Parameters in Forebody File vchn.inp (full).....	74
4.2-8	Description of Parameters in Input File vchn.inp (full).....	76
4.2-9	Summary of Parameters in Forebody File vchn.inp (condensed).....	96
4.2-10	Description of Parameters in Input File vchn.inp (condensed) .....	97
4.4-1	Description of HASC Files .....	101
B-1	Forebody A1 VTXCHN Input File .....	B-3
B-2	Forebody A2 VTXCHN Input File .....	B-4
B-3	Forebody B1 (smooth body) VTXCHN Input File.....	B-5
B-4	Forebody B1 (chined body) VTXCHN Input File .....	B-7
B-5	Forebody C1 VTXCHN Input File.....	B-9
B-6	Condensed VTXCHN Input File (vchn.inp) for an F-16 Forebody...B-11	B-11
B-7	Full VTXCHN Input File (vchn.inp) for an F-16 Forebody.....	B-13
C-1	HASC Input File hasc.inp for the Tailless Fighter Configuration.....	C-3
C-2	HASC Input File airfoil.inp for the Tailless Fighter Configuration.....	C-9
C-3	HASC Input File hasc.inp for the Falcon 21 Configuration .....	C-16
C-4	HASC Input File hasc.inp for the F-16XL Configuration .....	C-22
C-5	HASC Input File hasc.inp for the F-16 Configuration.....	C-32
C-6	HASC Input File vchn.inp for the F-16 Forebody .....	C-45
C-7	HASC Input File hasc.inp for the Model 200 Configuration .....	C-47
D-1	Sample of Output Information Written to Screen (unit 6).....	D-3
D-2	Sample of Primary HASC Output File (hasc.out).....	D-9

## LIST OF SYMBOLS

AEDC	Arnold Engineering Development Center
AFB	Air Force Base
AOA	angle of attack
AOS	angle of sideslip
CA	axial coefficient
CAS	Consulting Aviation Services
CD	drag coefficient
CDL	drag due to lift
CL	lift coefficient
CI	rolling moment coefficient
Clp	roll damping coefficient
Cm	pitching moment coefficient
Cmq	pitch damping coefficient
CN	normal force coefficient
Cn	yawing moment coefficient
Cnr	yaw damping coefficient
Cp	pressure coefficient
CY	side force coefficient
GDLST	General Dynamics Low Speed Tunnel
HASC	High Angle of Attack Stability and Control code
HT	horizontal tail
L/D	Lateral / Directional
LaRC	Langley Research Center
LE	leading edge flap
LH	left hand
LMTAS	Lockheed Martin Tactical Aircraft Systems
M	Mach number
NEAR	Nielsen Engineering & Research, Inc.
RH	right hand
TE	trailing edge flap
VORLAX	Vortex Lattice Method code
VTXCHN	Vortex Chine code
VTXCLD	Vortex Cloud code

## 1.0 INTRODUCTION

During the last two years the NASA Langley Research Center (NASA LaRC) has been leading an effort to develop non-linear aerodynamic prediction methods suitable for conceptual/preliminary design level applications. This effort at NASA LaRC has been led by Mike Logan. A requirements workshop, followed by an initial code evaluation workshop, have taken place at NASA LaRC. Recommendations have been collected from industry for developing a new analytical/semi-empirical aerodynamic prediction method and a more empirically based method. Development of these methods is expected to be a multi-year task. The current short-term effort as documented in this report was initiated to develop an improved aerodynamic prediction method by making modifications to an existing prediction code with funding from NASA LaRC. The HASC (High Angle of Attack Stability and Control) code was selected as the baseline code.

In 1992 the initial development of HASC was completed by Lockheed Aeronautical Systems Company for the Air Force Wright Laboratory (reference 1). The HASC code is primarily an integration of three routines (modules):

- 1) VORLAX - a generalized vortex lattice program by L.R. Miranda (reference 2),
- 2) VORLIF - a semi-empirical strake/wing vortex analysis code developed by Dixon (reference 3),
- 3) VTXCLD - a two dimensional, unsteady, separated flow analogy program for analyzing smooth forebody shapes by M.R. Mendenhall and D.J. Lesieutre (reference 4).

Additional modifications based on the work of C.E. Lan (reference 5) and L.E. Ericsson and J.P. Reding (reference 6) were also incorporated in the HASC code.

The NASA LaRC funded HASC modification effort included tasks to correct known software errors, improve the prediction accuracy through methodology enhancements, validate the code using several configurations, and document the results. These tasks were performed by Lockheed Martin Tactical Aircraft Systems (LMTAS) as prime contractor, with Nielsen Engineering & Research, Inc. (NEAR) and Consulting Aviation Services (CAS) as subcontractors. Modifications

were made to the latest available versions of both HASC and VTXCHN. The new HASC code, HASC95, is similar in structure to the original HASC code, except for the replacement of VTXCLD with VTXCHN. VTXCHN allows analysis of forebodies with chined cross-sections. The modified code HASC95 is referred to hereafter simply as HASC.

A major rewrite of the HASC software using C/C++ , and development of a graphical user-interface were outside the scope of this contract.

This report contains an overview of the modification tasks, a description of the code, user information, and validation results.

Section 2 presents an overview of the most significant accomplishments during the modification tasks. Many changes were made to the software to provide easier porting to various platforms and improved maintainability. Many errors, some of which are listed in section 2, were identified and corrected.

Section 3 contains a top-level description of the theory and empiricism implemented in HASC. Diagrams showing the calling structure of the subroutines as well as short descriptions of the subroutines are included.

Section 4 contains user guide information for HASC including VTXCHN.

Section 5 presents results from the VTXCHN validation on four forebody shapes, while section 6 presents the validation results of HASC on wing and aircraft configurations. Longitudinal and lateral/directional coefficients, control increments, and damping derivatives were computed and compared to wind tunnel test data.

Appendix A contains a description of a new utility program called HASCUTIL. Appendix B contains listings of VTXCHN input files. Appendix C and D provide samples of HASC input and output files. Finally, Appendix E is a discussion on a research application of HASC to buffet analysis as conducted by CAS with funding from Georgia Institute of Technology.

## 2.0 MODIFICATION TASK OVERVIEW

This section provides a summary of the major accomplishments by LMTAS, NEAR, and CAS during the subject contract.

- Several software errors, both large and small, were identified and corrected throughout the HASC code.
- Improvements in variable usage, common blocks, internal comments, maintainability, and portability were made.
- Time required for creating input files has been reduced through:
  - elimination of unnecessary formatted reads,
  - permitting comment lines in all input files,
  - writing a new HASC utility program, and
  - adding internal checks with appropriate warning messages.
- Output information has been enhanced through improving formats, renaming files, and additional diagnostic information.
- Output geometry files for Plot3d and Tecplot have been added.
- The calculation for the effects of multiple vortices has been considerably improved. HASC now includes an improved routine to predict the final burst of the vortex; i.e., from initial turbulent or spiral breakdown to chaotic burst.
- Several corrections were made to improve the vortex effects on configurations with two lifting surfaces (wing & horizontal tail, or canard & wing). Canard configurations can now be evaluated using VORLIF.
- Pitch, roll, and yaw rates with vortex breakdown effects have been included.

- A major change in computing the camber effects now allows accurate accounting for small leading and trailing edge deflections, bevels, and other camber devices. The computation of the zero lift angle of attack is more rigorous making the camber effects more accurate.
- A correction for the loss in spanwise lift carry-over is available for the conditions where the lifting surface unports from the fuselage when deflected.
- The robustness and accuracy of VTXCHN was improved. Major coding changes were made to improve the accuracy of the results for chined bodies at high angle of attack and at non-zero sideslip. In order to reduce flow modeling assumptions, the tracking of vortices shed from the body (including the chines) was moved from the physical plane to the transformed (or mapped) circle plane.
- Effects of steady-state angular rates were incorporated in VTXCHN. This process involved adding contributions to the velocity components in the flow tangency boundary conditions applied in the mapped circle planes.
- In VTXCHN, the pressure calculation performed in the physical plane was modified to include additional velocity contributions. A term was added in the compressible Bernoulli pressure expression to account for steady rotations. A lower limit in the pressure coefficient was also implemented.
- In VTXCHN, the position and strength of a vortex can now depend on the flow on the upper surface as well as the flow on the lower surface.
- HASC has been used to predict subsonic aerodynamics of 4 forebody shapes and 5 aircraft configurations. Baseline longitudinal and lateral/directional coefficients, leading edge and trailing edge control increments, and damping derivative predictions were compared to wind tunnel data.



### 3.0 HASC PROGRAM DESCRIPTION

Included in this section are brief descriptions of the theory and empiricism implemented in the HASC code. Section 3.1 presents the information on all subroutines except those unique to VTXCHN. The VTXCHN discussion is presented in section 3.2. A comprehensive description of the theory and equations is outside the scope of this report. However, several references exist where this information can be reviewed if desired.

HASC from its inception was developed as an integration of primarily three routines; 1) VORLAX, 2) VTXCLD, and 3) VORLIF. These modules have been modified and enhanced for use within HASC. The current version of HASC utilizes VTXCHN instead of VTXCLD thus enabling analysis of forebodies with chined cross sections. HASC can be ran either as a complete HASC code utilizing any or all of the analysis modules (VORLAX, VORLIF, VTXCHN), or it can be run executing VTXCHN only by placing "VTXCHN ONLY" in the top line of the primary HASC input file hasc.inp.

HASC is a conceptual/preliminary design level subsonic aerodynamic prediction code. Semi-empirical methods are used to estimate the effects of vortex lift and breakdown. Output files provide information on the input geometry, total configuration loads, component loads, and vortex characteristics.

Results can generally be obtained from several seconds to a few minutes. The execution time depends on the size of the input deck (number of horseshoe vortices and number of flow conditions), the analysis modules utilized, and the processor speed.

Figure 3.0-1 shows a top-level flow path of the calculation process within HASC. As noted in the figure, depending on the modules selected for analysis (VTXCHN, VORLAX, VORLIF), multiple runs are required to obtain the necessary upwash/downwash corrections. These runs are automatically ran by HASC, thus not requiring any additional input from the user. See Appendix D for an illustration of these multiple runs.

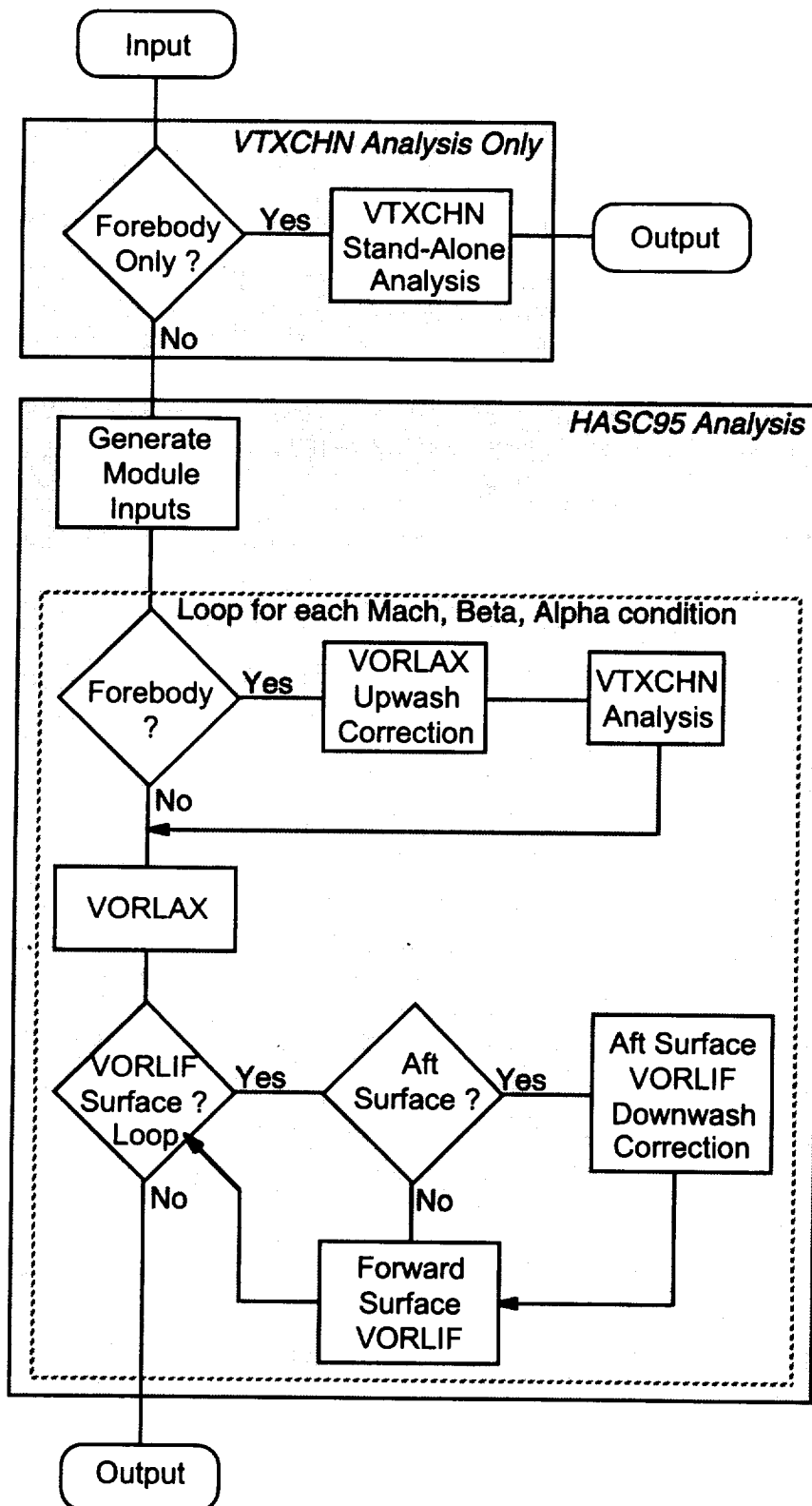


Figure 3.0-1 Overview of the HASC Analysis Flow Path

### **3.1 HASC (less VTXCHN)**

Separated vortex flow on lifting surfaces is modeled using a combination of a vortex lattice method (a modified VORLAX) and a vortex analysis code (VORLIF). The vortex lattice code provides leading-edge thrust values and stripwise forces and moments. The VORLIF code uses these values and geometric data to calculate the local streamwise section angle of attack, angle of zero lift, and lift curve slopes. This information is then used in a semi-empirically developed, two-dimensional routine to predict the vortex lift and drag and the total lift and drag for each streamwise section. The effect of airfoil thickness on leading edge separation is included. In a manner similar to that justified by parabolic fluid flow equations the vortex strength and position for the vortex is computed from its apex to its full span condition. The vortex induced and total forces and moments for the configuration are then calculated.

VORLIF uses flow data (pressure and velocities) calculated along the vortex core track to empirically predict the transition of the core from laminar to turbulent flow and to predict the breakdown (burst of the turbulent vortex) position. The influence of one vortex on another's velocity is included. These predictions can then be used to change the forces and moments due to the vortex breakdown.

The steps VORLIF follows are described below.

1. Local streamwise section angle of attack is obtained from the vortex lattice output. The angle of attack is corrected to an effective two-dimensional value and then used in a semi-empirical, two-dimensional analysis to obtain local streamwise force coefficients.
2. Vortex lift and drag coefficients (forces due to the leading edge shear layer), and the additional lift and drag coefficients (forces due to the trailing edge shear layer) are calculated for the configuration for a sharp leading edge. Total lift is the sum of these two components.
3. Vortex and additional lift and drag coefficients are corrected for finite airfoil effects on the loss in leading edge thrust. Vortex lift is proportional to the loss in leading edge thrust which is less for a finite airfoil than for a sharp edge wing.

4. Airfoil forces (reference 1) are used to determine the relation between leading edge thrust loss and/or recovery and the mass flow going into the vortex core.
5. The vortex lift is used to calculate the vortex circulation. The vortex lift has been empirically defined to match experimentally evaluated circulation.
6. The circulation across the core is used to calculate the vortex core velocity and the vortex stability analysis. The vortex core axial velocity and the core mass flow are used in the continuity equation to calculate the core radius.
7. The core radius is used in an empirical equation to approximate the position of the vortex over the wing. The equation involves the angle of attack of the free stream normal to the leading edge from which the vortex forms and the local vortex circulation.
8. The code is run through the first cycle of VORLIF to get the vortex or multiple vortex positions assuming the externally induced velocity in the vortex core is equal to the free stream velocity.
9. During the second cycle in VORLIF, the induced velocity is obtained from the vortex lattice code at the vortex core centerline as calculated in cycle one.
10. Cycle two analyzes the vortex stability defining the position along the vortex axis for its transition to a turbulent core.
11. Using the vortex position to define the aerodynamic center of the vortex lift, the moment is then calculated.
12. In VORLIF cycle two, the loads and moments are corrected for the change in the Kutta condition at the trailing edge in and near where the turbulent vortex crosses the trailing edge. An empirical correlation of the effective loss in local angle of attack with the vortex size and position is used.

13. The shift in section aerodynamic center due to the change in Kutta condition is found from the correlation and the moments corrected.

14. In cycle three the vortex position from cycle two is retained and the vortex core velocities including the vortex induced velocities and the externally induced velocities are recalculated.

15. Cycles two and three include the mutual effect of induced velocities from all free vortices and their images. This effect is on the free vortex axial velocities at all surfaces and the downwash at surfaces downstream of the vortex generating surface.

16. In cycle three the stability calculations are made again, and when the core axial velocity ratio approaches -0.6 the vortex is considered burst. New loads and moments are calculated assuming a stalled wing near and outside of the vortex burst.

17. All loads and yawing moment vectors are in planes normal to the surface being analyzed, and all pitching and rolling moment vectors are parallel to the planes being analyzed. HASC rotates and integrates these vectors to the body, wind, or stability axis of the configuration.

Additional information on important aspects of HASC are listed next.

- Nature of Vortex Breakdown

For moderately swept wings the vortex breakdown goes through two stages. The first stage is the transition to a turbulent vortex, and this is the spiraling of the previously laminar vortex core. Then there is a final chaotic burst of this spiraling core. Prior to burst this previously laminar core is still coherent, but it becomes turbulent and it is now spiraling within an envelope that is called the turbulent vortex diameter. Uberoi (reference 7) developed an equation for this diameter that is a function of the vortex circulation and distance from the origin of transition. This equation is used in HASC.

- Vortex Core Size

Vortex core size is based on the mass flow entrained and is calculated from continuity and pressure gradient terms as presented in reference 8.

- Vortex Stability

Two criteria are used to determine when the breakdown of the laminar vortex occurs. These are (1) a critical pressure gradient along the vortex axis (using 0.5), and (2) a critical vortex helix angle if the pressure gradient is at least 0.4.

- Effect of Breakdown on Forces and Moments

When the laminar vortex breaks down the turbulent core becomes large, and as it crosses the wing trailing edge it affects the Kutta condition causing an effective loss in local angle of attack. An empirical method based on data from a large scale test was developed to compute the effective loss in angle of attack. A shift in the aerodynamic center is computed also to correct the moments.

- Vortex Burst

HASC includes an improved routine to predict the final burst of the vortex; i.e., from initial turbulent or spiral breakdown to chaotic burst. A reverse flow along the free vortex axis is now computed. When core axial velocity ratio reaches a value of -0.58 the vortex burst and loads are affected accordingly. The only other burst criterion is a practical limit on the vortex core radius. If the radius exceeds 0.5 times the span of the leading edge where the vortex is formed, it is assumed the interference will cause the vortex to burst. The latter usually occurs only for turbulent vortices and on lifting surfaces with sweep less than 45 degrees.

When the final burst occurs, equations developed for a totally stalled airfoil are used to compute the forces and moments on the wing sections affected by the burst. The wing sections affected are determined empirically as a function of their relative position to the burst.

- Sweep Effects

For delta wings with sweeps less than 70 degrees a turbulent vortex can exist all the way from the apex to the trailing edge without chaotic burst. The extent depends on the sweep and the angle of attack. Loads and moments are significantly affected, but they are not severely affected until the vortex burst.

As the sweep approaches 70 degrees, the axial distance between the turbulent transition and the burst gets smaller until the two are almost together at the trailing edge. For sweep angles greater than 70 degrees the distinction between transition and burst can not be found.

- Effect of Negative Vortex Elements

At some spanwise position along the span, vortex elements that shed from the leading edge have negative circulation values; i.e., their circulation is the opposite sign of the free vortex. The explanation for this is that elements get their strength from the gradient of the vortex lift across the wing span. The vortex lift is increasing initially, but at some spanwise station it must start to approach zero at the wing tip. Therefore, where the vortex lift starts decreasing, the elements develop negative circulation.

For the HASC code these negative elements are assumed to wrap around the free vortex, and this causes a negative velocity along the vortex axis. Velocities are computed along the vortex axis from these elements and they produce a negative axial velocity.

An additional negative velocity is assumed to come from the core that is spiraling within the turbulent vortex diameter. The velocity from this entity is empirically developed as a function the strength of this spiraling core. These velocities are added to the other induced velocities and the free stream component.

- Analytical Development of Stall and Post Stall

Empirical factors that account for viscous effects are used in the angle of attack regions near stall and post stall. Values for these factors were determined primarily using test data from three wing configurations. The first configuration is the 59.3 degree delta wing investigated by Hubner (reference 9). The next configuration is a 63.03 degree delta wing (reference 10). The third configuration is the aspect-ratio-one Hummel wing (reference 11). All three configurations were used to investigate the proper values of these empirical factors.

Figure 3.1-1 presents the calling structure of the various subroutines of HASC. The subroutines for VTXCHN are presented in a later figure. Short descriptions of the subroutines follow in table 3.1-1.



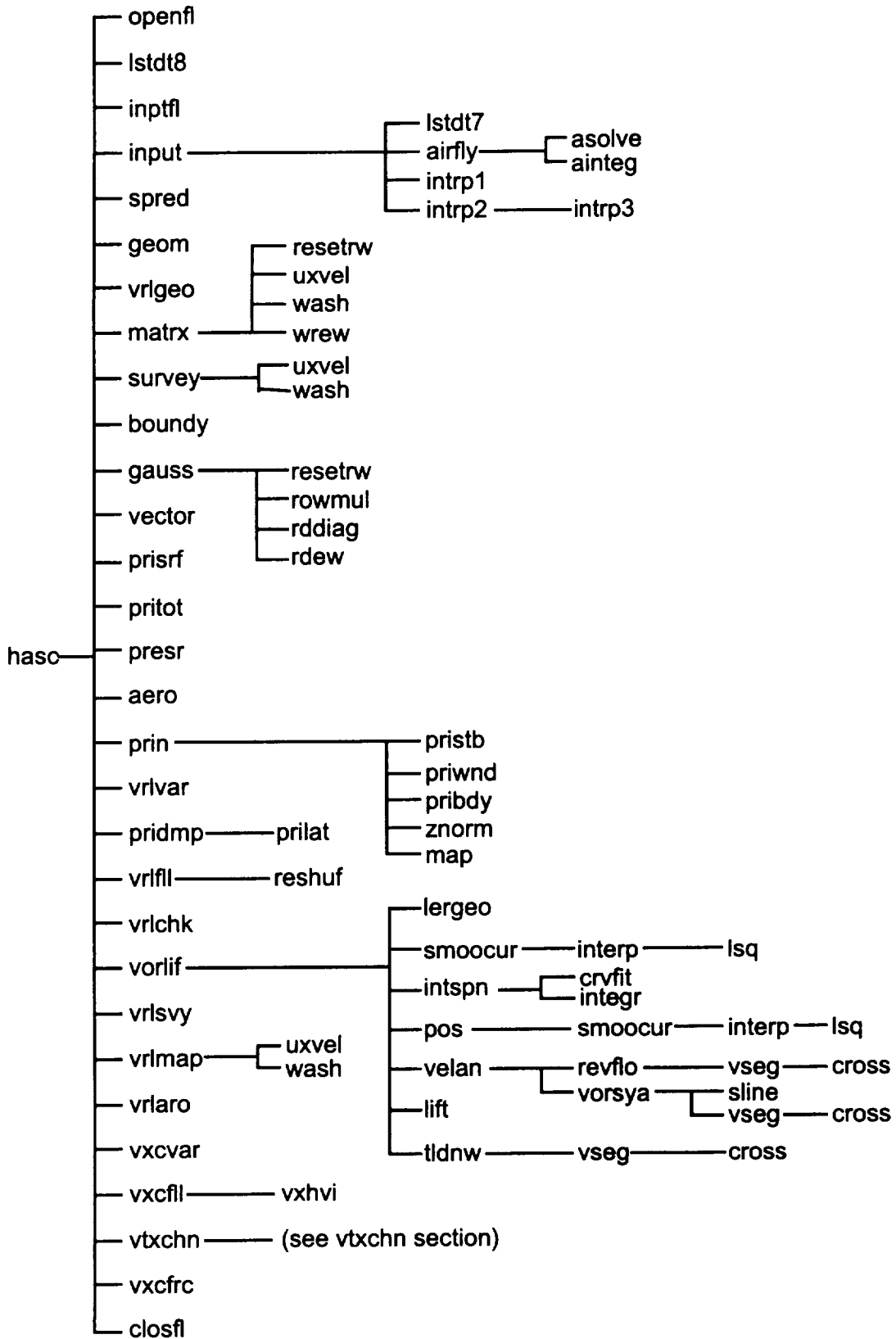


Figure 3.1-1 HASC(less VTXCHN) Subroutine Calls

Table 3.1-1 Listing of HASC Subroutine Descriptions

<b>AERO</b>	Force and moment coefficients are determined by integrating the pressure distribution and computing the leading edge suction forces in accordance with Lan's procedure (reference 5). Three classes of coefficients are computed, (1) total configuration coefficients, (2) panel coefficients, and (3) stripwise, or chordwise coefficients. The aero subroutine is called by HASC for every angle of attack, sideslip, and Mach number combination.
<b>AINTEG</b>	Integrates over a curve for force and moments.
<b>AIRFYL</b>	Reads in basic airfoil characteristics provided in file airfoil.inp. Computes airfoil parameters as required by HASC.
<b>ASOLVE</b>	Solves a matrix equation by Gauss-Jordan elimination.
<b>BOUNDY</b>	Calculates the onset of the flow component normal to the boundary surface at the vortex lattice control points. This is calculated by projecting the free-stream velocity vector along the surface normal taking into account a rigid body rotation.
<b>CLOSFL</b>	Closes input and output files.
<b>CROSS</b>	Calculates the vector product of two vectors.
<b>CRVFIT</b>	Curve fitting routine for both open and closed curves.
<b>DOT</b>	Calculates the scalar product of two vectors (function).
<b>DTRMNT</b>	Calculates matrix determinant (function).
<b>FAKIMA</b>	Computes y at desired x values (function).
<b>GAUSS</b>	Solves the boundary condition equations by the method of "controlled successive over-relaxation" (csor). The circulation strength of the

horseshoe vortices that satisfy the boundary condition of no mass-flux along the normal to the surface at the control points is performed iteratively row by row by using the csor method.

- GEOM** Computes the vortex lattice geometry and surface slopes at the control points.
- HASC** HASC main program.
- INPTFL** Reads the primary HASC input file and prepares it for multiple runs to obtain the necessary interactions between surface types.
- INPUT** Reads the input data and prepares it for use in the generation of vortex lattice geometry done in the subroutine geom.f. The geometry is based on a body fixed orthogonal coordinate system with the positive x axis pointing downstream along the centerline plane. Positive z points upward and the y axis points to the starboard.
- INTEGR** Integrates a single curve for forces and moments.
- INTERP** Fits a least-squares curve to data. Generates integrals and derivatives.
- INTGAM** Computes the total circulation strength by integration of the spanwise circulation components. This information can be used to asses the x-component of gamma which is used to improve lateral/directional predictions.
- INTRP1** Computes a three-point square root Lagrange polynomial interpolation for slope and z-ordinates from the input geometry data. This routine is only used for interpolation between the first and second points in the geometry data.
- INTRP2** Interpolates the input geometry curves to find the z-ordinates and slopes.

<b>INTRP3</b>	Interpolation routine using a locally-fitted cubic spline.
<b>INTSPN</b>	Adds the value at the root and tip to the span load array and returns the integral of the load from root to tip.
<b>LERGEO</b>	Computes the parameters required to obtain the residual leading-edge thrust using Carlson's method. The leading edge geometry is required for both the inboard and outboard stations of each panels of the lift surface. Geometry for stations between input stations is obtained by interpolation.
<b>LIFT</b>	Calculates all the section lift and drag coefficients.
<b>LSQ</b>	Least squares curve fit routine.
<b>LSTDT7</b>	Removes the comment lines from the airfoil definition input file unit 3, and writes resulting data to unit 7.
<b>LSTDT8</b>	Reads the primary HASC input file from unit 15, removes the blank lines and comment lines. Writes the remainder of the input to a VORLAX input file, unit 8.
<b>MAP</b>	Flow field quantities are computed at the nodal points of a 3-d grid defined around the configuration by a set of orthogonal planes. Velocities are calculated by the use of influence coefficient matrices based on the vortex lattice representation of the configuration. One matrix is computed in the subroutine survey.f for each velocity component. The pressure ratios and other related flow quantities are computed through the use of isentropic flow relationships
<b>MATRX</b>	Generates three aerodynamic influence coefficient matrices, (1) normalwash at the control points, (2) axialwash at the control points, and (3) normalwash at the leading edge. These matrices represent the induced velocity field due to the horseshoe vortices of the lattice.

**OPENFL** Opens files used by the HASC program. Information on what subroutine utilizes the file is included.

**POS** Computes the vortex position above and behind the wing.

**PRESR** Computes pressure load coefficients, or surface pressure coefficients, from the values of the induced velocities and circulation strengths.

**PRIBDY** Prints surface and total forces and moments in body axes.

**PRIDMP** Generates output file of panel geometry breakpoints.

**PRILAT** Produces a pseudo element lattice suitable for the output file unit 79.

**PRIN** Prints VORLAX program data. Data are arranged in three groups, as follows: (1) input data which have been converted to a format suitable for use by the program, (2) panel and total configuration force and moment coefficient data, and (3) data related either to chordwise strips or to individual horseshoe vortices. These three data groups are printed sequentially.

**PRISRF** Prints forces and moments for each surface in body, stability, and wind axes.

**PRISTB** Prints surface and total forces and moments in stability axes.

**PRITOT** Prints total forces and moments in body, stability, and wind axes.

**PRIWND** Prints surface and total forces and moments in wind axes.

**RESHUF** Reformats the check output of the sectional coefficients from the file unit 37, and writes the reformatted data to file 57.

- REVFLO** Computes velocity induced on the vortex axis by vortex elements which encircle and form the free vortex. These elements are shed for the leading edge and are allowed to circle the vortex at the location where the element joins the vortex. This routine is designed primarily to compute the self induced velocities at the vortex axis. Both positive and negative vortex elements are shed from the leading edge. Positive elements increase the circulation and induce positive velocities along the vortex axis. Elements with negative circulation induce negative axial velocities. This routine is used to correct the average axial vortex velocity.
- SLINE** Computes influences of a (unit strength) sinkline segment.
- SMOOCUR** Fits a least square curve to the values of the dependent variable. It also allows a progression from one set of data points to another while holding the coordinates at the last point of the previous set of data. Only four data points are smoothed each step. Output gives new smoothed coordinates and the first derivative.
- SPRED** Prints panel x, y, and z data to a file for use in spreadsheet plotting.
- SURVEY** Generates three aerodynamic influence coefficient matrices, (1) the upwash at the flow field survey points, (2) the axialwash at the flow field survey points, (3) the sidewash at the flow field survey points. These matrices represent the induced velocity field due to the horseshoe vortices of the lattice. This flow field is measured at the nodal points of a specified 3-d grid.
- TLDNW** Calculates a correction to the tail or aft surface downwash due to the loads being different than produced by potential flow from VORLAX. Downwash is computed at the aft surface before vortex breakdown and after. The difference is used to obtain the correction.
- UXVEL** Computes the axialwash induced by a skewed rectilinear vortex segment of unit circulation.

VECTOR	Solves the linear system of boundary condition equations by Purcell's method. Sets of linearly independent vectors are constructed which are successively orthogonal to each row. When all rows have been considered, there is only one vector which is normal (orthogonal) to all rows and contains the solution vector. Thus no matrix inversion is involved and only one row of the coefficient matrix is required at a time.
VELAN	Computes axial and normal velocities along vortex.
VORLIF	Semi-empirical strake/wing vortex analysis code developed by Dixon.
VORSYA	Calculates the velocities at the core of each free vortex due to the presence of other vortices.
VRLARO	Computes force and moment data by integration of the strip force and moment coefficients from VORLIF.
VRLCHK	Prints out the vlmdat.f and intgrm.f common blocks for checking the variables being passed to VORLIF from VORLAX.
VRLFLL	Fills the variables calculated in vrlvar.f into the appropriate VORLIF variables and arrays for the particular surface to be analyzed.
VRLGEO	Translates the VORLAX geometry in NASA VLM type outline geometry definition. This is the format the VORLIF segment requires for input data.
VRLMAP	Computes the flow field at the vortex core coordinates. The velocities are calculated from influence coefficient matrices based on the vortex lattice representation of the configuration. These matrices are computed in subroutine vrlsvy.f and are stored as one matrix per velocity component. The pressure ratios and other related flow quantities are computed through the use of isentropic flow relationships

VRLSVY	Generates three aerodynamic influence coefficient matrices, (1) upwash at the vortex core points, (2) axialwash at the vortex core points, (3) sidewash at the vortex core points. These matrices represent the induced velocity field due to the horseshoe vortices of the lattice. This flow field is measured at the core points calculated by VORLIF in cycle 1. These matrices include the coefficients at each angle of attack.
VSEG	Computes the velocity induced by a (unit strength) vortex segment (and its image) at arbitrary field point.
VXCFLL	Reads the top two data lines from the VTXCHN input file as modified for HASC.
VXCFRC	Adds the forces from VTXCHN to the force and moment summaries.
VXCVAR	Collects the variables for a given body surface for use in subroutine VXCFLL in constructing a VTXCHN input data set.
VXHM	Writes the VTXCHN input file to unit 53.
WASH	Computes the three velocity components induced at a given point by a generalized horseshoe vortex of unit strength.
ZNORM	Integrates the chordwise slope distribution from an input wing load distribution in order to obtain the surface camber ordinates.



## 3.2 VTXCHN

VTXCHN is an engineering prediction code developed to predict aerodynamic loads acting on a body including effects of nose vortex shedding. The bodies may have circular and noncircular cross sections which may include sharp chine edges. Flow conditions include subsonic flow, high angles of attack, non-zero angles of sideslip, and steady-state rotational flow. Axisymmetric bodies are represented by points transformed to a circle by either analytical or numerical conformal transformations. In the transformed plane, the circular body is modeled by three dimensional point sources and sinks, and two dimensional doublets. The lee side vortex wake is modeled in the transformed plane by discrete vortices in crossflow planes along the body; thus the three-dimensional steady flow problem is reduced to a two-dimensional, unsteady, separated flow problem for solution.

The predicted pressure distribution on the body under the influence of the stream and the separation vortex wake is calculated in the physical plane. The aerodynamic loads on the body are obtained from a pressure integration.

Conformal transformations used are of two types, analytical and numerical. For simple shapes like an ellipse, the transformation to the circle is through an analytical method. However, for complex noncircular shapes, the transformation is through a numerical method.

The body vortex shedding model for forebodies which chine is significantly different from the model for smoothed bodies. The major difference is in the formation of the discrete vortices themselves. Since the chine is the origin of separation it is not necessary to predict the separation location.

The volume of the body in the transformed plane is represented by discrete point sources and sinks, and the strength of the individual singularities is determined to satisfy a flow tangency condition on the body. Two dimensional doublets account for angles of incidence and roll. Compressibility effects on the body are included by a Gothert transformation which keeps the cross section shape unchanged but stretches the axial body coordinate.

The aerodynamic load calculation starts at a crossflow plane near the body nose, and the pressure distribution on the body is computed using the full compressible Bernoulli equation. The body shape determines the location of separation as the assumption is made that separation occurs at the sharp edge for a chined forebody, and the vortex sheet originates at that point. Strengths and positions of the incompressible vortices are determined by the requirement that the Kutta condition at the sharp edge be satisfied at the separation points. For smooth bodies separation is determined by the Stratford criteria. The trajectories of the discrete vortices between this crossflow plane and the next plane downstream are calculated by integration of the equations of motion of each vortex, including the influence of the free stream, the body, and other vortices. The vortex-induced velocity contribution to the body tangency boundary condition includes image vortices in the circle plane.

At the next downstream crossflow plane, new vortices are shed, adding to the vortex feeding sheet and cloud representing the wake on the lee side of the body. This procedure is carried out in a stepwise fashion over the length of the forebody.

Figure 3.2-1 presents the calling structure of the VTXCHN subroutines. Short descriptions of the subroutines are listed in table 3.2-1.

Further details are available in references 12 and 13.

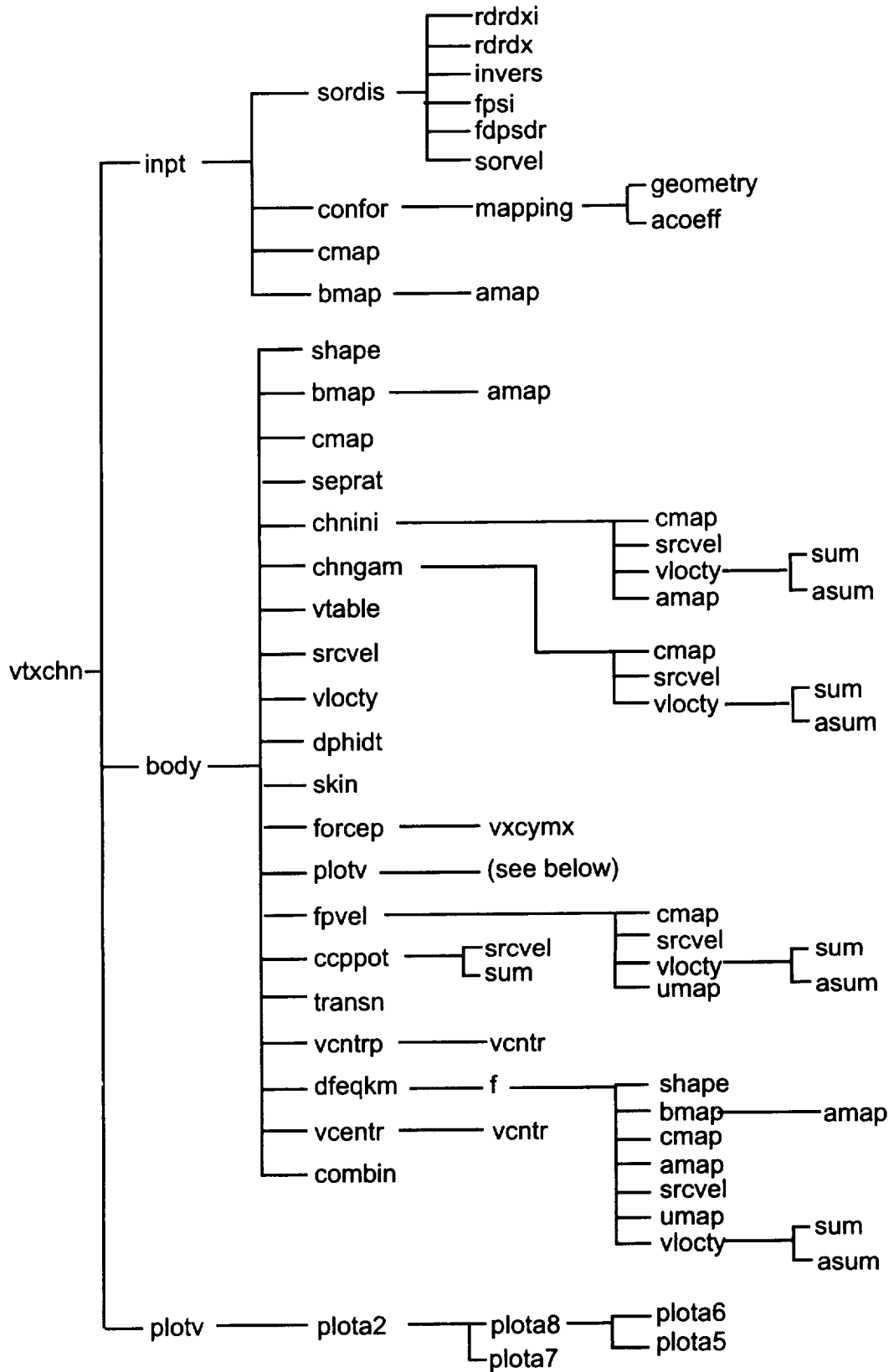


Figure 3.2-1 VTXCHN Subroutine Calls

Table 3.2-1 Listing of VTXCHN Subroutine Descriptions

AMAP	Transforms a specified point in the circle plane to its corresponding point in the body plane.
ASUM	Calculates the velocity term due to transformation for noncircular bodies.
BMAP	Sets up a table of points on the actual body corresponding to specified points on the circle. Actual mapping occurs in subroutine amap.f.
BODY	Organizes the flow throughout the VTXCHN module through calls to predict vortex shedding, to calculate surface velocities and pressures, and to calculate the overall forces and moments on the body. These data can be predicted for elliptic, non circular or chine cross sections. Options include asymmetry, initial flow field vorticity, reverse flow separation, and flow transition.
CCPPOT	Calculates a potential surface pressure distribution at a given x station (the effects of separated vortices are not present in the $C_p$ calculation). This is used in determining a turbulent separation point for the transition region.
CHNGAM	Calculates the strengths and locations of vortices shed from a chine cross section body. It is assumed that all chined bodies are symmetric about the body axis x-z plane and that only primary vortex separation occurs. In addition, the numerical conformal mapping requires symmetry about the z axis in the cross flow plane. Therefore, the separation location on a chined body are symmetric even if $\phi$ is non zero.

CHNINI	Calculates the initial strengths and locations of vortices shed from a chine cross section body. The vortex strength is approximated as body with a circular cross section with an attached strake modeled by vortex lattice. Effects of chine thickness on surface pressures are accounted for using the numerical conformal mapping.
CMAP	Transforms a specified point in the body plane to its corresponding point in the circle plane.
COMBIN	Combines vortices which are separated by a distance less than or equal to RGAM. The resulting vortex strength is the sum of the individual strengths, and its location is the centroid of the combined vortices.
CONFOR	Calculates the coefficients of the numerical conformal mapping function. Transforms the region outside of a polygonal shape with a vertical plane of symmetry to the region outside of a circle.
DFEQKM	Obtains vortex paths between stations $x$ and $x+\text{deltax}$ using Kutta-Merson integration scheme.
DNUDX	Calculates the $dnu/dx$ on the body surface.
DPHIDT	Calculates the two-dimensional unsteady pressure term for use in the Bernoulli equation.
DZDNU	Calculates the differential of the transform of a polygonal shape to a circle (function).
F	Calculates the derivatives of the vortex equations of motion which are used in conjunction with <code>dfeqkm.f</code> to obtain the vortex paths.
FDPSDR	Calculates the axial velocity due to a three-dimensional source distribution.

<b>FORCEP</b>	<b>Calculates the forces and moments on the body by integration of the surface pressure distribution.</b>
<b>FPSI</b>	<b>Calculates the axisymmetric body shape represented by a three-dimensional source distribution.</b>
<b>FPVEL</b>	<b>Calculates the velocity at specified field points.</b>
<b>GEOMETRY</b>	<b>Calculates geometric angles and side lengths.</b>
<b>INPT</b>	<b>Reads in and prints out the body geometry, the flow conditions, various program options, and restart quantities.</b>
<b>INVERS</b>	<b>Solves simultaneous linear equations.</b>
<b>LSTDT53</b>	<b>Removes the comment lines from VTXCHN input file for HASC (unit 56), and writes resulting data to unit 53.</b>
<b>MAPPING</b>	<b>Performs mapping function.</b>
<b>PLOTA2</b>	<b>Generates a character plot of simultaneous curves of y vs. x.</b>
<b>PLOTA5</b>	<b>Rounds off x values for plotting.</b>
<b>PLOTA6</b>	<b>Rounds off scaling to nearest acceptable plotting scale.</b>
<b>PLOTA7</b>	<b>Initializes a row of plotted output.</b>
<b>PLOTA8</b>	<b>Select scales, rounds maximum and minimum values to acceptable values, and locates x and y axes.</b>
<b>PLOTV</b>	<b>Creates a line printer plot of the body and its vortex wake at any given x station.</b>
<b>RDRDX</b>	<b>Calculates r and dr/dx at a given x station.</b>

RDRDXI	Initializes the calculation of $r$ and $dr/dx$ for subroutine <code>rdrdx.f</code> .
SEPRAT	Predicts the position in the cross flow plane where separation occurs based on the Stratford's criteria for laminar and turbulent flows.
SHAPE	Determines the body geometric parameters from a table look-up of input data.
SKIN	Estimates the axial skin friction force on the body.
SORDIS	Calculates the source distribution representing an axisymmetric body of revolution given the body shape and slope at each $x$ station.
SORVEL	Calculates perturbation velocities due to a three-dimensional source distribution. Used by subroutine <code>sordis.f</code> in calculation of the source distribution.
SRCVEL	Calculates perturbation velocities due to a three-dimensional source distribution.
SUM	Analytical mapping of an elliptical cross section.
TRANSN	Calculates the body separation points in the transition region.
UMAP	Calculates the axial velocity due to noncircular mapping and two-dimensional singularities.
VCENTR	Calculates the centroid of each vortex field.
VCNTR	Calculates the centroid of any set of vortices.
VCNTRP	Calculates the centroid of two arrays, $y$ and $z$ , with respect to the weighting array.
VINFLU	Calculates the influence of a unit strength vortex and its image inside a circle at a point.

- VLOCTY**      Calculates the velocity components in the cross flow plane at a specified field point on or off the body.
- VTABLE**      Sets up the arrays of free vorticity for two cases: (1) The vorticity in the working array GAM is distributed into the individual arrays GAMP, GAMM, GAMR, GAMA, or (2) the vorticity in the individual arrays GAMP, GAMM, GAMR, GAMA is distributed into the working array, GAM, in the proper order.
- VTXCHN**      This is the main subroutine for calculating the forces and moments on a slender body in a steady flow condition including the nonlinear effects of lee side separation vorticity for circular, elliptical, and chine bodies.
- Z**              Calculates the transformation of a polygonal shape to a circle.



## **4.0 USER'S GUIDE**

This section contains information on installing the HASC code, creating input files, running the code, and using the output files.

### **4.1 Installation**

HASC is written entirely in FORTRAN. The HASC code is currently separated into individual source files per subroutine (\*.f files). Most of the common blocks, excluding VTXCHN subroutines, are contained in separate common block files (\*.cmn files). A listing of the HASC source directory is given in figure 4.1-1. The common block files are attached with "attach \_\_\_\_cmn" statements within the appropriate source files. For some computer platforms it may be easier to gather the source files and common block files into just a few files as done with previous versions of HASC prior to compiling. The makefile used on a Silicon Graphics Indigo 2 platform to compile the HASC code is shown in figure 4.1-2. The -static and -r8 are required compiler options for HASC. Approximately 65 open files are used during a HASC run.

Makefile	freqncy.cmn	plota7.f	set20.cmn	velan.f
acoeff.f	frevor.cmn	plota8.f	set21.cmn	velvor.cmn
aero.f	gauss.f	plotv.f	set22.cmn	version.cmn
ainteg.f	geom.f	pos.f	set23.cmn	vinflu.f
airfyl.f	geometry.f	presr.f	set24.cmn	vlfrc.cmn
amap.f	grphic.cmn	pribdy.f	set25.cmn	vlmdat.cmn
asolve.f	hasc.f	pridmp.f	set3.cmn	vlmt.cmn
asum.f	hasc95*	priflg.cmn	set4.cmn	vlocty.f
asymon.cmn	inpt.f	prilat.f	set5.cmn	vorinf.cmn
bmap.f	inptfl.f	prin.f	set6.cmn	vorlif.f
body.f	input.f	print.cmn	set7.cmn	vorlmt.cmn
boundy.f	integr.f	prisrf.f	set8.cmn	vorsya.f
ccppot.f	interp.f	pristb.f	set9.cmn	vpos.cmn
chngam.f	intgrn.cmn	pritot.f	shape.f	vrlaro.f
chnini.f	intrp1.f	priwnd.f	skin.f	vrlchk.f
closfl.f	intrp2.f	rddiag.f	sline.f	vrlfll.f
cmap.f	intrp3.f	rdew.f	smoocur.f	vrlgeo.f
combin.f	intspn.f	rdrdx.f	sordis.f	vrlmap.f
confor.f	invere.f	rdrdxi.f	sorvel.f	vrlsvy.f
cross.f	invers.f	resetrw.f	spred.f	vrlvar.f
crvfit.f	lergeo.f	reshuf.f	srcvel.f	vseg.f
dfeqkm.f	lifdat.cmn	revflo.f	srffrc.cmn	vtable.f
dnudx.f	lift.f	rowmul.f	sum.f	vtcflg.cmn
dot.f	lsq.f	seprat.f	surtit.cmn	vtxchn.f
dphidt.f	lstdt53.f	set1.cmn	survey.f	vtxchn1.cmn
dtrmnt.f	lstdt7.f	set10.cmn	tail.cmn	vxcfl1.f
dzdnu.f	lstdt8.f	set11.cmn	templ.cmn	vxcfrc.f
f.f	map.f	set12.cmn	temph.cmn	vxcvar.f
fakima.f	mapping.f	set13.cmn	tldnw.f	vxcymx.f
fdpsdr.f	matrx.f	set14.cmn	transn.f	vxxhvi.f
flowopts.cmn	netn.cmn	set15.cmn	umap.f	wash.f
forcep.f	newmake	set16.cmn	uxvel.f	wrew.f
forces.cmn	openfl.f	set17.cmn	vcntr.f	z.f
fpsi.f	plota2.f	set18.cmn	vcntr.f	znorm.f
fpvel.f	plota5.f	set19.cmn	vcntrp.f	
freevr.cmn	plota6.f	set2.cmn	vector.f	

Figure 4.1-1 Listing of HASC Source Directory

```

#
# Makefile for the 'hasc' program
#

HASCOBJ=      acoeff.o      dnudx.o      intrp1.o      plota8.o      smoccur.o\
aero.o        dot.o          intrp2.o      plotv.o        sordis.o      vrlaro.o \
ainteg.o      dphidt.o      intrp3.o      pos.o          sorvel.o      vrlchk.o \
airfyl.o      dtrmnt.o      intspn.o      presr.o        spred.o       vrlfll.o \
amap.o        dzdnu.o       invere.o      pribdy.o       srcvel.o      vrlgeo.o \
asolve.o      f.o           invers.o      pridmp.o       sum.o         vrlmap.o \
asum.o        fakima.o      lergeo.o     prilat.o       survey.o      vrlsvy.o \
bmap.o        fdpsdr.o     lift.o        prin.o         vrlvar.o      wrew.o \
body.o        forcep.o     lsq.o         prisrf.o       tldnw.o       vseg.o \
boundy.o      fpsi.o       lstdt53.o    pristb.o       transn.o      vtable.o \
ccppot.o      fpvel.o      lstdt7.o     pritot.o       umap.o        vtxchn.o \
chngam.o      gauss.o      lstdt8.o     priwnd.o       uxvel.o       vxcfll.o \
chnini.o      geom.o       map.o         rdrdx.o        vcentr.o      vxcfrc.o \
closfl.o      geometry.o   mapping.o    rdrdxi.o       vcntr.o       vxcvar.o \
cmap.o        hasc.o       matrx.o      reshuf.o       vcntrp.o     vxcymx.o \
combin.o      inpt.o       openfl.o     revflo.o       vector.o      vxhvi.o \
confor.o      inptfl.o    plota2.o     sepat.o        velan.o       wash.o \
cross.o       input.o      plota5.o     shape.o        vinflu.o      z.o \
crvfit.o      integr.o     plota6.o     skin.o         vlocty.o      znorm.o \
dfeqkm.o     interp.o     plota7.o     sline.o        vorlif.o      vorsya.o \
resetrw.o    rowmul.o    rdew.o       rddiag.o

IRISLIBS=

ODFLG=  -O2 -r8 -mips2 -Nn16000 -Olimit 5000 -static -w0

LLFLG=  -g

hasc:  ${HASCOBJ}
       f77 ${LLFLG} -o hasc95 ${HASCOBJ}

.f.o:
       f77 ${ODFLG} -c $.f

.c.o :
       cc ${CCFLG} $(INCLUDES) -c $.c

```

Figure 4.1-2 HASC Makefile used on a Silicon Graphics Indigo 2 Platform

## 4.2 Input Description

HASC requires a minimum of two input files as listed below.

- hasc.inp** main input file containing program options, flow conditions, and geometry.
- emprcl.inp** empirical factors for VORLIF, this file is typically not changed by a user.

If any airfoil definition flag (IARFYL) is set to 2 then an additional input file is required.

- airfoil.inp** airfoil leading edge parameters

An additional input file is required for analysis of a forebody in VTXCHN.

- vchn.inp** input file for VTXCHN

Figure 4.2-1 presents the input and output filenames used by HASC. The input files are discussed in this section, while the output files are discussed in section 4.4.

Table 4.2-1 presents an overview of the input parameters for the primary HASC input file **hasc.inp**. New parameters are ALXP, ALZL, XGAP, and SRFTITL, while ISOLV is no longer required. The pitch, roll, and yaw inputs are now on a separate line. All reads are unformatted, therefore additional characters or comments can not follow the numerical values on a line. Several of the parameters have been renamed for easier recognition of data type and meaning. Input cases within a file can no longer be stacked as allowed in previous HASC versions. Comments must be on a line that begins with a \* in column 1. Table 4.2-2 provides the detailed descriptions, graphics, and useful information for creating the HASC input file **hasc.inp**.

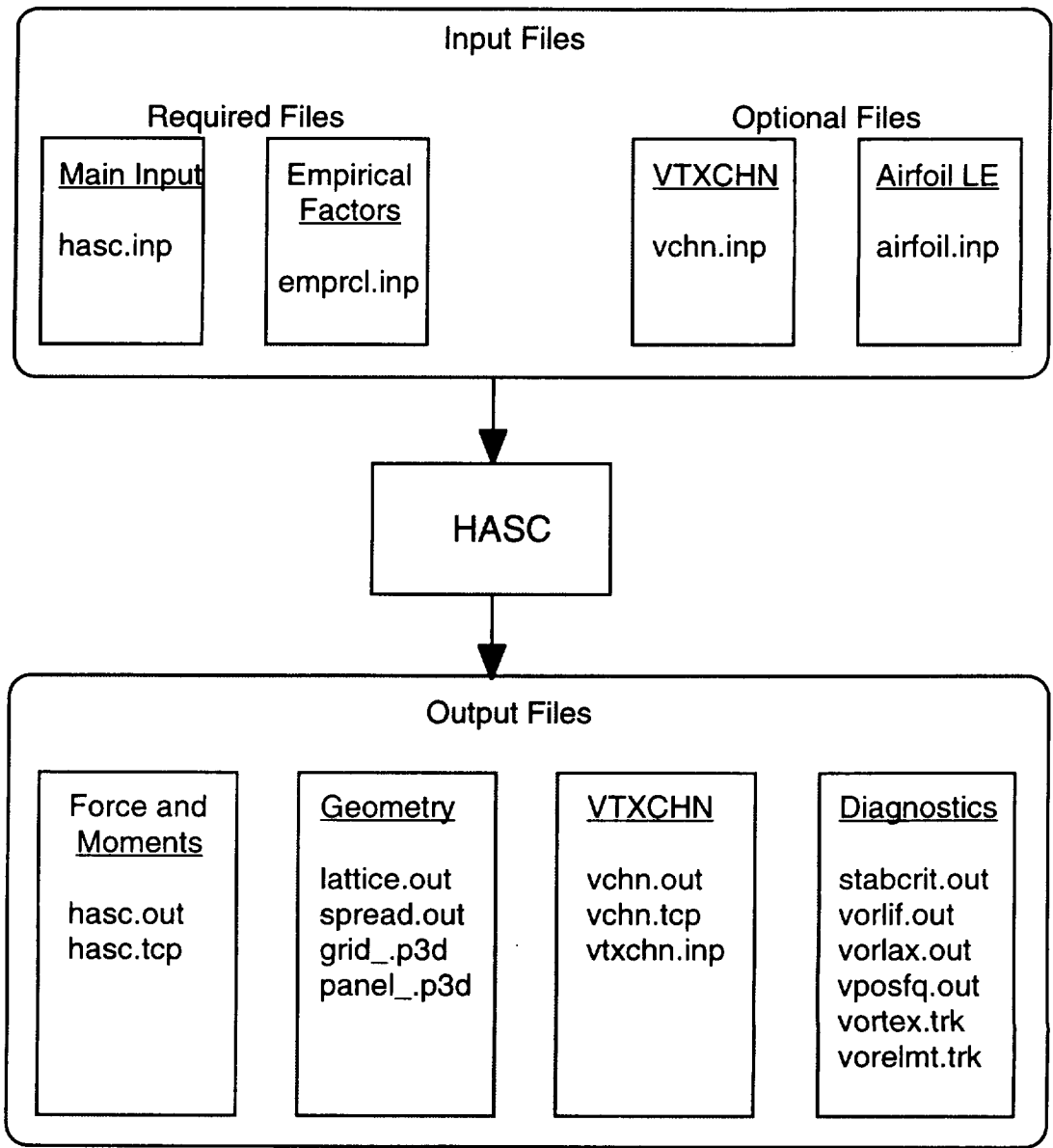


Figure 4.2-1 HASC Input/Output Files

Table 4.2-1 Summary of Parameters in Input File hasc.inp

Note: Parameters beginning with I,J,K,L,M, or N are integers.  
 Parameters JOBTITL and SRFTITL are character variables.  
 All remaining parameters are reals.  
 Parameters are read with unformatted read statements, for example:  
 read(unit,\*) PITCHQ, ROLLQ, YAWQ, VINF  
 Values for all parameters as required must be input.

**Item Variables**

1	JOBTITL						
2	LAX	LAY	HAG	IRSTFLG	NPAN	NSURF	ALXP
3	REY	NMACH	MACH(s)				
4	NALPHA	ALPSTB(s)					
5	NBETA	BETSTB(s)					
6	PITCHQ	ROLLQ	YAWQ	VINF			
7	SREF	CBAR	XREF	ZREF	SPAN		

Repeat items 8 through 16 for each surface.

8	SRFTITL						
9	ISRTYP	LNAPAN	ISYMFLG	ENETAR	FTAIL	ALZL	XGAP

*File vchn.inp is required if ISRTYP = 3.*

Repeat items 10 through 12, and 13 through 16 if required, LNAPN times.

10	X1	Y1	Z1	CORD1	AINC1		
11	X2	Y2	Z2	CORD2	AINC2		
12	ISPNDIV	ICHRDIV	SPC	IARFYL	NAP	IVTXFLG	

*File airfoil.inp is required if IARFYL = 2.*

*Item 13 is required if IARFYL = 1.*

13	TOC1	TOC2	ROC1	ROC2	TLOC1	TLOC2	DELLE1	DELLE2
----	------	------	------	------	-------	-------	--------	--------

*Items 14 through 16 are required only if NAP is > 3.*

14	XAF
15	ZC1
16	ZC2

Table 4.2-2 Descriptions of hasc.inp Input Variables

Item 1 - Job Title

JOBTITL Job identification heading, up to 80 characters on one line.

Item 2 - Program Options

Item 2 describes several of the program options including solution methods, spacing of vortices, ground effect height, and a selected angle of attack for a printout option.

LAX Chordwise or streamwise spacing of vortices.  
0 = cosine spacing  
1 = equal spacing with 1/4, 3/4 chord collocation.  
Note: Cosine spacing is recommended, LAX=0, since it gives more accurate leading edge thrust calculations.

LAY Spanwise spacing of vortices.  
1 = equally spaced  
2 = cosine spaced strips and control points  
LAY = 2 is required to allow calculation of side-edge thrusts. This option, although not recommended, can only be used when running all surfaces in VORLAX. When running VORLIF, LAY must be set to 1.

HAG Height above ground of the moment reference center. Set HAG = 0 for no ground effect. Ground effect is computed by the method of images. Note that this distance often varies with angle of attack during a wind tunnel angle of attack sweep.

IRSTFLG Restart status.  
0 = no restart to follow  
1 = initial run of restart series, file restart.inp is written  
2 = restarted run, requires restart.inp file  
Note: This restart option is not effective with VTXCHN calculations.

NPAN Total number of panels for entire configuration.

NSURF Total number of surfaces defining configuration. Limit  $NSURF \leq 20$ .

ALXP Selected angle of attack, as described below, for printing information to unit 100.

HASC includes an improved routine to predict the final vortex burst. A reverse flow along the free vortex axis is computed. To accomplish this, HASC computes the effect of vortex elements shed from the leading edge on the free vortex axial velocity. Only the elements that create negative circulation are included in the calculation. For one selected angle of attack the track or position of these elements is written to unit 100 (file vorelmt.trk). This selected angle of attack is ALXP.



### Item 3 - Reynolds Number and Mach Array

Item 3 specifies the Reynolds number based on CBAR and the array of desired Mach numbers. A unique Reynolds number can not be input for each Mach.

REY            Freestream Reynolds number based on CBAR and in consistent units with CBAR. If REY is input as 0.0 then a Reynolds number is calculated at 15,000 ft pressure altitude (1962 U.S. standard atmosphere) at the input Mach number and for the appropriate CBAR (assumed to be in feet). If this default calculation is used, then all input dimensions must be in feet.

NMACH        Number of Mach numbers to be analyzed. Limit  $NMACH \leq 6$ .

MACH         List of Mach numbers to be analyzed (NMACH values).

#### Item 4 - Angle of Attack Array

Item 4 contains the initial angle of attack values to be analyzed. A total of 30 angles of attack, including values added within HASC as described below, can be evaluated.

NALPHA      Number of angles of attack to be analyzed. Limit  $NALPHA \leq 30$ .

ALPSTB      List of angles of attack (NALPHA values).

When running HASC to get vortex effects with VORLIF (surface type 1 & 2), some caution is required in specifying the input angles of attack. A history of the vortex breakdown is included in VORLIF. As angle of attack increases and vortex breakdown occurs, the breakdown will continue to occur at the wing stations where it occurred at lower angles. Also, the breakdown will continue to move inboard as the angle of attack increases. This means that your lowest input angle should not indicate breakdown. If it does, then you should rerun the code starting at a lower angle. You can tell if the breakdown has occurred by checking the output file stabcrit.out. Look for the ratio of laminar vortex diameter to turbulent vortex diameter, RADR. If RADR is less than 1.00 then breakdown has occurred. Note: Cycle 2 and 3 results are given in stabcrit.out. RADR will be less than 1.00 only in the 3rd cycle which is the second or last part of the output for each surface.

### Item 5 - Angle of Sideslip Array

Item 5 is the set of angles of sideslip to be analyzed. The angles of attack listed in item 4 are analyzed for each sideslip angle listed in item 5.

- NBETA      Number of sideslip angles to be analyzed. Limit  $NBETA \leq 3$ . If only zero sideslip angle is requested set NBETA to 1 and set BETSTB = 0.
- BETSTB      List of stability axis sideslip angles following the sign convention of + sideslip is wind in pilot's right ear.(NBETA values).

### Item 6 - Rates

Item 6 lists the steady-state rate derivatives and a nondimensionalizing parameter VINF.

- PITCHQ      Pitch rate in degrees / second (+ for nose up).
- ROLLQ      Roll rate in degrees / second (+ for right wing down).
- YAWQ      Yaw rate in degrees / second (+ nose right).
- VINF      Reference free stream velocity. This parameter is only used when any of the angular rates is different from zero. It is used in the computation of the equivalent flow angle. For non-zero PITCHQ set  $VINF = C_{BAR}/2$ . For non-zero ROLLQ or YAWQ set  $VINF = WSPAN/2$ .
- VORLIF surfaces can be analyzed with non-zero values of PITCHQ, ROLLQ, and YAWQ.

### Item 7 - Reference Quantity Card

Item 7 contains values used to specify the reference geometry parameters. These references must be in consistent units with the remainder of the geometry parameters.

SREF        Reference area for force and moment coefficients.

CBAR        Pitching moment coefficient reference length, usually the mean aerodynamic chord length.

XREF        X-coordinate of moment reference point.

ZREF        Z-coordinate of moment reference point.

WSPAN      Total wing span.

Items 8 - 16 are repeated as a group for each surface.

### Item 8 - Surface Title

SRFTITL    Surface identification heading, up to 30 characters on one line.

## Surface Definitions

When analyzing an aircraft configuration in HASC, the configuration must first be divided into surfaces, or major components such as fuselage, wing, and tail. Solution options (VORLAX, VORLIF, or VTXCHN) apply to an entire surface as shown in figure 4.2-2. These surfaces must then be divided into panels to define breaks in the leading edge, trailing edge, or alignment with other fore/aft surfaces. Where the wing sweep varies across the span, the curvature should be defined well by using several panels. Vortex breakdown is significantly affected by the geometry. The vortex becomes more stable with increasing sweep and less stable with decreasing sweep. Wing strake panels must be included with the wing to correctly model the vortex flow. The entire wing and strake should be modeled as one surface with multiple panels.

The panels are then divided into sub-panels within the program based on input parameters ISPNDIV and ICHRDIV as shown in figure 4.2-3. In a HASC input file hasc.inp the order that the surfaces are listed, and panels within a surface, must follow what is shown in figure 4.2-3. Forward lifting surfaces are listed first (left then right side), followed by aft lifting surfaces (left then right side).

Due to the basic method of HASC being an enhanced vortex lattice method, some configurations may be difficult to represent accurately. For example any panel edge can have only one height (Z). Trailing edge and leading edge heights of this edge are represented only by incidence input (AINC).

A lifting surface (ISRTYP 1 or 2) can not have a panel with an exposed 90 degree edge (parallel to the freestream) anywhere except at the wing tip. Satisfying this requirement may require slight modifications to the geometry for some configurations.

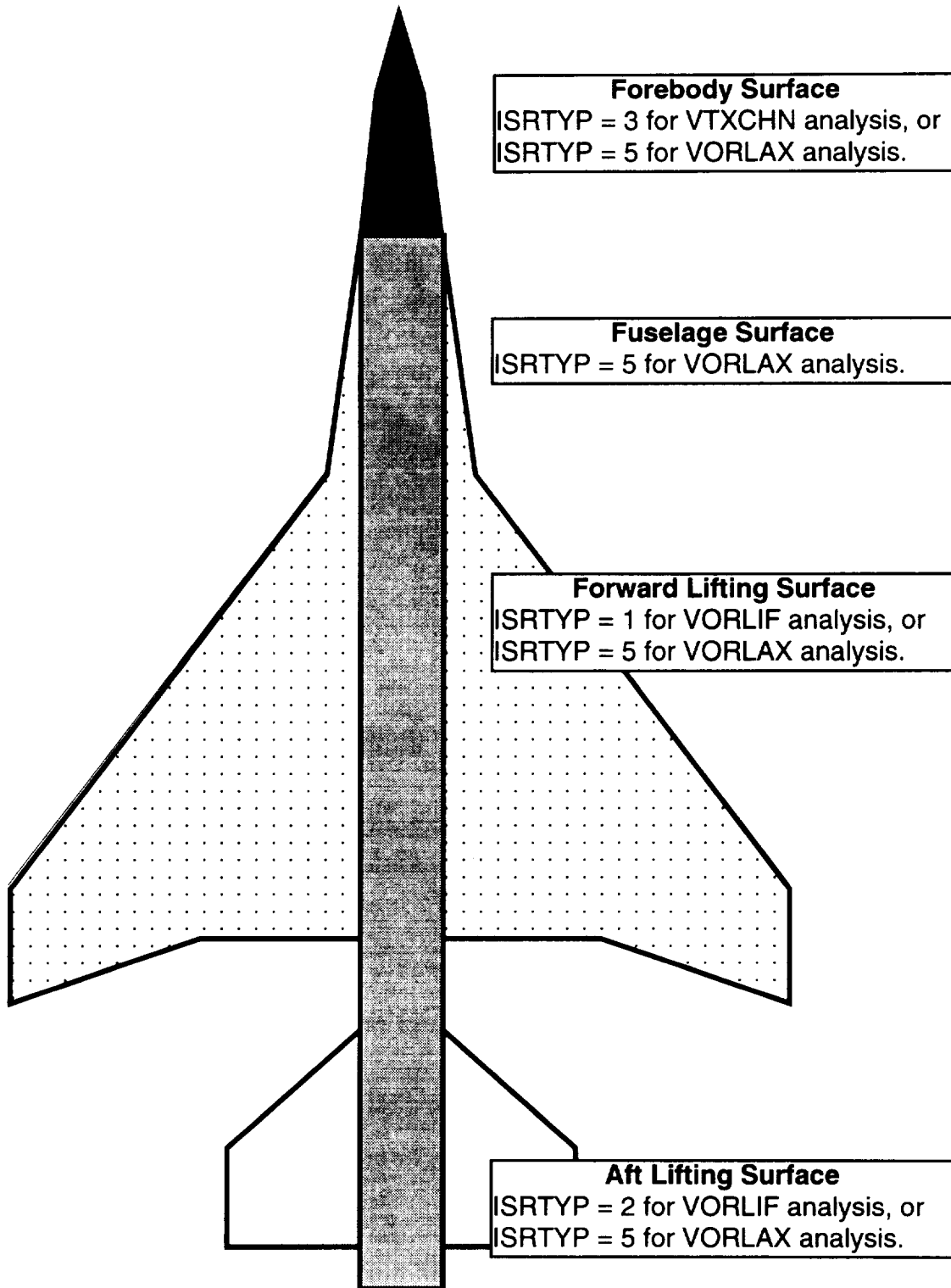


Figure 4.2-2 Surface Definitions and Solution Options

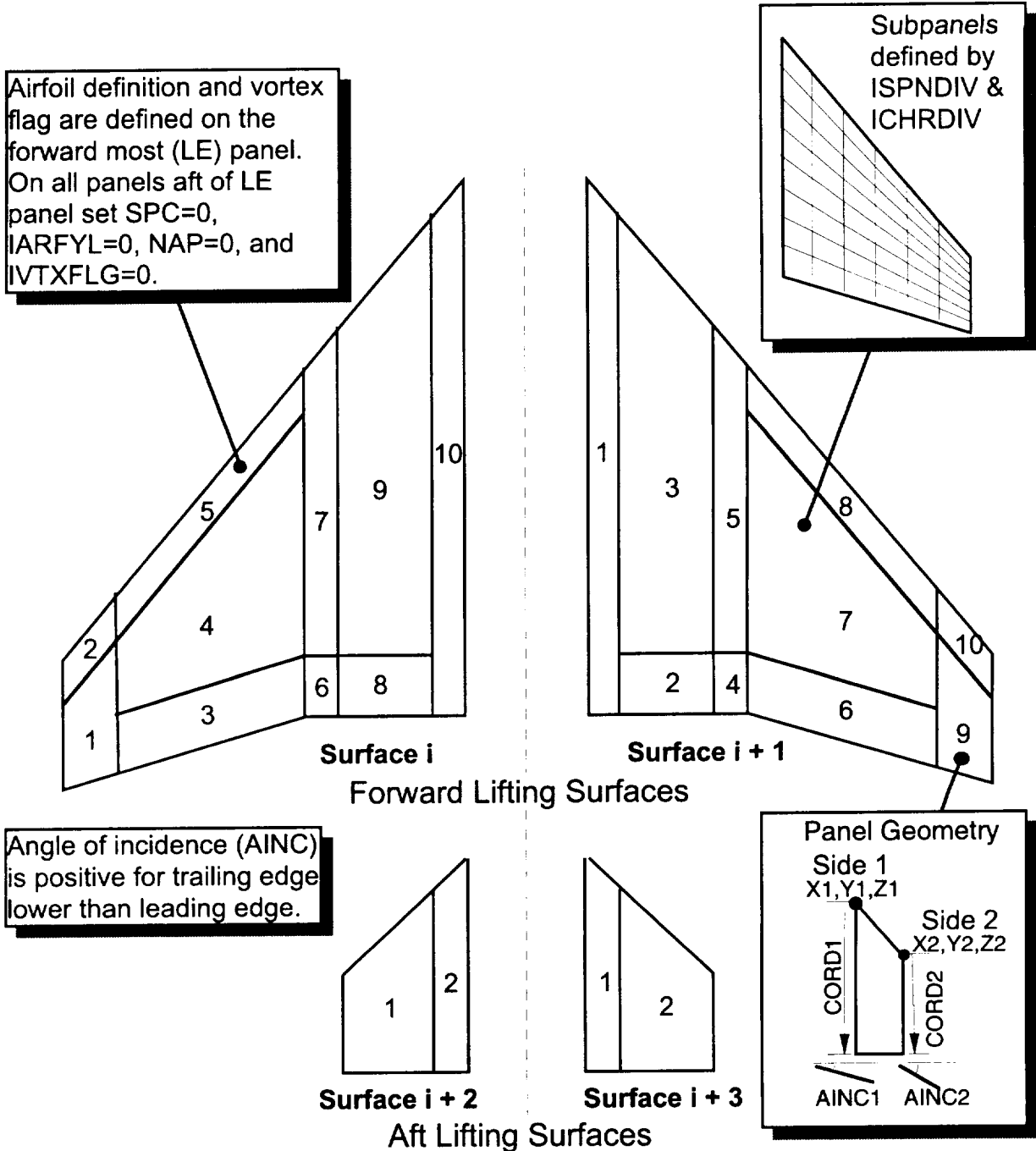


Figure 4.2-3 Panel Definitions and Input Order Requirements

## Item 9 - Surface Information (continued)

**ISRTYP** Specifies the type of solution requested for the current surface.

- 1 = VORLIF, use for aft lifting surface (tail, or wing behind a canard)
- 2 = VORLIF, use for forward, or only, lifting surface (canard, or wing)
- 3 = VTXCHN, used for forebody (requires input file vchn.inp). All forebody panels, both planform and sideview, should be listed as one surfaces. Only the forces and moments from VTXCHN (not from VORLAX/VORLIF) are included in the final results when ISRTYP = 3.
- 4 = VORLAX, use for interference surfaces. This options is useful for connecting surfaces where loads on the connecting surface are not to be included in the total configuration loads.
- 5 = VORLAX, use for non-lifting surfaces (fuselage surfaces) or for lifting surfaces where a VORLIF solution is not desired.

Note: Execution times and accuracy of solution varies strongly on the value of ISRTYP. It is recommended that all surfaces initially be run as type 5 (VORLAX calculations only) to verify input modeling. Then depending on time available and accuracy required, VORLIF and VTCHN options can be used.

**LNPAN** Number of panels that make up the current surface.  
Limit  $LNPAN \leq 20$ .

**ISYMFLG** Surface symmetry flag.

- 0 = no mirror image of surface requested
- 1 = mirror image of surface about X-Z axis. Use this option only with symmetric flow conditions (zero beta) and all VORLAX surfaces.

**ENETAR** Leading edge flap roundness. This parameter is used for VORLIF surfaces only. ENETAR specifies the fraction of the leading edge flap that is rounded at the flap knee with a value of from 0. to 1. This is used to position the vortex when a leading edge flap is employed. If no flap is present, a value of 0. should be input.



- FTAIL** Tail moment arm used for VORLIF aft lifting surfaces (ISRTYP=1). FTAIL is the distance from the forward surface .25 MAC to the trailing surface .25 MAC normalized by CBAR from item 7. FTAIL is a positive number.
- ALZL** Estimated angle of attack for zero lift. ALZL is used only for VORLIF surfaces. The value of ALZL as compared to the original angle of attack listing in item 4 is critical. HASC will modify the initial list of requested angles of attack in order to place the angle of attack for zero lift within a certain range. To minimize the number of additional angles added by HASC, If even numbers are used in the initial angle of attack listing, then use an even ALZL value. If odd numbers are used in the initial angle of attack listing, then use an odd ALZL value.
- XGAP** XGAP can be set to denote a gap between the root chord and the fuselage (unporting). If this gap is actually on the airplane, input 1.0. For no gap input 0.0. Often this gap is caused by a deflection of the surface that unports the root-fuselage junction. XGAP modifies a correction for lift carry-over across the junction. The term applied only to surfaces analyzed in VORLIF.

### Item 10 - Side One Panel Geometry

- X1 X or longitudinal coordinate of the leading edge of the first (left or port side) of a panel.
- Y1 Y or lateral coordinate of the leading edge of the first side of a panel.
- Z1 Z or vertical coordinate of the leading edge of the first side of a panel.
- CORD1 Chord length of the first side of a panel measured from X1, Y1, Z1 in the positive X direction and parallel to the X axis. Note: CORD1  $\neq$  0.0.
- AINC1 Incidence angle of the first panel side in degrees. Sign convention follows the right hand rule about an axis running from panel side one to panel side two: + = trailing edge down. This parameter is used to define the wing twist and/or control surface deflection for the left side of a panel. The control surface deflection (measured streamwise) must be added to the basic wing twist to determine the value for AINC1.

### Item 11 - Side Two Panel Geometry

- X2 X or longitudinal coordinate of the leading edge of the second (right or starboard side) of a panel.
- Y2 Y or lateral coordinate of the leading edge of the 2nd side of a panel.
- Z2 Z or vertical coordinate of the leading edge of the 2nd side of a panel.
- CORD2 Chord length of the second side of a panel measured from X2, Y2, Z2 in the positive X direction and parallel to the X axis. Note: CORD2  $\neq$  0.
- AINC2 Incidence angle of the second panel side in degrees. This parameter is used to define the wing twist and/or control surface deflection for the right side of a panel.

A cambered, twisted airfoil must be decomposed as shown in figure 4.2-4. Twist angle is entered using AINC1 and AINC2 parameters. The camber is determined after removing the twist. Camber parameters ZC1 (side one) and ZC2 (side two) are computed as percent  $dY/\text{chord}$  for NAP  $X/\text{chord}$  stations. Additional description of the camber parameters XAF, ZC1, and ZC2 is provided in the description of items 14 through 16.

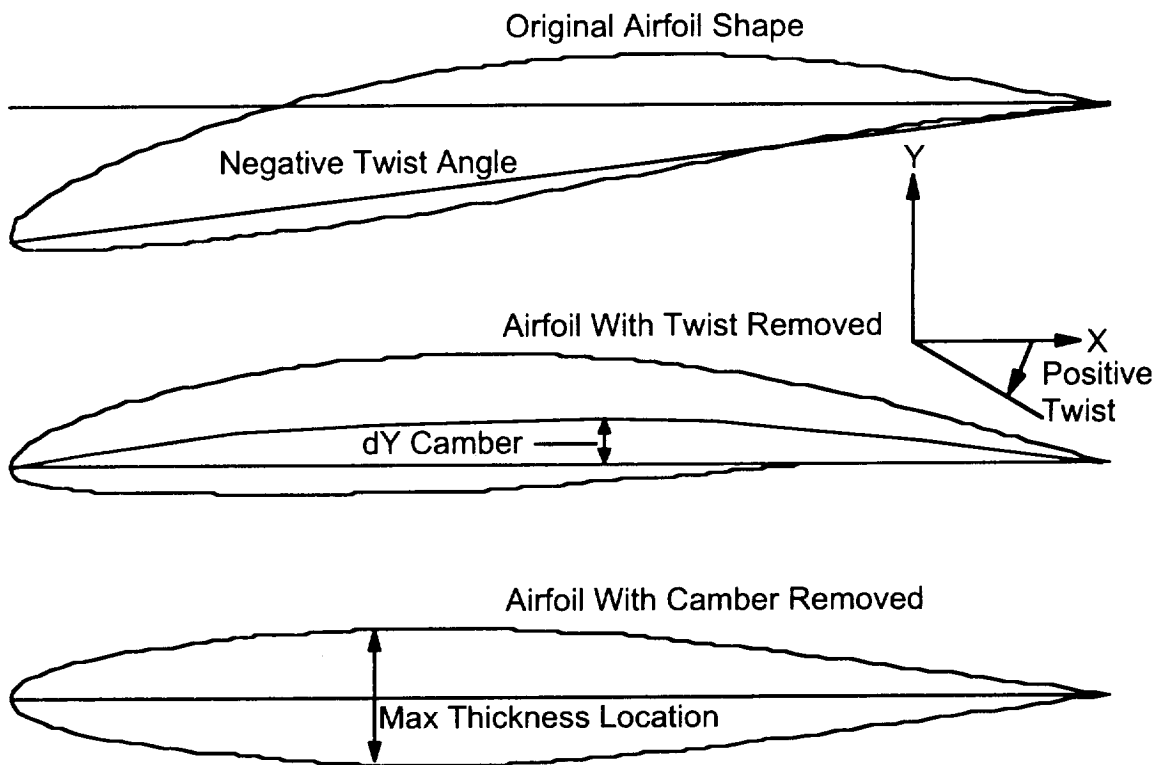


Figure 4.2-4 Airfoil Decomposition for HASC Input

## Item 12 - Panel Options

The density of horseshoe vortices represented by ISPNDIV x ICHRDIV of are spaced according to the LAY and LAX parameters.

ISPNDIV      Number of spanwise strips on panel.

Note:  $ISPNDIV \leq 101$

The number of spanwise strips can be critical to achieving good results when analyzing a surface in VORLIF. To get good vortex stability a total of at least 6 spanwise stations, preferably more, should be used on the surface generating the vortex. If a second vortex is generated outboard (from setting IVTXFLG = 1) then an additional 6 or more spanwise stations should be used.

Some effect on the aerodynamic coefficients from the number of spanwise stations may occur when the vortex breaks down. Currently the code will not allow the initial vortex transition to occur inboard of the fourth spanwise station for each vortex. The reason for this is that in the starting process there are numerical instabilities, and it takes 3 to 4 stations for this to settle. This means that the effect of the turbulent vortex on the loads may be under predicted. This anomaly may be corrected by increasing the number of spanwise stations. Alternatively it may be corrected by repaneling of the surface. Make a small panel at the vortex apex so that the first four stations of the vortex are confined to a small part of the span. Large jumps in the spanwise spacing should be avoided from panel to panel.

ICHRDIV      Number of chordwise vortices on each spanwise strip.  
Note: ICHRDIV < 51

The ideal number of chordwise elements depends on the camber and location of the panel. For panels where the leading edge thrust is not important, such as aft fuselage panels with no camber, 4 to 6 elements should be sufficient. Where accurate leading edge thrust is required, such as for wings and strakes, six to eight elements are required.

Several techniques can affect the speed of a HASC run. All are basically a trade off of level of analysis or accuracy for run time. A significant contributor to the run time is the iterative solution of the vortex lattice circulation strength matrix. There are several ways to reduce the time required for a solution.

1.      The most obvious is to decrease the number of horseshoe vortices (IPSN DIV x ICHRDIV). The VORLIF module requires a fair number of spanwise stations for accuracy so care should be exercised too avoid reducing IPSNDIV to low. Section 6 contains plots showing sensitivity of spanwise and chordwise spacing.

2.      Another method is to vary ISRTYP. If tail surfaces are defined with ISRTYP = 1, then a separate wing-off run is performed. Using ISRTYP = 5 sacrifices a vortex stability analysis on the tail but speeds up the run time. In a similar manner, a forebody surface with ISRTYP = 3 results in a forebody-off run. Using ISRTYP = 5 for the forebody will also decrease the run time.

A summary of total wall-clock times for various HASC runs is provided in table 4.2-3. Several examples showing how the execution times vary according to the number of horseshoe vortices and ISRTYP are included in the table.

Table 4.2-3 Summary of HASC Run Times on a SG Indigo 2

Note:

- o Clock times are from running on a dedicated Silicon Graphics Indigo 2 with a 150Mhz R4400 processor and 192M RAM.
- o Each run was for 19 angles of attack at 1 Mach number and 1 angle of sideslip.

Tailless Fighter Configuration

	horseshoe <u>vortices</u>	wall-clock <u>time(sec.)</u>
All surfaces in VORLIF	192	52
All surfaces in VORLIF	224	57
All surfaces in VORLIF	352	104
All surfaces in VORLAX	224	8

Falcon 21 Configuration

	horseshoe <u>vortices</u>	wall-clock <u>time(sec.)</u>
VORLIF wing, VTXCHN forebody	320	102
VORLIF wing, VORLAX forebody	320	83
All surfaces in VORLAX	320	12
All surfaces in VORLAX with TE flap	644	57

F-16XL Configuration

	horseshoe <u>vortices</u>	wall-clock <u>time(sec.)</u>
VORLIF wing, VTXCHN forebody	496	240
VORLIF wing, VORLAX forebody	496	201
All surfaces in VORLAX	496	32

F-16 Configuration

	horseshoe <u>vortices</u>	wall-clock <u>time(sec.)</u>
VORLIF wing & HT, VTXCHN forebody	744	468
VORLIF wing & HT, VORLAX forebody	744	396
VORLIF wing, VORLAX forebody & HT	744	326
All surfaces in VORLAX	744	72

Model 200 Configuration

	horseshoe <u>vortices</u>	wall-clock <u>time(sec.)</u>
VORLIF wing & canard	382	107
All surfaces in VORLAX	382	14

SPC            Leading edge suction multiplier.  
0.0 = no suction  
1.0 = 100% suction, values in between 0.0 and 1.0 may be input  
Negative value = rotates thrust using Polhamus suction analogy.  
All lifting surfaces analyzed by VORLIF (ISRTYP 1 or 2) should have SPC values set to 1.0 on all leading edge panels. On panels aft of the leading edge SPC should be 0.0 when running VORLAX or VORLIF . Partial suction values (between 0 and 1) may be utilized for VORLAX surfaces. See section 6 for a sensitivity plots of different values of SPC.

IARFYL        Airfoil definition  
0 = default to NACA 64A006 series  
1 = input known thickness and radius on following item  
2 = blunt or wedge airfoil, required additional input file airfoil.inp

It is imperative that the airfoils, camber, and twist be input accurately. Vortex breakdown is very sensitive to these geometric entities. These values affect the free vortex circulation gradient. HASC takes into account airfoil thickness and leading edge radius. It does this to calculate residual thrust and to proportion the vortex lift. HASC can handle a wide range of airfoils. The most basic is the NACA 6 series using Carlson's method. For these airfoils, if thickness and radius are known, input these values directly as item 13 in input file hasc.inp. Non-standard airfoils can be input through the optional airfoil definition file airfoil.inp. An effective radius and thickness is obtained for these non-standard airfoils by a method that uses the integral of the area of the cross section. Set IARFYL to 0 for all non leading edge panels.

Item 13 - Panel Leading Edge and Thickness Definition, omit if IARFYL  $\neq$  1.

TOC1	Max section thickness for panel side 1 as a fraction of the local chord.
TOC2	Max section thickness for panel side 2 as a fraction of the local chord.
ROC1	Effective LE radius for panel side 1 as a fraction of the local chord.
ROC2	Effective LE radius for panel side 2 as a fraction of the local chord.
TLOC1	Chordwise location of maximum section thickness value (TOC1) on panel side 1 as a fraction of the local chord.
TLOC2	Chordwise location of the maximum section thickness value (TOC2) on panel side 2 as a fraction of the local chord.
DELLE1	Slope of upper surface leading edge between end of the semicircle defined by the leading edge radius value and the maximum thickness point measured in degrees for panel side 1.
DELLE2	Slope of upper surface leading edge between end of the semicircle defined by the leading edge radius value and the maximum thickness point measured in degrees for panel side 2.
NAP	Number of stations along the panel chord at which camber is defined. NAP must be greater than 3 to specify camber. If camber is defined then items 14 through 16 must follow.
IVTXFLG	Vortex Flag. 1 = a vortex is initiated on the inboard section of the panel. 0 = no new vortex is initiated. Set IVTXFLG = 1 on the most inboard LE panel of a VORLIF surface and where wing breaks occur or other large changes in wing geometry. IVTXFLG should be 0 for panels aft of the leading edge. This parameter is only used in VORLIF. Section 6 presents plots showing the sensitivity to this parameter.



Parameters in item 13 are illustrated in figure 4.2-5.

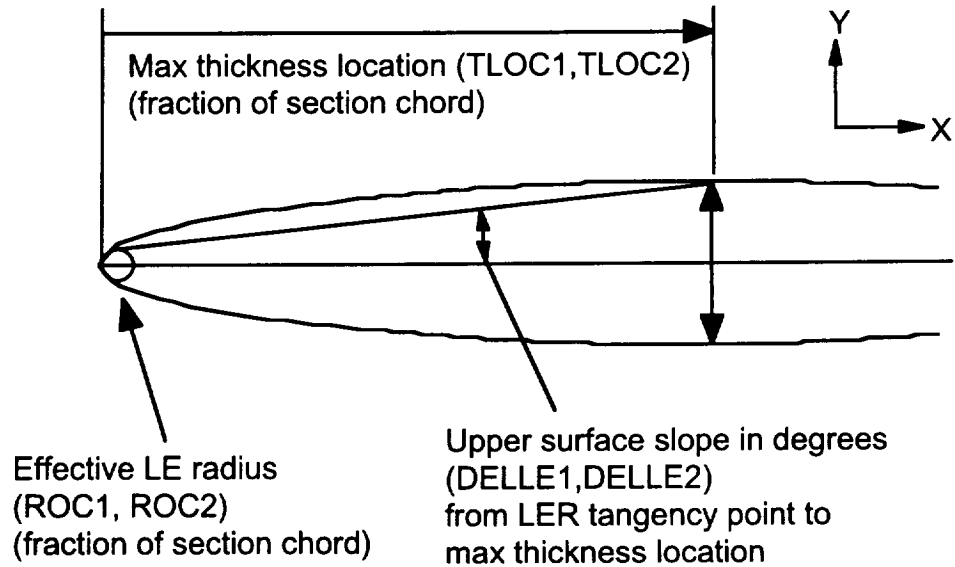


Figure 4.2-5 Definitions of Airfoil Leading Edge Parameters

If IARFYL = 0 the following defaults are set.

TOC1, TOC2	= .06 (or 6%)
ROC1, ROC2	= .00246
TLOC1, TLOC2	= .40 (or 40%)
DELLE1, DELLE2	= .06874

*Items 14 through 16 (camber definition) are only required where NAP > 3.*

Item 14 - Camber Chord Location

**XAF** Percent chord values at which camber coordinates (ZC1 & ZC2) will be defined (NAP values). Arbitrary spacing may be used to define the camber, however the same spacing applies for both sides of the panel. The first XAF value must be 0.0 and the last value must be 100. HASC uses a cubic spline to connect the camber ordinates. To input a "kink" for a flap deflection, enter a negative XAF value at the appropriate location. For example, the following input for XAF places a kink at the 75% chord station (0., 25., -75., 100.). Although flap deflections can be input following this method, the preferred method is to use the AINC1 and AINC2 parameters to represent a deflected panel. The following is a section from a HASC input deck showing the correct method of entering the camber items 14 through 16.

```

*ISPNDIV  ICHRDIV  SPC      IARFYL  NAP      IVTXFLG
2          8        1.0      2        23       0
*SECTION CAMBER LOCATIONS (XAF) - X LOCATIONS (%), ITEM 14
0.00      1.00      2.50      5.00      10.00     15.00     20.00     25.00
30.00     35.00     40.00     45.00     50.00     55.00     60.00     65.00
70.00     75.00     80.00     85.00     90.00     95.00     100.00
*SECTION CAMBER DEFINITION (ZC1) - SIDE1 VALUES (%), ITEM 15
0.00      0.318     0.589     0.824     0.974     0.934     0.879     0.824
0.768     0.713     0.658     0.603     0.548     0.493     0.438     0.383
0.327     0.275     0.220     0.162     0.107     0.052     0.000
*SECTION CAMBER DEFINITION (ZC2) - SIDE2 VALUES (%), ITEM 16
0.000     0.379     0.757     1.180     1.648     1.866     1.919     1.877
1.766     1.644     1.513     1.387     1.264     1.138     1.007     0.881
0.755     0.632     0.502     0.375     0.252     0.122     0.000

```

Item 15 - Side One Camber Ordinates

**ZC1** Side 1 camber ordinates in percent panel side 1 chord corresponding to the XAF stations. Enter 10% chord as 10.0, not 0.1.

Item 16 - Side Two Camber Ordinates

**ZC2** Side 2 camber ordinates in percent panel side 2 chord corresponding to the XAF stations. Enter 10% chord as 10.0, not 0.1.

## Description of Optional Input File airfoil.inp

The optional airfoil file airfoil.inp must be used if IARFYL = 2. The airfoil definition within this file must be for only those panels within hasc.inp that have IARFYL set to 2. Figure 4.2-6 illustrates the parameters required in this file. Table 4.2-4 describes these parameters in more detail.

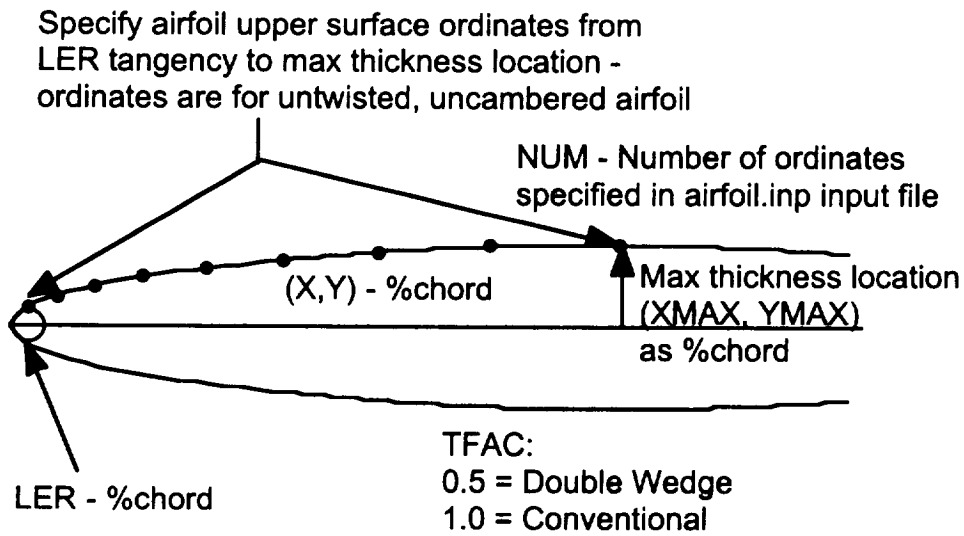


Figure 4.2-6 Definitions of Airfoil File airfoil.inp Parameters

Table 4.2-4 Description of Parameters in Input File airfoil.inp

Item 1 - Side One Airfoil Definition

LER1	Leading edge radius in % chord.
XMAX1	X location of maximum thickness in % chord.
YMAX1	Y ordinate of maximum thickness measured from chord reference line (1/2 of actual thickness from lower to upper surface) in % chord.
NUM1	Number of X, Y coordinates input to define airfoil upper surface.
TFAC1	Airfoil type factor. 0.5 = double wedge airfoil, use for airfoils with surface slope discontinuities 1.0 = conventional airfoil, use for smooth airfoils

Item 2 - Side Two Airfoil Definition

LER2	Leading edge radius in % chord.
XMAX2	X location of maximum thickness in % chord.
YMAX2	Y ordinate of maximum thickness measured from chord reference line (1/2 of actual thickness from lower to upper surface) in % chord.
NUM2	Number of X, Y coordinates input to define airfoil.
TFAC2	Airfoil type factor. 0.5 = double wedge airfoil, use for airfoils with surface slope discontinuities 1.0 = conventional airfoil, use for smooth airfoils

### Item 3 - Upper Surface Coordinates

NUM coordinates starting just aft of the leading edge radius and progressing back over the top to the maximum thickness location. Input the upper surface of the airfoil only.

X            X ordinate of point on airfoil in percent local chord.

Y            Y ordinate of point on airfoil in percent local chord.

## Description of Empirical Factor File

Table 4.2-5 presents a listing of the empirical factors contained within the input file emprcl.inp. A short description of the factors is provided in table 4.2-6. These factors, primarily used within the vorlif.f subroutine, are generally not altered by the user. Additional research, validation, and implementation information is required prior to modifying these factors.

Table 4.2-5 Summary of Empirical Factor File emprcl.inp

### Line Empirical Factors

1	FS	FV	FG	FPPR	FKRN	VFIX	VFFACT	RFAC
2	CTFACT	FDNT	CBFACT	FMG	VABR	TFC	FAL	FSPAN
3	XVBR	VOTRA	FTINC	BLAMX	FMLV	VMUVL	RLEND	VISCS
4	GCPDL	MVLFAC	DPROW	CPTT	ACPT	FVAG	FKSTL	BOTOM
5	RLORT	FMXACV	FMXACB	DRAGF	DRAGP	CBFACN	CLTFAC	VOTRA2
6	RFIN	RFOU	RALNOR	NNAG				

Note: These factors are read with unformatted read statements.

Table 4.2-6 Description of the Empirical Factors in emprcl.inp

Line 1

FS = 1.0	Factor to correct the bound element lift coefficient. Based on experimental laser velocimeter tests.
FV = 0.77	Factor to correct the free vortex lift coefficient. Based on experimental laser velocimeter tests.
FG = 1.0	Correction factor for vortex position.
FPPR = 0.08	Integral of circulation function across a laminar vortex core. Based on theory with corroboration by laser velocimeter experiments.
FKRN = 0.15	Empirical factor for vortex height. Based on several delta wing tests. Used in defining the effective circular space that contains the vortex. This space remains in a position protected from the force of relative wind.
VFIX = 0.8	Empirical factor to change the critical pressure gradient. This is a temporary fix to account for the effect of merging vortices.
VFFACT = 1.0	Empirical factor to change the critical vortex burst velocity. This is a temporary fix to account for the effect of merging vortices.
RFACT = .4	Factor used in determining turbulent vortex size. Based on theory and experiments by Uberoi (reference 7).

Line 2

CTFACT=1000.	Critical pressure gradient along vortex axis for turbulent vortex. Currently set at 1000.0 so that turbulent vortex does not breakdown due to critical pressure gradient.
FDNT = 3.0	Currently not used.
CBFACT = .50	Critical laminar vortex pressure gradient.
FMG = .25	Empirical correction to vortex lift moment arm. This makes the vortex lift aerodynamic center at 25% of the distance from the wing leading edge to the center of the vortex.
VABR = -0.58	Axial velocity for which the turbulent vortex burst. Currently the axial velocity is the main breakdown criterion for the turbulent vortex since the turbulent vortex is not allowed to breakdown due to critical pressure gradient.
TFC = 0.8	Factor applied to loss in lift due to turbulent vortex crossing the trailing edge of the wing.
FAL = .2	Factor to account for effect of vortex strength on its position.
FSPAN = .23	Correction to the wing span affected by the turbulent vortex.



Line 3

XVBR = .1	Fraction of wing span along the vortex axis and aft of the wing trailing edge where burst of the turbulent vortex begins to affect the wing loads.
VOTRA = 0.5	Factor that makes the vortex burst accelerate towards the vortex origin. (See RLORT & VORTR2.) Smaller values will increase the acceleration.
FTINC = 10.0	Factor to correct the empirical profile drag when there is a finite value of sideslip.
BLAMX = 0.5	Taper ratio of the aft lifting surface. Small changes in BLAMX will have insignificant effect on the total forces and moments.
FMLV = 0.0	Currently not used.
VMUVL = 1.0	Currently not used.
RLEND = 0.165	Factor for correcting the vortex self induced velocity caused by the spiraling core of the turbulent vortex.
VISCS = 1.1	Factor used in an approximate correction for viscous effects on circulation growth after positive vorticity is no longer fed to the vortex.

Line 4

GCPDL = 0.0	Factor used in preventing vortex breakdown if pressure gradient downstream of the one being evaluated is less than the evaluated one. The evaluated vortex pressure gradient is corrected to a value less than the critical value.
MVLFAC = 3.0	Not used currently.
DPROW = .6	Factor used to correct theoretical vortex height.
CPTT = 1.0	Factor used on the total pressure loss during sideslip.
ACPT = 0.9	Critical pressure gradient for wings with sweep less than or equal to 45 degrees. ACPT is used only when the succeeding pressure gradient is less than the one being evaluated.
FVAG = .30	Factor used in averaging the vortex core velocity.
FKSTL = 1.0	Factor used in calculating the aerodynamic coefficients over the stalled portion of the wing; i.e., sections affected by turbulent vortex burst.
BOTOM = 0.63	Factor used in curve fitting for the change in aerodynamic center caused by the turbulent vortex crossing trailing edge.

Line 5

RLORT = .70	Factor that makes the acceleration of the vortex burst towards the vortex origin change at 70% of the vortex span. This is done by changing the value of the empirical constant, VOTRA to VORTRA2.
FMXACV = .32	Factor used in curve fitting for the change in vortex lift (leading-edge vortex shedding) aerodynamic center; i.e., the change caused by the turbulent vortex crossing the trailing edge.
FMXACB = .10	Factor used in curve fitting for the change in bound lift (trailing-edge vortex shedding) aerodynamic center; i.e., the change caused by the turbulent vortex crossing the trailing edge.
DRAGF = .025	Factor used in the profile drag term.
DRAGP = 1.0	Factor used in the profile drag term.
CBFACN = 0.40	Critical pressure gradient for laminar vortex when critical helix angle is reached.
CLTFAC = 1.0	Factor used in equation that calculates the analytical lift coefficient to compare with lift coefficients obtained by integrating wing pressures.
VOTRA2 = 1.0	See RLORT.

Line 6

- RFIN = 0.1      Factor that determines the amount of wing span affected by the bursted turbulent vortex when the burst is still downstream of the wing trailing edge.
- RFOU = 0.70      Factor that determines the amount of wing span affected by the bursted turbulent vortex when the burst is upstream of the wing trailing edge. This affects the post stall lift, drag, and pitching moment. It appears this factor may be a little high, but more test data for small wings in large tunnels is needed before making changes.
- RALNOR = 1.5      Factor to limit the height of the free vortex when conditions such as yaw rate or sideslip causes the free vortex to move ahead of the wing leading edge.
- NNAG = 6      Initial number of the angle of attack values listed in the input angle of attack array in input file hasc.inp for determining the angle to use for computing the lift curve slope.

## Description of Input File vchn.inp

An overview of all the parameters for a complete VTXCHN input file is given in table 4.2-7. Descriptions of the parameters are provided in table 4.2-8. When analyzing just a forebody shape in VTXCHN independent of the rest of HASC (VORLAX & VORLIF) then use tables 4.2-7 and 4.2-8. To run VTXCHN independent (stand-alone) from the remainder of HASC place "VTXCHN ONLY" in the top most line of the hasc.inp file. This form of the vchn.inp file is called the complete form. If a forebody surface is to be analyzed as part of an airplane configuration by setting ISRTYP = 3 in the hasc.inp file then use the information in tables 4.2-9 and 4.2-10. This file contains fewer parameters as many of the VTXCHN parameters are computed within HASC prior to calling VTXCHN. This form of the vchn.inp file is called the condensed form. HASC writes a complete VTXCHN input file (vtxchn.inp) based on information from hasc.inp and vchn.inp. This vtxchn.inp is then submitted to VTXCHN automatically by HASC. The vtxchn.inp file is saved if the user wishes to check the input file executed by VTXCHN.

Lines with a \* in column one are treated as comment lines. Parameters are read with unformatted read statements. Values for all parameters as required must be input.

Table 4.2-7 Summary of Parameters in Forebody File vchn.inp (full)

<u>Item</u>	<u>Variables</u>							
1	NCIR	NCF	ISYM	NBLSEP	NSEPR	NDFUS	NDPHI -	
	INP	NXFV	NFV	NVP	NVR	NVM	NVA	NASYM
2	NVPHI	NCHINE	NDADT					
3	NHEAD	NPRNTP	NRPNTS	NPRNTV	NPLOTV	NPLOTA	NTH -	
	NCORE	NSKIN	NCOMP					

Repeat item 4 for each NHEAD(item 3).

4	TITLES							
5	REFS	REFL	XM	SL	SD			
6(a)	ALPHAC	PHI	RE	MACH				
6(b)	PRATE	QRATE	RRATE	XROT	YROT	ZROT		
7	XI	XF	DX	XTR1	XTR2	EMKF	RGAM	VRF
8	E5	XTABL	XASYMI	XASYMF	DBETA	SEPL	SEPT	RCORE
9	NSOR	NRPT						

Omit items 10 and 11 if  $NSOR(\text{item } 9) \leq 0$ .

10	XSRC
11	QS
12	NXR
13	XR
14	R
15	DR

Omit items 16 and 17 if cross section shape is not elliptical,  $NCIR(\text{item } 1) \neq 1$ .

16(a)	AE
16(b)	BE
17(a)	DAE
17(b)	DBE

Omit item 18 if cross section is elliptical,  $NCIR = 0$ .

18(a)	RO
18(b)	DRO

*Omit items 19 through 27 if cross section is circular or elliptical,  $NCIR < 2$ .*

*Omit item 19 if  $NTH(\text{item } 3) = 0$ .*

19 TH

20(a) MNFC MXFC

20(b) XFC

*Omit item 21 if the body does not have a chined cross section,  $NCHINE \leq 0$ .*

21 NCSEP

*Omit items 22 and 23 if  $NCF(\text{item } 1) > 0$ .*

22 NR

23(a) XRC

23(b) YRC

*Omit items 24 through 27 if  $NCF = 0$ .*

24 ZZC RZC

25 NR

26(a) XRC

26(b) YRC

26(c) THC

27 AFC

*Omit items 28 and 29 if  $NCHINE(\text{item } 2) \leq 0$ .*

28 NSTRTC FVCHN

29(a) XCHNB XCHNE

29(b) NCH(1) NCH(2) NCH(3)

29(c) NCBL(1) NCBL(3)

29(d) VRFC(1) VRFC(3)

*Omit items 30 and 31 if  $NXFV(\text{item } 1) = 0$ .*

30 XFV

*Omit item 31 if  $NFV(\text{item } 1) = 0$ .*

31 YFV, ZFV

Description of the restart items (32 through 37) are not included.

Table 4.2-8 Description of Parameters in Input File vchn.inp (full)

Note: Comments are included indicating where parameters are set or computed within HASC prior to running VTXCHN. When VTXCHN is run independent of HASC then these pre-sets and calculations are not executed.

Item 1 - Program Flags

NCIR	Cross section flag, determines the type of body cross section. 0 = circular body 1 = elliptical body 2 = arbitrary body with similar cross sections at all axial stations 3 = arbitrary body with nonsimilar cross sections
NCF	Mapping flag, specifies whether the required mapping is input or calculated, applies to arbitrary body cross sections (NCIR = 2 or 3). 0 = calculate mapping 2 = input mapping NCF is set to 0 in HASC.
ISYM	Vortex shedding symmetry flag. 0 = symmetric shedding, saves computation time 1 = nonsymmetric shedding, if PHI $\neq$ 0 then VTXCHN sets ISYM = 1. ISYM is set to 0 in HASC.
NBLSEP	Separation flag. 0 = no separation 1 = laminar separation 2 = turbulent separation
NSEPR	Reverse flow or secondary separation flag. 0 = no reverse flow separation (preferred) 1 = reverse flow separation NSEPR is set to 0 in HASC.



**NDFUS**      Vortex core model flag.  
0 = potential vortex model  
1 = diffuse vortex model (preferred)  
NDFUS is set to 1 in HASC.

**NDPHI**      Two-dimensional unsteady pressure term flag.  
0 = omit  $d\phi/dx$  terms in  $C_p$  equation  
1 = include these terms in  $C_p$  equation  
NDPHI is set to 1 in HASC.

**INP**        Nose force flag.  
0 = estimate nose forces ahead of the first axial station (preferred)  
1 = zero nose forces ahead of the first axial station (for restarts)  
INP is set to 0 in HASC.

**NXFV**      Number of x stations at which the flow field is calculated and/or  
special output is generated. Note:  $0 \leq NXFV \leq 8$ .  
NXFV is set to 1 in HASC.

**NFV**        Number of field points for flow field calculation. Note  $0 \leq NFV \leq 500$ .  
NFV is set to 0 in HASC.

**NVP**        Number of positive vortices on +y side of body for a restart  
calculation. Note:  $0 \leq NVP \leq 70$ .  
NVP is set to 0 in HASC.

**NVR**        Number of reverse flow vortices on +y side of body for a restart  
calculation. Note:  $0 \leq NVR \leq 30$ .  
NVR is set to 0 in HASC.

**NVM**        Number of positive flow vortices on -y side of body for a restart  
calculation. Note:  $0 \leq NVM \leq 70$ .  
NVM is set to 0 in HASC.

- NVA**            Number of reverse flow vortices on -y side of body for a restart calculation. Note:  $0 \leq NVA \leq 30$ .  
NVA is set to 0 in HASC.
- NASYM**        Asymmetric vortex shedding flag. This option is not used on chine portion of a body.  
0 = no asymmetry  
1 = forced asymmetry (not recommended)  
NASYM is set to 0 in HASC.

## Item 2 - Additional Program Flags

- NVPHI**       $d\theta/dx$  flag, specifies how vortices are treated in the  $d\theta/dx$  calculation.  
-1 = all vortices are considered independent for the calculation  
 $\geq 0$  the most recent NVPHI vortices ( on each side of the body) are considered independent for the calculation, and the remaining vortices are included by a centroid representation. The NVPHI vortices considered independent can be considered as the feeding sheet. Note: NVPHI = -1 is suggested.  
NVPHI is set to -1 in HASC.
- NCHINE**      Chine flag, determines whether the body has a chine shaped cross section.  
0 = no chine section, body shape determined by the NCIR parameter  
1 = chine section for all or part of the body
- NDADT**      Flag which determines option for calculation of  $dv/dx$ .  
0 =  $dAk/dx$  term not included  
1 =  $dAk/dx$  term is included  
NDADT is set to 1 in HASC.

### Item 3 - Program Options

- NHEAD**      Number of title lines.  
NHEAD is set to 1 in HASC.
- NPRNTP**     Pressure distribution print flag.  
0 = pressure distribution output only at specified output stations  
(NXFV > 0)  
1 = pressure distribution output at each x station  
NPRNTP is set to 0 in HASC.
- NPRNTS**     Vortex separation print flag.  
0 = no separation output  
1 = separation point summary (preferred)  
2 = detailed separation calculation (for diagnostic purposes only)  
NPRNTS is set to 1 in HASC.
- NRPNTV**     Vortex field summary output flag.  
0 = vortex field is printed at special output stations only (NXFV>0)  
1 = vortex field is printed at every x station  
NRPNTV is set to 1 in HASC.
- NPLOTV**     Vortex field printer-plot flag.  
0 = no plots  
1 = plot full cross section, constant scale  
2 = plot half cross section, constant scale  
3 = plot full cross section, variable scale  
NPLOTV is set to 0 in HASC.
- NPLOTA**     Additional output flag. Option to have pressure distribution, vortex  
field summary, and a plot of the vortex field regardless of the above  
set options.  
0 = no additional output  
1 = additional output only at specified x stations (NXFV > 0)  
2 = additional output at each station  
NPLOTA is set to 0 in HASC.

NTH Numerical conformal mapping angle flag.  
0 = calculate circle values for mapping at 5° increments (preferred)  
1 = input values  
NTH is set to 0 in HASC.

NCORE Vortex core radius flag.  
0 = maximum allowable local vortex core size is  $.05 \cdot D$   
1 = no upper limit on the local vortex core size, the vortex core size is given by  $RCORE \cdot D$   
NCORE is set to 0 in HASC.

NSKIN Axial skin friction drag estimation flag.  
0 = skin friction not estimated  
1 = axial skin friction estimated  
NSKIN is set to 0 in HASC.

NCOMP Compressibility correction flag.  
0 = incompressible calculation  
1 = compressibility correction applied (Mach number must be input in item 6)  
NCOMP is set to 1 in HASC.

#### Item 4 - Title(s)

TITLES      NHEAD title lines  
TITLES is set within HASC from hasc.inp input.

#### Item 5 - References

REFS        Reference area, REFS > 0.  
REFS is set within HASC from hasc.inp input.

REFL        Reference length, REFL > 0.  
REFL is set within HASC from hasc.inp input.

XM           Axial position of the moment center, measured from the body nose.  
XM is set within HASC from hasc.inp input.

SL           Total body length, L.

SD           Maximum body diameter, D.

Item 6(a) - Flow Conditions

ALPHAC     Angle of incidence (degrees). Note:  $0^\circ \leq \text{ALPHAC} < 90^\circ$   
ALPHAC is set within HASC from hasc.inp input.

PHI         Angle of roll (degrees). For chine bodies the user should be aware that separation is forced at the sharp edge of the chine regardless of the value of PHI. It is the user's responsibility to determine the limit of PHI for a given chine shape.  
PHI is set within HASC from hasc.inp input.

RE          Reynolds number based on the maximum body diameter.  
RE is set within HASC from hasc.inp input.

MACH       Free-stream Mach number.  
MACH is set within HASC from hasc.inp input.

Item 6(b) - Flow Conditions for Steady-State Rates

- PROT      The non-dimensional roll rate defined as  $p \cdot \text{REFL} / \text{VINFL}$ , where  $p$  is the roll rate in radians per second. Positive is right wing down when viewed from the rear.  
PROT is set within HASC from hasc.inp input.
- QROT      The non-dimensional pitch rate defined as  $q \cdot \text{REFL} / \text{VINFL}$ , where  $q$  is the pitch rate in radians per second. Positive is nose up.  
QROT is set within HASC from hasc.inp input.
- RROT      The non-dimensional yaw rate defined as  $r \cdot \text{REFL} / \text{VINFL}$ , where  $r$  is the yaw rate in radians per second. Positive is nose to the right when viewed from above.  
RROT is set within HASC from hasc.inp input.
- XROT      The dimensional x position of the rotation center from the nose.  
XROT is set within HASC from hasc.inp input.
- YROT      The dimensional y position of the rotation center from the center line.  
YROT is set within HASC from hasc.inp input.
- ZROT      The dimensional z position of the rotation center from the center line.  
ZROT is set within HASC from hasc.inp input.



## Item 7 - Extent, Transition, and Vortex Wake Parameters

- XI** Initial X station for calculations,  $XI > 0$ , dimensional quantity.
- XF** Final X station for calculations,  $XF > XI$ , dimensional quantity.  
XI and XF are set within HASC from hasc.inp input.
- DX** X increment for vortex shedding calculation. For bodies with chine cross sections it is recommended that DX be between  $0.10 \cdot D$  and  $0.25 \cdot D$ , otherwise use  $D/2$ .
- XTR1** Beginning of transition region, dimensional quantity. This option is not recommended for use, thus XTR1 has been set to a large positive number (99998.) in HASC.
- XTR2** End of transition region, dimensional quantity. This option is not recommended for use, thus XTR2 is set to a large positive number (99999.) in HASC.
- EMKF** Minimum shed vortex starting distance from the body surface. This value is not used on a chined portion of the body.  
1.0 = shed vortices located according to stagnation point criterion  
 $\geq 1.0$  minimum radii position of shed vortices. Typical value of EMKF = 1.05.  
EMKF is set to 1.05 in HASC.
- RGAM** Vortex combination factor.  
0.0 = vortices are not combined (preferred)  
 $\geq 0.0$  radial distance within which vortices are combined  
RGAM is set to .0 in HASC.
- VRF** Vortex reduction factor to account for decreases in vortex strength.  
0.6 = for bodies with bases  
1.0 = for closed bodies  
If NCHINE = 1 this parameter is not used.  
VRF is set to .6 in HASC.

## Item 8 - Tolerance, Asymmetry, and Separation Criteria

- E5** Error tolerance for the vortex trajectory calculation. Typical range of E5 is 0.01 to 0.05.
- XTABL** Location at which a table of points on the body and on the circle is printed.  
0.0 = no table of points is printed (preferred)  
>0.0 table of points for all  $x < XTABL$   
XTABL is set to .0 in HASC.
- XASYMI** Initial x station for asymmetric perturbation. This option is not available on a chined portion of the body.  
XASYMI is set to .0 in HASC.
- XASYMF** Final x station for asymmetric perturbation. This option is not available on a chined portion of the body.  
XASYMF is set to .0 in HASC.
- DBETA** Angular displacement of separation points for asymmetry perturbation. This option is not available on a chined portion of body.  
DBETA is set to .0 in HASC.
- SEPL** Stratford's laminar criterion (not used on a chined portion of body).  
0.0 = program uses SEPL = 0.087 (preferred)  
> 0.0 program uses input value of SEPL  
SEPL is set to .0 in HASC.
- SEPT** Stratford's turbulent criterion (not used on a chined portion of body).  
0.0 = program uses SEPT = .350 (preferred)  
> 0.0 program uses input value  
SEPT is set to .0 in HASC.
- RCORE** Ratio of the local core radius to the local body diameter. Default value is .025. Maximum allowable value is  $.025 * D/R$   
RCORE is set to .05 in HASC.

### Item 9 - Source Distribution

- NSOR      Source distribution flag.  
-1 = calculate the source distribution from the geometry input  
0 = no sources (not recommended)  
> 0 = number of sources to be input  
NSOR is set to -1 in HASC.
- NPRT      Source distribution print flag.  
0 = output source locations and strengths  
1 = above output plus input and source geometry comparison  
2 = above output plus source-induced surface velocities  
NPRT is set to 0 in HASC.

*Omit items 10 and 11 if NSOR ≤ 0.*

### Item 10 - Source Locations

- XSRC      Nondimensional source locations, x/L.

### Item 11 - Source Strengths

- QS      Nondimensional source strengths.

Item 12 - Number of Entries to Specify Body

NXR            Number of entries in the body geometry table ( $1 \leq \text{NXR} \leq 101$ ).

Item 13 - Axial Stations

XR            Non-dimensional axial stations in the geometry table,  $x/L$  (NXR values).

Item 14 - Body Radius

R            Non-dimensional area body radius at the NXR  $x/L$ -stations,  $r/L$  (NXR values).

Item 15 - Body Slope

DR            Body slope at the NXR  $x/L$ -stations,  $dr/dx$ . (NXR values)

*Omit Items 16 and 17 if  $\text{NCF} \neq 1$  (only required for elliptical bodies).*

Item 16 - Half Axis Lengths

AE            Non-dimensional horizontal half axis length of the elliptical cross section at the NXR  $x/L$ -stations,  $a/L$  (NXR values).

BE            Non-dimensional vertical half axis length of the elliptical cross section at the NXR  $x/L$ -stations,  $b/L$  (NXR values).

Item 17 - Slopes of Half Axis Lengths

DAE            Slope of the horizontal half axis length of the elliptical cross section at the NXR  $x/L$ -stations,  $da/dx$  (NXR values).

DBE            Slope of the vertical half axis length of the elliptical cross section at the NXR  $x/L$ -stations,  $db/dx$  (NXR values).

*Omit items 18(a) and 18(b) if NCIR = 0 (circular body).*

Items 18(a) and 18(b) contain the mapped body geometry information at the NXR x/L-stations specified in item 13.

Item 18(a)

RO Non-dimensional transformed (mapped) body radius at the NXR(item 13) x/L stations,  $r_0/L$ . For an ellipse,  $r_0 = (a + b)/2$ .

Item 18(b)

DRO Body slopes at the NXR x/L-stations,  $dr_0/dx$ .

*Omit items 19 through 27 if NCIR < 2 (required only for arbitrary cross sections).*

Items 19 through 27 are used to specify a body or arbitrary cross section shape. The body should be polygonal in shape (i.e., negative interior angles can cause problems in the numerical conformal mapping procedure).

Item 19, omit if NTH = 0.

TH Special table of circle angles for arbitrary body mapping, (i=1,73), to be used only if the density of points on the cross section needs adjusting to improve the resolution of pressure distribution. Not recommended under normal conditions.

Item 20(a)

MNFC      Number of mapping coefficients for the arbitrary body ( $MNFC \leq 100$ ). Generally good mappings can be obtained with 20 to 30 coefficients.

MXFC      Number of axial stations at which the arbitrary body is specified ( $1 \leq MXFC \leq 10$ ). For bodies with a similar shape at all cross sections set  $MXFC = 1$ .

Item 20(b)

XFC      x stations at which the arbitrary body is specified (MXFC values). For a similar cross section body,  $MXFC=1$ ,  $XFC(1) \leq XI$ .

Item 21 - Omit item 21 if  $NCHINE \leq 0$  (required for chine shaped cross sections)

Item 21 is a set of MXFC integers to indicate which input corner point of each input cross section is to be considered as the chine edge. The input corner points are read in items 22 and 23 (MXFC values).

NCSEP      Number of the input corner point defining the chine edge. Corner points are read in items 22 and 23. It is recommended that NCSEP be the same for all input chine cross sections ( $0 \leq NCSEP \leq NR$ ).

Items 22 and 23, omit if  $NCF \geq 0$ .

Items 22 and 23 are repeated for each of the MXFC axial stations when the transformation coefficients are to be calculated ( $NFC = 0$ ).

Item 22 - Number of Points Describing Arbitrary Body

NR            Number of points describing the arbitrary body cross section ( $2 \leq NR \leq 30$ ). Note: NR must be the same for all x stations.

Item 23(a) - Horizontal Coordinates

XRC          Horizontal coordinates of the arbitrary body cross section (NR values). The convention for ordering the coordinates from bottom to top in a counter-clockwise fashion is observed. This corresponds to inputting the +y side geometry. Right/left body symmetry is required.

Item 23(b) - Vertical Coordinates

YRC          Vertical coordinates of the arbitrary body cross section following the same input as used for XRC values (NR values).

*Items 24 through 27, not required if NCF = 0.*

Items 24 through 27 are repeated as a group for each of the MXFC axial stations if the numerical transformations are available from a previous calculation. Inputting the mapping parameters eliminates the need to recompute the numerical mapping in subsequent runs, thus saving computation time.

Item 24

ZZC Mapping offset distance.

RZC Radius of transformed cross section.

Item 25

NR Number of points describing the arbitrary body cross section ( $NR \leq 30$ ). NR must be the same for all x stations.

Item 26(a)

XRC Horizontal coordinates of the arbitrary body cross section (NR values).

Item 26(b)

YRC Vertical coordinates of the arbitrary body cross section (NR values).

Item 26(c)

THC Circle angles of body points (NR values).

Item 27

AFC Mapping coefficients (MNFC values).



Omit items 28 and 29 if  $NCHINE \leq 0$  (required only for sections of chine shape).

Item 28 - Information for Starting Chine Solution

NSTRTC      Number of axial stations at which the vortex lattice approximation of the chine is used to start the solution. A value between 0 and 5 generally works the best.

FVCHN        Fraction of the exposed strake span where the boundary condition is applied to determine the initial chine strength using a vortex lattice approximation. Suggested value is 0.50.

Item 29(a) - Chine Separation Region

XCHNB        Axial station at which chine separation begins.

XCHNE        Axial station at which chine separation ends.

Item 29(b) - Cross Section Shape Parameters

NCH(1)       Value of NCIR for portion of body in front of axial station XCHNB(item 29a). Only NCIR values of 0, 2, or 3 are available here. If the body has an elliptical nose section, it should be run as a non-circular body (NCIR = 2 or 3).

NCH(2)       Value of NCIR for portion of body between axial station XCHNB and XCHNE. For the chine section, NCIR is 2 or 3. If  $NCH(1) = 0$  and  $NCH(2) = 3$ , then the first input body cross section should be a circle with a radius equal to the body radius at the start of the chine section. This is required to ensure transition from the circular portion of the body to the chine portion.

NCH(3)       Value of NCIR for portion of body after axial station XCHNE. Only NCIR values of 0,2,or 3 are available here. If the body has an elliptical afterbody section, it should be run as a non-circular body (NCIR = 2 or 3).

Item 29(c) - Separation Parameters for Chine Body

NCBL(1) Value of NBLSEP for portion of body in front of axial station XCHNB.

NCBL(3) Value of NBLSEP for portion of body after axial station XCHNE.

Note: NCBL(2) value is set in VTXCHN but is not used.

Item 29(d) - Vortex Reduction Factors for Chine Body

VRFC(1) Value of VRF for portion of body in front of axial station XCHNB.

VRFC(3) Value of VRF for portion of body after axial station XCHNE.

Note: The value of VRFC(2) is set in VTXCHN but is not used.

Item 30 - Additional Output Stations. omit if NXFV = 0.

XFV X stations at which additional output is printed or calculated ( $XFV \leq 8$ ).

Item 31 - Field Points for Velocity Component Calculations.

omit if NXFV = 0 or NFV = 0

YFV, ZFV Coordinates of the field points for the velocity field calculation. It is recommended that all points lie outside the body surface at all axial stations.

Items 32 through 37. omit if  $NVP+NVR+NVM+NVA = 0$ ).

Refer to reference 12 for a discussion of the parameters in items 32 through 37. These items are only used during a restart of VTXCHN. Restarts are only allowed when running VTXCHN in the stand-alone mode.

### Description of Condensed Input file vchn.inp

The top 9 items of the full vchn.inp file as previously discussed have been reduced down to just 2 items as shown in table 4.2-9 for the condensed form of vchn.inp. The differences in used between the two files are summarized below.

- 1) When analyzing just a forebody configuration in VTXCHN independent of the rest of HASC, follow the input requirements for the full vchn.inp file as presented in tables 4.2-7 and 4.2-8. Place "VTXCHN ONLY" in the top most line of the hasc input file hasc.inp.
- 2) When running an aircraft configuration where the forebody is one of the surfaces, set ISRTYP = 3 for the forebody surface and follow the input requirements for the condensed vchn.inp file as presented in tables 4.2-9 and 4.2-10. The results from VTXCHN will be added to the results from VORLAX and VORLIF in the final output.

Table 4.2-9 Summary of Parameters in Forebody File vchn.inp (condensed)

<u>Item</u>	<u>Variables</u>
1	NCIR NBLSEP NCHINE DROOP DX E5
2	TNOSE ENOSE RNOSE FBLNTH SL SD
3	NXR
4	XR
5	R
6	DR
<i>Omit items 7 and 8 if cross section shape is not elliptical, NCIR ≠ 1.</i>	
7(a)	AE
7(b)	BE
8(a)	DAE
8(b)	DBE
<i>Omit item 9 if cross section is elliptical, NCIR = 0.</i>	
9(a)	RO
9(b)	DRO
<i>Omit items 10 through 15 if cross section is circular or elliptical, NCIR &lt; 2.</i>	
10(a)	MNFC MXFC
10(b)	XFC
<i>Omit item 11 if the body does not have a chined cross section, NCHINE ≤ 0.</i>	
11	NCSEP
<i>Omit items 12 and 13 if NCF &gt; 0.</i>	
12	NR
13(a)	XRC
13(b)	YRC
<i>Omit items 14 and 15 if NCHINE ≤ 0.</i>	
14	NSTRTC FVCHN
15(a)	XCHNB XCHNE
15(b)	NCH(1) NCH(2) NCH(3)
15(c)	NCBL(1) NCBL(3)
15(d)	VRFC(1) VRFC(3)
16	XFV

The parameters not described in table 4.2-10 are listed in table 4.2-10.

Table 4.2-10 Additional Parameters in Input File vchn.inp (condensed)

DROOP	Droop angle of forebody in degrees. DROOP is used to adjust the effective angle of attack prior to running VTXCHN. A positive value indicates the forebody has negative incidence.
TNOSE	Forebody type. 1 = ogive 0 = cone
ENOSE	Forebody ellipticity (use 1 for circular).
RNOSE	Forebody radius. 0 = sharp nose 1 = blunt
FBLNTH	Length of forebody section of varying cross sectional area plus length of constant section. This length is used to determine the limits of integration. The total length of the body (SL) is the summation of FBLNTH plus the base closure length as shown in figure 4.2-7. This total length is used to nondimensionalize various parameters.

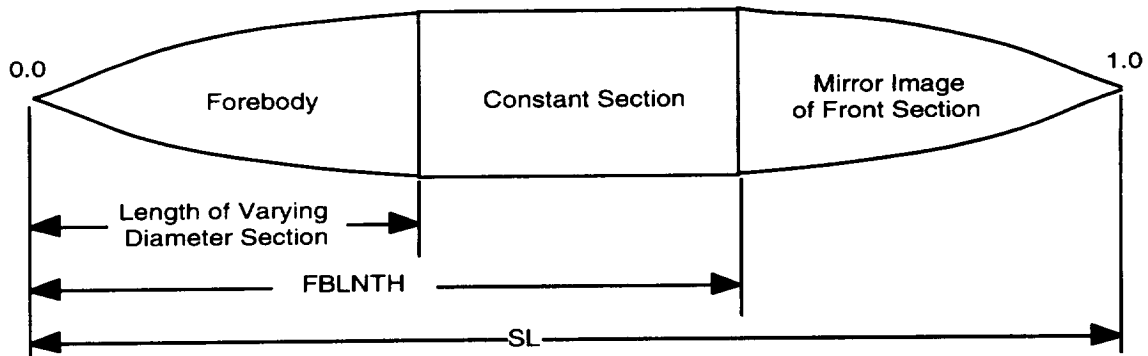


Figure 4.2-7 Illustration of Forebody Lengths

The remaining VTXCHN parameters must be input as described in tables 4.2-7 and 4.2-8. Refer to Appendix B for examples of VTXCHN input files. A full and condensed listing for the F-16 forebody is provided in Appendix B.

### Note on Using VTXCHN:

The following method should be used to determine the source/sink (R) and mapped radius (R0) distribution for a geometry with an arbitrary cross section.

The first step required is to execute VTXCHN with the required geometry description for the cross-sections and with XI set equal to XF, refer to the input description, table 4.2-8. The initial source/sink and mapped radius distributions should be set to some generic distribution such as a tangent ogive. The source/sink distribution is unimportant at this point. In addition the XF value is set equal to XI so VTXCHN will not calculate a flow field.

Once the code has finished the initial run, the mapped radius for each of the specified cross-sections should be used to determine the mapped radius distribution required by the code for subsequent runs.

In general, the mapped radius distribution is required at more stations than the input geometry cross-sections. Therefore, the mapped radii between the input cross-sections need to be determined by the user using some type of curve fit. It is important that the resulting mapped radii at the input geometry cross-sections match the actual mapped radii at the input stations. If there is a difference, the body will be scaled up or down.

The final step is to set the radius distribution (R) for the source/sink distribution calculation equal to the mapped radius distribution (R0).

### 4.3 Running the Code

The user information required to setup an input deck correctly is contained in the previous sections. The typical process for running HASC is outlined below.

1. Study the configuration 3-views. Divide the configuration into surfaces. Develop a list of buttlines that will provide easily adding controls surfaces later if desired. Provide alignment in the spanwise direction of fore/aft panels.
2. Develop the basic input file using HASCUTIL or with a text editor. Run HASCUTIL to develop geometry files for viewing the paneling in plotting tools such as Plot3d, Excel, or Tecplot. Modifying an existing HASC deck with good comments may be the best way to create a new HASC input file.
3. Submit the job with all surfaces as type 5 (VORLAX analysis). Debug if necessary. Since HASC uses input files with predefined names be sure to rename your input files to the names required by HASC, and rename the default output files to unique names if desired so they won't be overwritten by the next job submittal.
4. Modify the lifting surface definitions to include wing twist, camber, etc. if desired and rerun using VORLIF (type 1 or 2) on the appropriate surfaces. If a bomb occurs after a successful VORLAX run, then try altering the sub-panel definitions with ISPNDIV or ICHRDIV. Be sure to check the values of IVTXFLG and SPC. Evaluate the output files hasc.out, vorlax.out, vorlif.out, stabcrit.out and vortex.trk as required.
5. Create a forebody VTXCHN input file (vchn.inp) if desired. All forebody paneling should be done within a single surface (top and side view). Change the ISRTYP to 3 for the forebody. Resubmit job for a complete VORLAX, VORLIF, VTXCHN analysis of the configuration.

Depending on the configuration being analyzed and your experience with the code it may be possible to develop the HASC input deck full-up with the correct ISRTYP parameters, wing definition, and forebody definition prior to the first

submittal. If problems are experienced in obtaining a successful solution, then the problem deck may be simplified as required to resolve problems.



## 4.4 Output Description

Several output files are generated from a successful HASC run. Files range from geometry of the input model, summary of force and moments, to detailed summary of vortex characteristics. The output information depends on which solution options are used (VORLAX, VORLIF, or VTXCHN). Table 4.4-1 summarizes input, temporary, and output files of HASC. A brief summary of many of these files is provided in table 4.4-1. Appendix D contains listings of selected output files.

Table 4.4-1 Description of HASC Files

Note: Input files are underlined.  
Output files are shown in **bold**.

<u>Unit</u>	<u>File</u>	<u>Description</u>
2	<b>vorlax2.tmp</b>	VORLAX work file: axial wash coefficient matrix.
3	<u>airfoil.inp</u>	airfoil input file: airfoil leading edge definition file.
4	<b>vorlax4.tmp</b>	VORLAX work file: axial wash influence coefficient matrix.
6	(screen dump)	A useful assortment of information is printed to the standard output file (unit 6). This information includes input listings, warnings, program stop messages, intermediate solutions, and progression statements. Often problems with an input file can be found from reviewing the information in this screen dump.
7	<b>vorlax7.tmp</b>	VORLAX work file: airfoil definition file stripped of comment lines.
8	<b>vorlax8.tmp</b>	VORLAX work file: generated by HASC and used to generate the final input file.

- 9     **vorlax9.tmp**     VORLAX work file: leading edge normal wash coefficient matrix.
- 10    **vorlax10.tmp**    VORLAX work file: side wash influence coefficient matrix.
- 11    **vorlax11.tmp**    VORLAX work file: temporary data storage.
- 12    **vorlax12.tmp**    VORLAX work file: temporary data storage.
- 13    **alpn.tmp**        VORLIF work file: vorlif tail incidence data.
- 14    **stabcrit.out**    VORLIF output file: output file of vortex velocity and stability characteristics.
- 15    hasc.inp        primary HASC input file: program option flags, references, flow conditions, and geometry input file.
- 16    **vorlax.out**     VORLAX output file: primary output of VORLAX including a listing of the input deck, summary of geometry including panel slopes, plus calculated loads per sub-panel and panel strip. This is a useful file for verifying input deck and understanding results. See reference 2 additional information on this output file.
- 17    emprcl.inp     VORLIF input file: empirical factors and corrections used by the vorlif module.
- 18    **gama.tmp**        VORLIF work file: created in the second cycle of vorlif for data required for the third cycle.
- 19    **vorlif.out**     primary VORLIF output file: spanwise and integrated force and moment data, including vortex characteristics. This is the primary output from VORLIF. Several parameters are given as a function of the wing span for each angle of attack. Total loads and moments and vortex radius constant are given as a function of angle of attack. Total

loads and moments are based on both the local surface area and configuration reference area. Description of many of the output parameters are printed in the file.

- |    |                   |  |
|----|-------------------|--|
| 21 | mulvor.tmp        | VORLIF work file: vortex strengths and locations at the trailing edge for each leading edge vortex at each angle of attack.  |
| 22 | mulvor2.tmp       | VORLIF work file: same as unit 21 file mulvor but with corrections for vortex transition.  |
| 23 | vposa.tmp         | VORLIF work file: vortex positions and other parameters used to predict induced velocities from vortices.  |
| 24 | vpos.tmp          | VORLIF work file: vortex positions used for the next vorlif cycle.   |
| 25 | vorlax25.tmp      | VORLAX work file: VORLAX input file stripped of comment files.   |
| 27 | vchn.tcp          | VTXCHN output file: results formatted for Tecplot.   |
| 28 | <b>vposfq.out</b> | output file: predicted frequency for the peak unsteady aerodynamic forcing function (Appendix D). Inboard and outboard coordinates of the vortex core edges, ratio of laminar vortex core radius to the turbulent core radius, and peak forcing function reduced frequency are included. |
| 29 | vorlax1.tmp       | VORLAX work file: horseshoe vortex control points normal wash influence coefficient matrix.  |
| 31 | vorlax31.tmp      | VORLAX work file: ew matrix.   |
| 38 | vorlax38.tmp      | VORLAX work file: spanwise vortex density values for entire alpha range for use in calculating vortex core velocities.   |

39	<code>vorlax39.tmp</code>	VORLAX work file: vortex core normal wash coefficient matrix.
40	<code>vorlax40.tmp</code>	VORLAX work file: vortex core axial wash coefficient matrix.
41	<code>vorlax41.tmp</code>	VORLAX work file: vortex core sidewash coefficient matrix.
50	<code>vorlif50.tmp</code>	VORLIF work file: vortex core u, v, w values.
52	<u><code>restart.inp</code></u>	vortex restart file: gamma arrays used for restart run.
53	<code>vtxchn.inp</code>	VTXCHN work file: complete input file for VTXCHN created within HASC. The file can be resubmitted for a "VTXCHN ONLY" analysis run.
54	<u><code>vchn.out</code></u>	VTXCHN output file: VTXCHN output quantities are labeled and each page is headed with descriptive information, additional description can be found in reference 11.
55	<code>vtxchn55.tmp</code>	VTXCHN work file: VTXCHN vortex characteristic output file.
56	<b><code>vchn.inp</code></b>	VTXCHN input file: input file required for analyzing a forebody in VTXCHN module.
70	<code>vorlif70.tmp</code>	VORLIF work file.
71	<code>vorlax71.tmp</code>	VORLAX work file.
73	<code>hasc.tcp</code>	HASC output file: output file in Tecplot format of total and per surface force and moment coefficients in body, wind, and stability axis system.
75	<b><code>hasc.out</code></b>	primary HASC output file: tabular listing of total and per surface force and moments in body, wind, and stability axis system.

76	<b>vorlif76.tmp</b>	VORLIF work file.
77	<b>vorlif77.tmp</b>	VORLIF check file.
78	<b>vortex.trk</b>	VORLIF output file: x, y, and z positions of the vortex axis for each angle of attack per vorlif cycle.
79	<b>lattice.out</b>	geometry output file: x, y, and z coordinates of sub-panel corner points.
80	<b>vorlif80.tmp</b>	VORLIF work file: used in tail downwash correction.
81	<b>vorlif81.tmp</b>	VORLIF work file: used in tail downwash correction.
85	<b>spread.xyz</b>	geometry output file: x, y, and z coordinates of panel corner points for spreadsheet plotting.
93	<b>grid_.p3d</b>	geometry output file: file in plot3d ASCII format of x, y, and z corner points of sub-panels. Multiple files are generated if multiple runs are required within HASC to obtain interference / downwash information. The x in the file name will be 1, 2 or 3 depending on the run number. If all surfaces are analyzed in VORLAX only, then the resulting file name will be grid1.p3d as only one run is required. However, if a configuration with two lifting surfaces (wing and tail or canard and wing) analyzed in VORLIF and with a forebody analyzed in VTXCHN then three files will be generated; grid1.p3d, prid2.p3d, and grid3.p3d. These files can be plotted to view the geometry being analyzed as HASC obtains the required interference / downwash information.
94	<b>panel_.p3d</b>	geometry output file: same as unit 93 grid_.p3d except the x, y, and z values represent only the panel corner points, not the sub-panel corners.

100 **vorelmt.trk** vortex characteristic output file: Subroutine revflow.f computes the effect of vortex elements shed from the leading edge on the free vortex axial velocity. Only the elements that create negative circulation are included in the calculation. For a selected angle of attack (ALXP) this file includes (1) the spanwise station ( $2y/b$ ) where the element is shed from the leading edge, (2) the circulation of the element, (3) the X, Y, and Z components of the velocity, (4) the center line of the free vortex (XD, YD, ZD), and (5) the coordinates of the track of the element (XR, YR, ZR).

## 5.0 VTXCHN VALIDATION

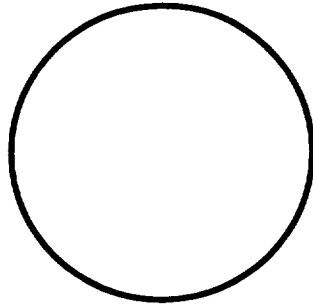
This section describes the VTXCHN validation effort by NEAR. Four different forebody shapes, A1, A2, B1, and C1 were selected from reference 14 as the validation cases for the improved VTXCHN code. The cross sections are shown in figure 5.0-1. The input decks for these forebodies are provided in Appendix B.

For the longitudinal comparisons, VTXCHN was run up to an angle of attack of 50 degrees in increments of 10 degrees. For the lateral comparisons, VTXCHN was run for 0, 5, and 10 degrees of sideslip at angles of attack of 10, 20, 30, and 40 degrees.

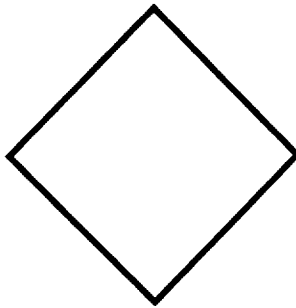
It should be noted that the present version of VTXCHN can not handle cases involving combinations of low angle of attack and high angle of sideslip when forced separation at the chine edges is employed. In these cases, the separation points do not necessarily occur at the chine edges. VTXCHN is applicable to shapes which are either smooth or have a distinct sharp edge. VTXCHN has difficulty achieving an accurate solution at higher angles of attack with shapes, such as the B1 body, which are neither smooth nor chined. Another point to note is that VTXCHN will not predict vortex asymmetry for symmetric forebodies at very high angles of attack and zero angle of sideslip.

Along with the current results, the results predicted previously by the original version of VTXCHN and the experimental results presented in reference 14 are shown. The current results are labeled as "VTXCHN". The predicted results from reference 14 are labeled as "VTXCHN, Orig".

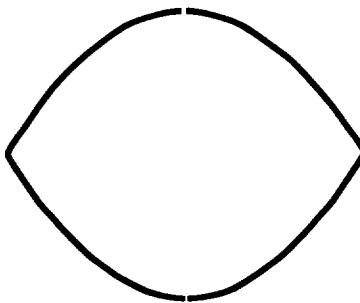
In general, for cases within its realm, VTXCHN does a good job of agreeing with experimental data. However, VTXCHN overpredicts the lateral characteristics for chined bodies at angles of attack greater than 20 degrees.



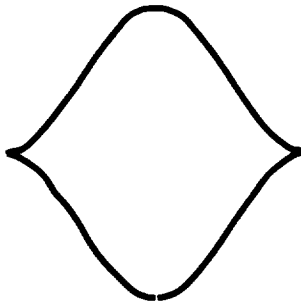
Forebody A1



Forebody A2



Forebody B1



Forebody C1

Figure 5.0-1 Cross Sections of Forebodies Used in VTXCHN Validation



## 5.1 A1 Forebody

Figure 5.1-1 shows that the longitudinal characteristics predicted for the circular cross section A1 by VTXCHN are in good agreement with the experimental data. For cases with sideslip, figures 5.1-2 through 5.1-4, the characteristics are predicted quite well at angles of attack of 10, 20, and 30 degrees. When the angle of attack reaches 40 degrees (figure 5.1-5), VTXCHN is unable to predict the asymmetry that is indicated by the experimental data. The current version of VTXCHN does not contain an asymmetric shed vortex model. VTXCHN does show good agreement in the slopes of side force and yawing moment as a function of angle of sideslip.

The pressure distribution at  $x=7.03$  is shown in figure 5.1-6. The pressure on the lower surface (dashed line) is in good agreement with data. For the pressure distribution on the upper surface (solid line), the predictions on the sides are slightly higher, while the prediction at the center is slightly lower. Overall, VTXCHN captures the pressure distribution to the first order. Second order effects caused by secondary vortices and other details of the flow in the separation region are not modeled by VTXCHN.

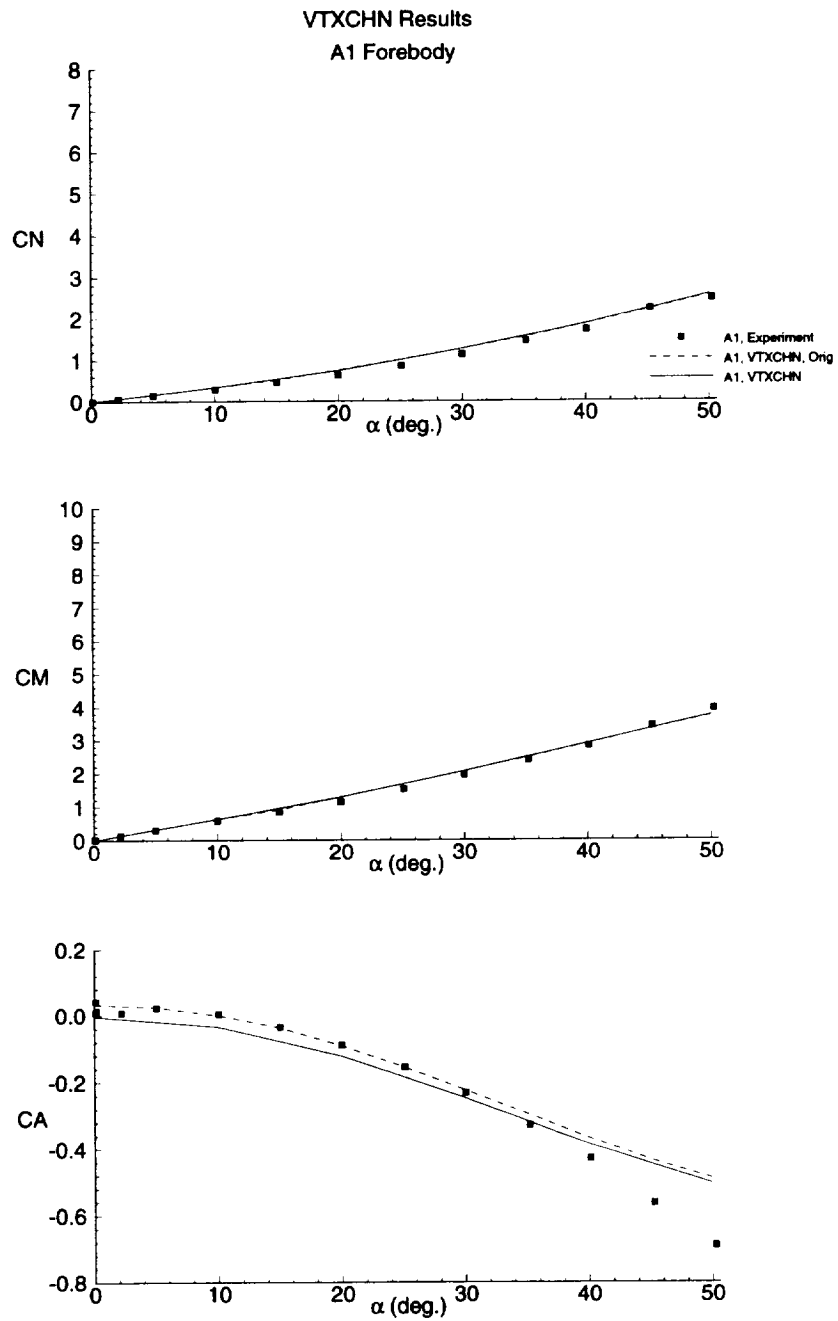


Figure 5.1-1 Longitudinal Characteristics for Forebody A1, M=0.2

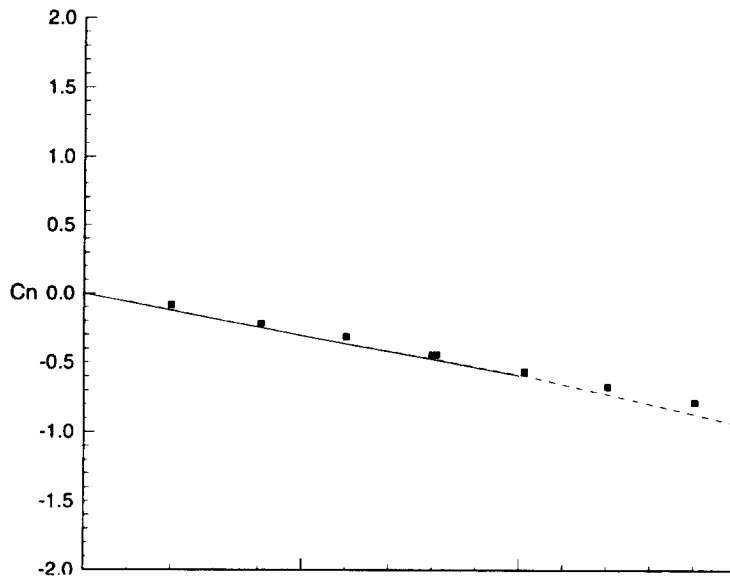
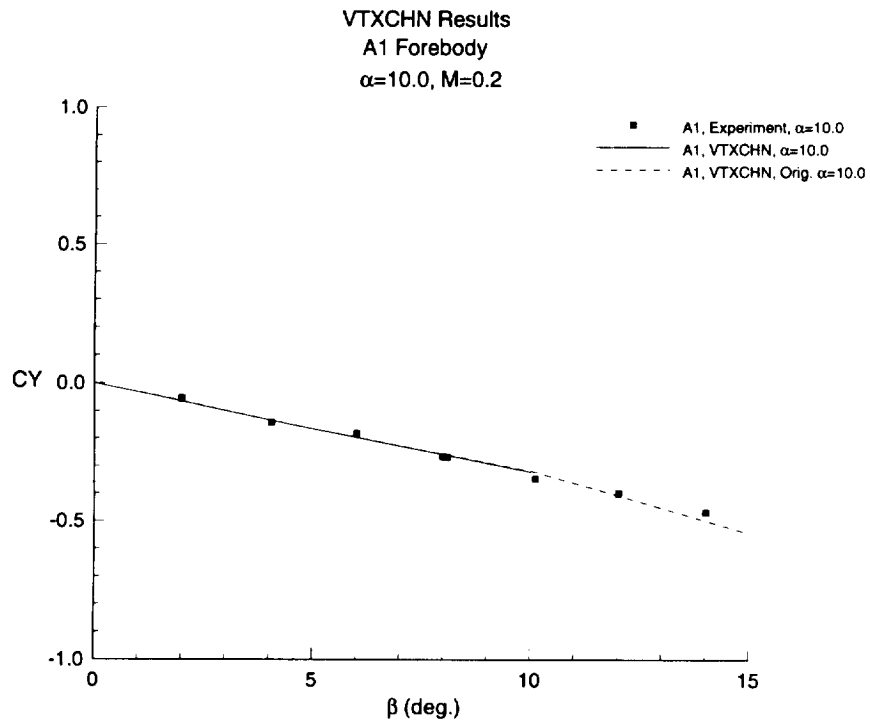


Figure 5.1-2 Lateral Characteristics for Forebody A1, AOA=10°, M=0.2

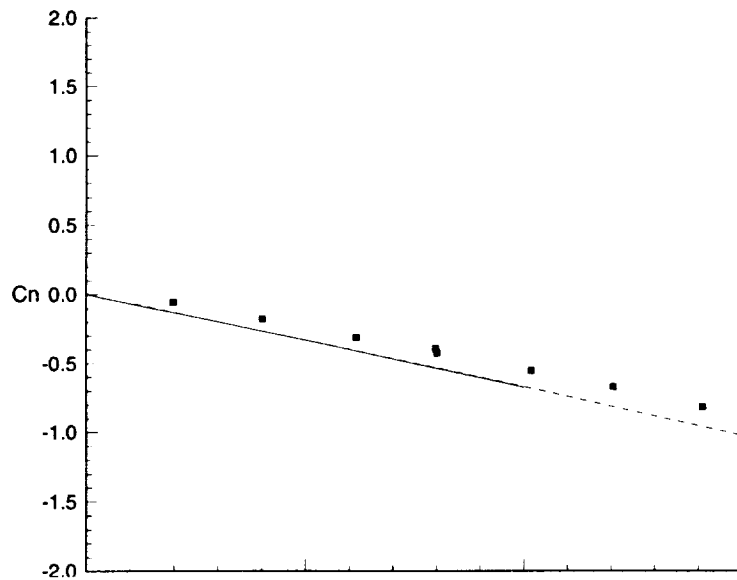
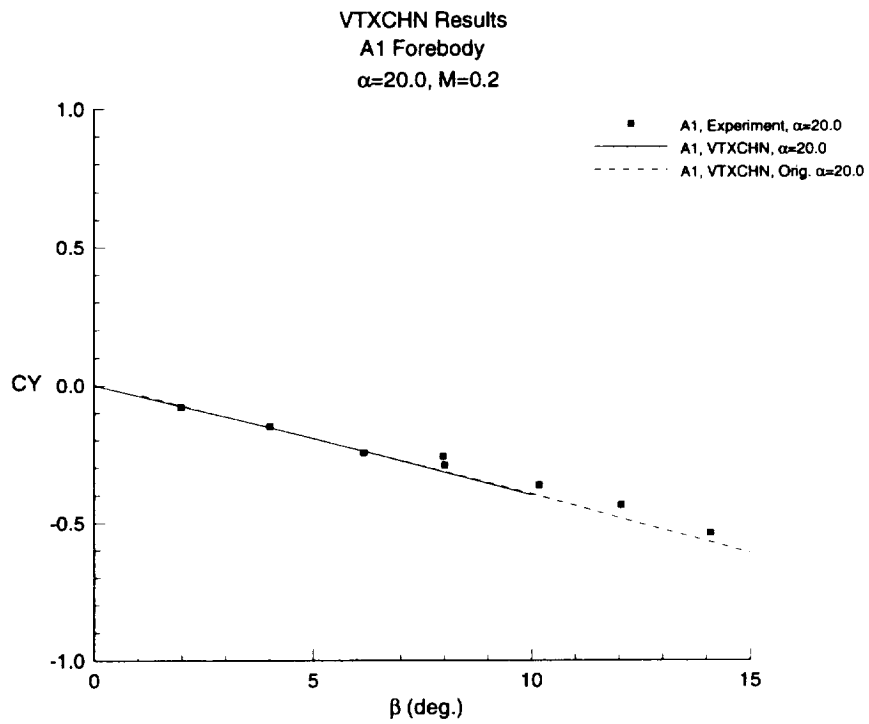


Figure 5.1-3 Lateral Characteristics for Forebody A1, AOA=20°, M=0.2

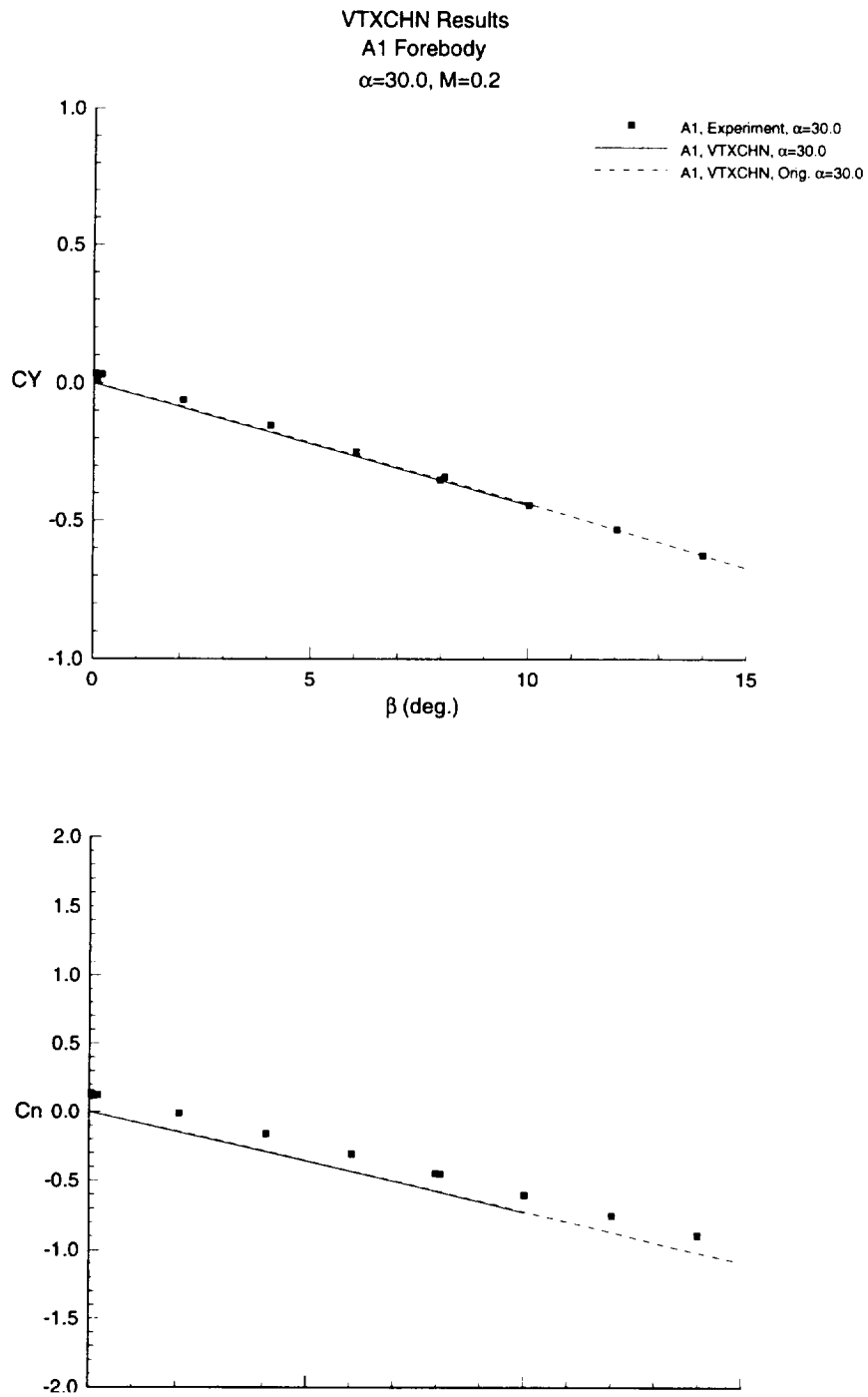


Figure 5.1-4 Lateral Characteristics for Forebody A1, AOA=30°, M=0.2

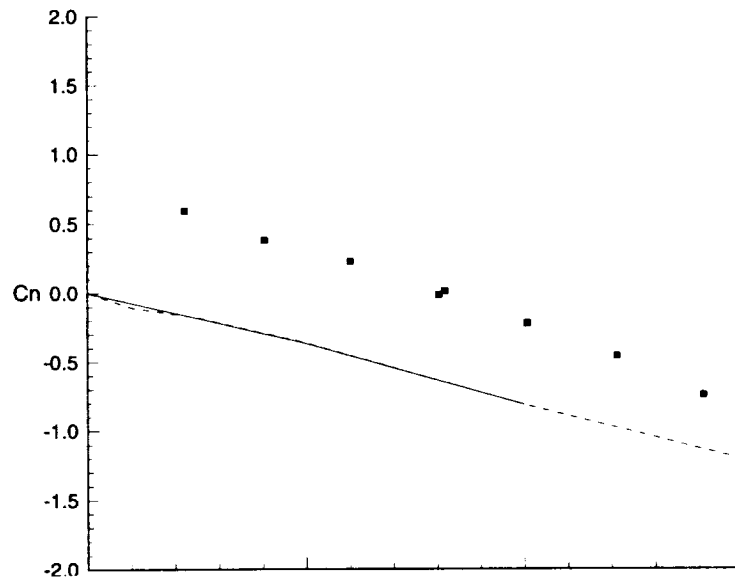
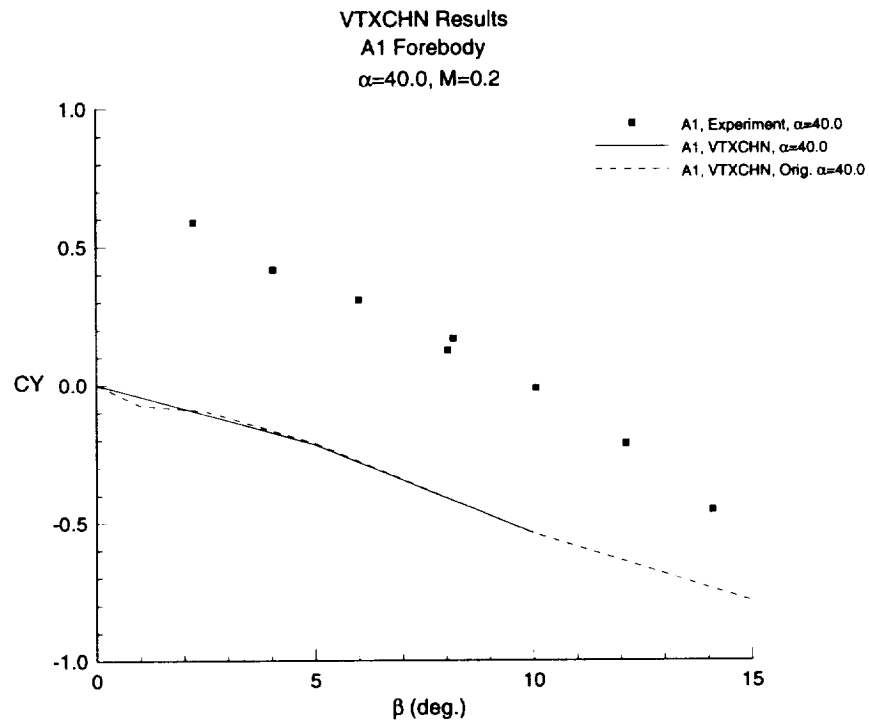


Figure 5.1-5 Lateral Characteristics for Forebody A1, AOA=40°, M=0.2

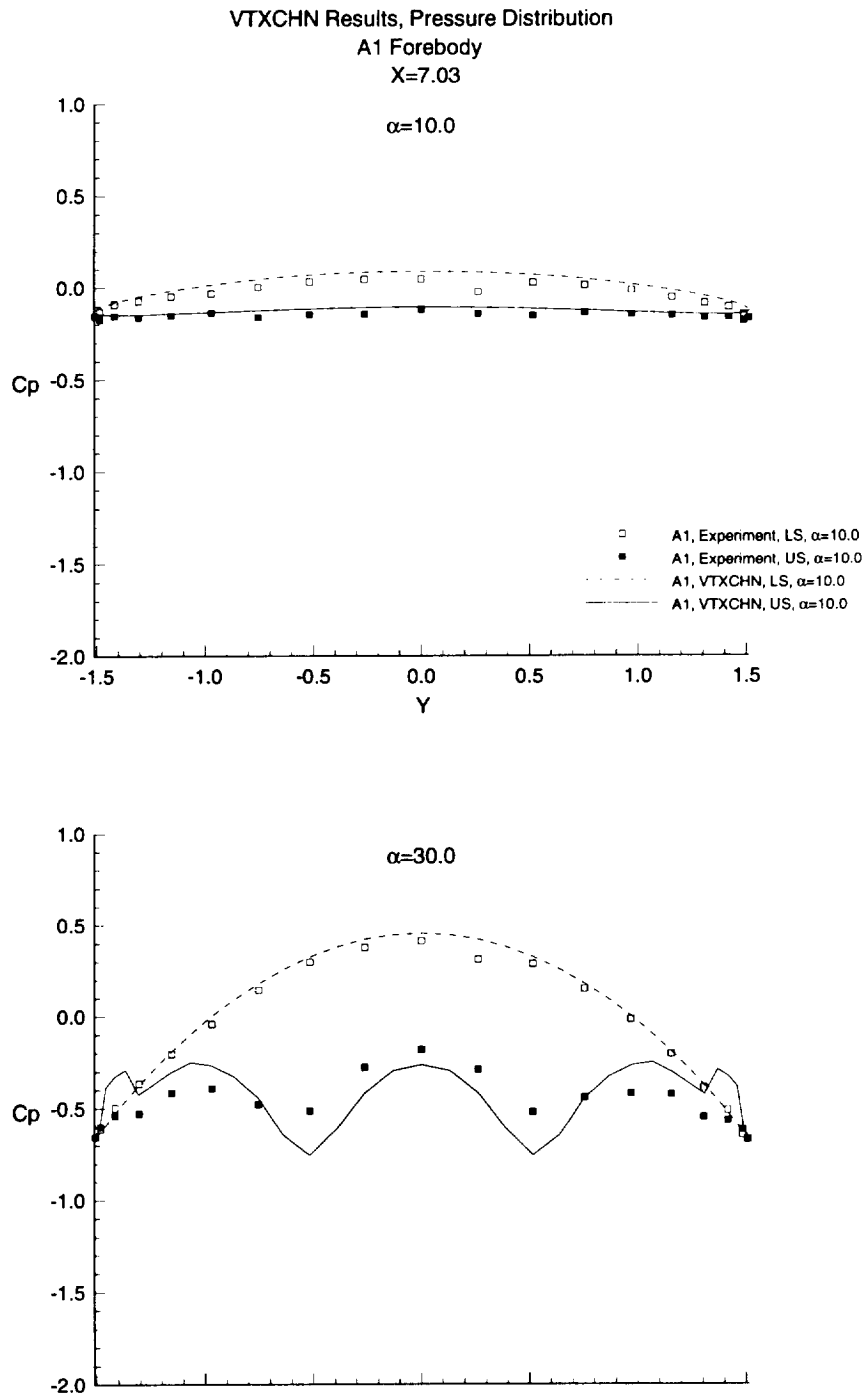


Figure 5.1-6 Pressure Coefficient for Forebody A1, M=0.2

## 5.2 A2 Forebody

Figure 5.2-1 shows the longitudinal data for the A2 forebody. Separation was forced at the corners in the horizontal plane by setting the corners to be chines within VTXCHN. Once again, the longitudinal results are in good agreement to the experimental data. As with all the cases, VTXCHN does not predict asymmetry in the vortex formation when the angle of attack is in excess of 40 degrees. This is indicated in the lateral results.

The lateral results for the A2 forebody are shown in figures 5.2-2 through 5.2-5. The results for nonzero sideslip at angles of attack of 10 and 20 degrees show an improvement over the results from reference 14 and are in good agreement with the experimental results. At an angle of attack of 30 degrees VTXCHN overpredicts the values slightly but the results show the right trend. At an angle of attack of 40 degrees, VTXCHN severely overpredicts the side force results, but the yawing moment is in fair agreement. At high angles of attack, the vorticity shed from the chines is strong and the poor results for the side force may be a result of these strong vortices being forced too close to the body by the sidewash.

The pressure distribution for the A2 forebody is shown in figure 5.2-6. The spikes at the edges and the middle of the graph are a result of the large mapping gradients at the right, left, top, and bottom corners of the A2 forebody. For an angle of attack at 30 degrees, the pressure close to the chine on the upper and lower surfaces is shifted. As was mentioned in the previous section, VTXCHN does not model the higher order flow details in the separation region.



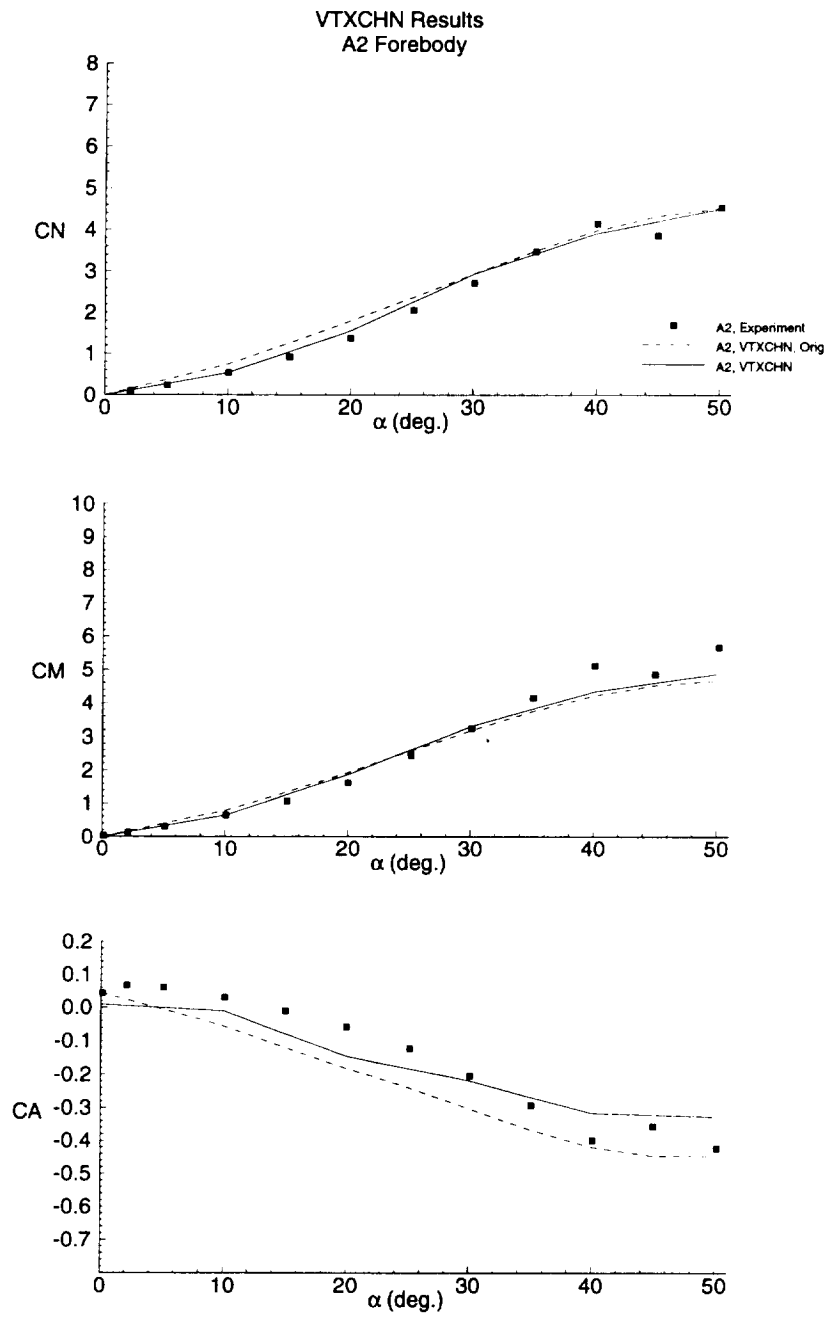


Figure 5.2-1 Longitudinal Characteristics for Forebody A2, M=0.2

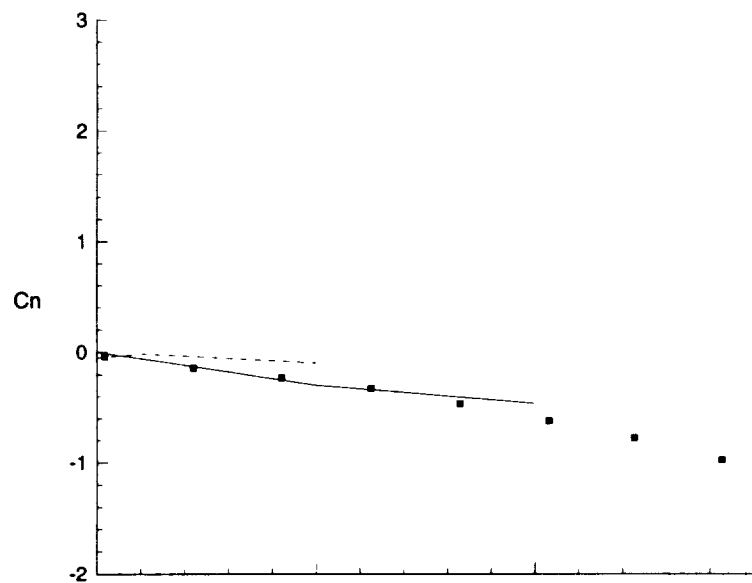
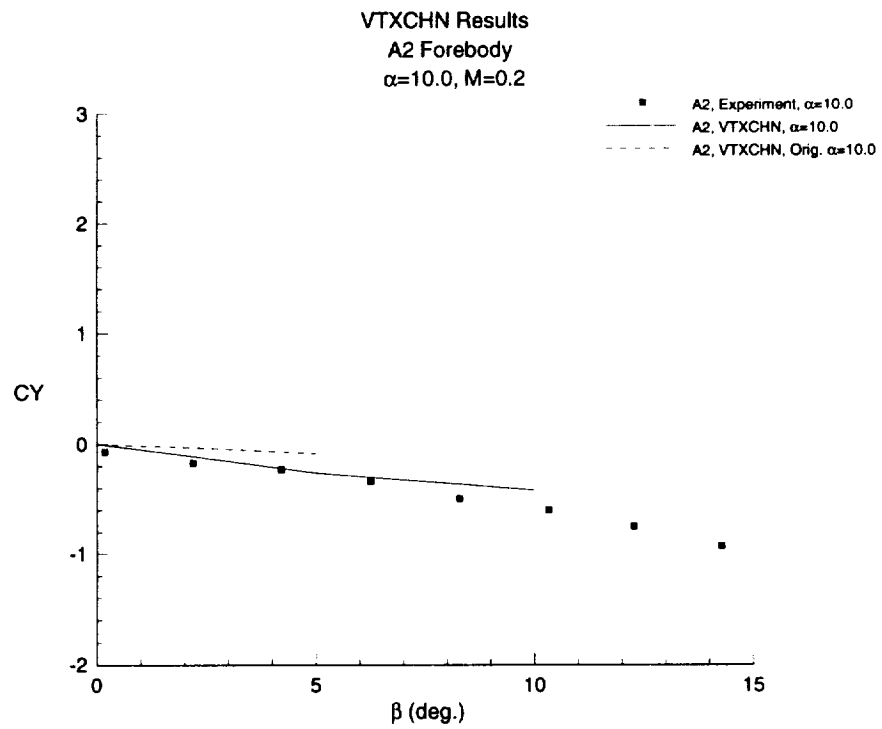


Figure 5.2-2 Lateral Characteristics for Forebody A2, AOA=10°, M=0.2

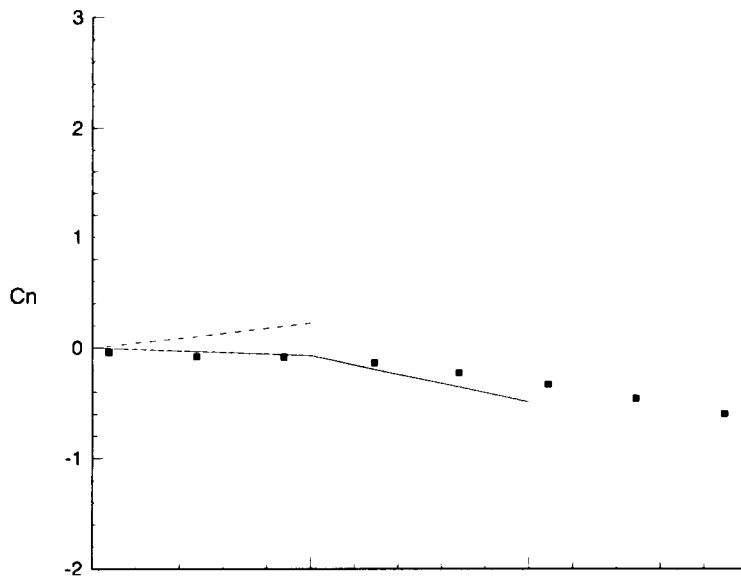
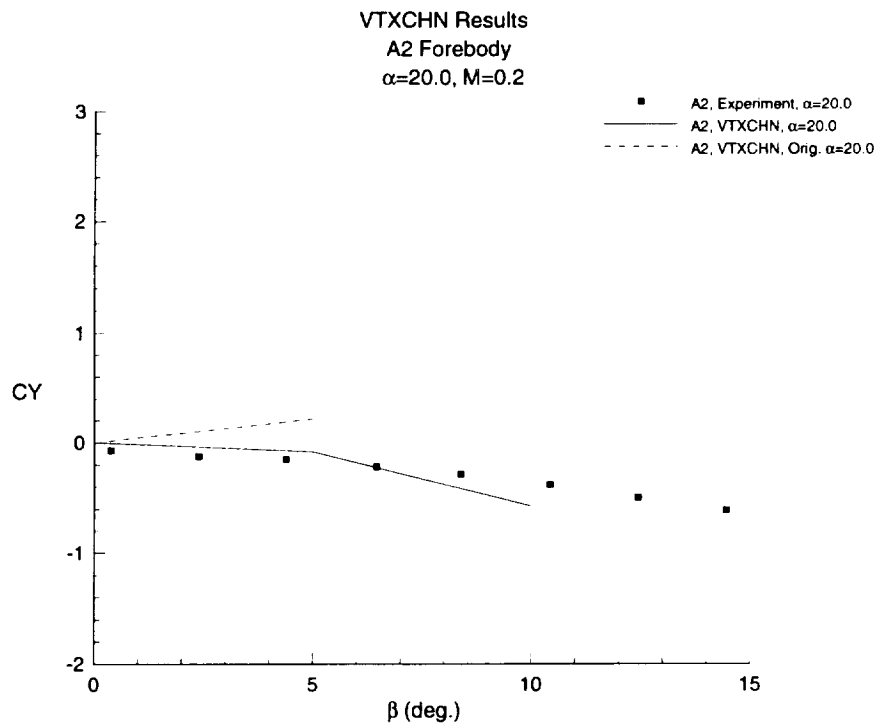


Figure 5.2-3 Lateral Characteristics for Forebody A2, AOA=20°, M=0.2

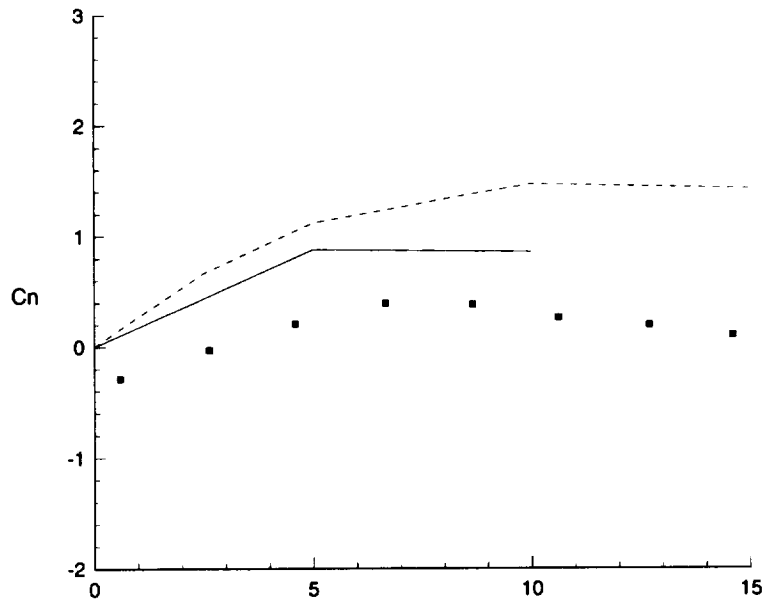
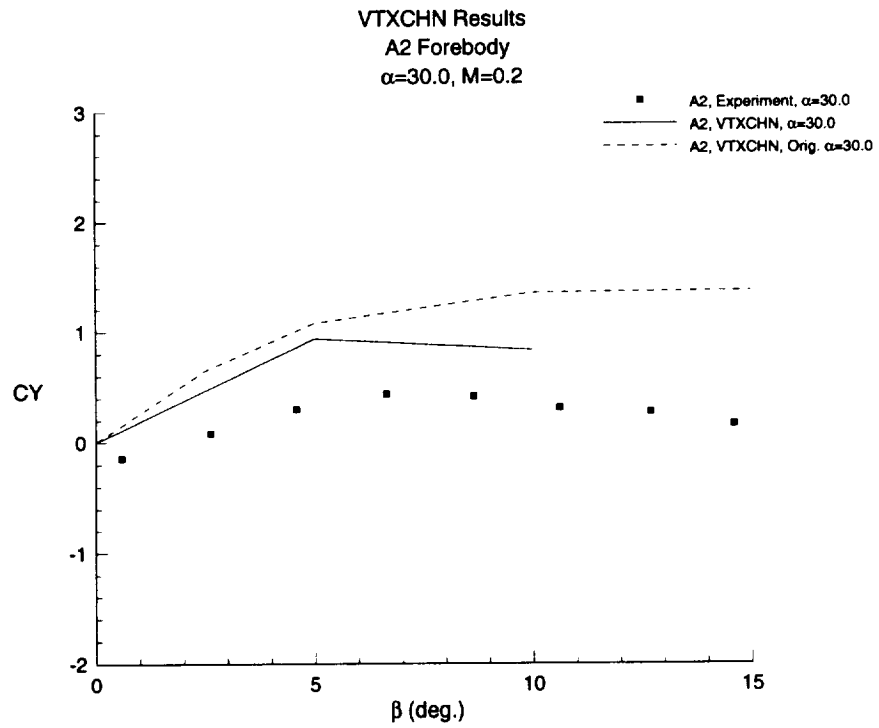


Figure 5.2-4 Lateral Characteristics for Forebody A2, AOA=30°, M=0.2

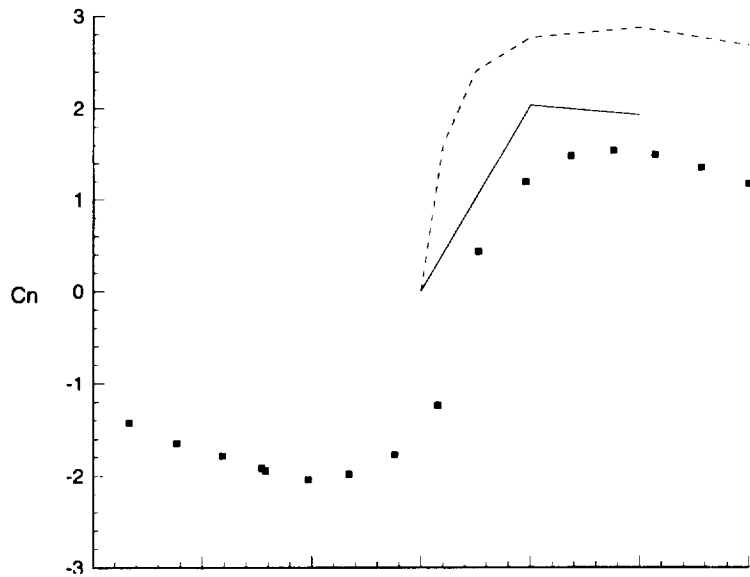
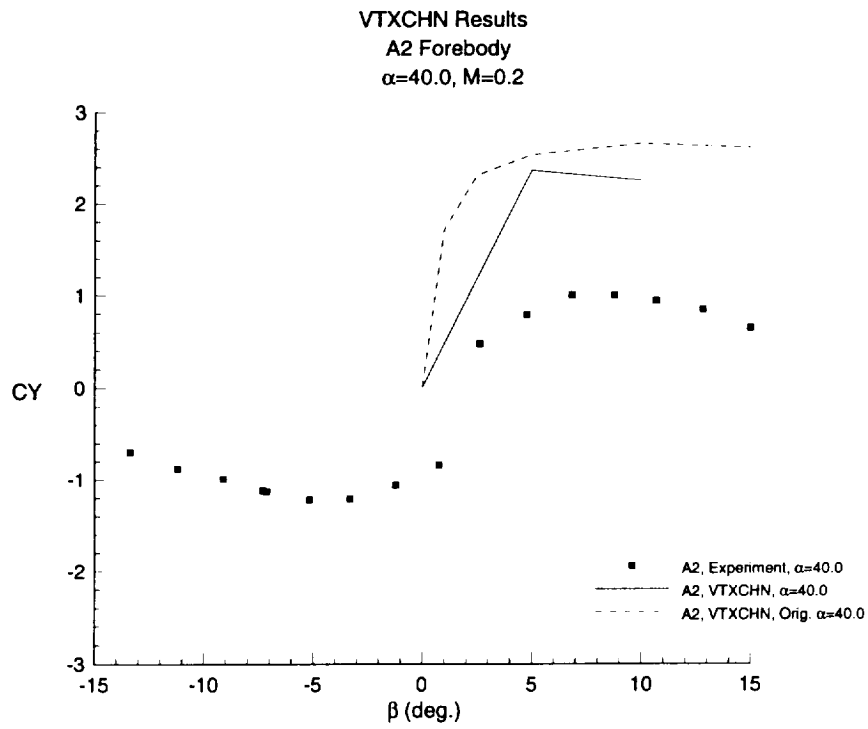


Figure 5.2-5 Lateral Characteristics for Forebody A2, AOA=40°, M=0.2

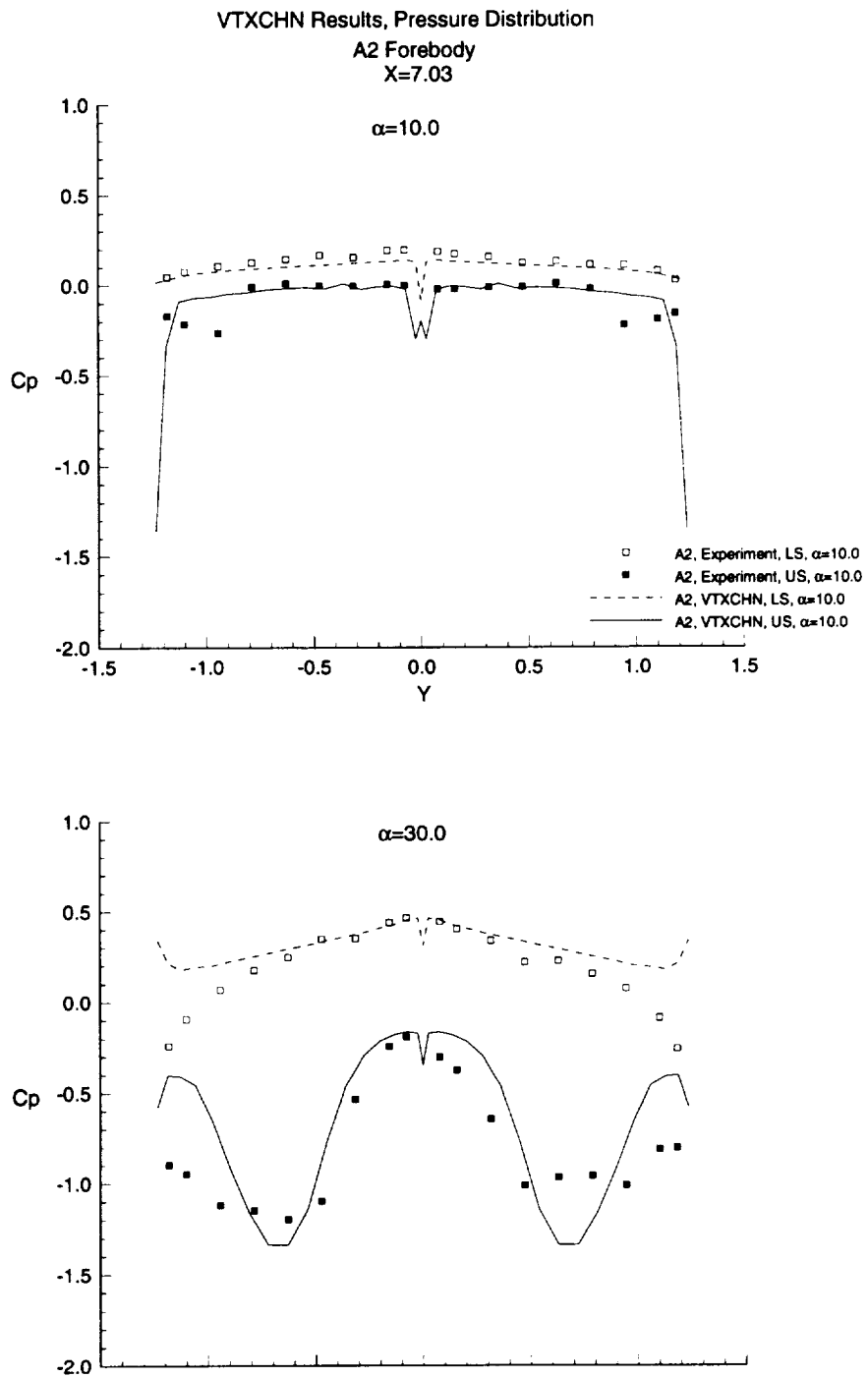


Figure 5.2-6 Pressure Coefficient for Forebody A2, M=0.2

### 5.3 B1 Forebody

Of the four bodies, the B1 forebody is unique in that it is neither a chined body, nor a smooth body. Because of this, the corners were treated in two different ways. The first was to force separation at the edge, the same way as the A2 and C1 bodies were handled. The second was to handle the shape as a smooth body, allowing VTXCHN to calculate the separation point using a Stratford flow separation criteria applied to the circumferential pressure distributions.

Figure 5.3-1 shows the longitudinal results for forebody B1. Up to 30 degrees angle of attack, the results from both methods are in good agreement to the data. At 40 degrees, the smooth body results are reasonable, but the forced separation results for both 40 and 50 degrees have risen back to those presented in reference 14. This is most likely a result of the higher vortex strengths that are predicted by a chined separation. At 50 degrees angle of attack, a result with the smooth body separation could not be obtained since the vortex tracker could not successfully track the vortices. The fact that the program could not track the vortices is purely due to a numerical constraint on the smooth body vortex tracking in the present version of the VTXCHN program.

Figures 5.3-2 through 5.3-4 show the lateral results with forced separation. Solutions in sideslip could not be obtained with smooth body separation for the same reason mentioned above. The lateral results up to 30 degrees angle of attack show good agreement with experiment. At 40 degrees angle of attack, the solution encounters a problem due to the large vorticity strengths.

Figure 5.3-6 shows the pressure distribution for the B1 forebody at an axial station of 7.03. For this cross section, at an angle of attack of 30 degrees, VTXCHN is unable to capture the low pressures on the sides of the top surface (solid line). The reason for this is presently unknown.

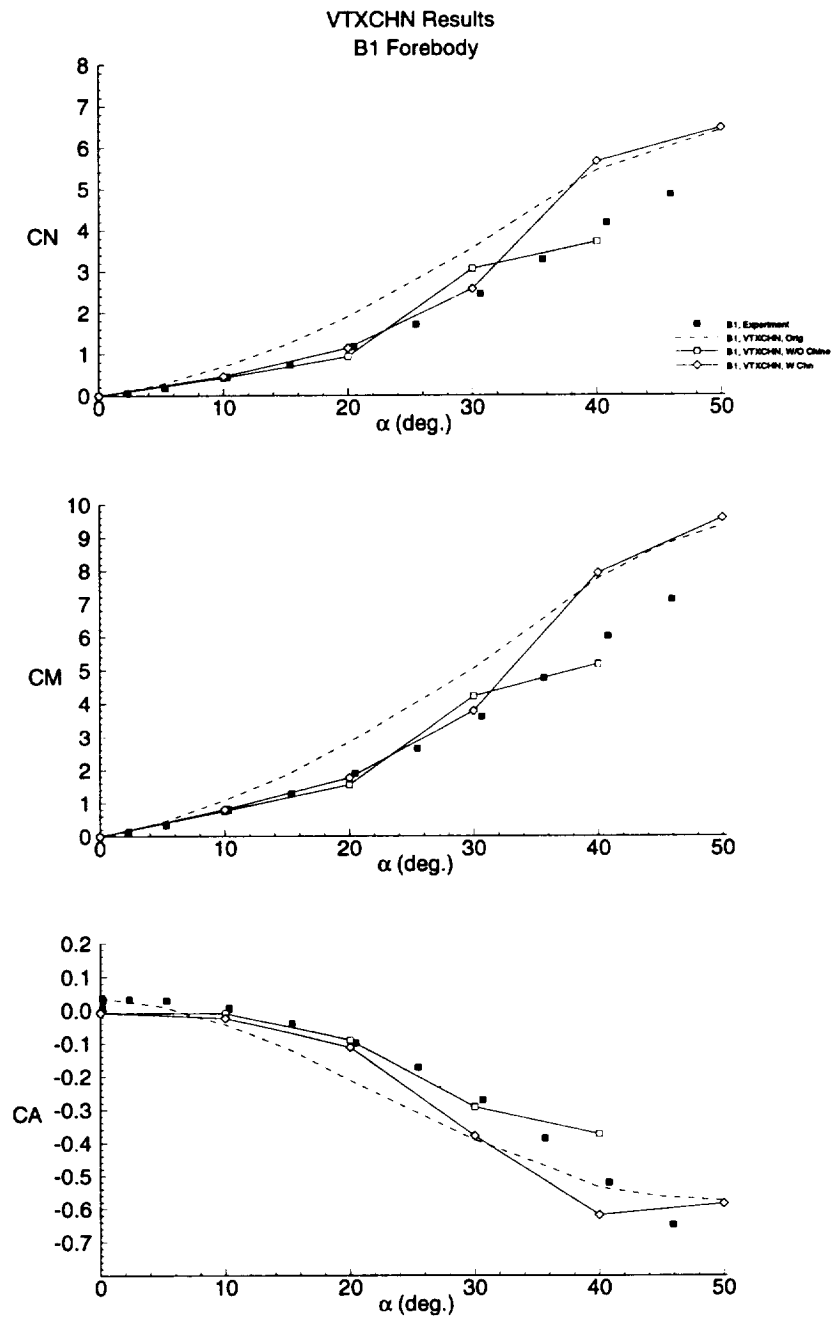


Figure 5.3-1 Longitudinal Characteristics for Forebody B1, M=0.2



VTXCHN Results  
 B1 Forebody  
 $\alpha=10.0$ ,  $M=0.2$

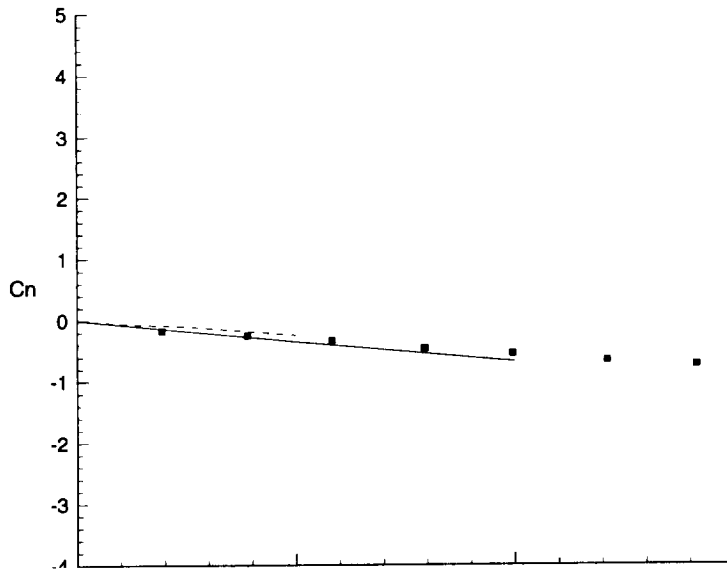
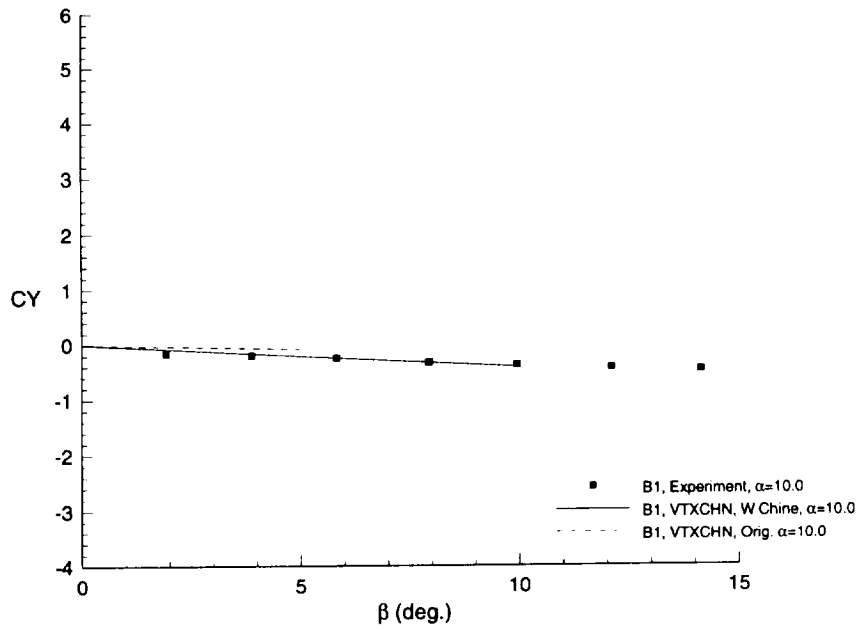


Figure 5.3-2 Lateral Characteristics for Forebody B1, AOA=10°, M=0.2

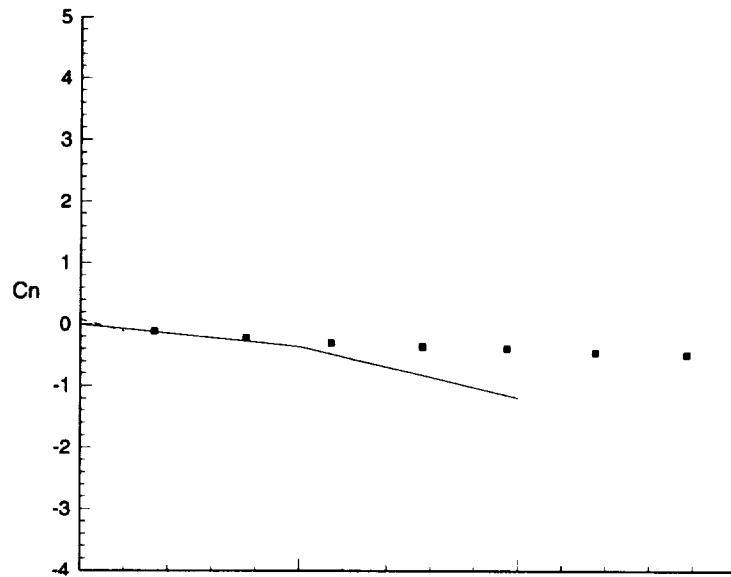
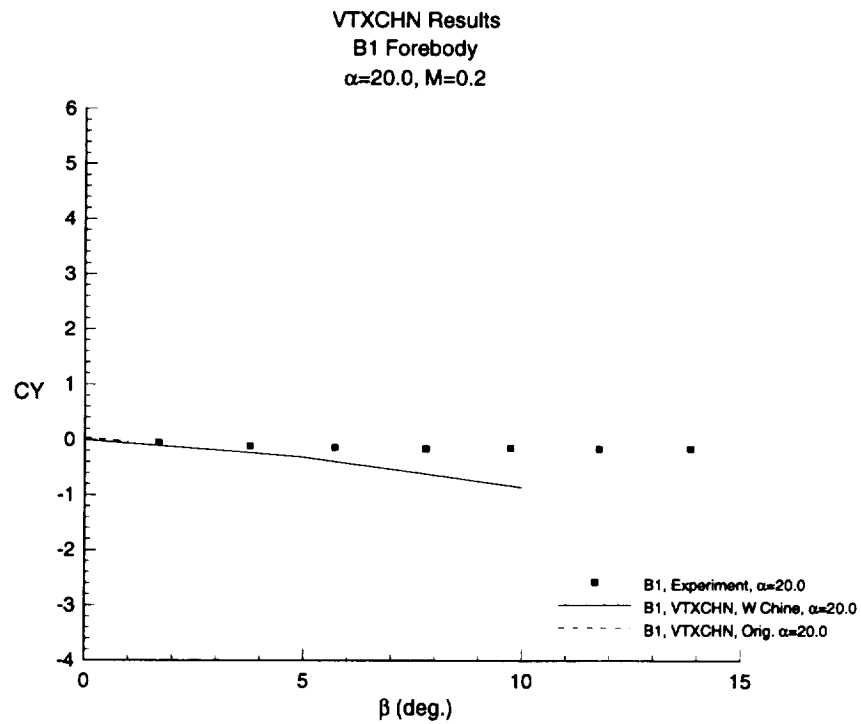


Figure 5.3-3 Lateral Characteristics for Forebody B1, AOA=20°, M=0.2

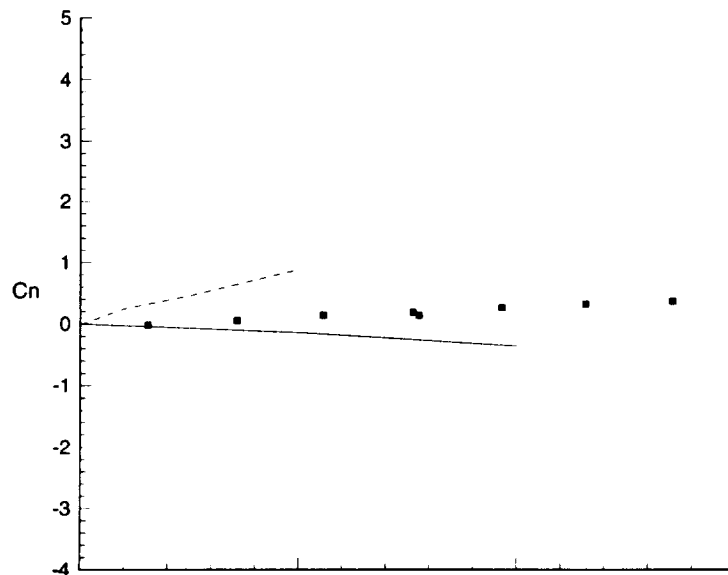
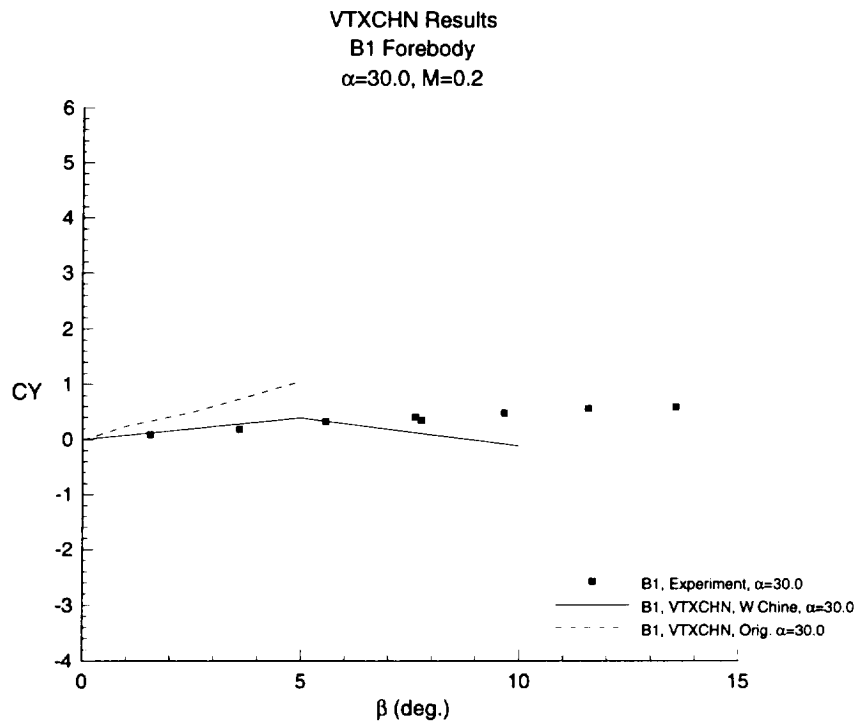


Figure 5.3-4 Lateral Characteristics for Forebody B1, AOA=30°, M=0.2

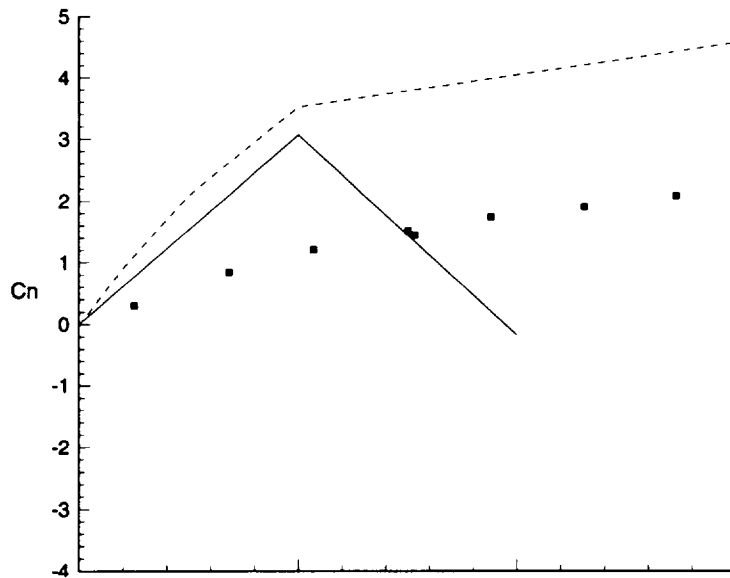
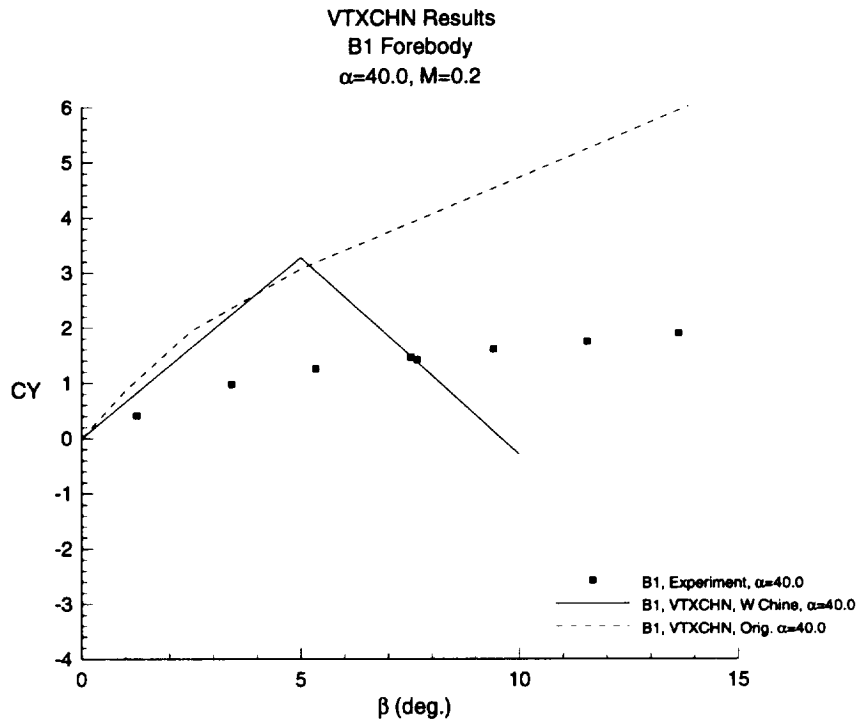


Figure 5.3-5 Lateral Characteristics for Forebody B1, AOA=40°, M=0.2

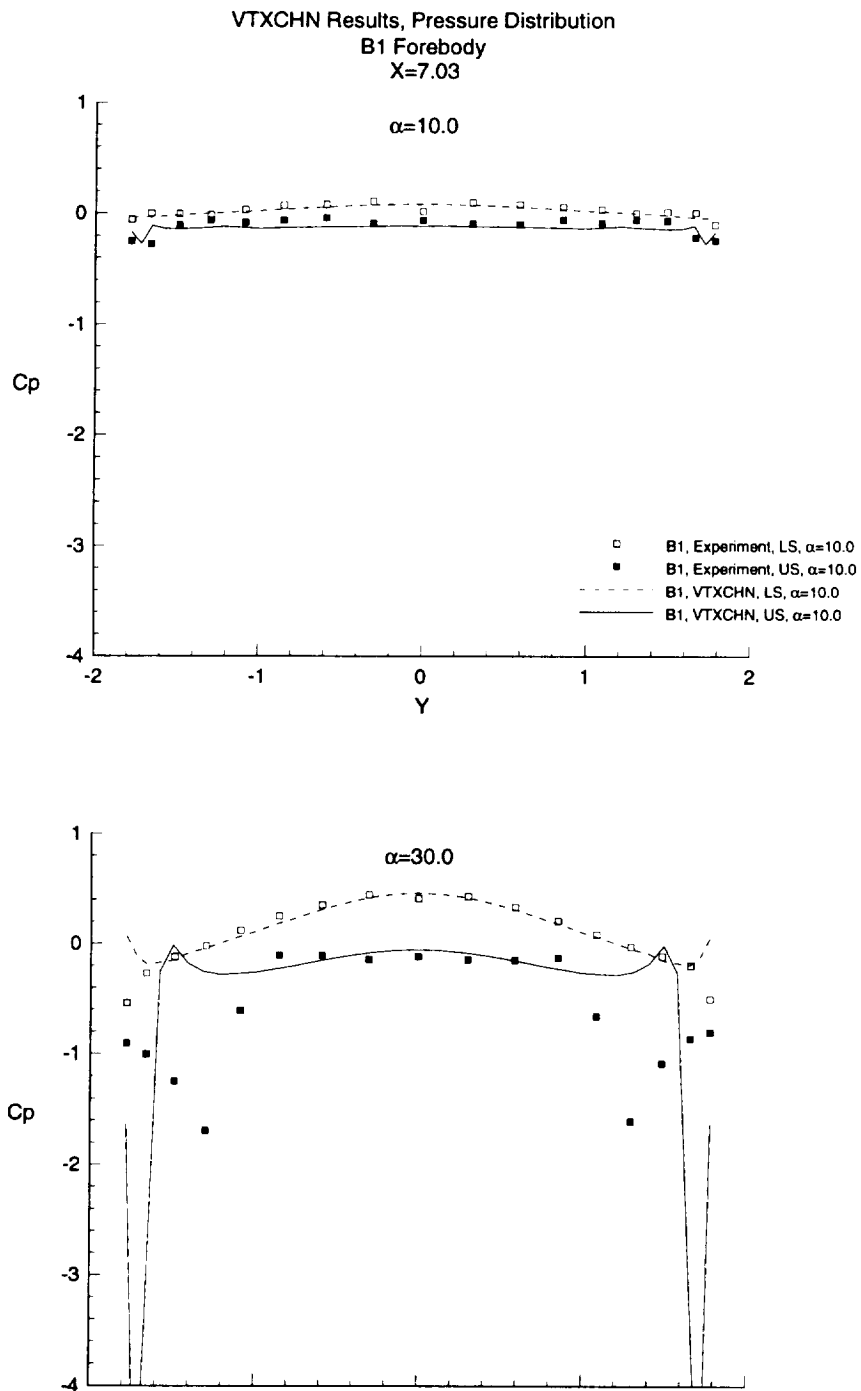


Figure 5.3-6 Pressure Coefficient for Forebody B1,  $M=0.2$

## 5.4 C1 Forebody

Figure 5.4-1 presents the longitudinal values for the sharp chined C1 forebody. The results agree with experiment up to 30 degrees angle of attack. Above this angle, the VTXCHN predictions are low probably due to the vortex cloud being too far from the body.

Figures 5.4-2 through 5.4-5 display the lateral characteristics. In general, the new predictions show an improvement over the results given in reference 14. The lateral results at an angle of attack of 30 and 40 degrees do not exhibit the flat characteristic of the experimental data. Again, this may be a result of the vortex cloud being washed into the side of the body.

The pressure distribution acting on the C1 forebody is given in Figure 5.4-6. Similar to B1, the agreement with test data is better on the lower surface than it is on the upper surface.

Figures 5.4-7 through 5.4-10 show the vortex field at  $x=7.06$  and  $x=14.06$  for 0 and 5 degrees angle of sideslip. It is interesting to note that at 40 degrees angle of attack, an angle of sideslip of 5 degrees drastically changes the flow field. Since the lateral aerodynamic characteristics are over predicted at this condition, it is likely that the flow field under these conditions is not predicted adequately.

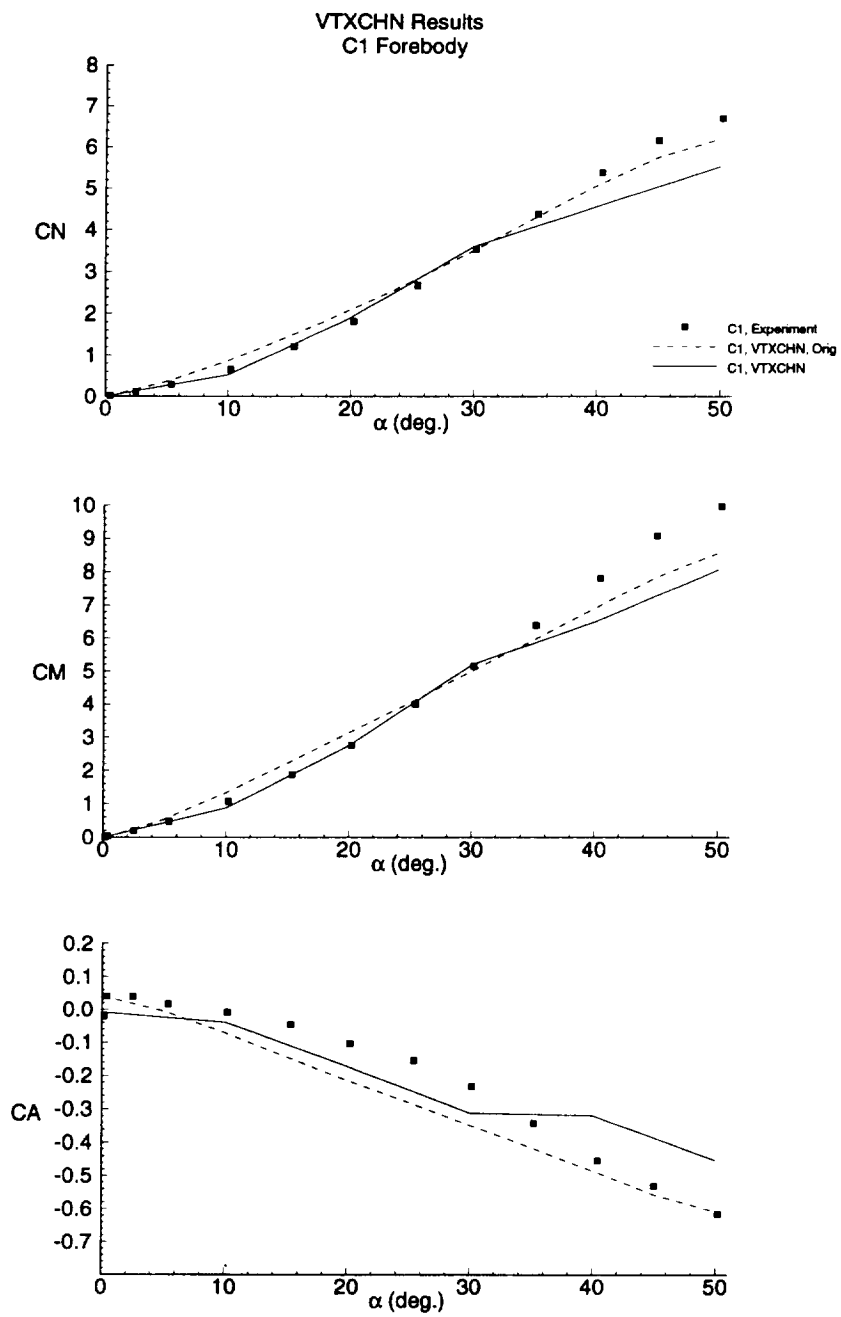


Figure 5.4-1 Longitudinal Characteristics for Forebody C1, M=0.2

VTXCHN Results  
 C1 Forebody  
 $\alpha=10.0$ ,  $M=0.2$

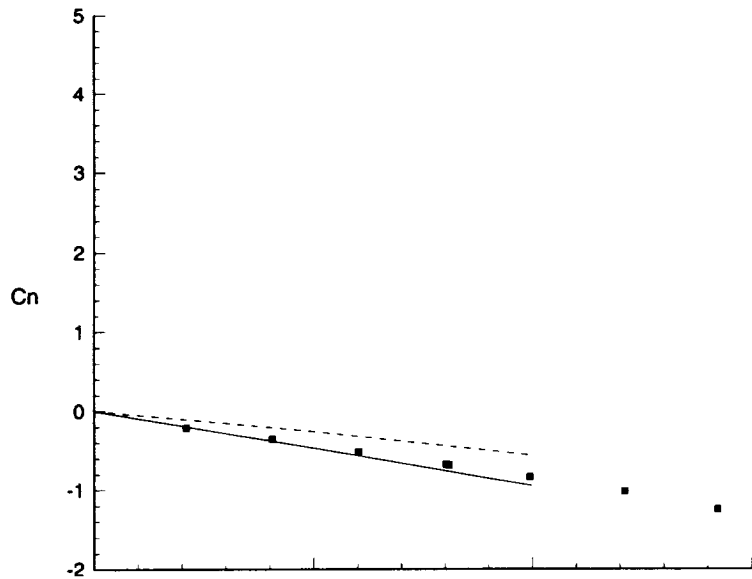
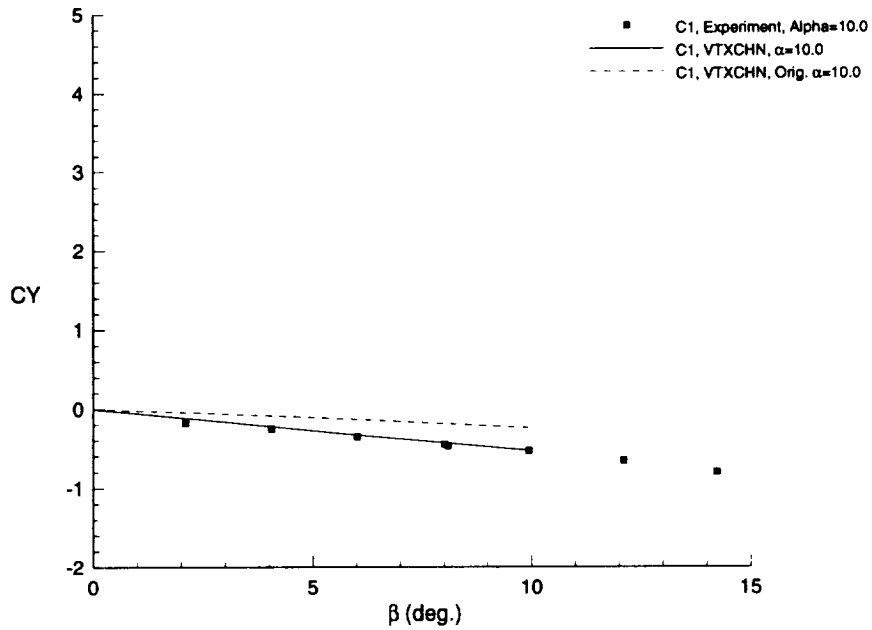


Figure 5.4-2 Lateral Characteristics for Forebody C1, AOA= $10^\circ$ ,  $M=0.2$



VTXCHN Results  
 C1 Forebody  
 $\alpha=20.0$ ,  $M=0.2$

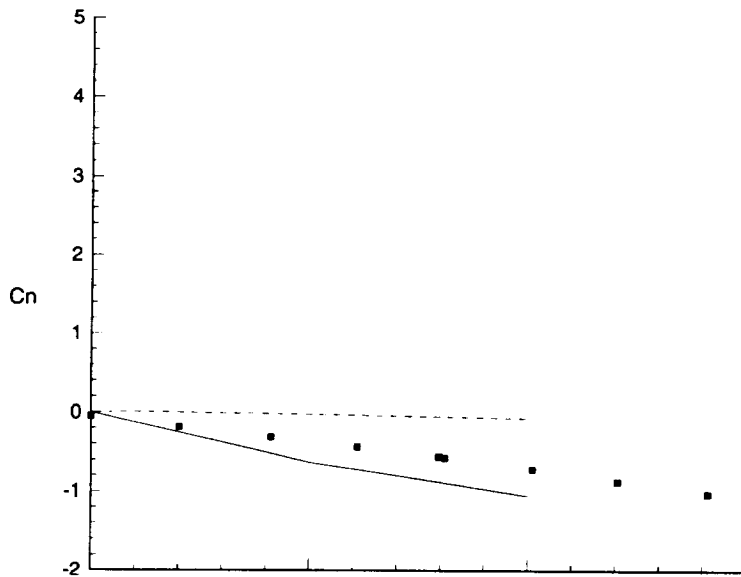
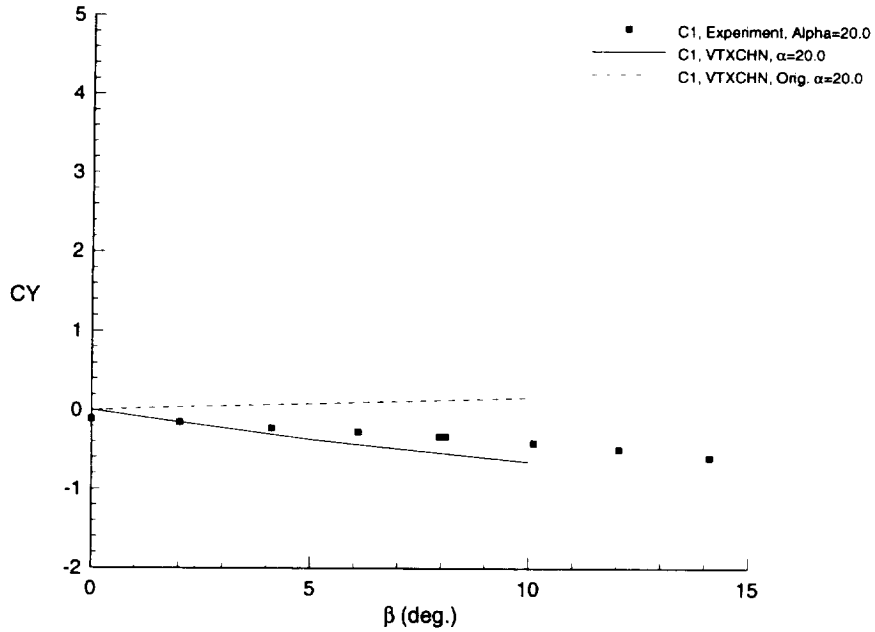


Figure 5.4-3 Lateral Characteristics for Forebody C1, AOA=20°, M=0.2

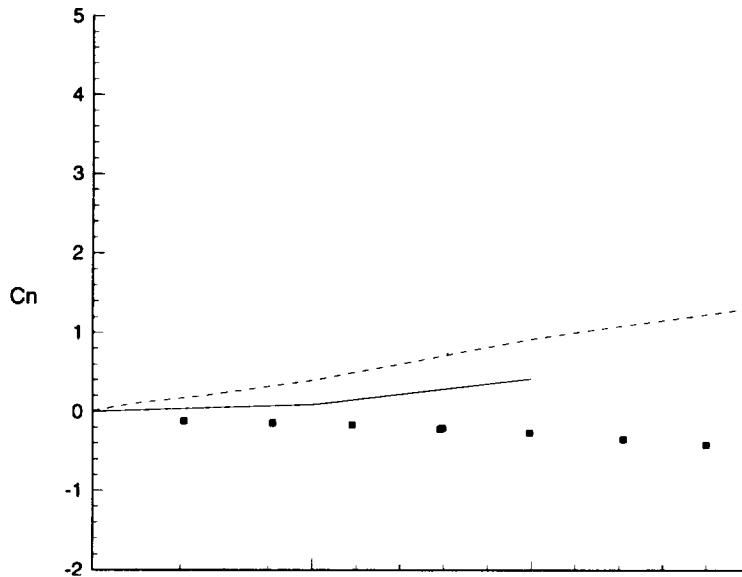
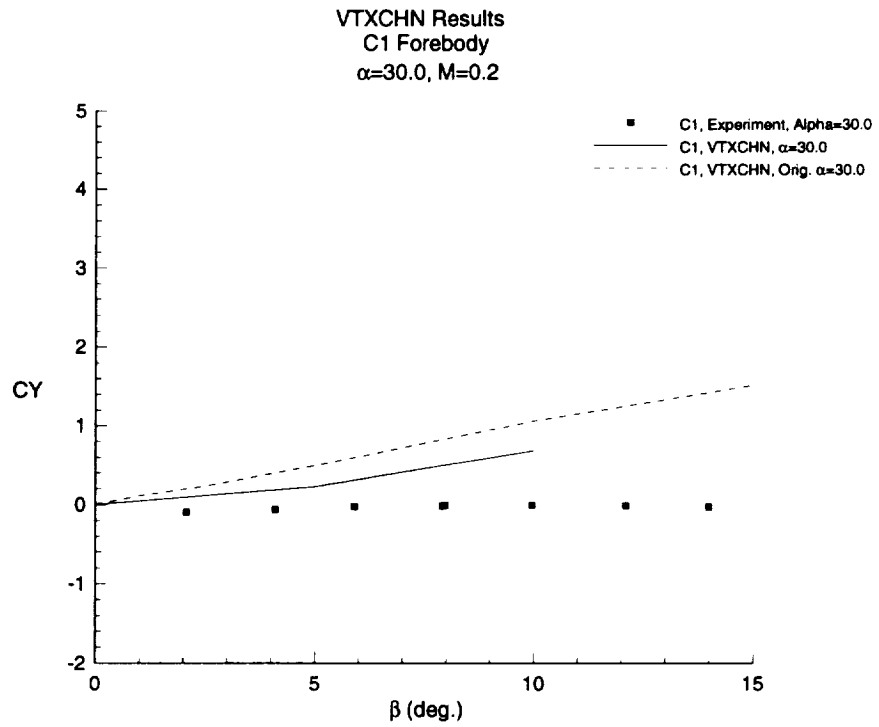


Figure 5.4-4 Lateral Characteristics for Forebody C1, AOA=30°, M=0.2

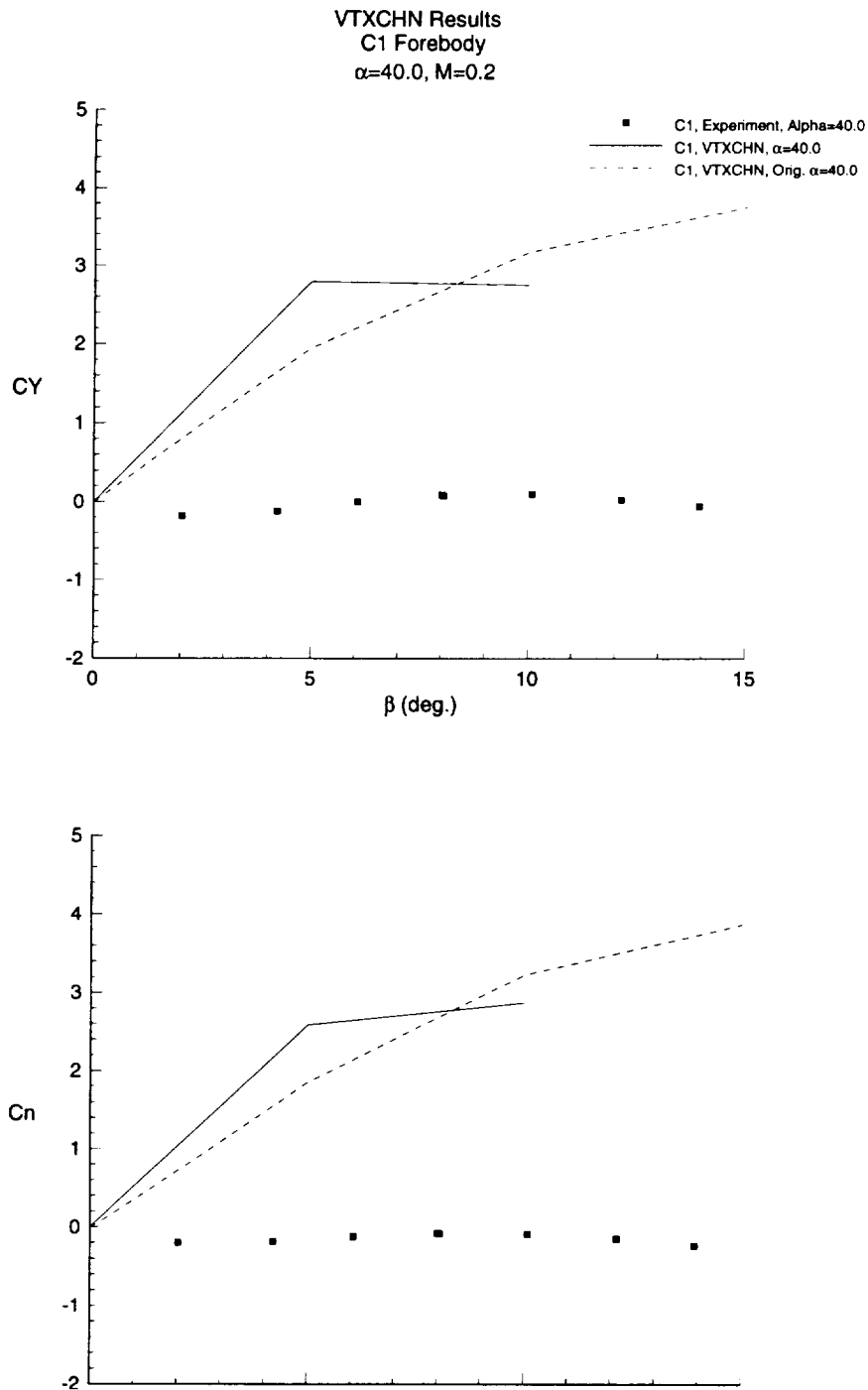


Figure 5.4-5 Lateral Characteristics for Forebody C1, AOA=40°, M=0.2

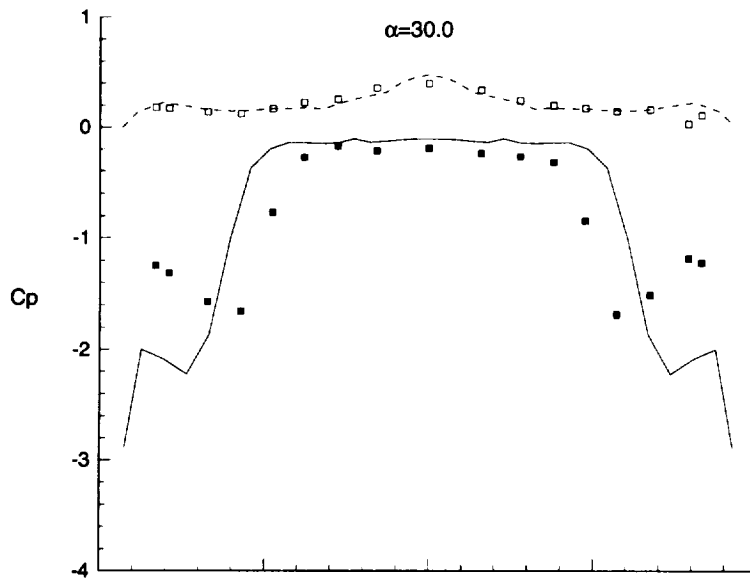
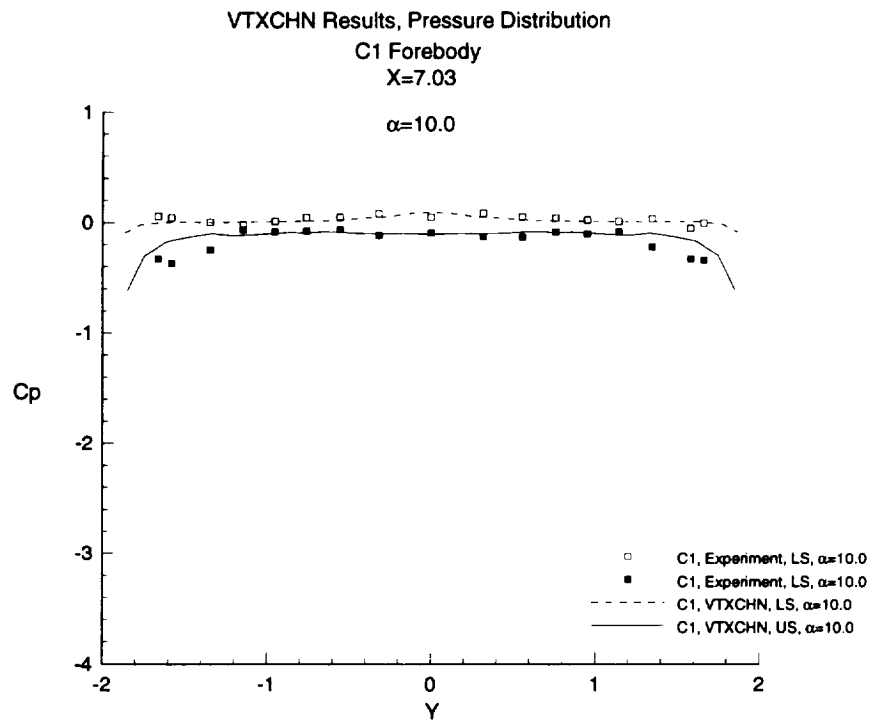


Figure 5.4-6 Pressure Coefficient for Forebody C1, M=0.2

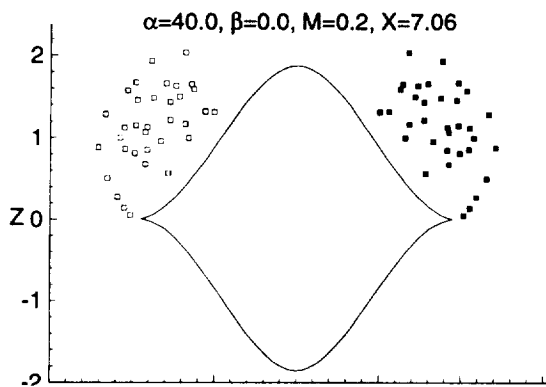
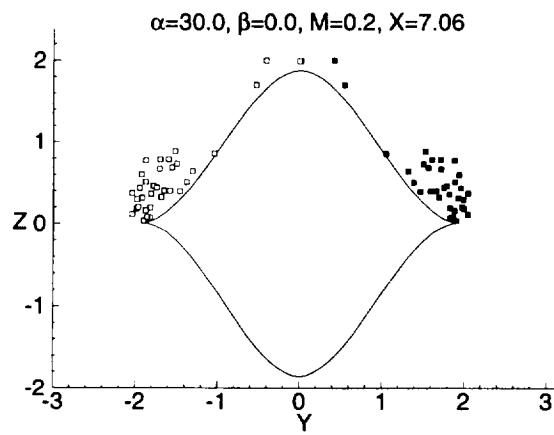
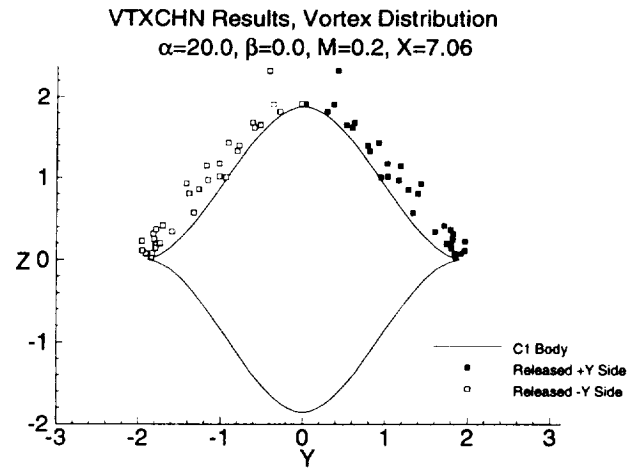


Figure 5.4-7 Vortex Distribution for Forebody C1, X=7.06, Beta=0°, M=0.2

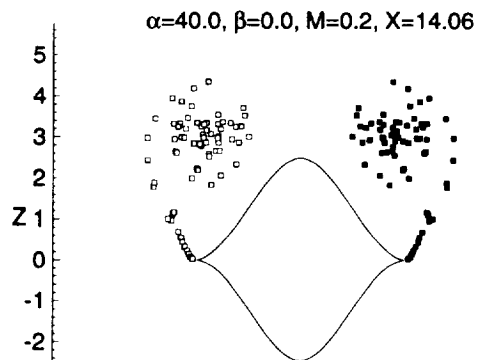
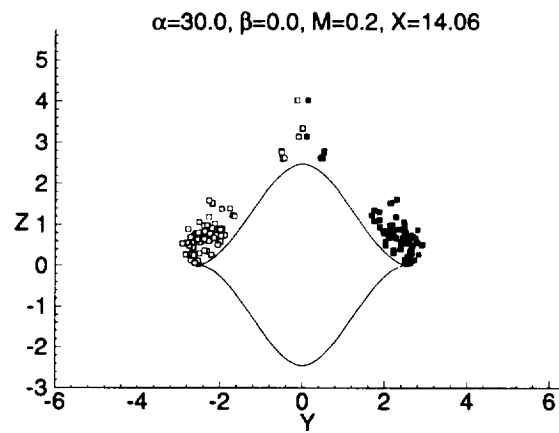
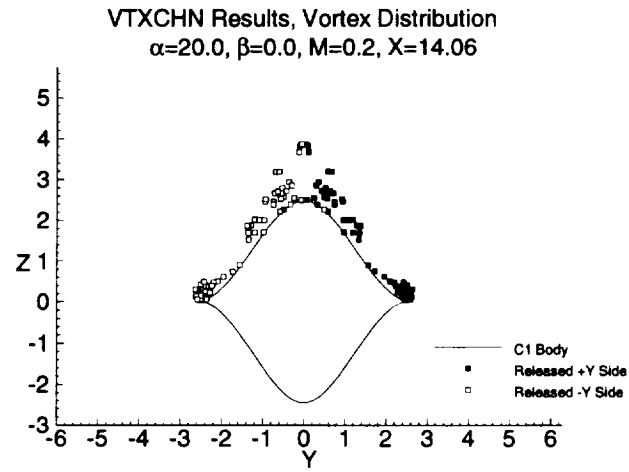
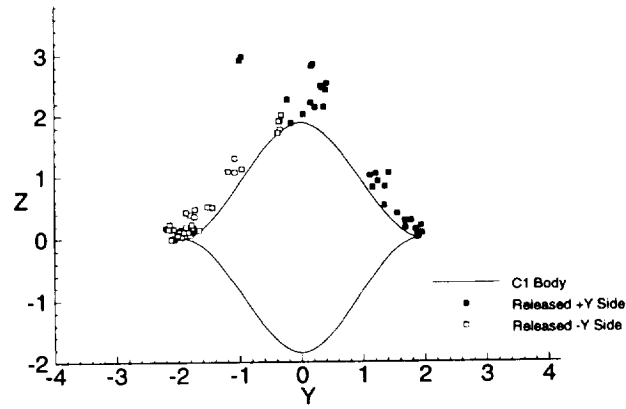
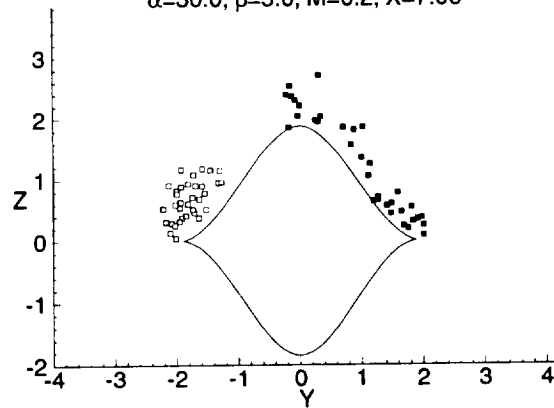


Figure 5.4-8 Vortex Distribution for Forebody C1,  $X=14.06$ ,  $\text{Beta}=0^\circ$ ,  $M=0.2$

VTXCHN Results, Vortex Distribution  
 $\alpha=20.0$ ,  $\beta=5.0$ ,  $M=0.2$ ,  $X=7.06$



$\alpha=30.0$ ,  $\beta=5.0$ ,  $M=0.2$ ,  $X=7.06$



$\alpha=40.0$ ,  $\beta=5.0$ ,  $M=0.2$ ,  $X=7.06$

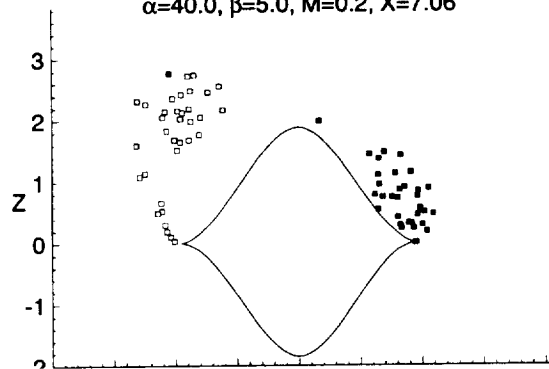


Figure 5.4-9 Vortex Distribution for Forebody C1,  $X=7.06$ ,  $\beta=5^\circ$ ,  $M=0.2$

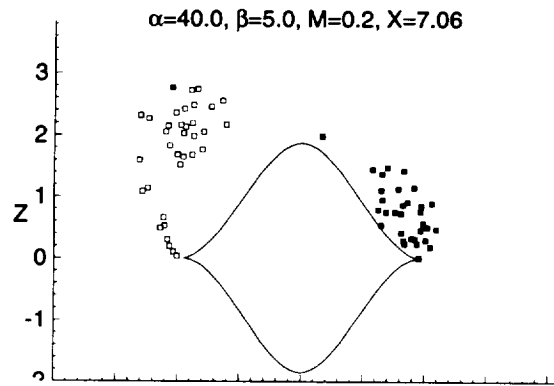
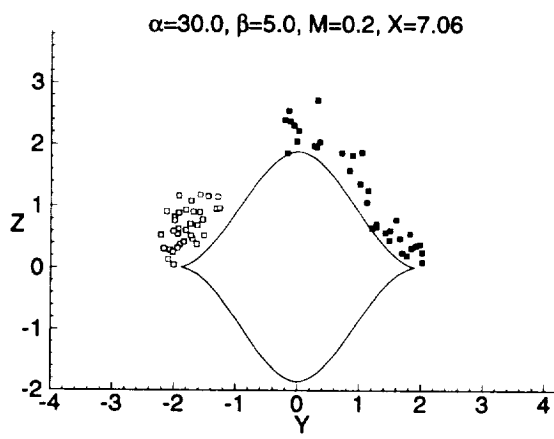
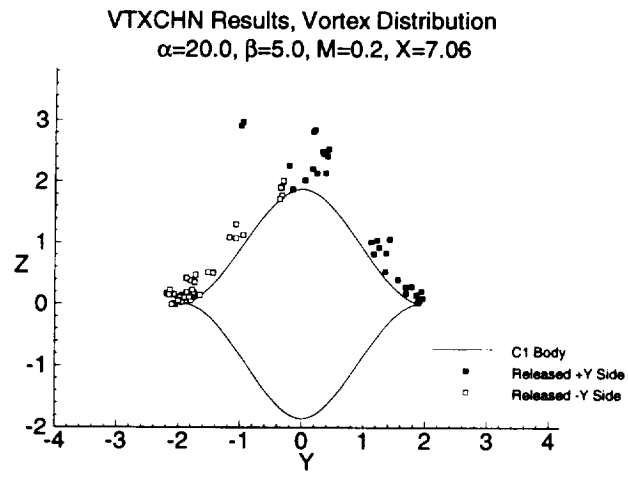


Figure 5.4-10 Vortex Distribution for Forebody C1,  $X=14.06$ ,  $\text{Beta}=5^\circ$ ,  $M=0.2$



## 5.5 VTXCHN Validation Summary

A number of problem areas and code limitations were identified during the reported investigation. They are listed below.

- 1) For the shapes that were investigated, the current version of VTXCHN gave the best longitudinal results when the angle of attack was less than 30 degrees. For lateral cases, the results compare well with experimental when the angle of attack was less than 20 degrees.
- 2) Vortex tracking can be very sensitive to changes in flow conditions and vortex related input variables. This is a consequence of the buildup of effects in the vortex tracking integration.
- 3) If the vortex core radius is too small, a vortex can be pulled down the side of the body by its image. This can cause the flow on the bottom of the chine to reverse and move away from the chine edge. Increasing the vortex core radius input parameter will reduce the possibility of the vortex being pulled down the side.
- 4) The numerical mapper creates cross sections which tend to be a slightly stretched from the original input cross section. The stretching occurs along the vertical axis and is a result of the method used in determining the mapping coefficients.
- 5) The numerical mapper creates singularities at all sharp corners on the body. This causes the velocities at those corners to be very large and the pressure coefficients to become undefined. This in turn causes all the integrated loads to become undefined.
- 6) It is important that the calculated source/sink radius distribution in the mapped plane match the mapped radius distribution.

For the four forebodies analyzed, including B1, the current version of VTXCHN shows significant improvement for the normal and pitching moment coefficients below an angle of attack of 30 degrees. This improvement is the result of the new tracker and the fixes in the mapping derivatives  $dv/dx$ . Likewise, the lateral coefficients have shown improvement for angles of attacks less than 20 degrees and angles of sideslip less than 10 degrees.

## 6.0 HASC VALIDATION

VTXCHN was validated by NEAR on four forebody shapes as presented in section 5 using the VTXCHN program prior to its integration into HASC. The VORLIF subroutines were validated by CAS. HASC, with the new VTXCHN and VORLIF subroutines, was validated by LMTAS. Figure 6.0-1 presents an overview of this validation process as documented in this report.

Several of the validation plots compare the different methods of running HASC. Included in sections 6.2 through 6.6 are plots and discussion comparing the results from VTXCHN vs. VORLAX, and from VORLAX vs. VORLIF. All predictions in section 6.1 are from using VORLIF on the lifting surfaces.

<p><b>VTXCHN Validation</b> (section 5) Nielsen Engineering &amp; Research, Inc.</p> <ol style="list-style-type: none"> <li>1. Forebody A1 (circular)</li> <li>2. Forebody A2 (diamond)</li> <li>3. Forebody B1 (smooth chine)</li> <li>4. Forebody C1 (sharp chine)</li> </ol>	<p><b>VORLIF Validation</b> (section 6.1) Consulting Aviation Services</p> <ol style="list-style-type: none"> <li>1. 63° delta wing</li> <li>2. Hummel wing</li> <li>3. 44° Trapezoidal Wing &amp; Canard</li> <li>4. 65° delta wing</li> </ol>						
<p align="center"><b>HASC Validation</b> (section 6.2-6.6) Lockheed Martin Tactical Aircraft Systems</p> <table border="0"> <tr> <td data-bbox="354 1199 784 1373"> <p><u>1. Tailless Fighter</u></p> <ul style="list-style-type: none"> <li>• Baseline longitudinal</li> <li>• Panel sensitivity</li> <li>• VORLAX vs VORLIF</li> <li>• RH elevon (long., lat/dir.)</li> </ul> </td> <td data-bbox="816 1199 1166 1339"> <p><u>3. F-16XL</u></p> <ul style="list-style-type: none"> <li>• Baseline longitudinal</li> <li>• Vortex flag sensitivity</li> <li>• Symmetric elevon</li> </ul> </td> </tr> <tr> <td data-bbox="354 1415 784 1625"> <p><u>2. Falcon 21</u></p> <ul style="list-style-type: none"> <li>• Baseline longitudinal</li> <li>• Forebody comparison</li> <li>• LE flap</li> <li>• Sym. TE flap</li> <li>• Asym. TE flap</li> </ul> </td> <td data-bbox="816 1381 1166 1625"> <p><u>4. F-16</u></p> <ul style="list-style-type: none"> <li>• Baseline long. &amp; lat/dir.</li> <li>• Vortex flag sensitivity</li> <li>• Horizontal tail</li> <li>• LE flap</li> <li>• Rudder</li> <li>• Damping derivatives</li> </ul> </td> </tr> <tr> <td></td> <td data-bbox="816 1667 1166 1730"> <p><u>5. Convair Model 200</u></p> <ul style="list-style-type: none"> <li>• Baseline longitudinal</li> </ul> </td> </tr> </table>		<p><u>1. Tailless Fighter</u></p> <ul style="list-style-type: none"> <li>• Baseline longitudinal</li> <li>• Panel sensitivity</li> <li>• VORLAX vs VORLIF</li> <li>• RH elevon (long., lat/dir.)</li> </ul>	<p><u>3. F-16XL</u></p> <ul style="list-style-type: none"> <li>• Baseline longitudinal</li> <li>• Vortex flag sensitivity</li> <li>• Symmetric elevon</li> </ul>	<p><u>2. Falcon 21</u></p> <ul style="list-style-type: none"> <li>• Baseline longitudinal</li> <li>• Forebody comparison</li> <li>• LE flap</li> <li>• Sym. TE flap</li> <li>• Asym. TE flap</li> </ul>	<p><u>4. F-16</u></p> <ul style="list-style-type: none"> <li>• Baseline long. &amp; lat/dir.</li> <li>• Vortex flag sensitivity</li> <li>• Horizontal tail</li> <li>• LE flap</li> <li>• Rudder</li> <li>• Damping derivatives</li> </ul>		<p><u>5. Convair Model 200</u></p> <ul style="list-style-type: none"> <li>• Baseline longitudinal</li> </ul>
<p><u>1. Tailless Fighter</u></p> <ul style="list-style-type: none"> <li>• Baseline longitudinal</li> <li>• Panel sensitivity</li> <li>• VORLAX vs VORLIF</li> <li>• RH elevon (long., lat/dir.)</li> </ul>	<p><u>3. F-16XL</u></p> <ul style="list-style-type: none"> <li>• Baseline longitudinal</li> <li>• Vortex flag sensitivity</li> <li>• Symmetric elevon</li> </ul>						
<p><u>2. Falcon 21</u></p> <ul style="list-style-type: none"> <li>• Baseline longitudinal</li> <li>• Forebody comparison</li> <li>• LE flap</li> <li>• Sym. TE flap</li> <li>• Asym. TE flap</li> </ul>	<p><u>4. F-16</u></p> <ul style="list-style-type: none"> <li>• Baseline long. &amp; lat/dir.</li> <li>• Vortex flag sensitivity</li> <li>• Horizontal tail</li> <li>• LE flap</li> <li>• Rudder</li> <li>• Damping derivatives</li> </ul>						
	<p><u>5. Convair Model 200</u></p> <ul style="list-style-type: none"> <li>• Baseline longitudinal</li> </ul>						

Figure 6.0-1 Summary of HASC Validation Cases

## 6.1 CAS Validation Configurations

### The 63.03 Delta Wing

A 63.03 degree delta wing (reference 10) is considered a baseline configuration for the development and verification of the HASC code. This wing was tested at nearly full scale Reynolds number, plus a comprehensive set of pressure data is available. Several configurations, including this 63.03 degree wing, were used to set the empirical factors in HASC. Figure 6.1-1 shows excellent agreement with the lift and pitching moment coefficients comparing the test results to the HASC predictions.

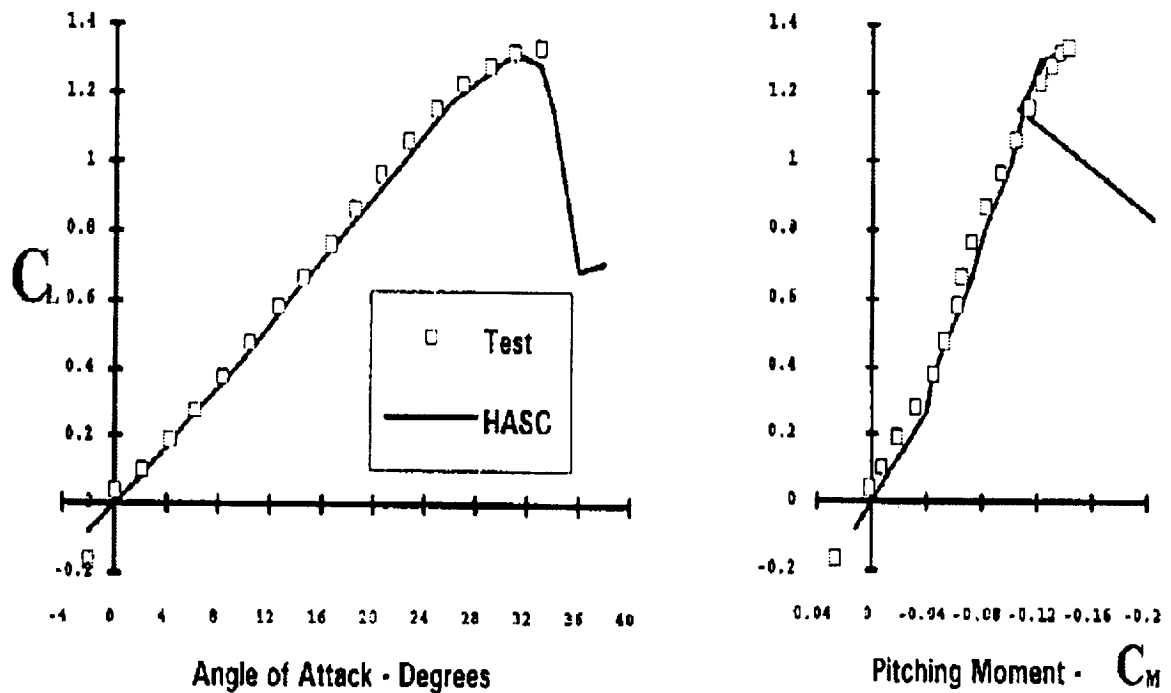


Figure 6.1-1 63.03 Degree Wing Baseline Comparison

## The Hummel wing

The Hummel wing (reference 11), shown in figure 6.1-2, is a high-swept, aspect-ratio-one wing with camber due to beveling on the lower surface. Good results were obtained with the HASC code, however some improvements in the stall range could be made. High sweep configurations have the free vortices so close together that their mutual interference effects are not fully captured in HASC.

The free vortices are not currently represented in the boundary conditions for the basic vortex lattice part of the code. To do this would require a major change, however it should be done to eliminate some of the empiricism that is presently required for these high swept delta wings. This will also improve the cases where multiple vortices such as formed by a strake and wing combination.

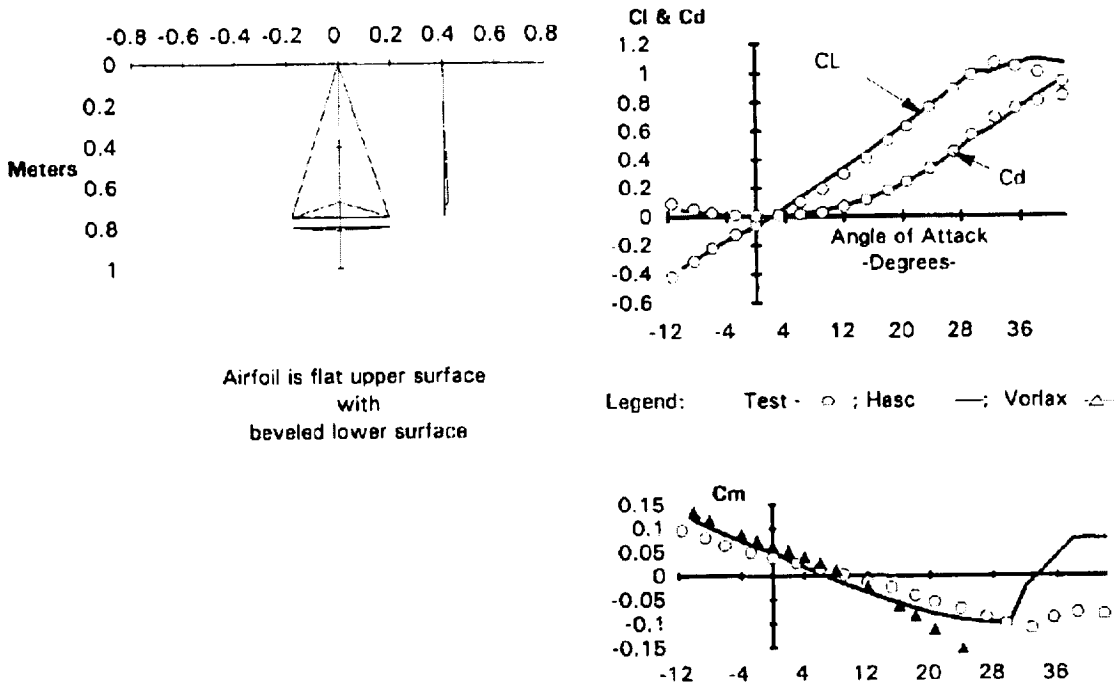


Figure 6.1-2 Hummel Wing Baseline Comparison

## 44 Degree Trapezoidal Wing with Canard

A canard configuration was taken from Carlson's report (reference 15) to illustrate the prediction capability of HASC on configurations with two lifting surfaces both analyzed with VORLIF to include vortex breakdown effects. Figure 6.1-3 shows the HASC predictions and the test results for the selected canard configuration. The configuration test data came from a generic test conducted by Carlson, et. al., at NASA Langley Research Center. Both the wing and canard are 44 degree trapezoidal planforms. The canard is located at the top of the fuselage, and the wing is at mid fuselage. Airfoils for the wing are uncertain, but reference 15 indicates the wing is probably a NACA 6 series with 6% thickness at the root and 4% at the wing tip. Maximum thickness is at 40% of the chord.

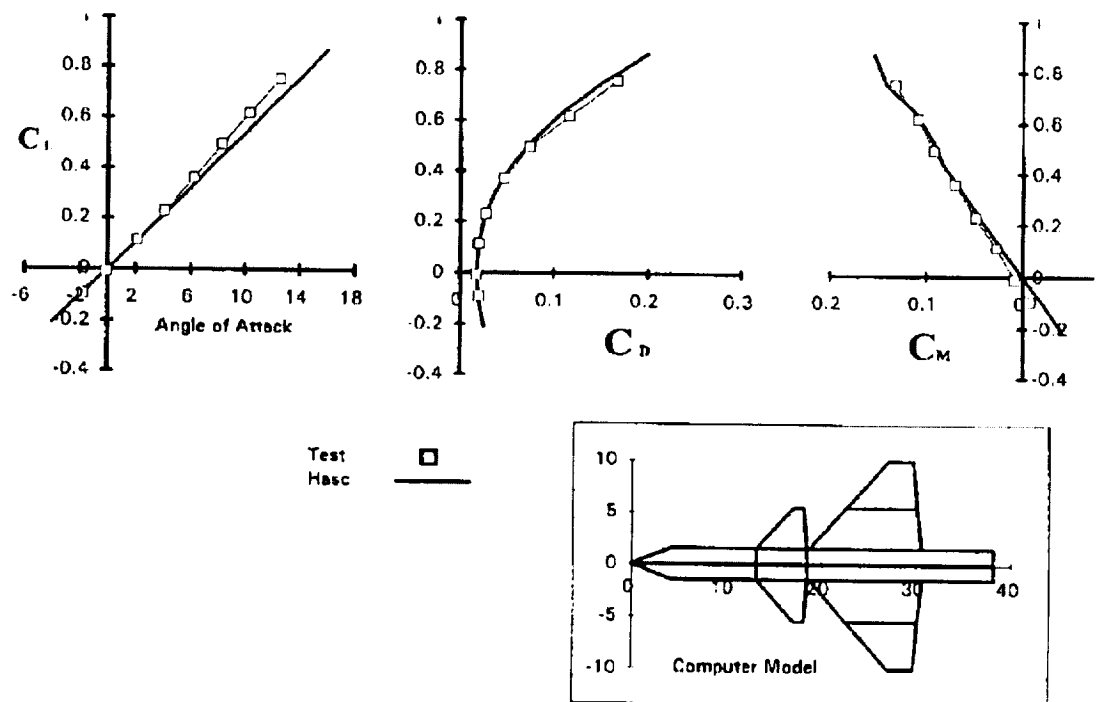


Figure 6.1-3 44 Degree Trapezoidal Wing and Canard Baseline Comparison

The canard is also a NACA 6 series airfoil and is assumed to have the same airfoil types as the wing. The latter may be the reason the HASC predicted lift is a lower than the test data. If the canard has thinner airfoils, more vortex lift will occur as the angle of attack increases.

The HASC code was run for the same configuration with the canard at a mid-fuselage position and at a low position. The results showed that the mid-fuselage position produced less lift than the high-position. In modeling the mid-fuselage canard the fuselage portion of the canard was the same as the fuselage for the wing. The high canard required another panel to represent the fuselage between the canard left and right surfaces. This fuselage could be input as a type 4 surface so that no loads are added; i.e., only its influence is considered. The correct surface, however, is a type 5, because there is additional carry over of lift from the canards to the fuselage.

The low canard (below the wing level) produced characteristics almost the same as the mid-fuselage canard; that is, until the wake from the canard crossed the wing. At this angle of attack the aerodynamic characteristics became irrational. Above this angle the characteristics came back to normal. This is not surprising since this happens on the actual airplane with less severe effect.

The configuration did have vortex breakdown. Unfortunately, the test data did not go high enough in angle of attack to compare the effects of vortex bursting. In HASC any change in the lift of the forward surface due to vortex breakdown or burst is reflected as a change in downwash at the aft surface. These effects are more pronounced for a configuration such as the F-16 having a tail in the wake of a wing.

## 65 Degree Delta Wing

Steady roll, yaw, and pitch rate effects can be analyzed in HASC with vortex breakdown included (VORLIF). Some examples, conditions, and suggestions are given in the following section for predicting steady-state rate derivatives.

### Pitch Rate Derivatives:

Figure 6.1-4 shows the predicted pitch rate derivatives for a 65 degree delta wing (references 16 and 17) with 20 degree symmetrically beveled leading edges. As noted in the figure, the breaks in the curves are primarily due to vortex breakdown. To obtain the pitch rate derivative  $C_{mq}$  the difference between the absolute values with and without the pitch rate is obtained. Some caution is suggested for interpretation of these results.

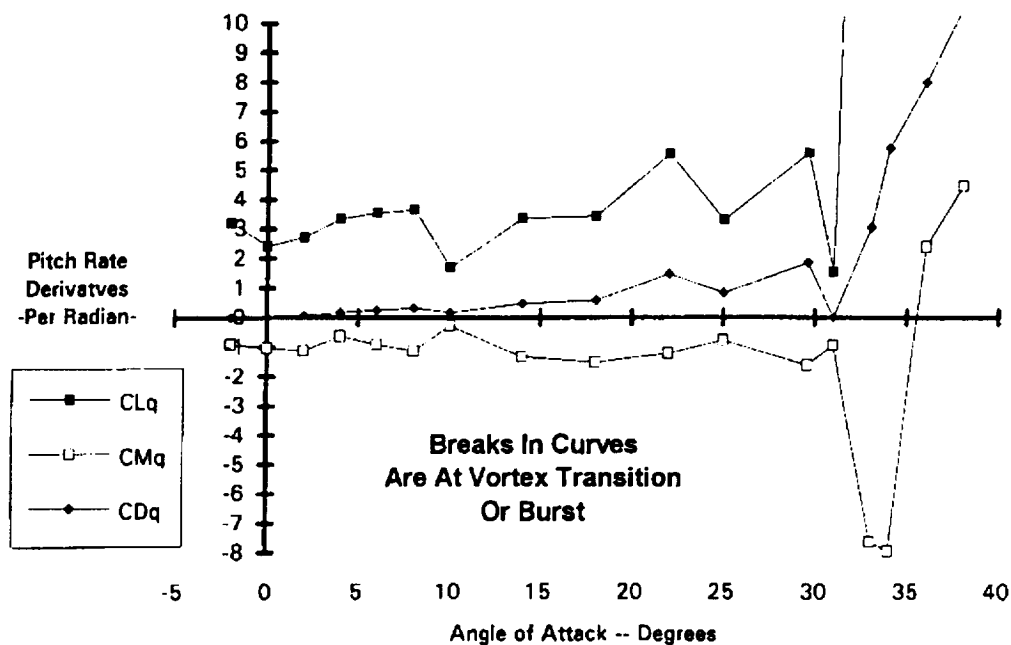


Figure 6.1-4 Predicted Pitch Rate Derivatives for a 65 degree Delta Wing



The break at 10 degrees angle of attack in figure 6.1-4 is due to transition of the vortex on both the zero and non-zero pitch rate cases. The effect is initially more severe for the case with the pitch rate, but progresses more slowly than the zero pitch rate case. Vortex burst begins with the zero pitch rate case at about 22 degrees, then with the 0.01 pitch rate case at 25 degrees. The maximum lift angle of attack is delayed 3 degrees for the case with the pitch rate. If the pitch rate is made an order of magnitude higher, the breakdown and burst may be delayed to a much higher value. Therefore it is suggested that the configuration be run at pitch rates that are expected on the actual airplane.

The low value of pitch rate was used so that the resulting effective camber would be small. This did not cause a large negative angle of zero lift. If larger values of pitch rate were used the estimated angle of zero lift would have to be input at a larger negative value. A problem with using a low pitch rate is that the difference between two large numbers becomes the pitch rate derivative. This leaves room for errors.

#### Roll and Yaw Rate Derivatives:

The 65 degree delta wing was run at roll and yaw rates of 0.1 radian. VINP was set to 1/2 the wing span. With these two conditions, the roll and yaw rate derivatives can be obtained by multiplying the final rolling and yawing moment coefficients by 10.0. As with the pitch rate problem, caution is suggested for interpretation. Roll and yaw rates also change the vortex breakdown characteristics.

To evaluate the HASC results the steady state and oscillating roll results of reference 17 were reviewed. First, a steady state simulation of the 65 degree wing with its longitudinal axis at 30 degrees and a roll angle of 10 degrees was made with HASC. This was done by running the HASC code at the effective stability axis angle of attack and sideslip angle. The rolling moment at this condition according to HASC is 0.022. Data in reference 17 gives 0.025 for the value. Considering that in the HASC prediction the wing is approaching maximum lift and vortex breakdown has occurred on the windward wing, this comparison is very good.

## 6.2 Tailless Fighter Configuration

### Background

Five different aircraft configurations were used at LMTAS to validate the new HASC code. The first configuration was a 65 degree swept all-wing configuration. Mach =0.30 data from a 1/18-scale force and moment model tested at the Subsonic Aerodynamic Research Laboratory (SARL) wind tunnel at Wright Patterson Air Force Base was used for comparison to the HASC predictions. The tailless fighter configuration, with lines representing the HASC spanwise panel boundaries, is shown in figure 6.2-1.

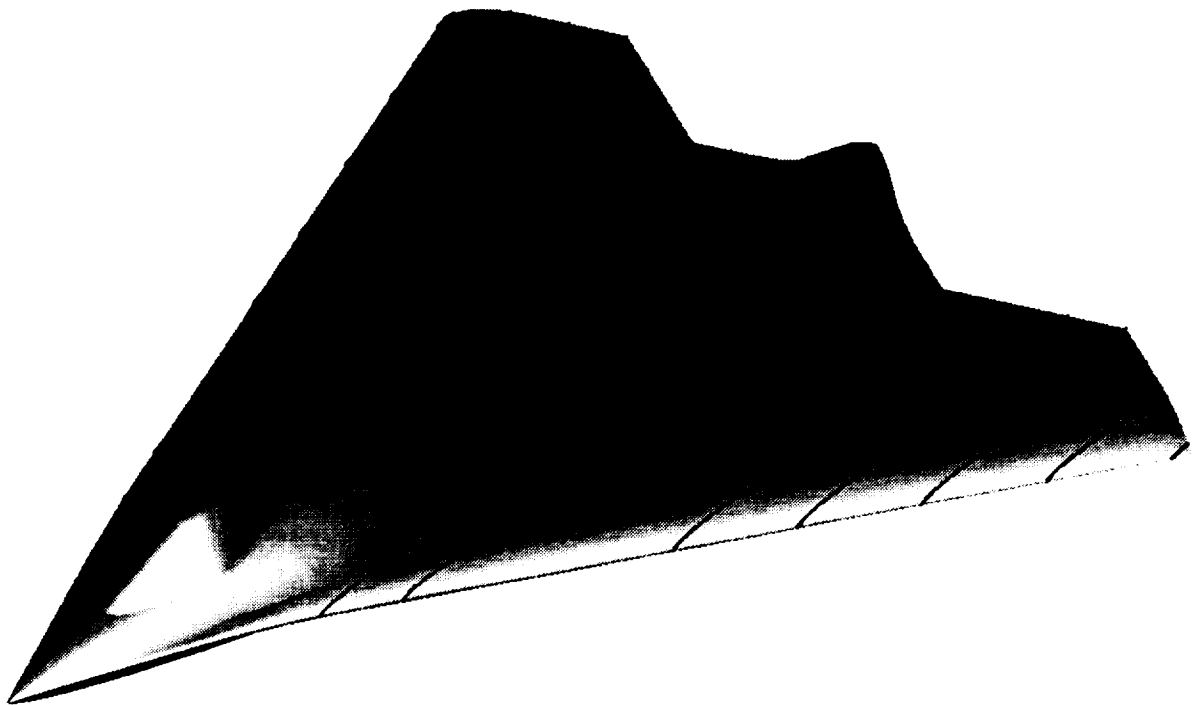


Figure 6.2-1 Tailless Fighter Configuration

The validation figures in sections 6.2 through 6.6 contain small plots of the geometry model used in the HASC runs. These plots show the sub-panels with linear chordwise spacing, however cosine spacing was used in the actual runs. Also, since HASC does not predict minimum drag levels, only the drag due to lift results are compared. Appendix C contains several examples of HASC input files

### Baseline Validation

Figure 6.2-2 presents the comparison of the tailless fighter configuration with undeflected controls. Included on the plot are HASC results from running the entire configuration in VORLIF(ISRTYP=2) and from running the configuration in VORLAX(ISRTYP=5) with SPC = -1. A forebody was not modeled in VTXCHN for this configuration. The HASC model for these predictions included wing twist, camber, and the optional airfoil input file airfoil.inp. The predictions using VORLIF produced good agreement in lift through 18 degrees angle of attack and in pitching moment through 12 degrees angle of attack. The VORLAX lift predictions compare very well to the test data through 30 degrees angle of attack. The VORLIF predicted drag due to lift at  $CL = .4$  is within 3% of the test drag due to lift.

HASC allows the user to vary the SPC (leading edge suction parameter) between -1.0 to +1.0 including fractions when analyzing a surface in VORLAX. The results of using SPC's of -1, 0, and +1 are shown in figure 6.2-3. Good agreement with the test pitching moment in the low angle of attack range occurs when using SPC values of 0 and +1. However, the lift and drag agreement is best when using a SPC value of -1.

Figures 6.2-4 and 6.2-5 illustrate the sensitivity of varying the chordwise and spanwise sub-paneling of the input model. The chordwise (ICHRDIV) and spanwise (ISPNDIV) parameters were decreased and increased without changing the number of surfaces or panels. The job execution time increases as the number of sub-panels increases. Above 18 degrees angle of attack the pitching moment begins deviating significantly as the number of chordwise panels is varied. The deviation begins at an even lower angle of attack (12 degrees) as the number of spanwise panels is varied. The lift and drag predictions are not as

strongly impacted by the number of sub-panels as is pitching moment. This apparent sensitivity to paneling is a major concern and requires additional research.

Figure 6.2-6 presents the sensitivity of the VORLIF predictions to wing camber. The previous figures 6.2-2 through 6.2-5 were run with the wind tunnel's model camber included in the HASC model. Figure 6.2-6 compares the cambered solution to a solution with the camber removed, thus not representative of the wind tunnel model. Although the agreement in  $C_{mo}$  is lost with the uncambered wing, the general shape of the pitching moment curve and lift agreement is improved with the uncambered wing.

# Baseline Comparison

Test vs HASC

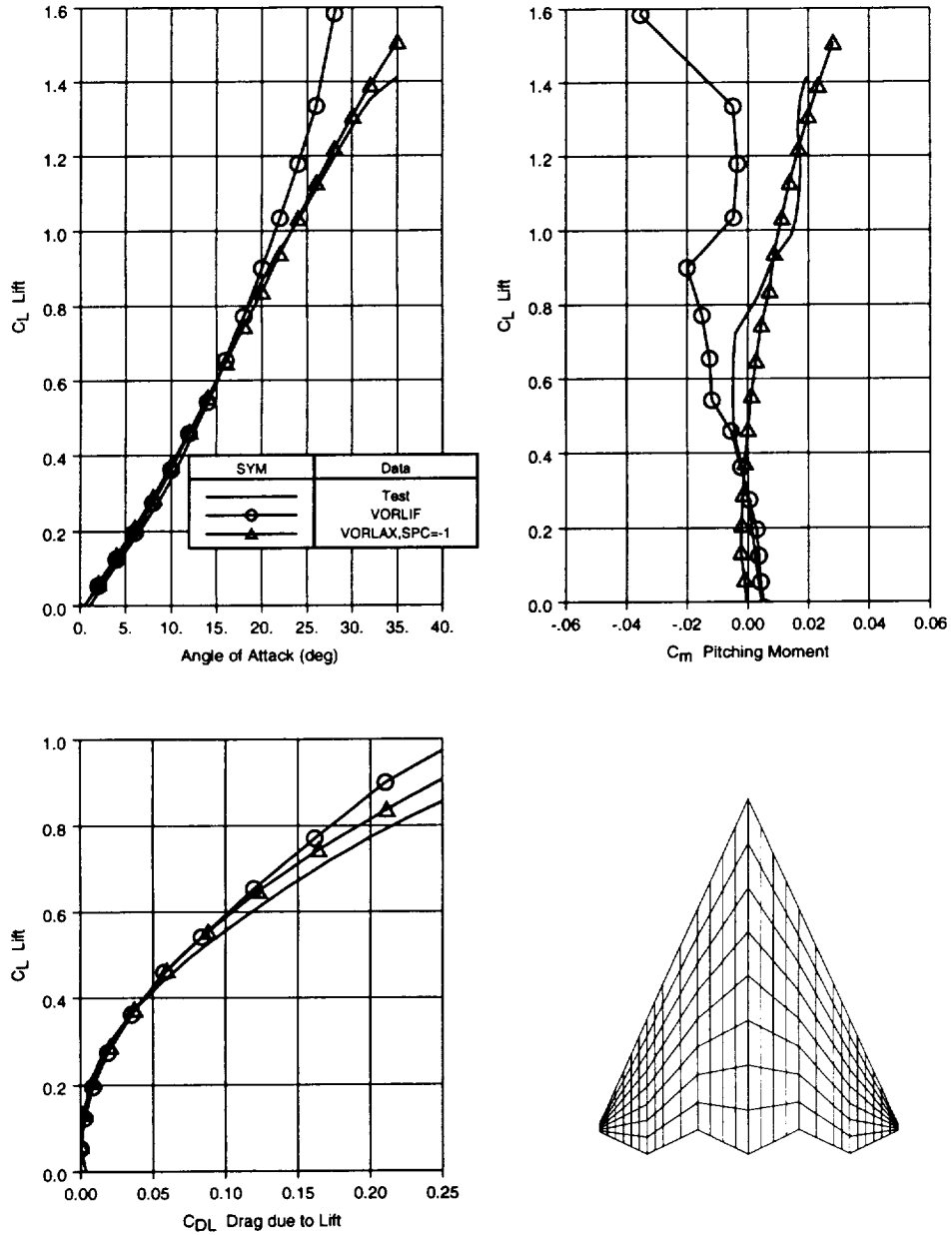


Figure 6.2-2 Tailless Fighter Baseline Comparison,  $M=.3$ , Controls=0

# Effect of Varying SPC

Test vs HASC, VORLAX wing

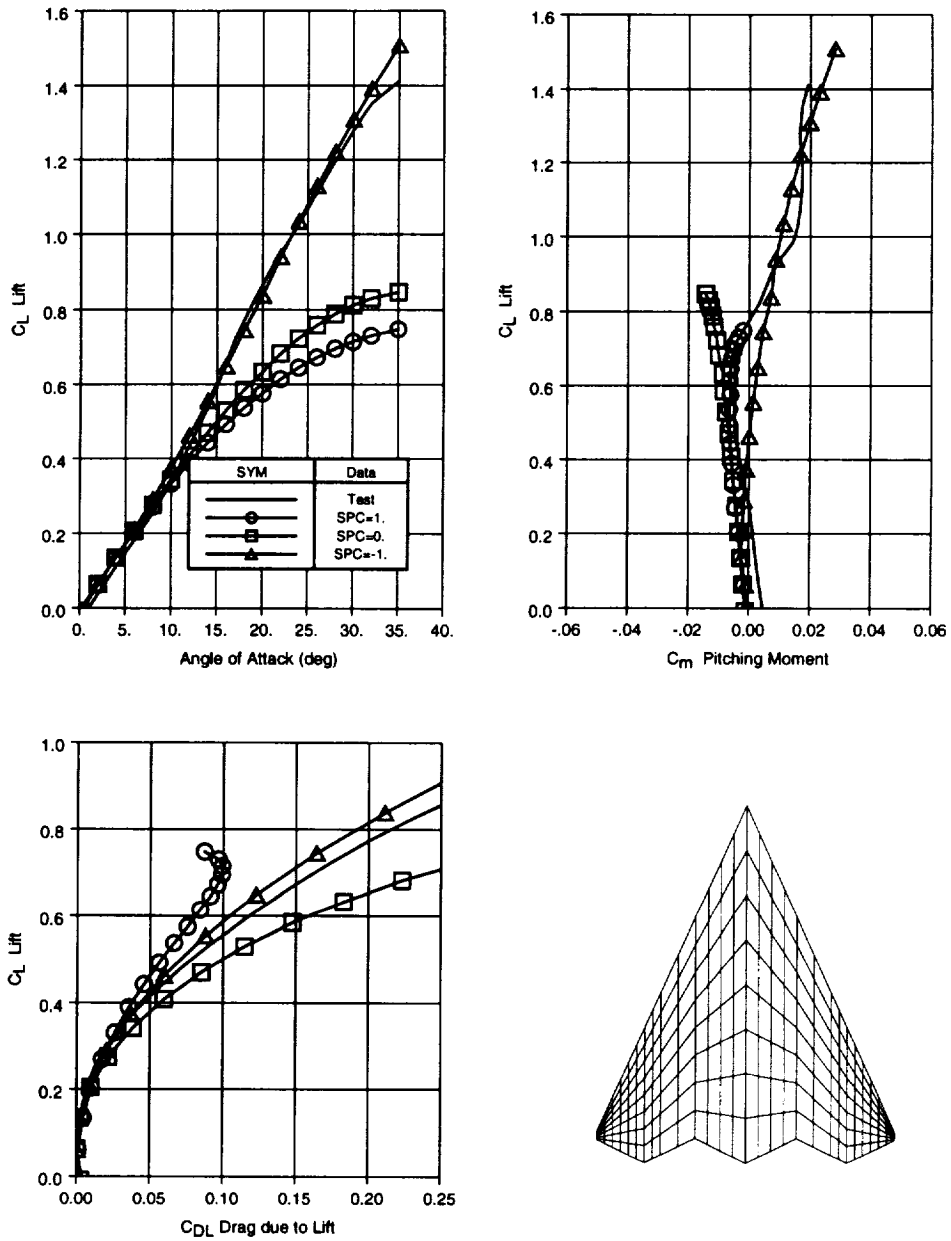


Figure 6.2-3 Sensitivity to SPC Parameter on Tailless Fighter

# Chordwise Paneling Sensitivity

Test vs HASC, VORLIF wing

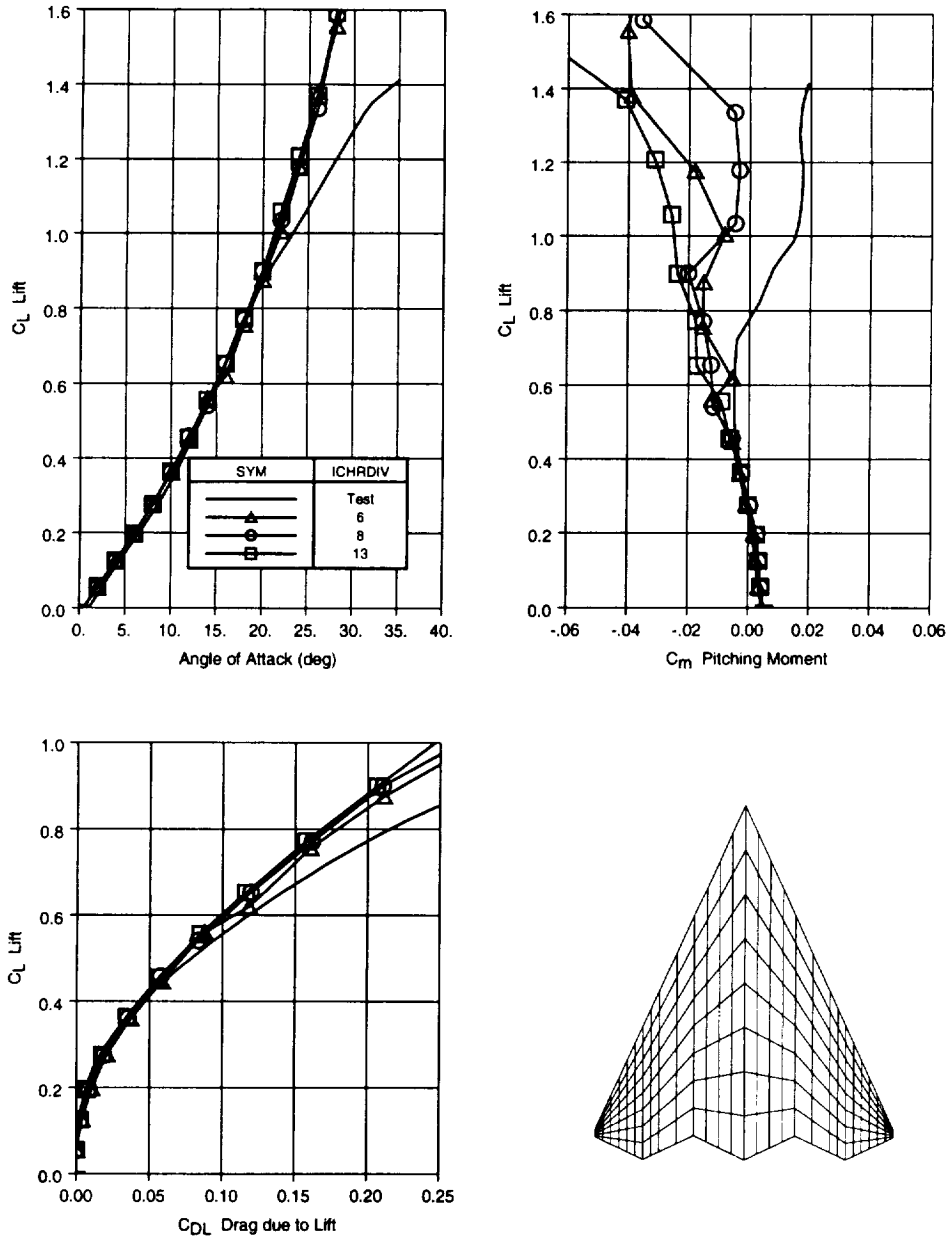


Figure 6.2-4 Sensitivity to Chordwise Paneling on Tailless Fighter

# Spanwise Paneling Sensitivity

Test vs HASC, VORLIF wing

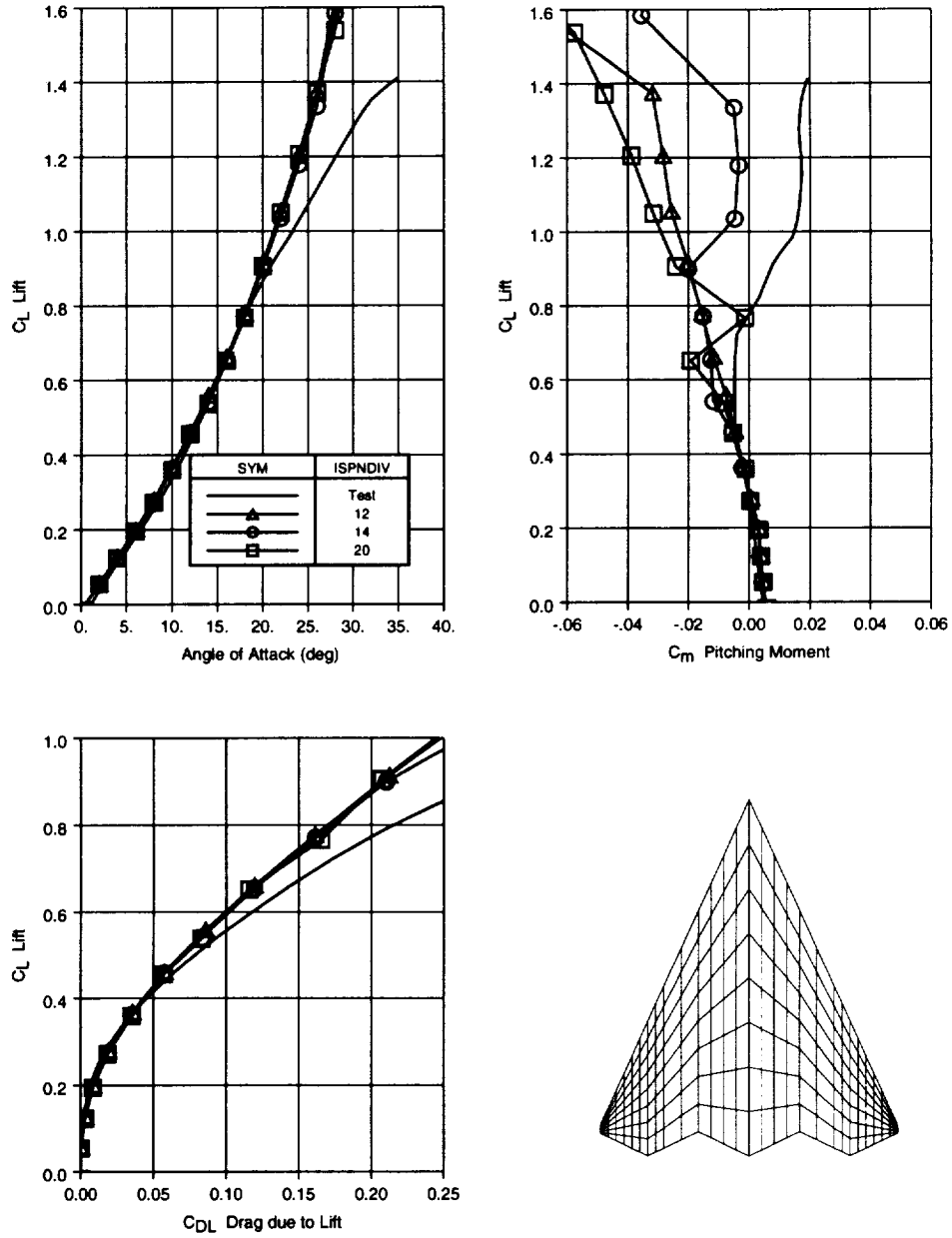


Figure 6.2-5 Sensitivity to Spanwise Paneling on Tailless Fighter



# Baseline Comparison

Test vs HASC, VORLIF wing

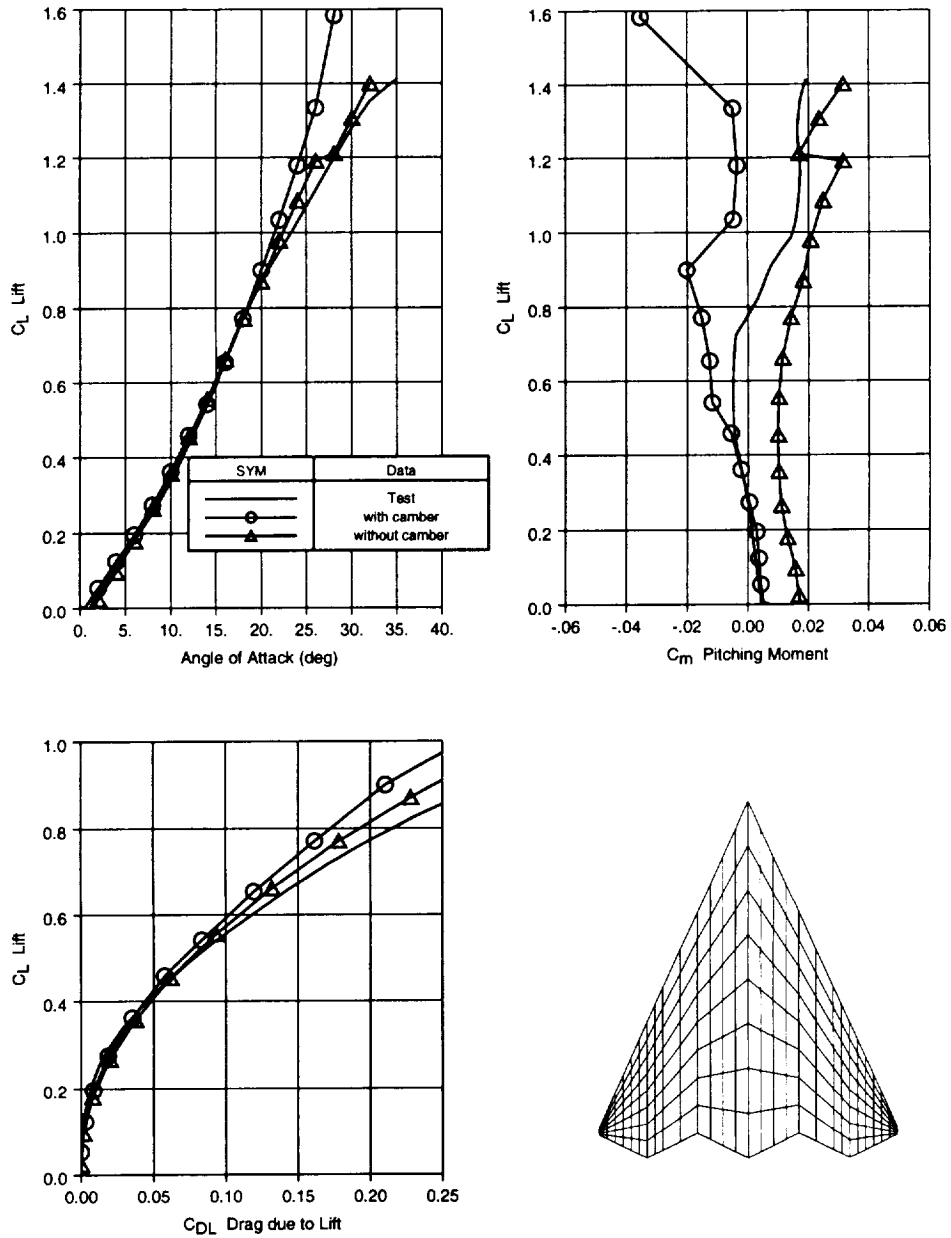


Figure 6.2-6 Sensitivity to Wing Camber Definition on Tailless Fighter

## Control Effectiveness Validation

The baseline HASC model was modified to include trailing edge flaps. Figures 6.2-7 through 6.2-14 compare increments from HASC to test data for right hand elevon deflections of -30, -10, +10, and +30 degrees. When modeling trailing edge control deflections, the geometric streamwise deflection of the control surface should be adjusted according to the theoretical/effective ratio obtained from page 190 of reference 18. This adjusted deflection is then added to the undeflected AINC values to correctly model a trailing edge flap deflection. This approach was used for all the trailing edge flap comparisons presented in this report. Both longitudinal and lateral/directional (L/D) comparisons are shown using both VORLIF and VORLAX predictions.

The longitudinal comparisons using VORLIF(ISRTYP = 2) predictions are shown in figures 6.2-7 and 6.2-8, while the predictions using just VORLAX(ISRTYP = 5) are presented in figures 6.2-9 and 6.2-10. VORLAX results are generally in better agreement with the test data.

The lateral/directional increments from the right hand elevon deflections were also compared to the test data. Figures 6.2-11 and 6.2-12 show the results from the VORLIF predictions, while figures 6.2-13 and 6.2-14 show the results using VORLAX. As with the longitudinal coefficients, the VORLIF results tend to be erratic and deviate from the test data above 20 degrees angle of attack.

## RH Elevon (-10,+10) Comparison

Test vs HASC, VORLIF wing

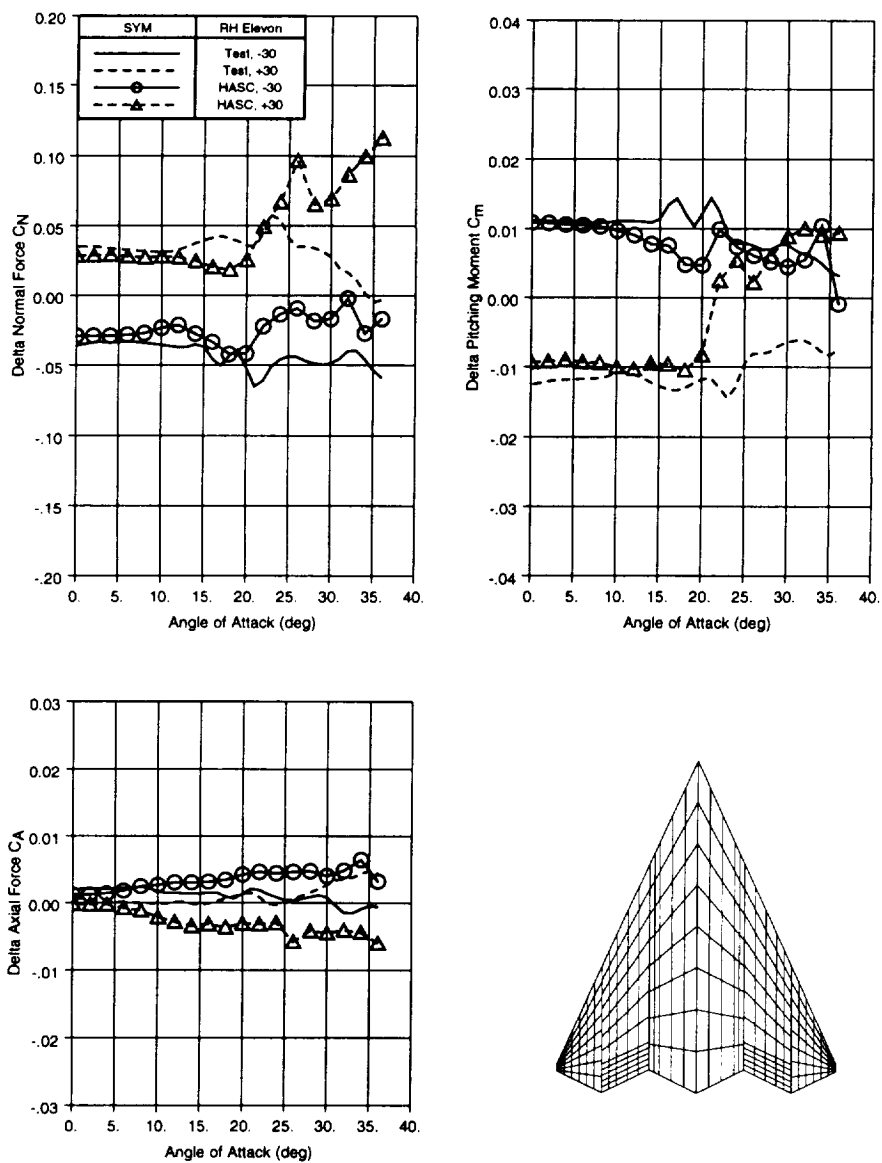


Figure 6.2-7 Tailless Fighter 10 deg. RH Elevon Long. Comparison, VORLIF

# RH Elevon (-30,+30) Comparison

Test vs HASC, VORLIF wing

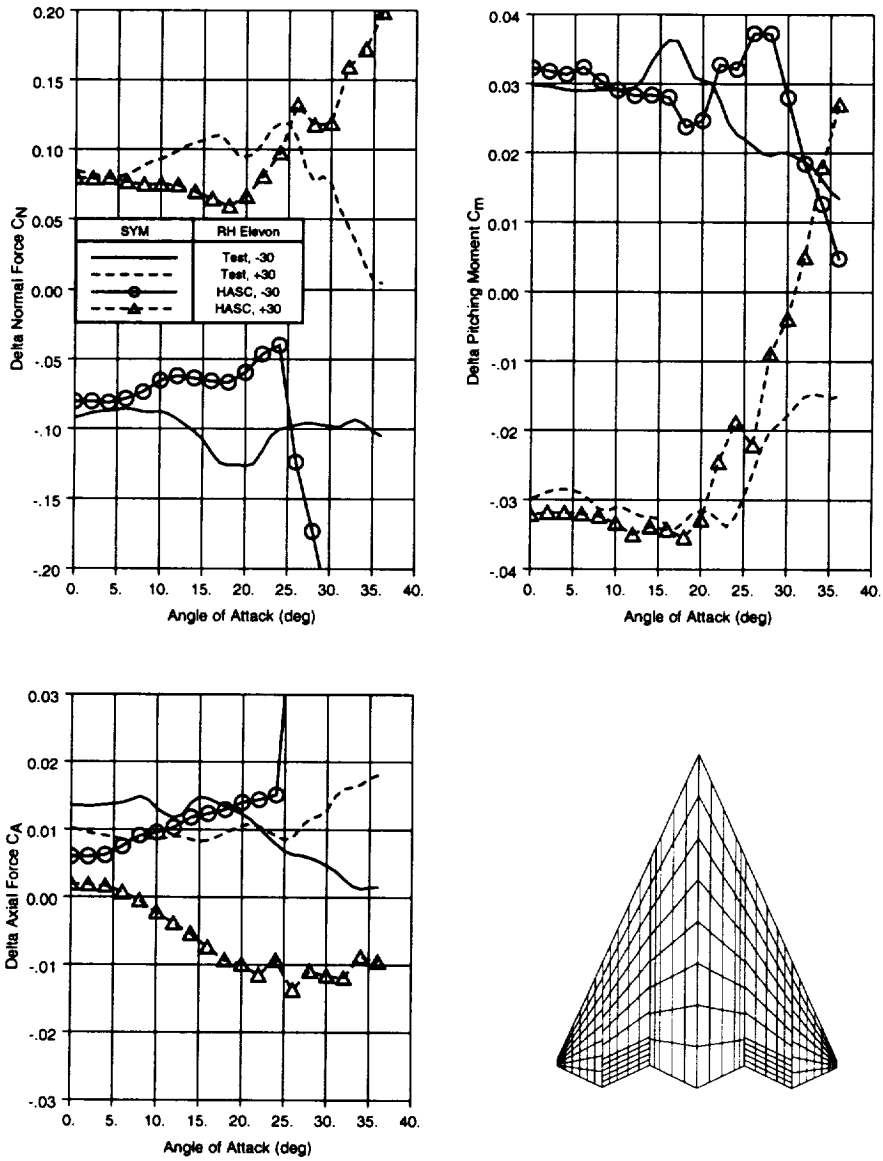


Figure 6.2-8 Tailless Fighter 30 deg. RH Elevon Long. Comparison, VORLIF

## RH Elevon (-10,+10) Comparison

Test vs HASC, VORLAX wing using SPC=-1

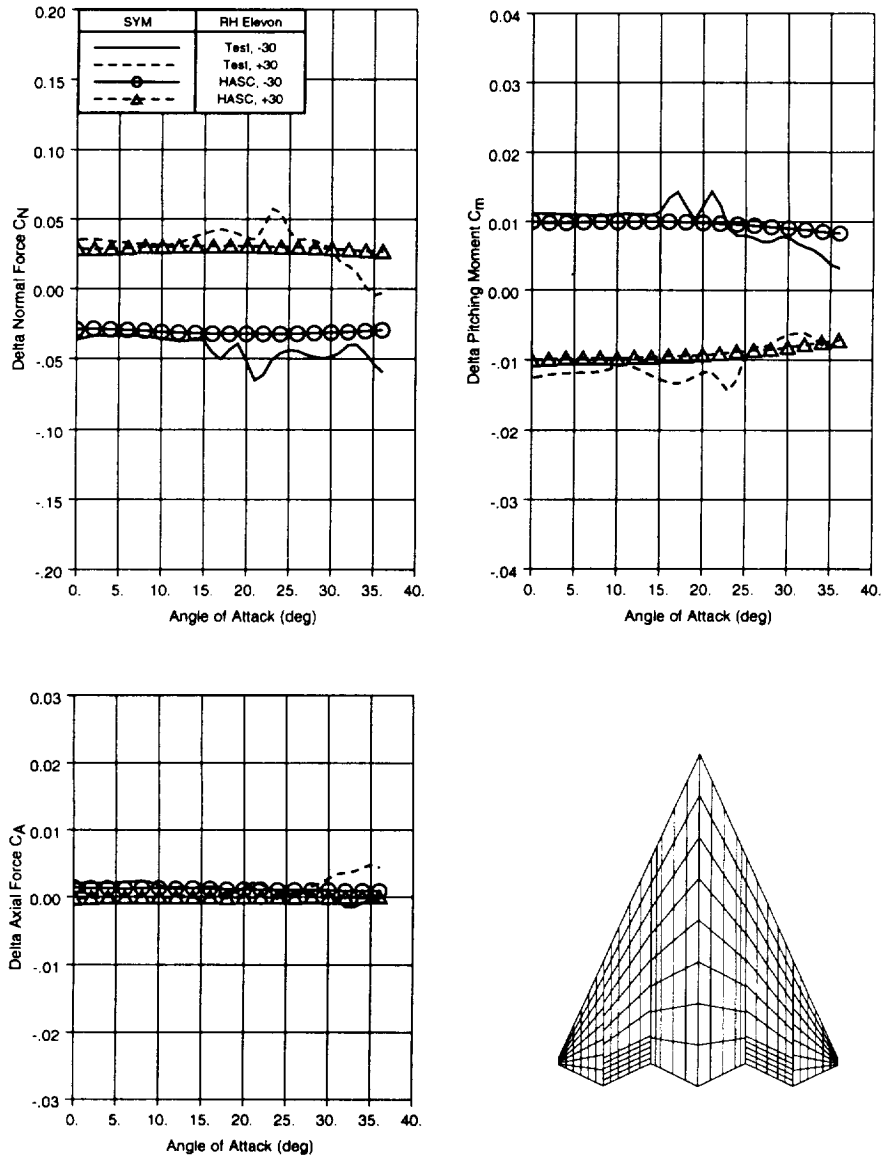


Figure 6.2-9 Tailless Fighter 10 deg. RH Elevon Long. Comparison, VORLAX

## RH Elevon (-30,+30) Comparison

Test vs HASC, VORLAX wing using SPC=-1

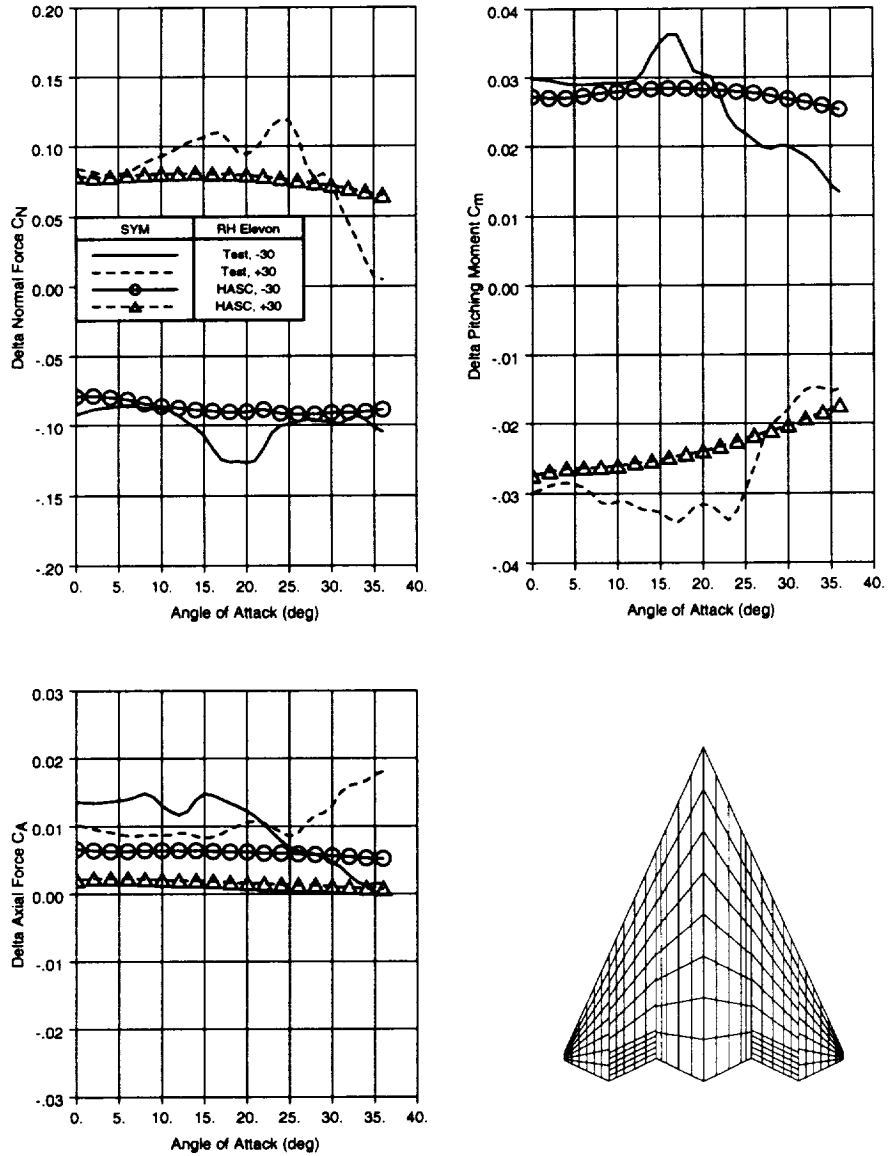


Figure 6.2-10 Tailless Fighter 30 deg. RH Elevon Long. Comparison, VORLAX

### Lat/Dir RH Elevon(-10,+10) Comparison

Test vs HASC, VORLAX wing using SPC=-1

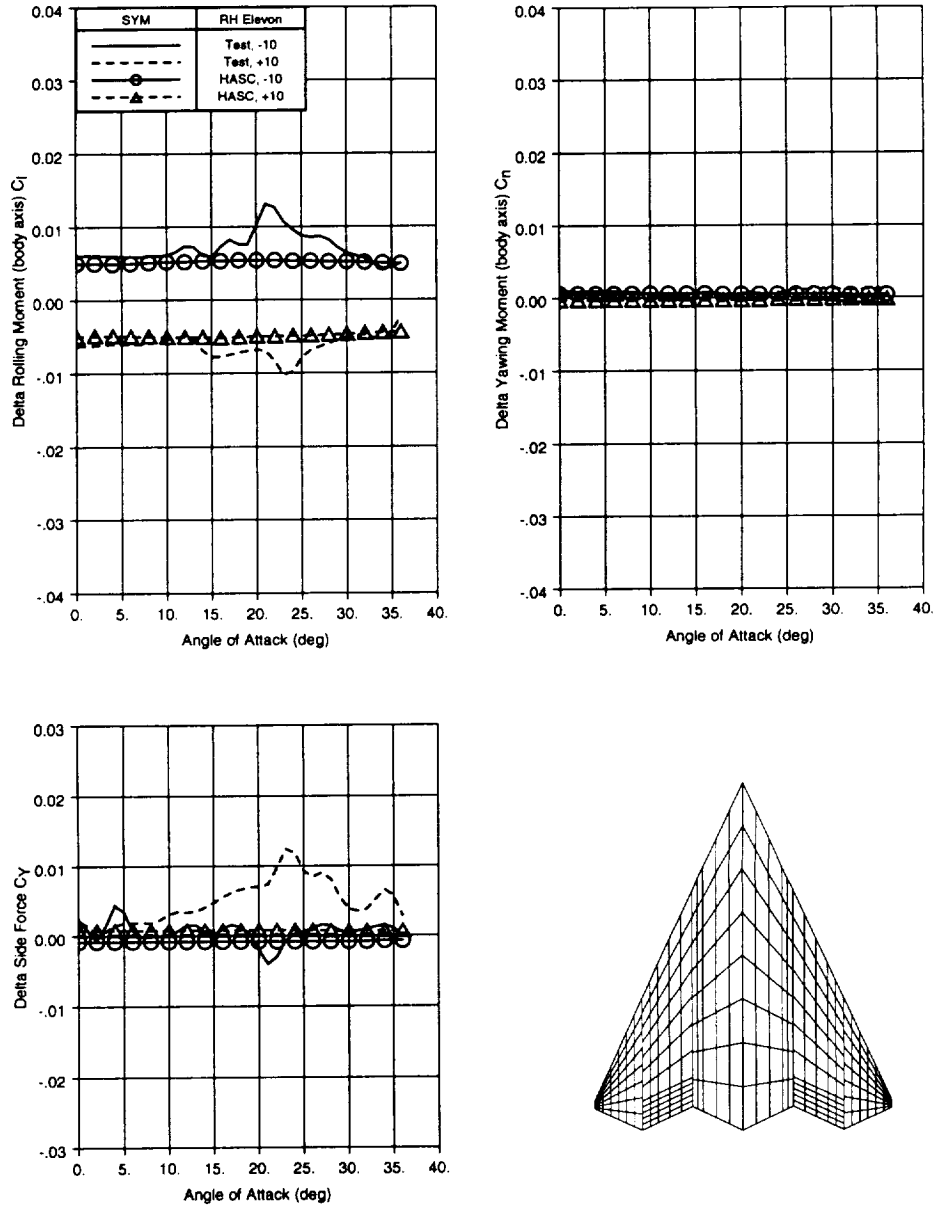


Figure 6.2-11 Tailless Fighter 10 deg. RH Elevon L/D Comparison, VORLIF

### Lat/Dir RH Elevon(-30,+30) Comparison

Test vs HASC, VORLIF wing

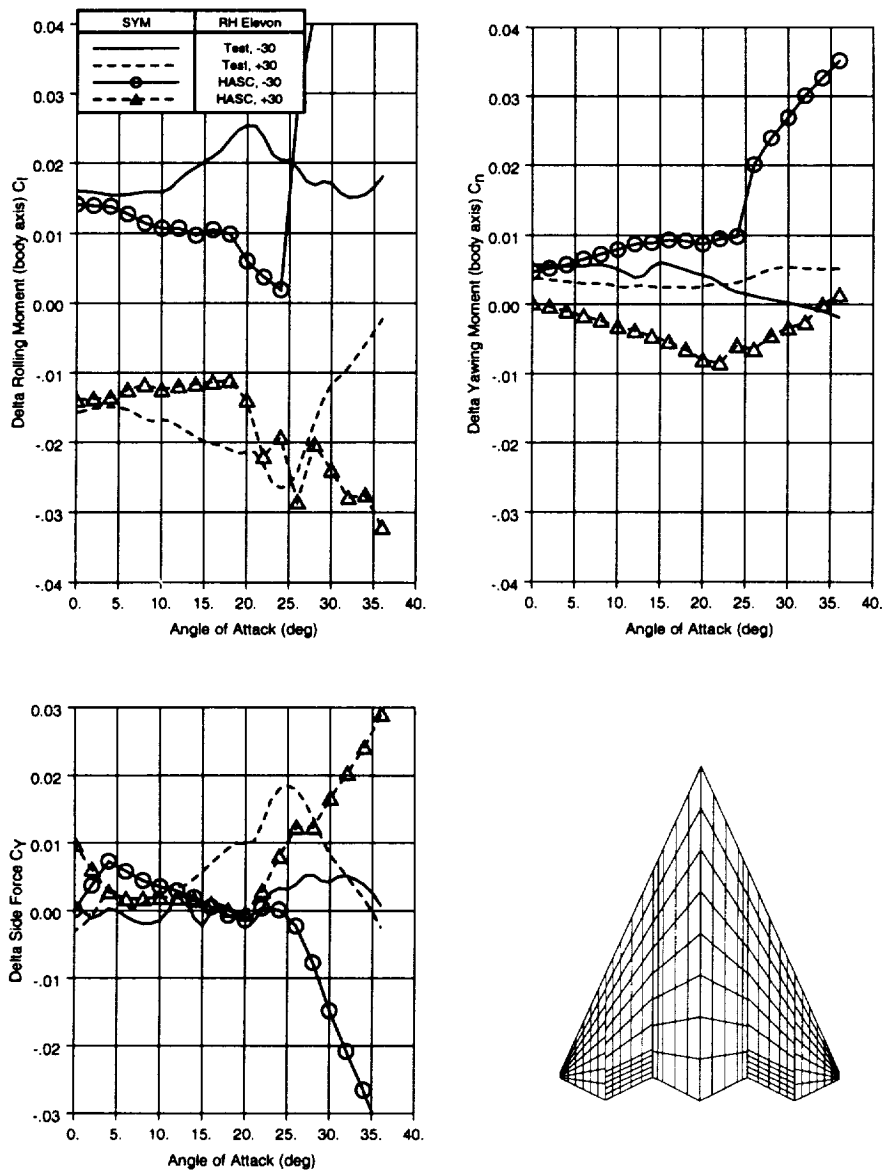


Figure 6.2-12 Tailless Fighter 30 deg. RH Elevon L/D Comparison, VORLIF



### Lat/Dir RH Elevon(-10,+10) Comparison

Test vs HASC, VORLAX wing using SPC=-1

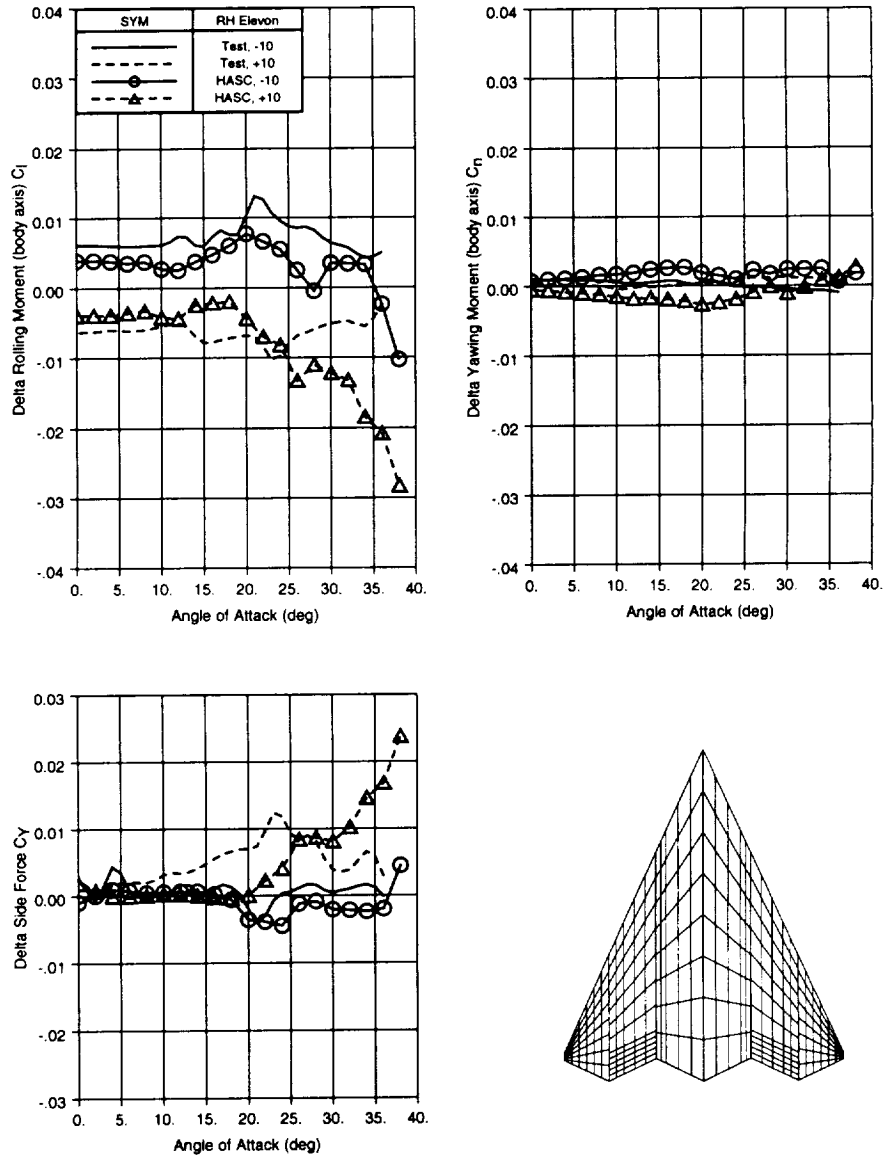


Figure 6.2-13 Tailless Fighter 10 deg. RH Elevon L/D Comparison, VORLAX

## Lat/Dir RH Elevon(-30,+30) Comparison

Test vs HASC, VORLAX wing using SPC=-1

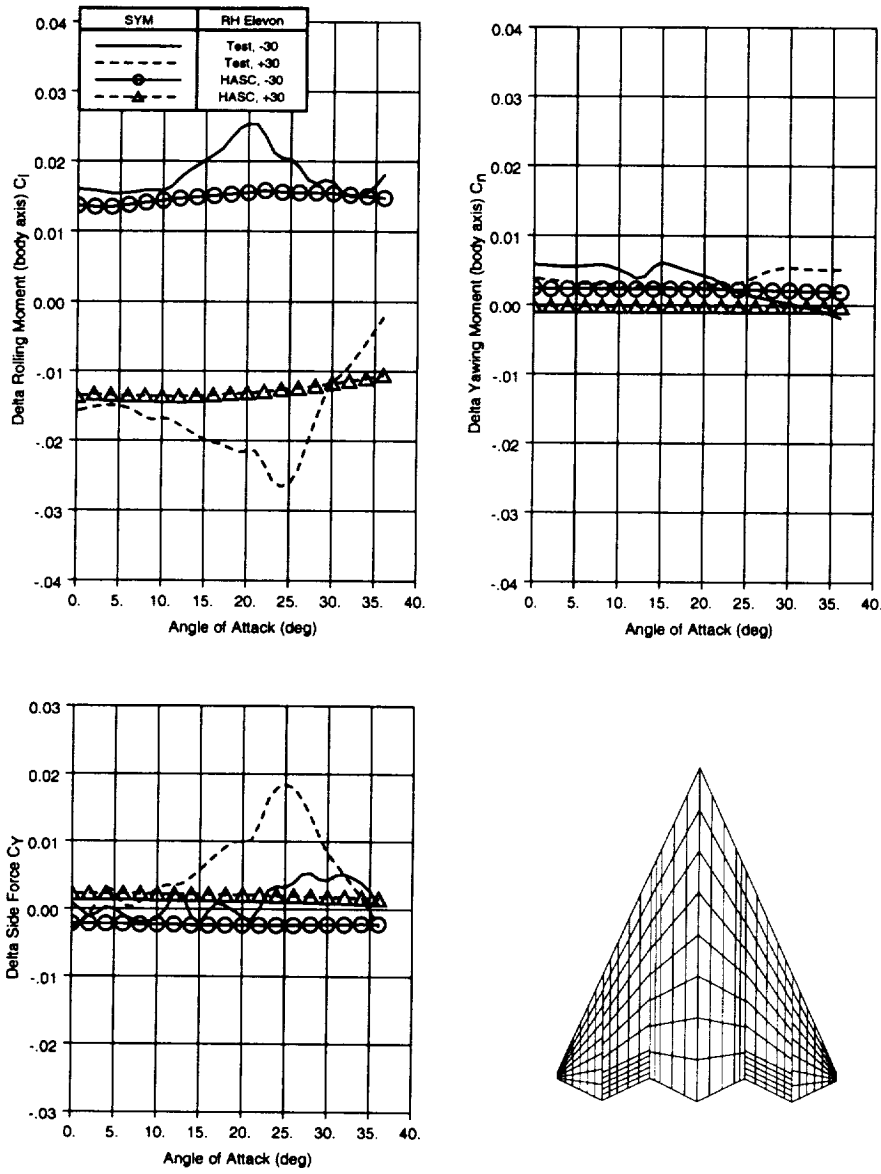


Figure 6.2-14 Tailless Fighter 30 deg. RH Elevon L/D Comparison, VORLAX

### 6.3 Falcon 21 Configuration

#### Background

The next configuration used during the HASC validation was the Falcon 21 configuration. LMTAS developed the Falcon 21 configuration in the late 1980's as an F-16 derivative with an F-16 fuselage and vertical tail, but with a trapezoidal 50 degree swept wing. A full-span leading edge flap is integrated into the wing. A highly swept strake blends the wing into the fuselage.

A low speed tunnel test at the General Dynamics Low Speed Tunnel (GDLST) of a 1/15-scale force and moment Falcon 21 model provided the validation test data. All validation comparisons are at Mach = 0.20. The Falcon 21 configuration, with the HASC spanwise panel boundaries, is shown in figure 6.3-1.

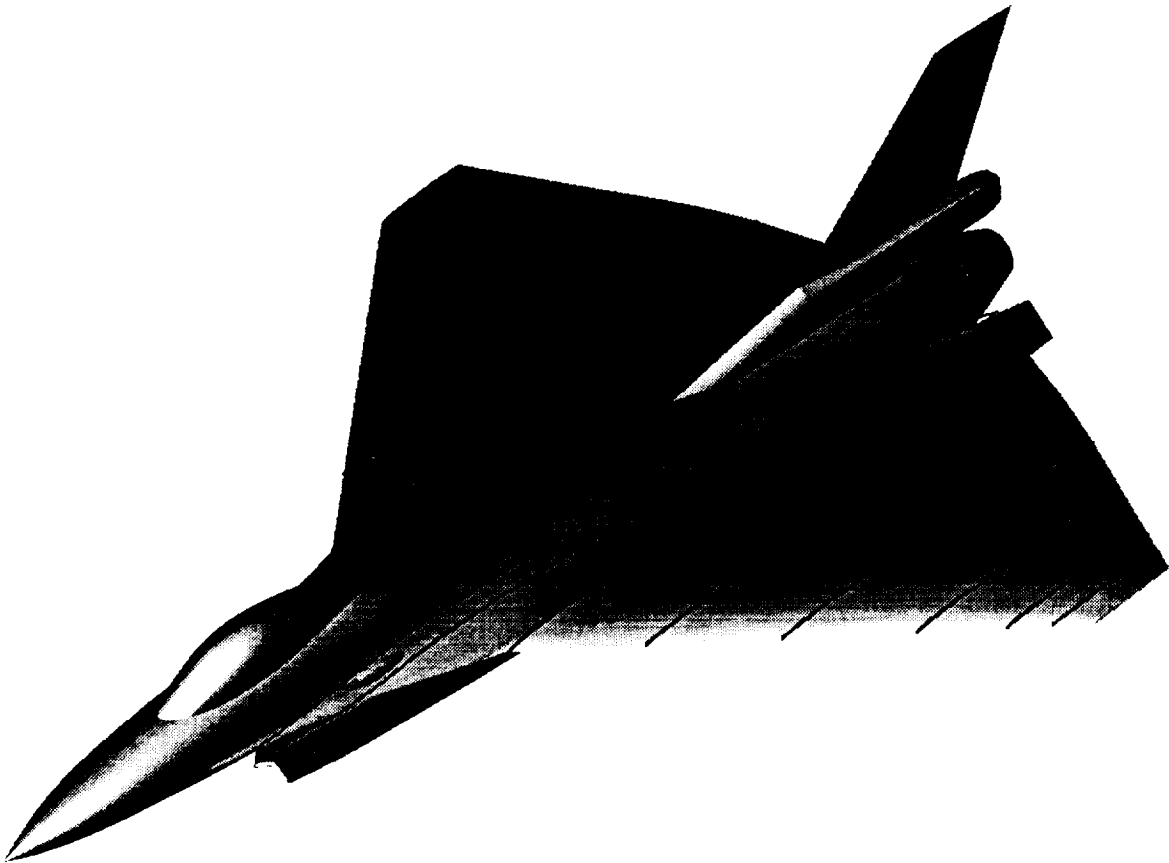


Figure 6.3-1 Falcon 21 Configuration

## Baseline Validation

The Falcon 21 configuration was modeled in HASC in a manner similar to that for a conceptual airplane design with a minimum amount of configuration definition available. The wing camber and airfoil definitions for the wind tunnel model were not located, so an uncambered wing with default airfoils was used in the HASC model. However, both the wing was analyzed using both VORLIF and VORLAX.

Figure 6.3-2 presents the comparison of the baseline (controls = 0) configuration coefficients with results from HASC predictions using VORLIF, VORLAX using SPC = -1, and VORLAX using SPC = +1. The best pitching moment agreement with the test data occurs when running HASC using VORLAX with SPC = +1, while the best lift and drag agreement occurs when using VORLIF. The predicted drag due to lift using VORLIF at  $CL = .4$  is within 5% of the test drag due to lift. These comparisons are partly inconclusive because of the lack of the wing and airfoil definition in the HASC models.

Figure 6.3-3 shows the difference in the predicted results when running the forebody portion of the Falcon 21 configuration in VTXCHN vs. VORLAX. Significant differences occur only in pitching moment. These differences increase with angle of attack. The time required to model the forebody in VTXCHN and the increased computational time for a VTXCHN analysis must be traded off with the change in accuracy.

## Baseline Comparison with LEF=0

Test vs HASC, wing camber not modeled, default airfoil, VORLAX forebody

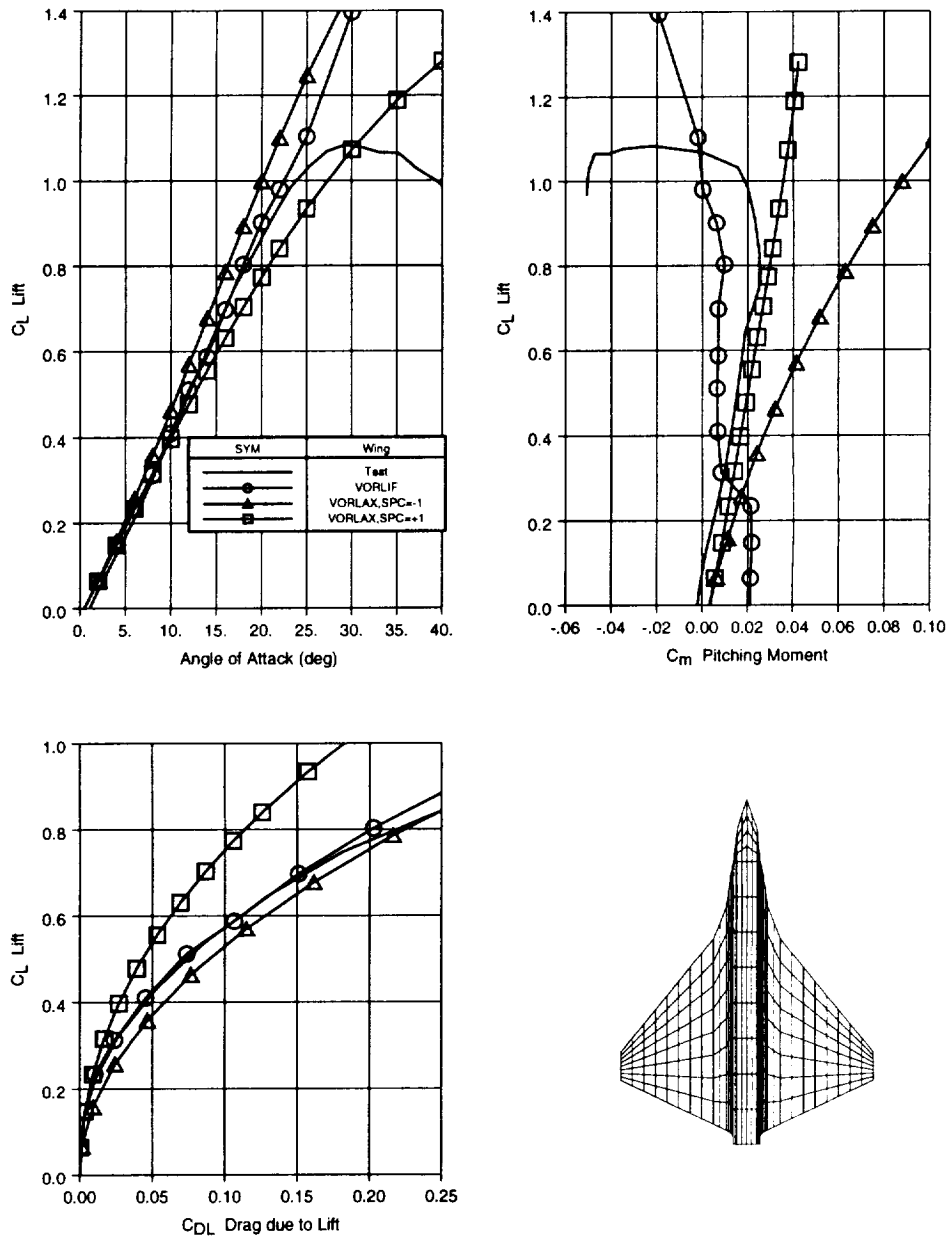


Figure 6.3-2 Falcon 21 Baseline Comparison,  $M=0.2$ , Controls=0

# Forebody Calculation Comparison

Test vs HASC, VORLIF wing

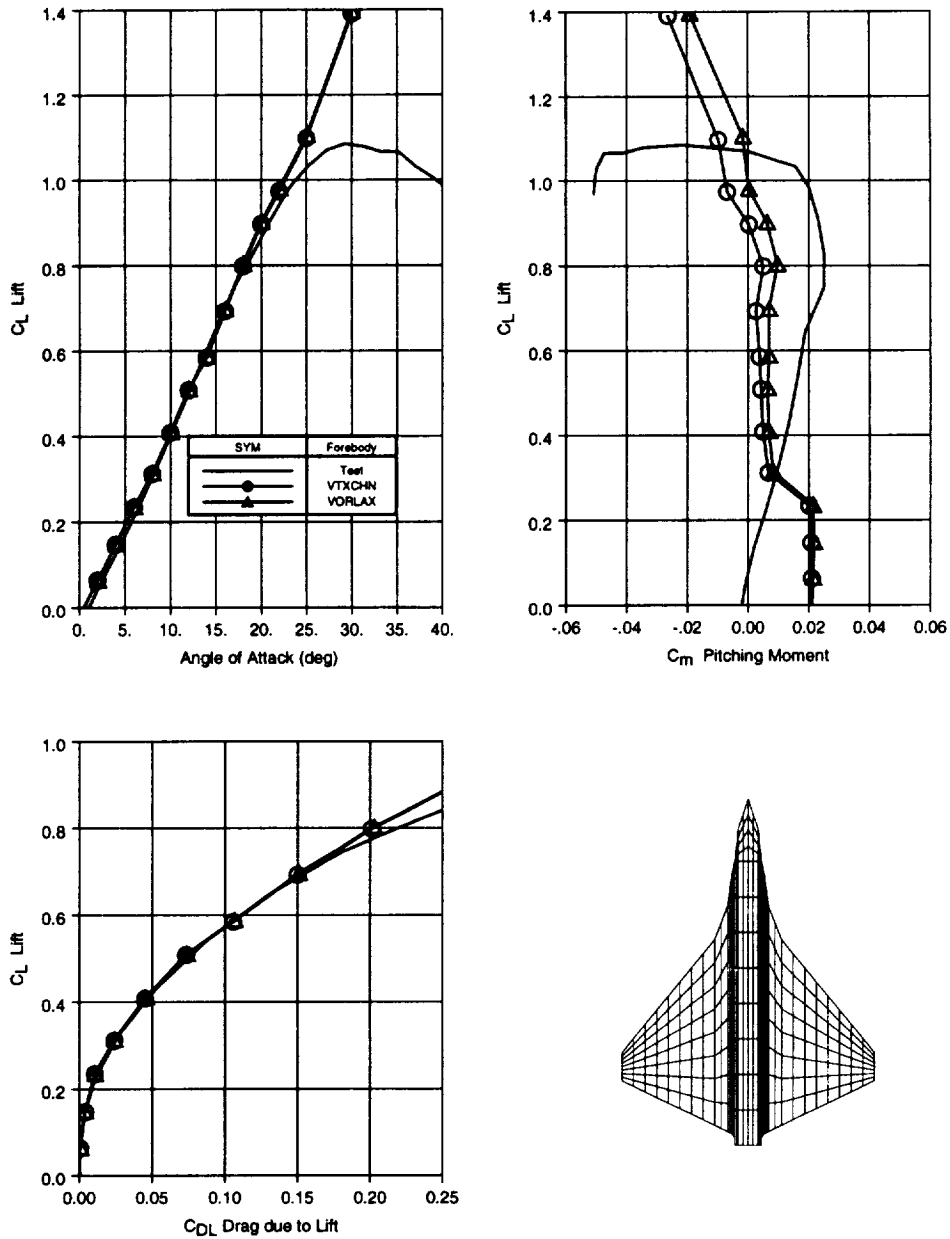


Figure 6.3-3 Comparison of Forebody Calculation Methods on Falcon 21

## Control Effectiveness Validation

The baseline Falcon 21 HASC model was modified to include panels representing the leading edge flaps. Increments from a 10 degree leading edge flap deflection were computed using first VORLIF and then VORLAX on the wing surface. These leading edge flap runs were made with the forebody modeled in VORLAX. The comparison of the two HASC predictions to the test data are shown in figure 6.3-4. The VORLAX predictions result in good agreement in normal force, pitching moment, and drag up to approximately 15 degrees angle of attack. The VORLIF results do not agree well with the test data.

The Falcon 21 HASC model was the modified to include trailing edge flap panels. Runs of symmetric trailing edge flap deflections were run in VORLAX. These predictions were made using SPC values of -1. The HASC predictions compared to the test data for -10 and +10 degree trailing edge flap effectiveness is presented in figure 6.3-5. The comparison for the -30 and +30 degree effectiveness is shown in figure 6.3-6. Good agreement with the test data is obtained for the positive deflections in normal force and pithcing moment. The axial increments do not agree well with the test data.

Figure 6.3-7 presents a comparison of an asymmetric trailing edge flap deflection configuration (-10 degrees on the left wing, +10 degrees on the right wing). The VORLAX predictions agree closer to the test data in rolling and yawing moment, however the VORLIF results agree closer in side force.

# 15deg. Leading Edge Flap Comparison

Test vs HASC, VORLAX forebody

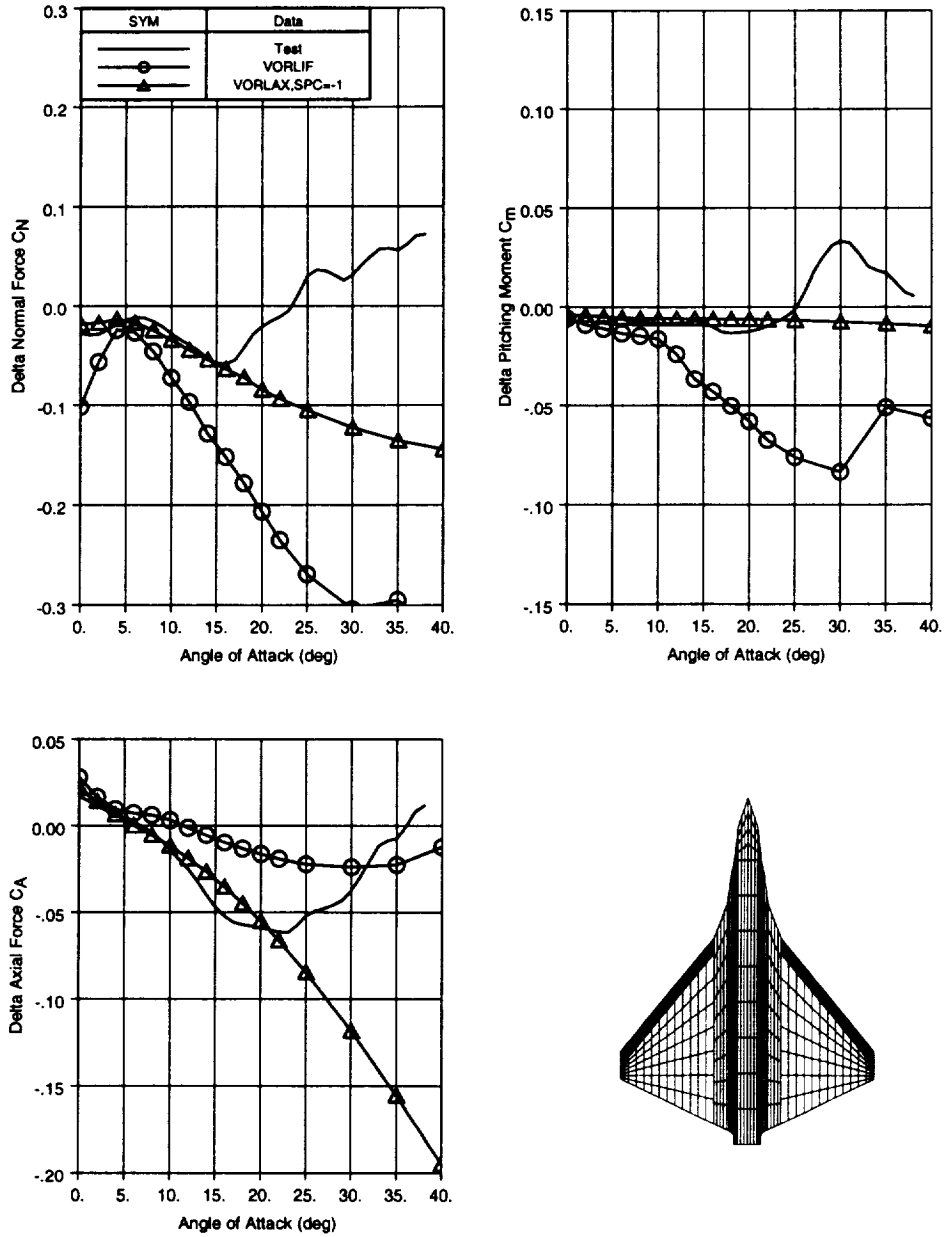


Figure 6.3-4 Falcon 21 15 deg. Leading Edge Flap Comparison



## Sym. TE Flap(-10,+10) Comparison

Test vs HASC, VORLAX wing with SPC=-1, VORLAX forebody

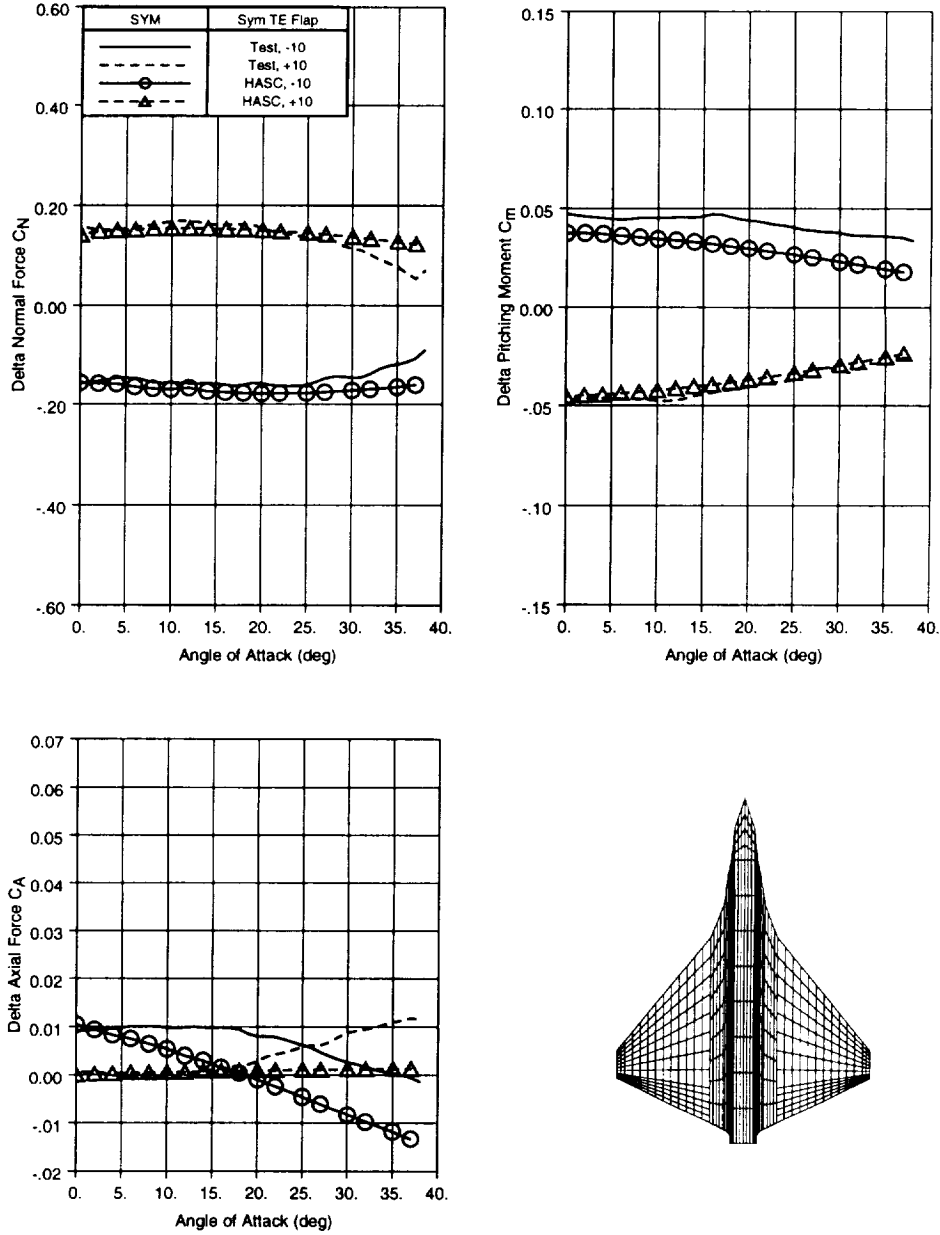


Figure 6.3-5 Falcon 21 Symmetric 10 deg. Trailing Edge Flap Comparison

# Sym. TE Flap(-30,+30) Comparison

Test vs HASC, VORLAX wing with SPC=-1, VORLAX forebody

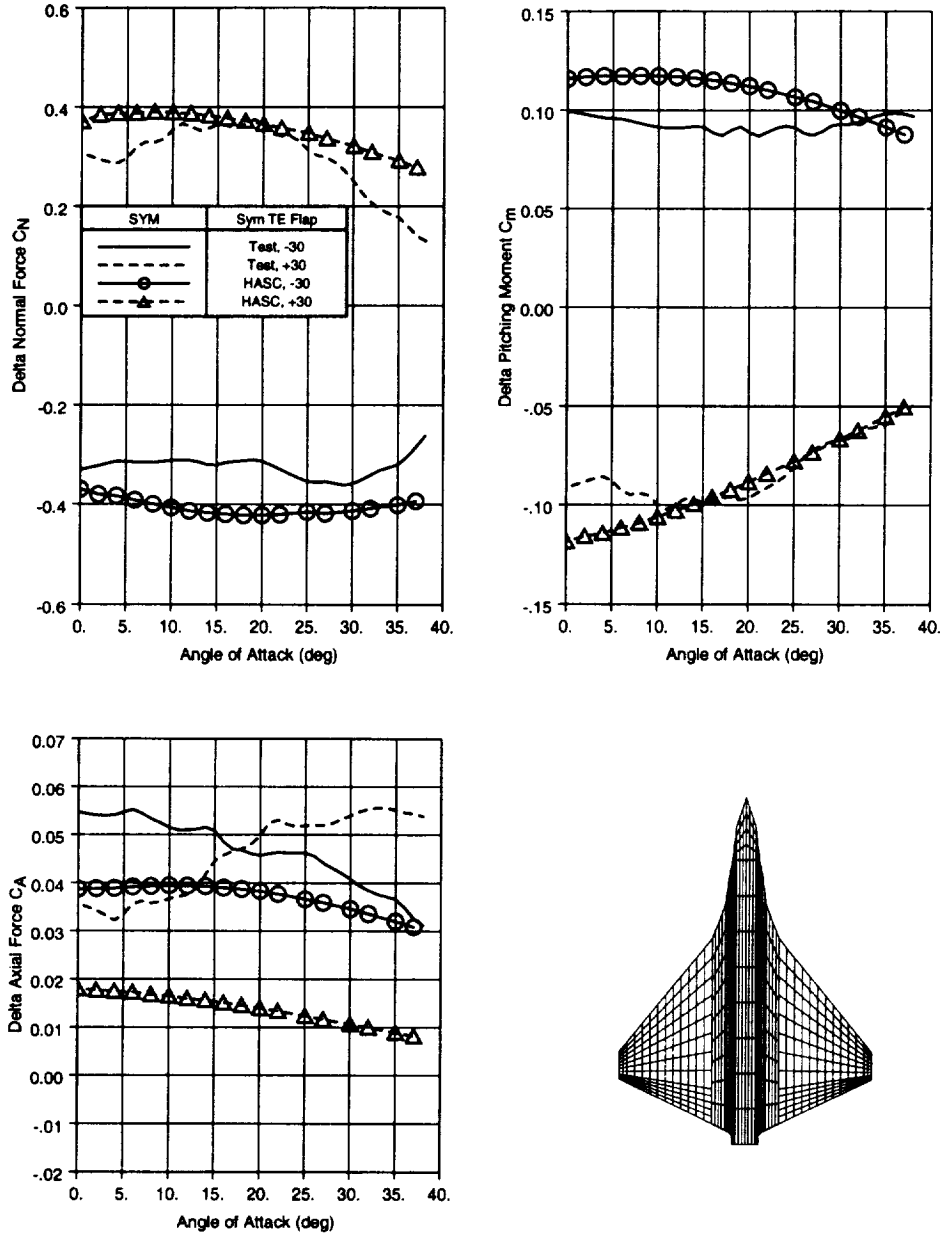


Figure 6.3-6 Falcon 21 Symmetric 30 deg. Trailing Edge Flap Comparison

# Asymmetric TE Flap (-10LH/+10RH)

Test vs HASC, VORLAX forebody

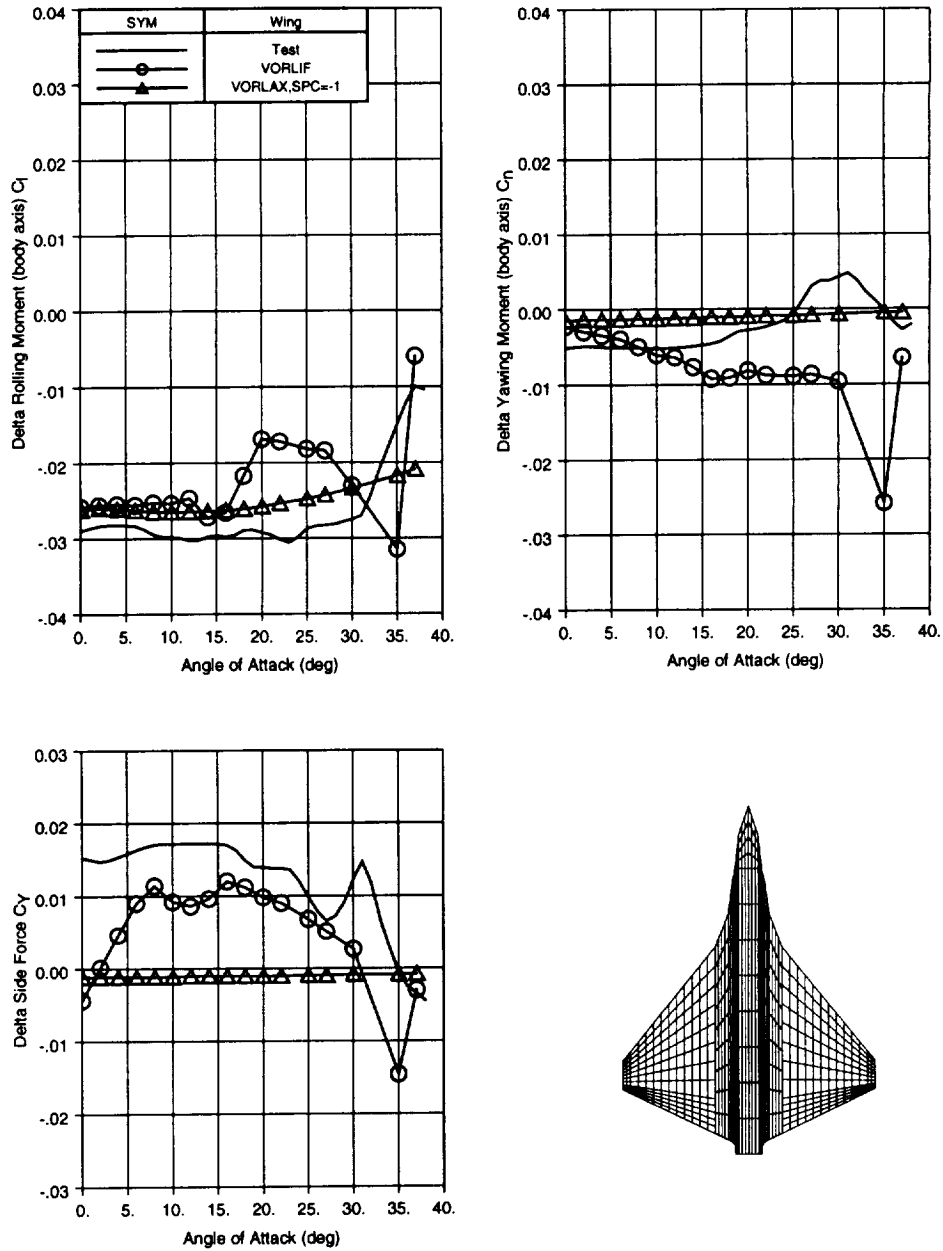


Figure 6.3-7 Falcon 21 Asymmetric 10 deg. Trailing Edge Flap Comparison

## 6.4 F-16XL Airplane

### Background

The F-16XL aircraft was also used as a configuration for the HASC validation effort. The F-16XL incorporates a strake with a cranked arrow wing planform resulting in unique challenges for HASC. Mach = 0.20 data from a 0.18 scale wind tunnel model tested at the NASA LaRC 30x60 facility (reference 19) was used for comparison to the HASC predictions. The F-16XL configuration is shown in figure 6.4-1. The wing-tip launchers and missiles were not part of the wind tunnel model and were not included in the HASC model



Figure 6.4-1 F-16XL Configuration

## Baseline Validation

Figure 6.4-2 presents the comparison of the longitudinal coefficients from the wind tunnel to the HASC predictions for the baseline F-16XL configuration (controls=0). The strake/wing surface of the F-16XL HASC panel model was analyzed using VORLIF and VORLAX as shown in figure 6.4-2. The wing twist, camber, and airfoil definitions were included in the HASC model. The VORLAX results are generally in better agreement with the test data than the VORLIF results for this baseline configuration. However, the predicted drag due to lift from VORLIF at  $CL = .4$  is within 2% of the test drag due to lift. The forebody was analyzed in VTXCHN.

Figure 6.4-3 shows the difference in the predicted results between modeling the F-16XL forebody in VORLAX vs. VTXCHN. VTXCHN predicts more nose down pitching moment from the forebody than does VORLAX. No significant differences are seen in lift or drag.

The predictions from VORLIF can be sensitive to the input wing definition as illustrated in figure 6.4-4. The VORLIF results from figure 6.4-2 are compared to VORLIF results when using the default uncambered NACA 6-series airfoils in HASC. Wing twist was included in both runs. Pitching moment appears to be the most sensitive as large differences exist between the two predictions above 12 degrees angle of attack.

HASC predictions can also be sensitive to the setting of the vortex flag parameter IVTXFLG as shown in figure 6.4-5. The results in figure 6.4-2 are from setting the IVTXFLG parameter to 1 at the most inboard panel (strake) and at the butline where the wing sweep changes (BL 136) as recommended in section 4.2. Figure 6.4-5 also contains a prediction from HASC where the outboard IVTXFLG was changed from 1 to 0. Large differences occur in pitching moment and in lift at the higher angles of attack. This illustrates the importance of setting the IVTXFLG correctly when using the VORLIF option for analyzing lifting surfaces.

# Baseline Comparison

Test vs HASC, VORLAX forebody

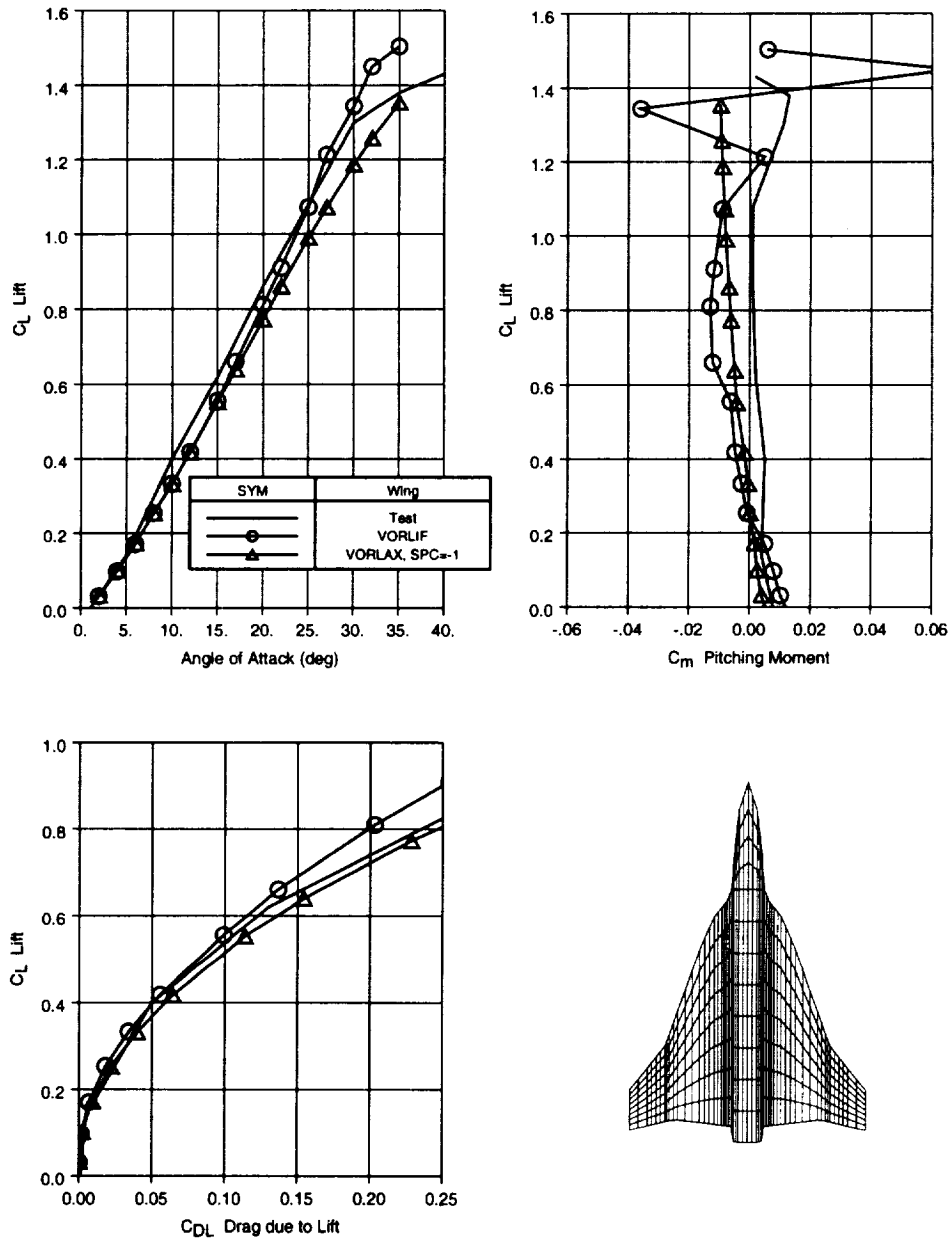


Figure 6.4-2 F-16XL Baseline Comparison,  $M=.2$ , Controls=0

# Forebody Computation Comparison

Test vs HASC, VORLIF Strake/Wing

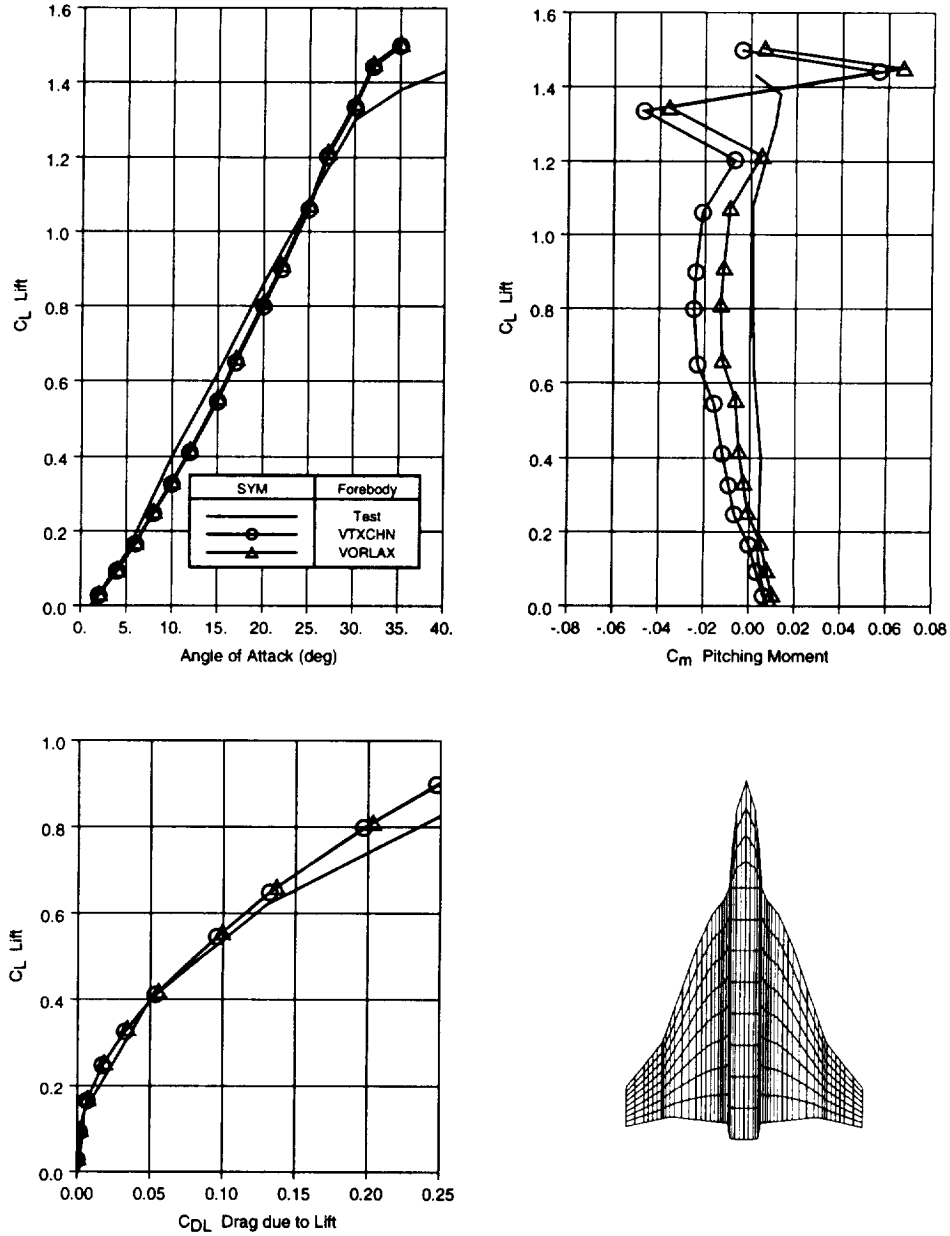


Figure 6.4-3 Comparison of Forebody Calculation Methods on F-16XL

# Wing Definition Sensitivity

Test vs HASC, VORLIF wing/strake, VTXCHN forebody

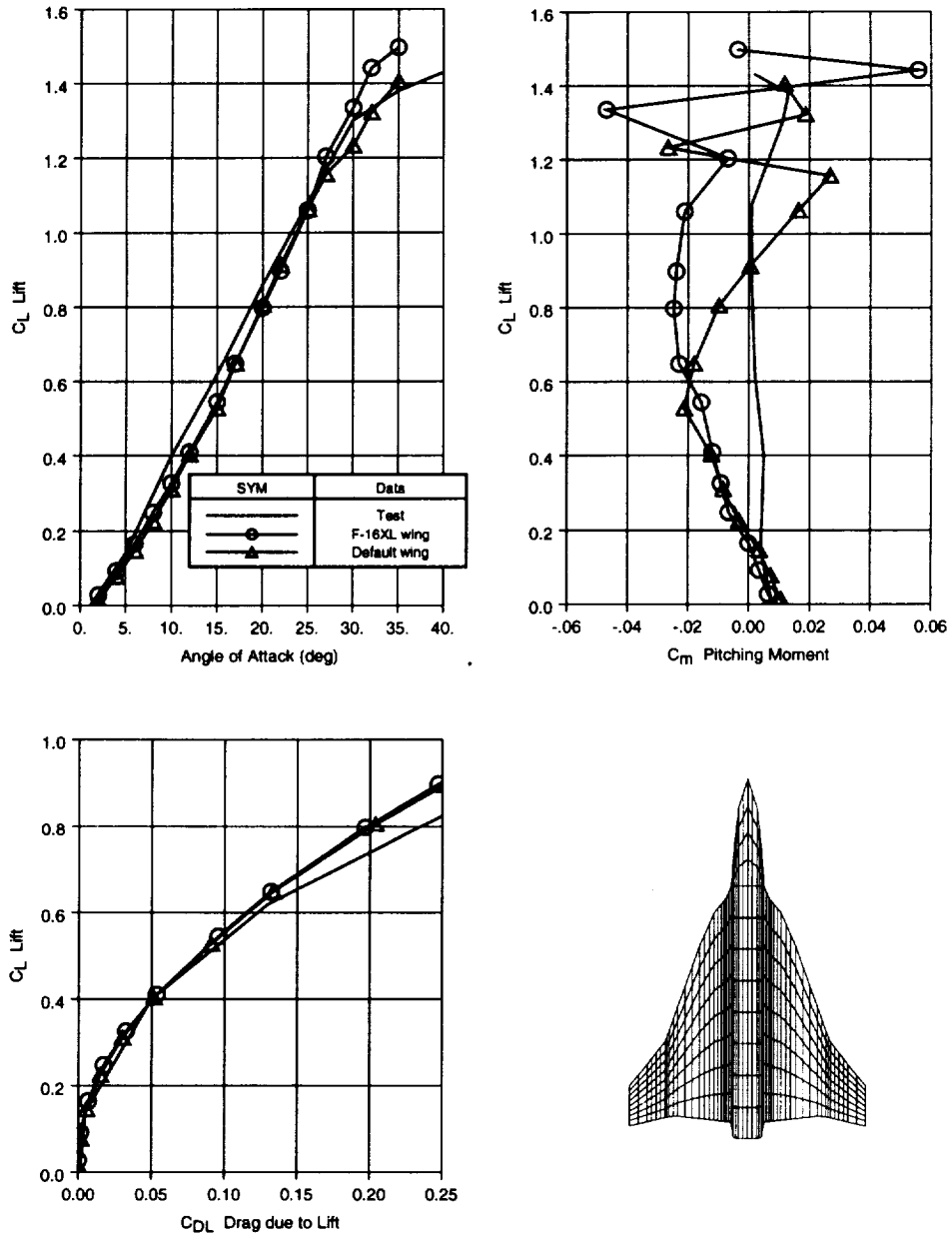


Figure 6.4-4 Sensitivity to Wing Definition on F-16XL



# Vortex Flag (IVTXFLG) Sensitivity

Test vs HASC, VORLIF strake/wing, VORLAX forebody

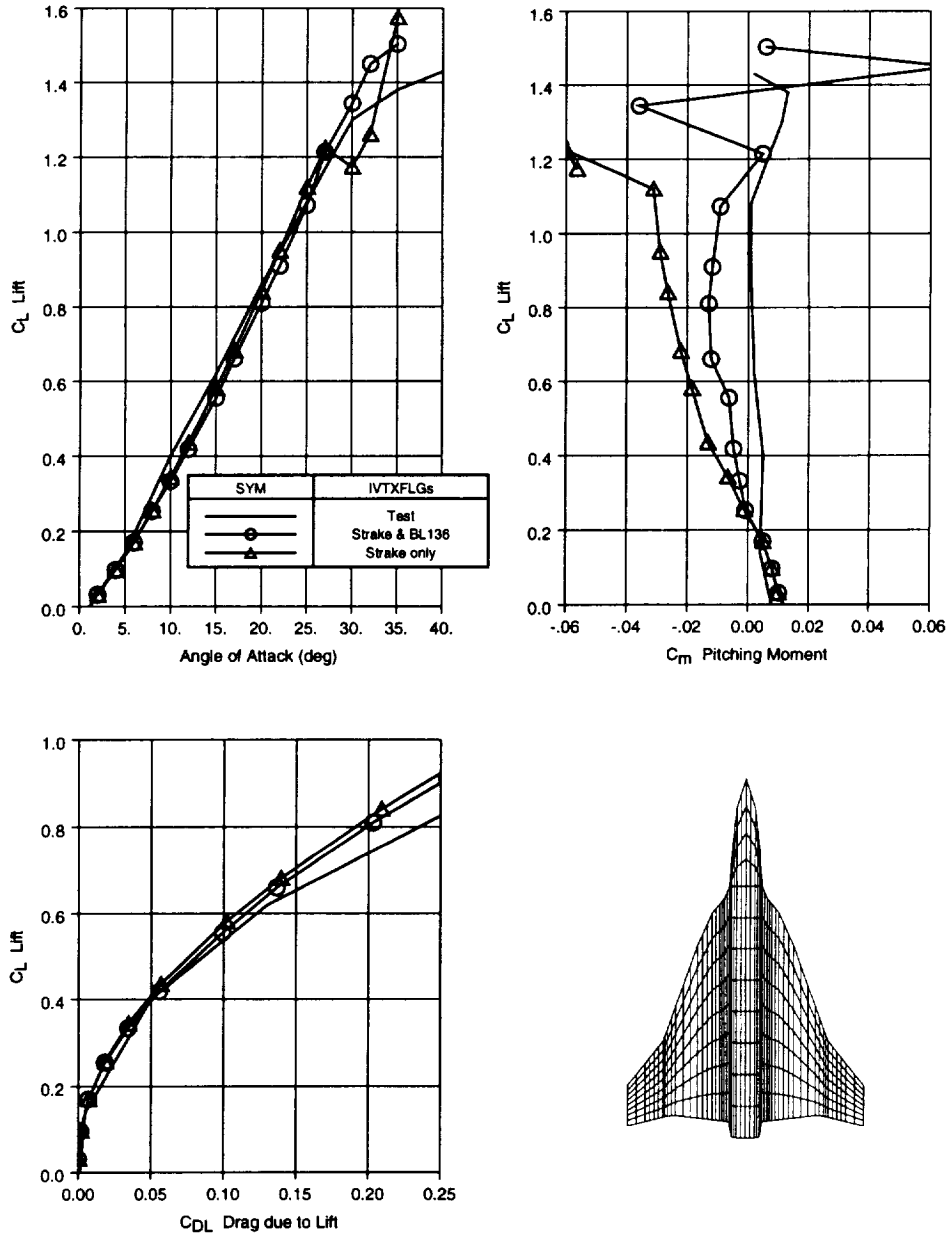


Figure 6.4-5 F-16XL Sensitivity to Vortex Flag (IVTXFLG)

## Control Effectiveness Validation

The baseline HASC model was modified by adding panels to the wing surface to allow deflected elevons. Figure 6.4-6 shows the comparison of the HASC predictions using VORLAX to the test data for -10 and +10 degree elevon increments. Figure 6.4-7 shows this comparison for the -30 and +30 degree elevons.

## Sym. Elevon (-10,+10) Comparison

Test vs HASC, VORLAX wing with SPC=-1

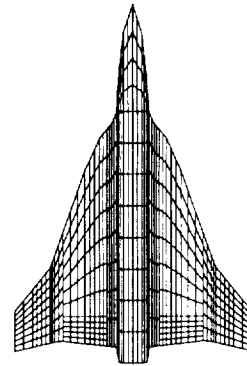
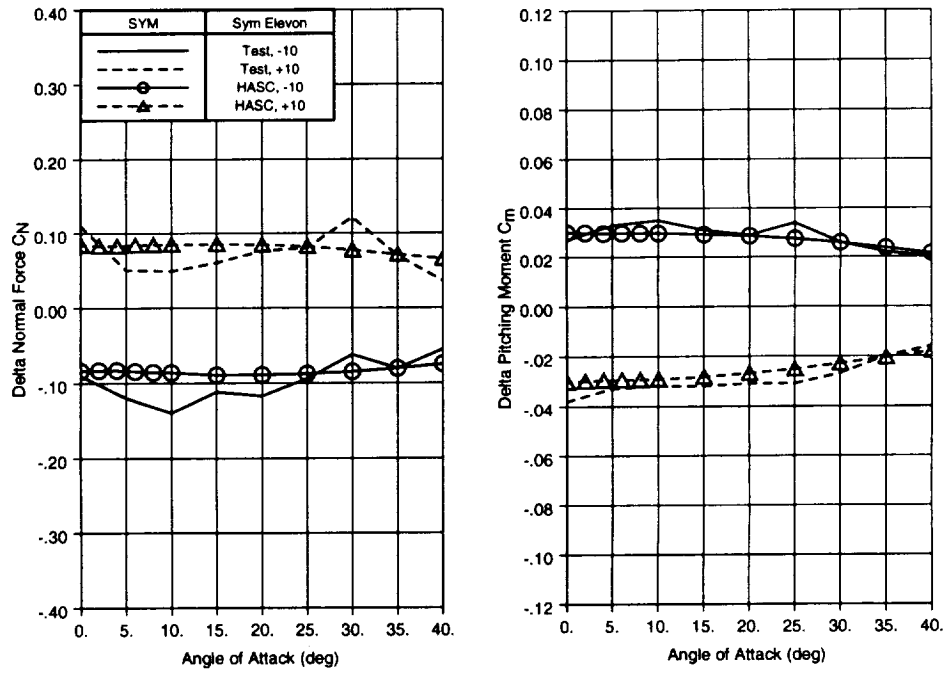


Figure 6.4-6 F-16XL Symmetric 10 deg. Elevon Comparison

## Sym. Elevon (-30,+30) Comparison

Test vs HASC, VORLAX wing with SPC=-1

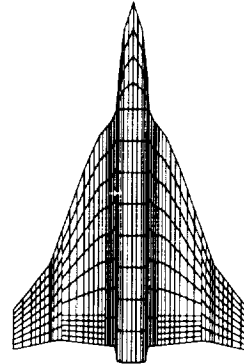
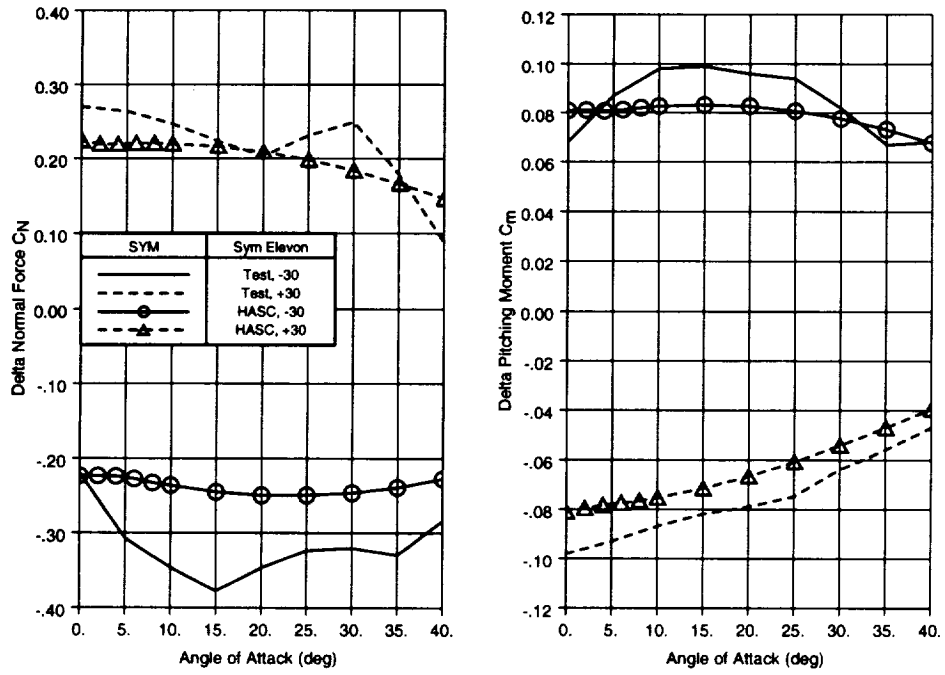


Figure 6.4-7 F-16XL Symmetric 30 deg. Elevon Comparison

## 6.5 F-16 Airplane

### Background

The F-16 airplane was also chosen as a HASC validation configuration. The F-16 has many of the geometric variables that are significant in vortex flow analysis. Camber, twist, and airfoils vary across the span. In addition the planform is complex in that the sweep of the strake is reducing in the outboard spanwise direction. Also, the tail is under heavy influence of the wing downwash that is changing due to angle of attack and wing vortex breakdown or burst. Mach = 0.60 data from a 1/9-scale force and moment model of the F-16 tested in the Arnold Engineering Development Center 16T facility was used for comparison with the HASC predictions. Wing-tip launchers and missiles were included both on the wind tunnel model and in the HASC model.

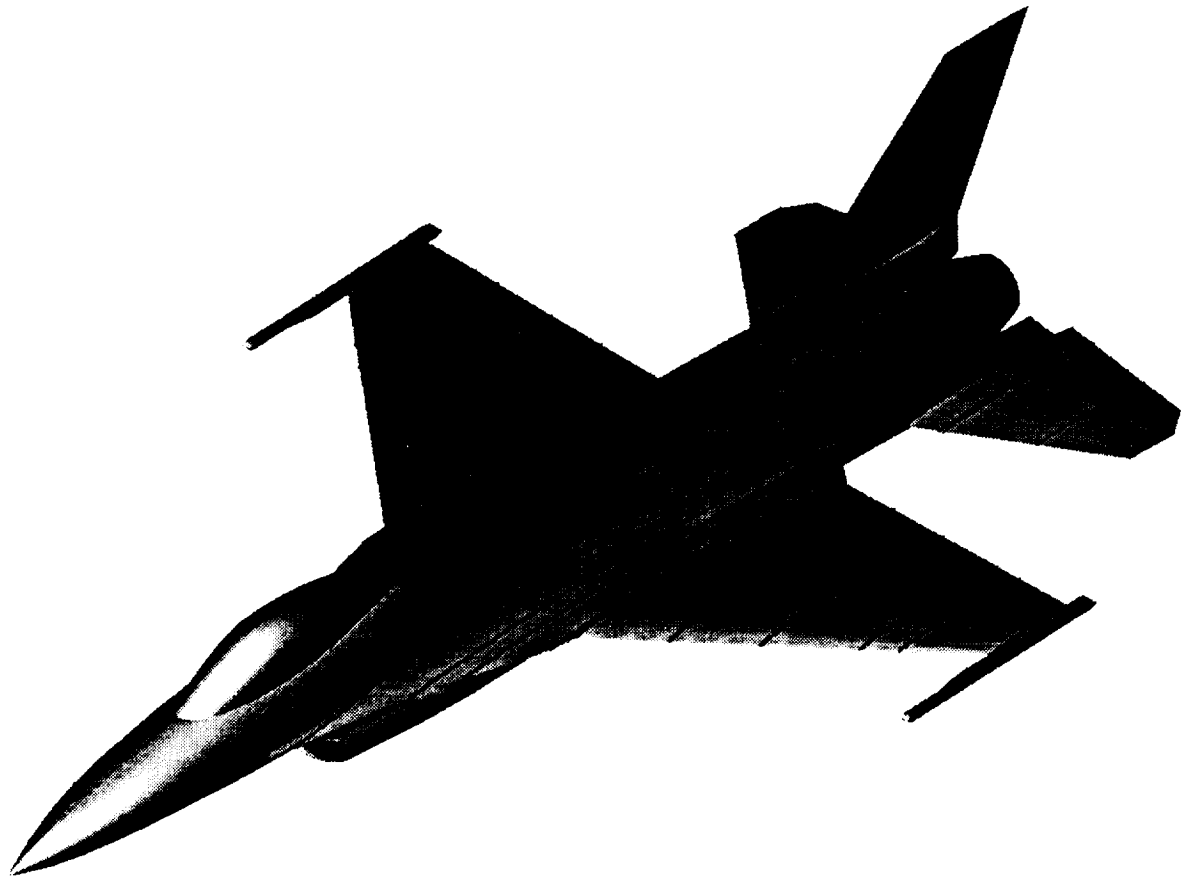


Figure 6.5-1 F-16 Configuration

## Baseline Validation

The comparison of the baseline F-16 with all controls undeflected is shown in figure 6.5-2. Predictions from using VORLIF both on the wing and horizontal tail and from using VORLAX on the wing and horizontal tail are compared to the test data. The forebody was analyzed with VTXCHN. Wing twist, camber, and leading edge definitions were included in the HASC model. The lift predicted from using VORLIF agrees with the test data only up through 12 degrees angle of attack. The VORLIF pitching moment results are in general agreement with the test data, however the predicted results show a non-linearity between CLs of .7 and 1.0 that is not in the test data. The VORLAX Cmo prediction is closer to the test data than that from VORLIF. At a CL = .4 the predicted drag due to lift from VORLIF is within 3% of the test drag due to lift.

The comparison between using VTXCHN and VORLAX on the forebody of the F-16 is shown in figure 6.5-3. Small differences are seen in pitching moment, No significant differences are apparent in lift or drag.

In figure 6.5-2 both the wing and horizontal tail were analyzed in VORLIF. Figure 6.5-4 shows change in the HASC prediction if the horizontal tail is analyzed in VORLAX, while the wing is analyzed in VORLIF. The pitching moment comparison at the higher angles of attack is better when analyzing both surfaces in VORLIF. As discussed earlier in the report, the computational time is longer when running two lifting surfaces in VORLIF (wing & tail) vs. one surface in VORLIF (wing) and one in VORLAX (tail).

The highly vortex dominated flowfield of the F-16 results in the HASC predictions being sensitive to placement of the vortex flag. The baseline runs shown in figure 6.5-2 are with the vortex flag IVTXFLG set to 1 at the inboard panel (strake) and where the wing begins (leading edge sweep change). These settings are according to recommendations in the user's guide. Changing the outboard IVTXFLG from 1 to 0 dramatically worsens the comparison as shown in figure 6.5-5. It is extremely important to assure correct setting of the vortex flags, as well as correct modeling of the wing geometric parameters, when analyzing surfaces in VORLIF.

# Baseline Comparison

Test vs HASC, VORLAX Forebody

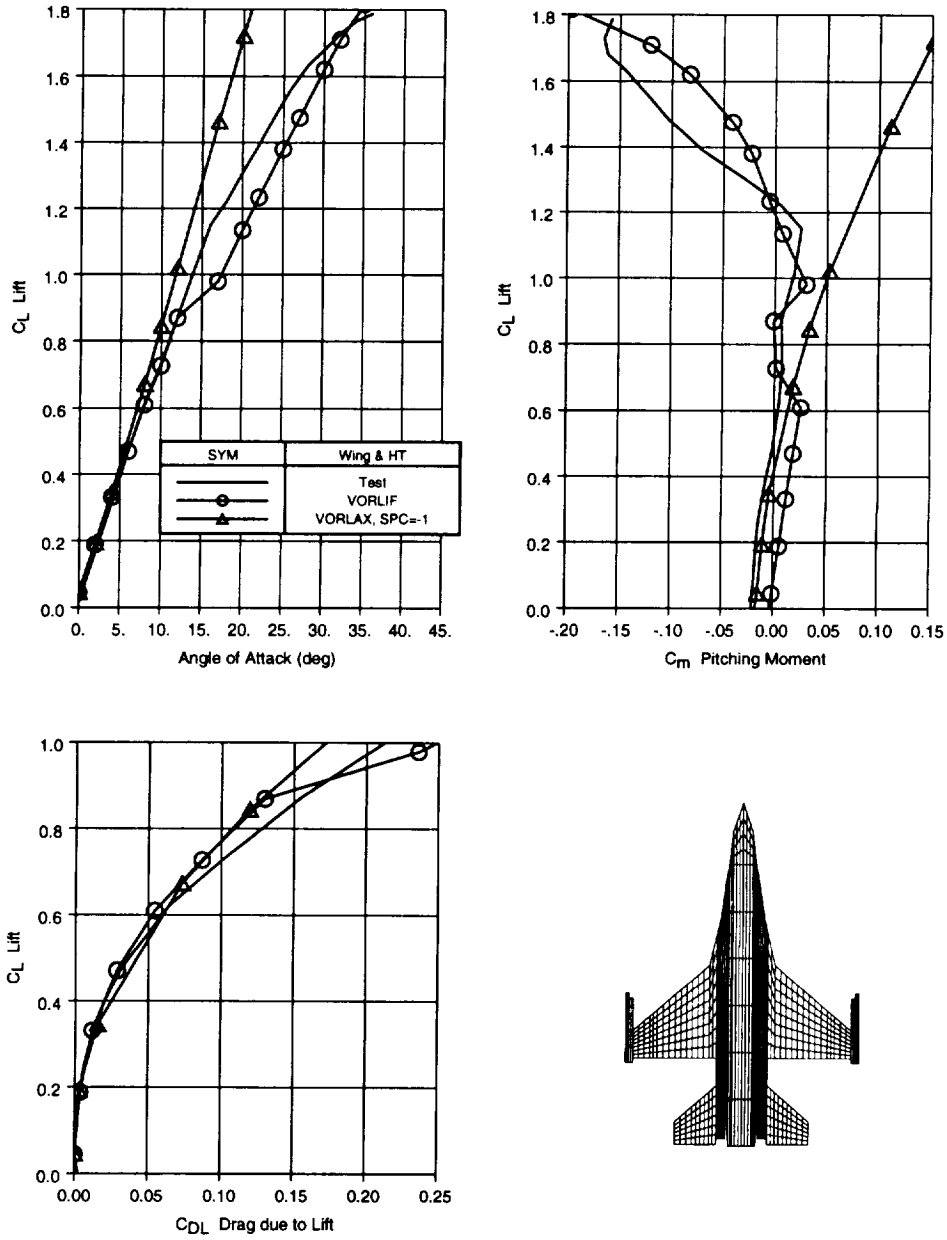


Figure 6.5-2 F-16 Baseline Comparison, M=.6, Controls=0

# Forebody Computation Comparison

Test vs HASC, VORLIF wing & HT

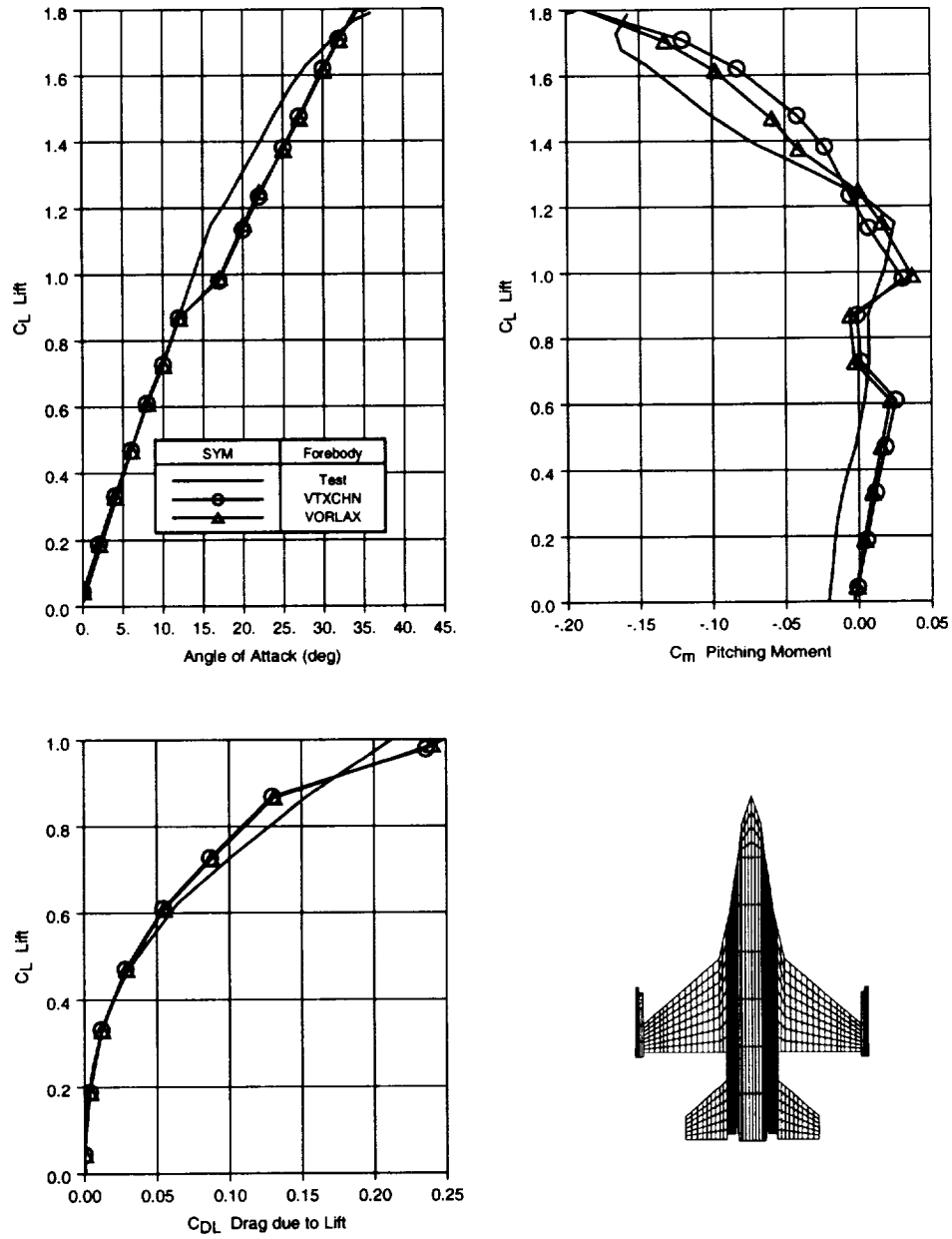


Figure 6.5-3 Comparison of Forebody Calculation Methods on F-16



## Control Effectiveness Validation

The F-16 HASC model was modified to include panels representing the full span leading edge flap. Leading edge flap increments were predicted using VORLIF for the wing and VORLAX for the forebody and horizontal tail. Figure 6.5-6 shows the comparison to the test data for a 15 degree leading edge flap deflection, while figure 6.5-7 shows the comparison for a 25 degree leading edge flap deflection.

The horizontal tail increments from -10 and +10 degree deflections were computed next. Results from analyzing the tail in VORLIF are shown in figure 6.5-8, while results from using VORLAX on the tail are shown in figure 6.5-9. The VORLAX results are in better agreement to the test data than the VORLIF results especially at the higher angles of attack. The horizontal tail increment (on-off) was also computed. The normal force and pitching moment agreement is good through 12 degrees angle of attack as shown in figure 6.5-10. HASC under predicts the tail presence increment above 12 degrees.

## HASC Model with Sideview Paneling for Lateral/Directional Effects

The HASC model was then modified to include the sideview projection of the forebody, fuselage, vertical tail, and rudder. Rudder effectiveness for a 30 degree deflection were computed with HASC and compared to test data as shown in figure 6.5-11.

The F-16 HASC model with the sideview paneling was then run at 5 degrees of sideslip for comparison of the lateral/directional coefficients. Figure 6.5-12 present the HASC predictions from using both VORLAX and VTXCHN on the forebody and VORLAX on the wing and tail. The predicted rolling moment, yawing moment, and side force do not compare well to the test data. Some differences are apparent between VORLAX and VTXCHN in yawing moment and side force.

Figure 6.5-13 shows the change in the predicted results in sideslip when analyzing the wing in VORLIF to VORLAX. The yawing moment comparison is improved, however the rolling moment and side force comparison is worse. Figures 6.5-12 and 6.5-13 indicate an area of future research and development for HASC.

# Baseline Comparison

Test vs HASC, VORLIF wing, VTXCHN forebody

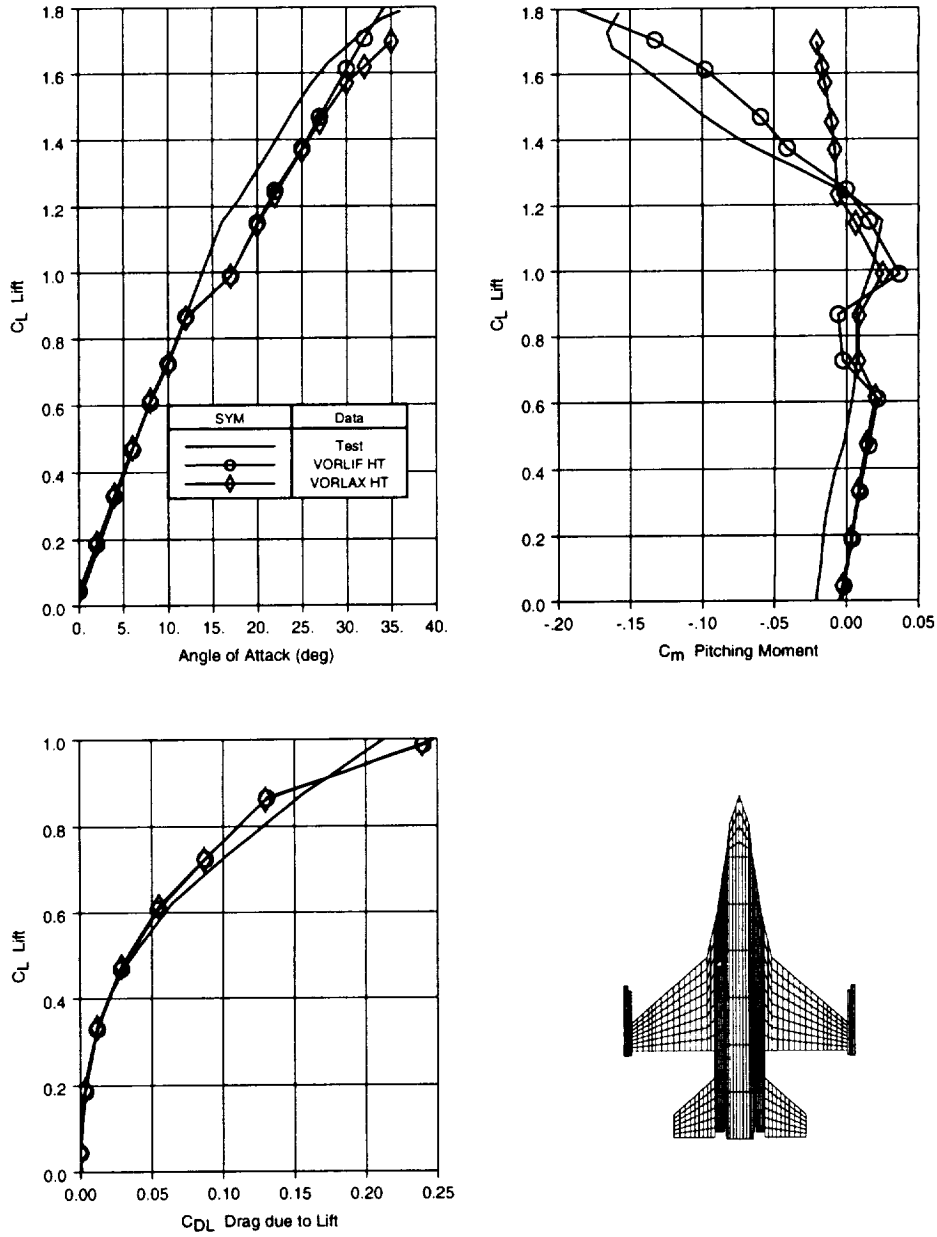


Figure 6.5-4 Comparison of Computation Methods on F-16 Horizontal Tail

# Vortex Flag (IVTXFLG) Sensitivity

Test vs HASC, VORLIF wing & HT, VORLAX forebody

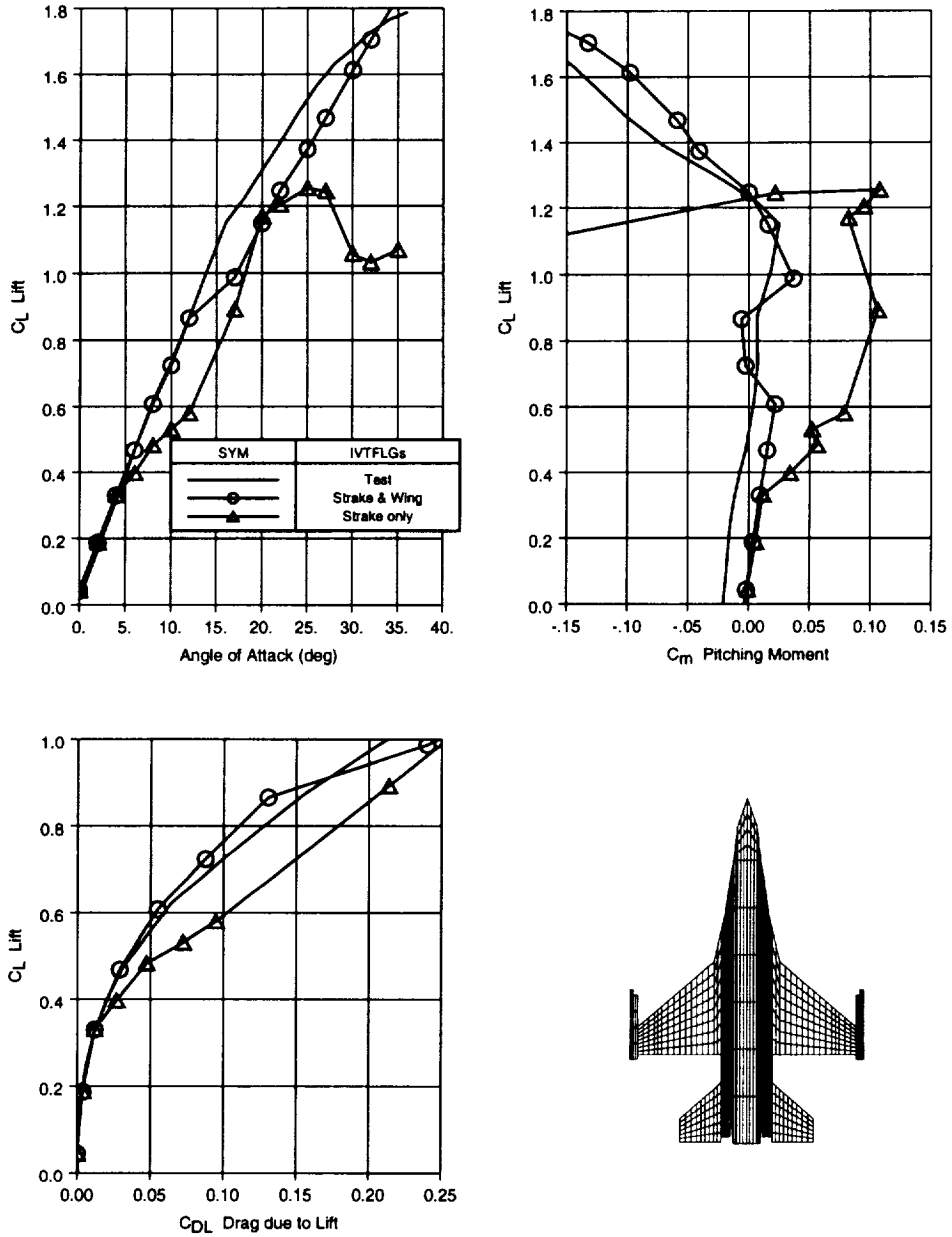


Figure 6.5-5 F-16 Sensitivity to Vortex Flag (IVTXFLG)

# 15deg. Leading Edge Flap Comparison

Test vs HASC, VORLIF wing, VORLAX HT & forebody

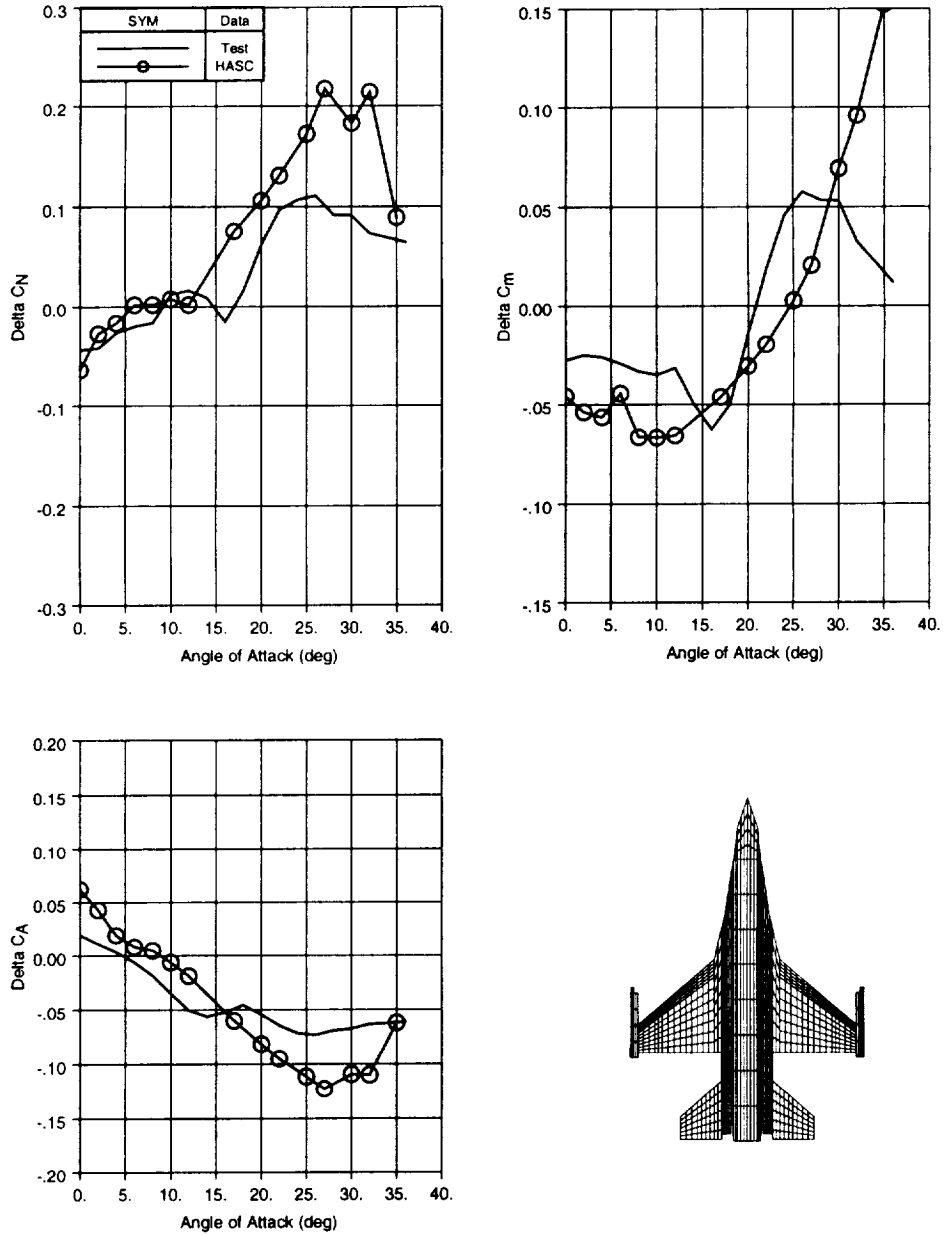


Figure 6.5-6 F-16 15 deg. Leading Edge Flap Comparison

## 25deg. Leading Edge Flap Comparison

Test vs HASC, VORLIF wing, VORLAX HT & forebody

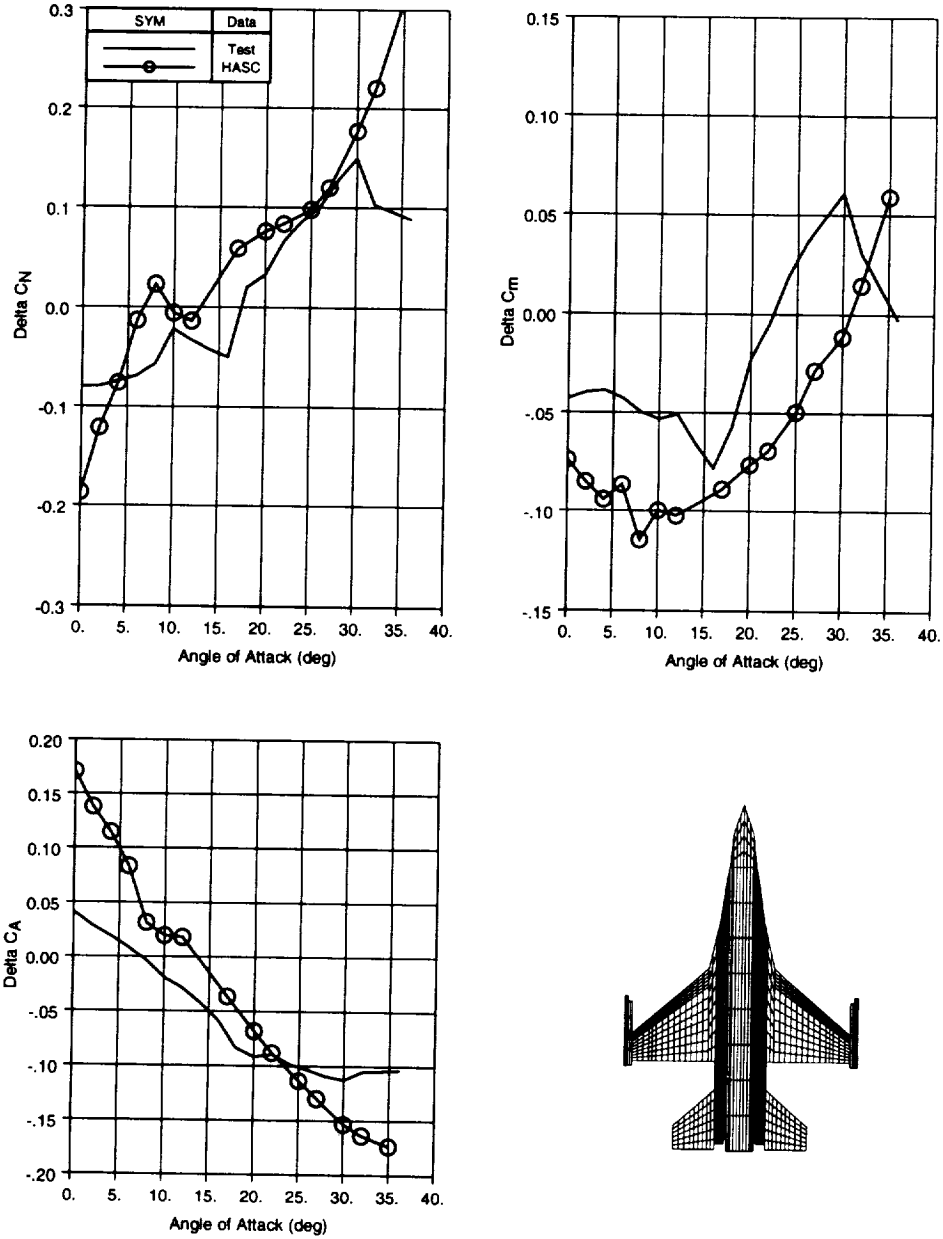


Figure 6.5-7 F-16 25 deg. Leading Edge Flap Comparison

## HT Tail(-10,+10) Comparison

Test vs HASC, VORLIF wing, VORLAX HT w/SPC=-1, VORLAX forebody

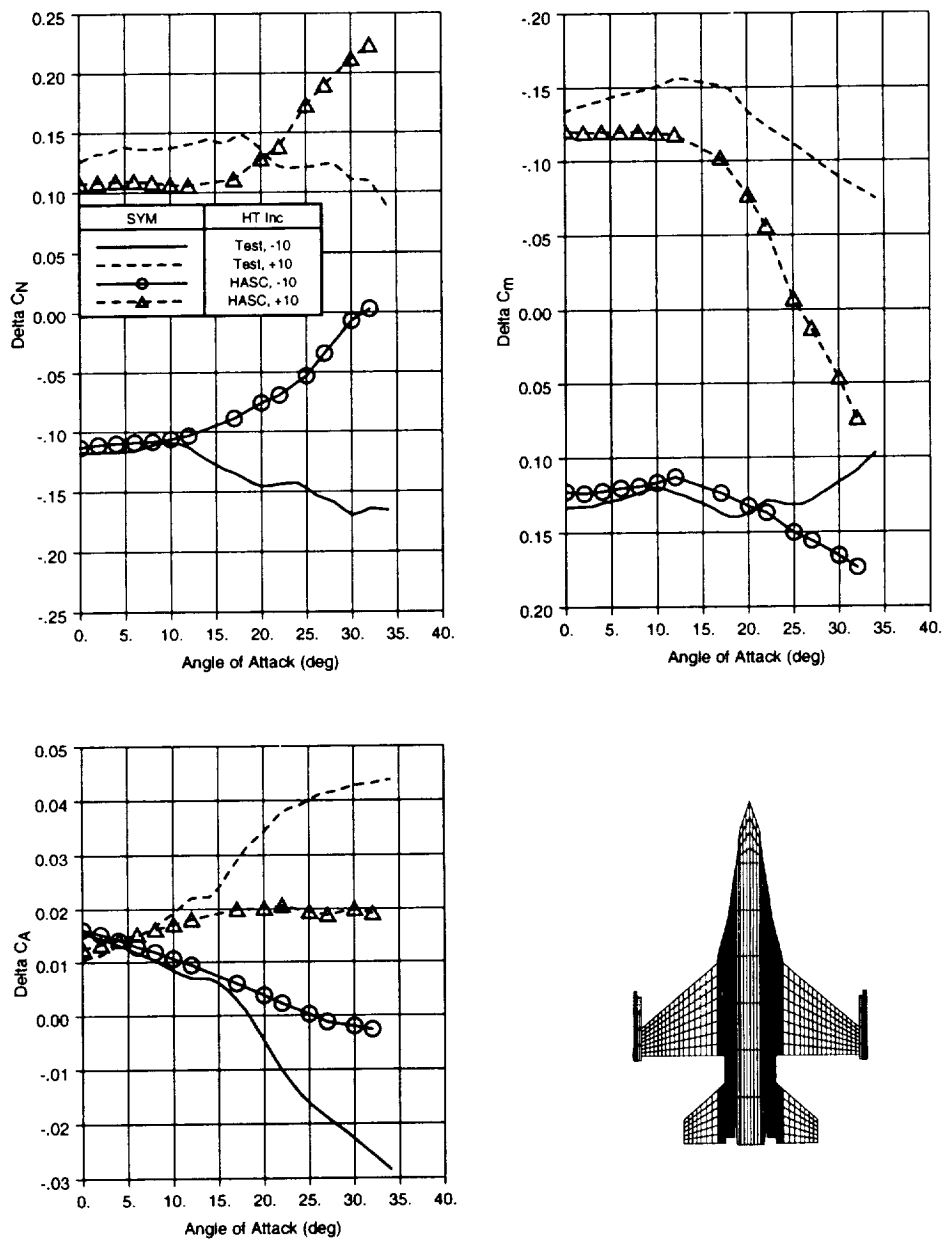


Figure 6.5-8 F-16 10 deg. Horizontal Tail Comparison, VORLIF

# HT Tail(-10,+10) Comparison

Test vs HASC, VORLAX wing & HT w/SPC=-1, VORLAX forebody

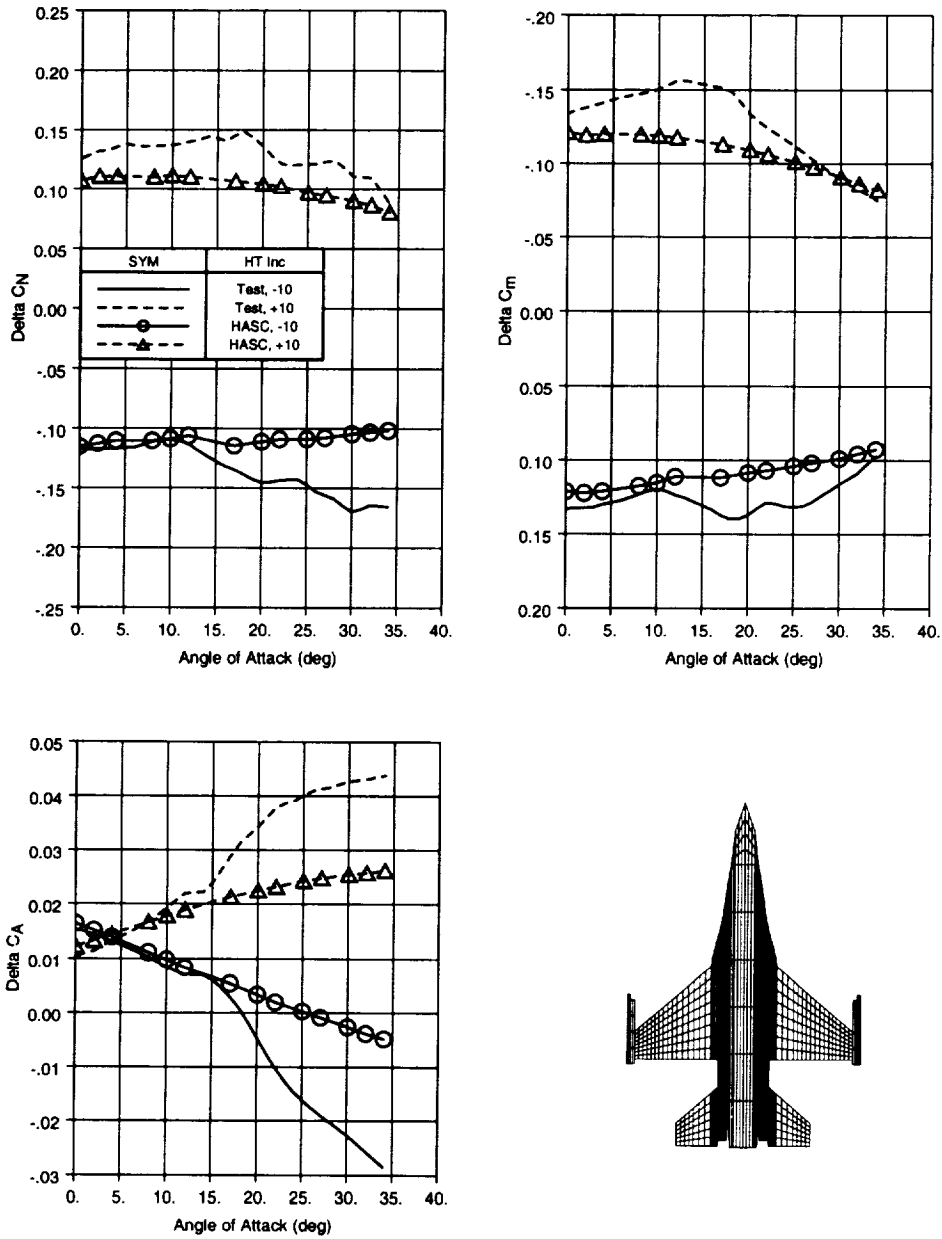


Figure 6.5-9 F-16 10 deg. Horizontal Tail Comparison, VORLAX



# HT Tail (on-off) Comparison

Test vs HASC

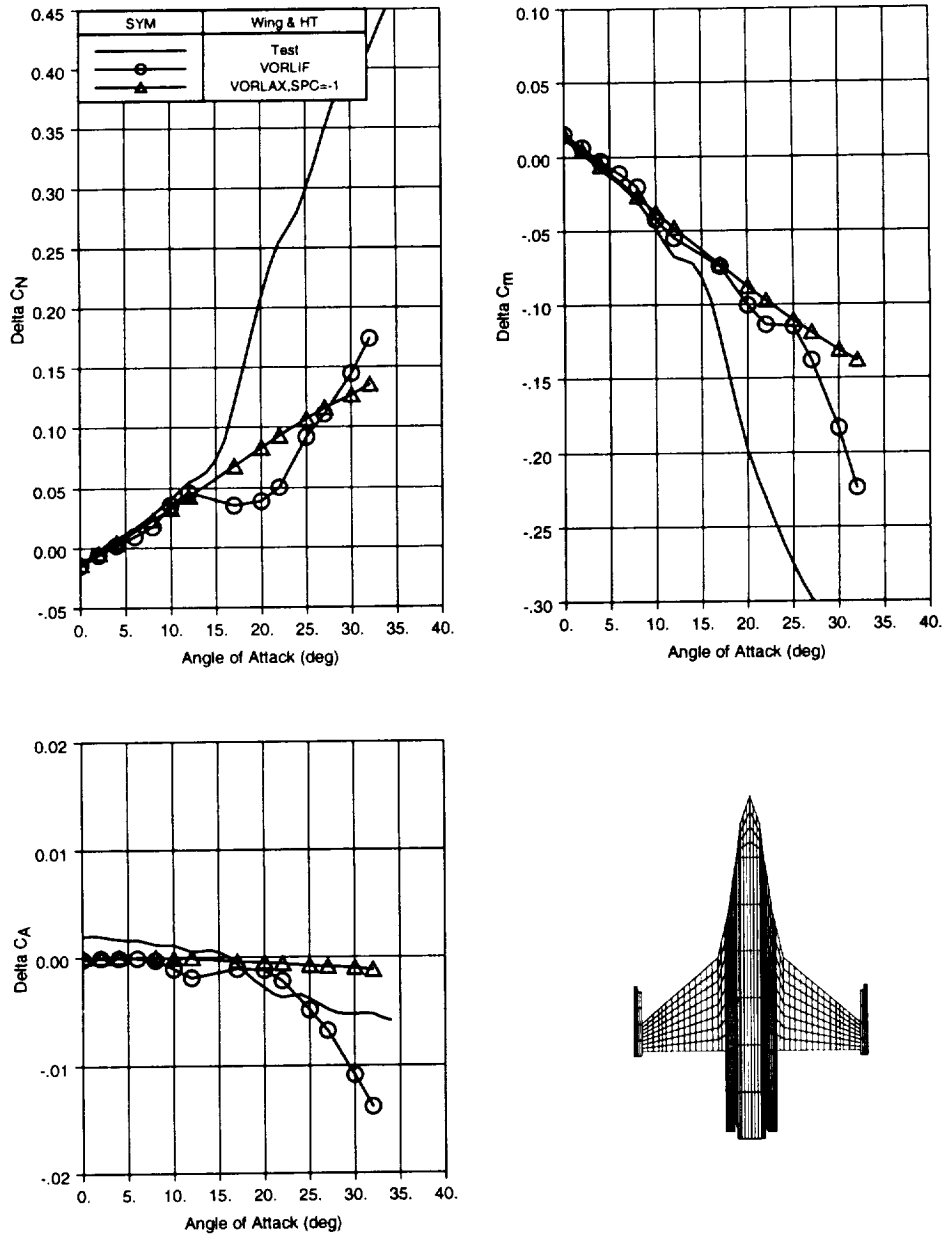


Figure 6.5-10 F-16 Horizontal Tail Increment (on-off) Comparison

### 30degree Rudder Comparison

Test vs HASC, VORLIF wing & HT, VORLAX forebody & VT

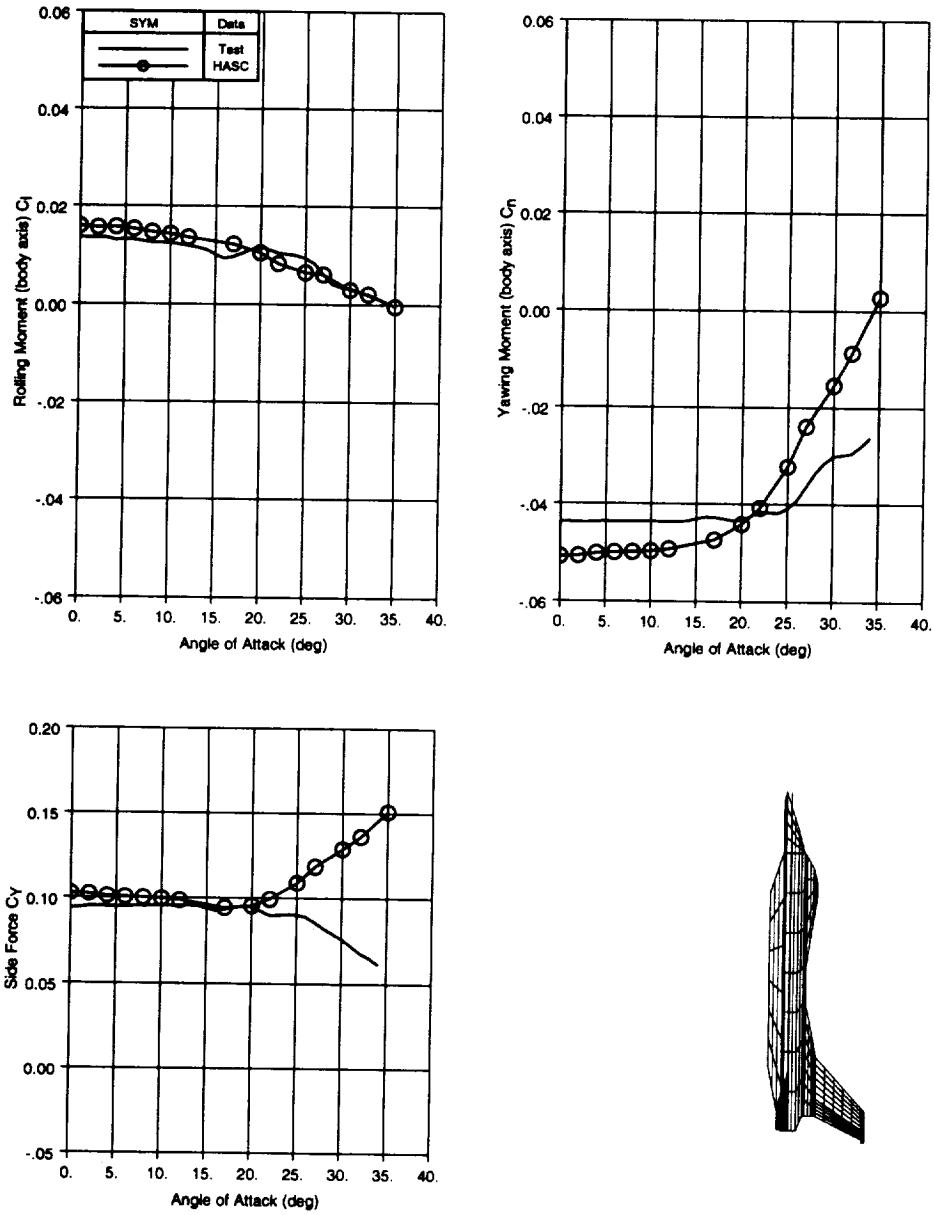


Figure 6.5-11 F-16 30 deg. Rudder Comparison

## Forebody Comparison, Lat/Dir at Beta = 5

Test vs HASC, VORLAX wing & HT

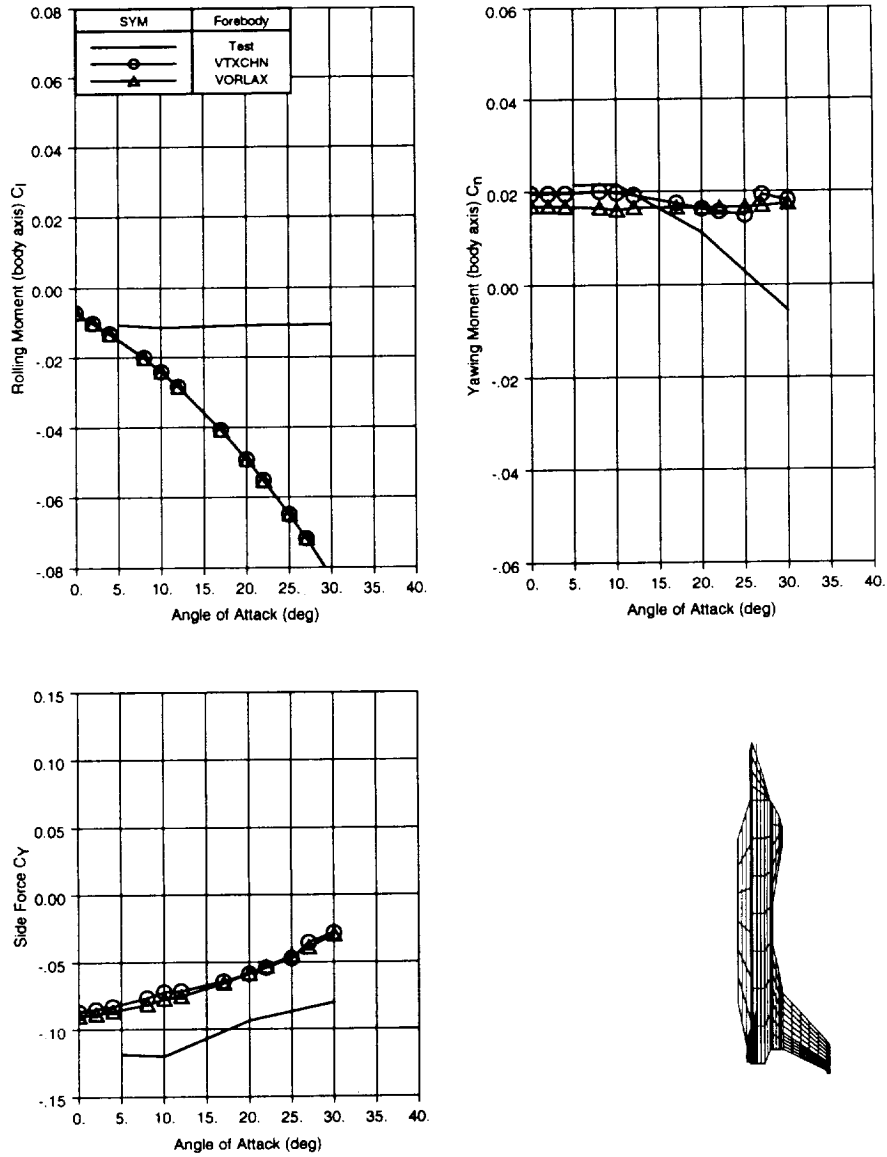


Figure 6.5-12 F-16 Comparison of Forebody Methods at 5 deg. Sideslip

# Lat/Dir at Beta = 5 Comparison

Test vs HASC

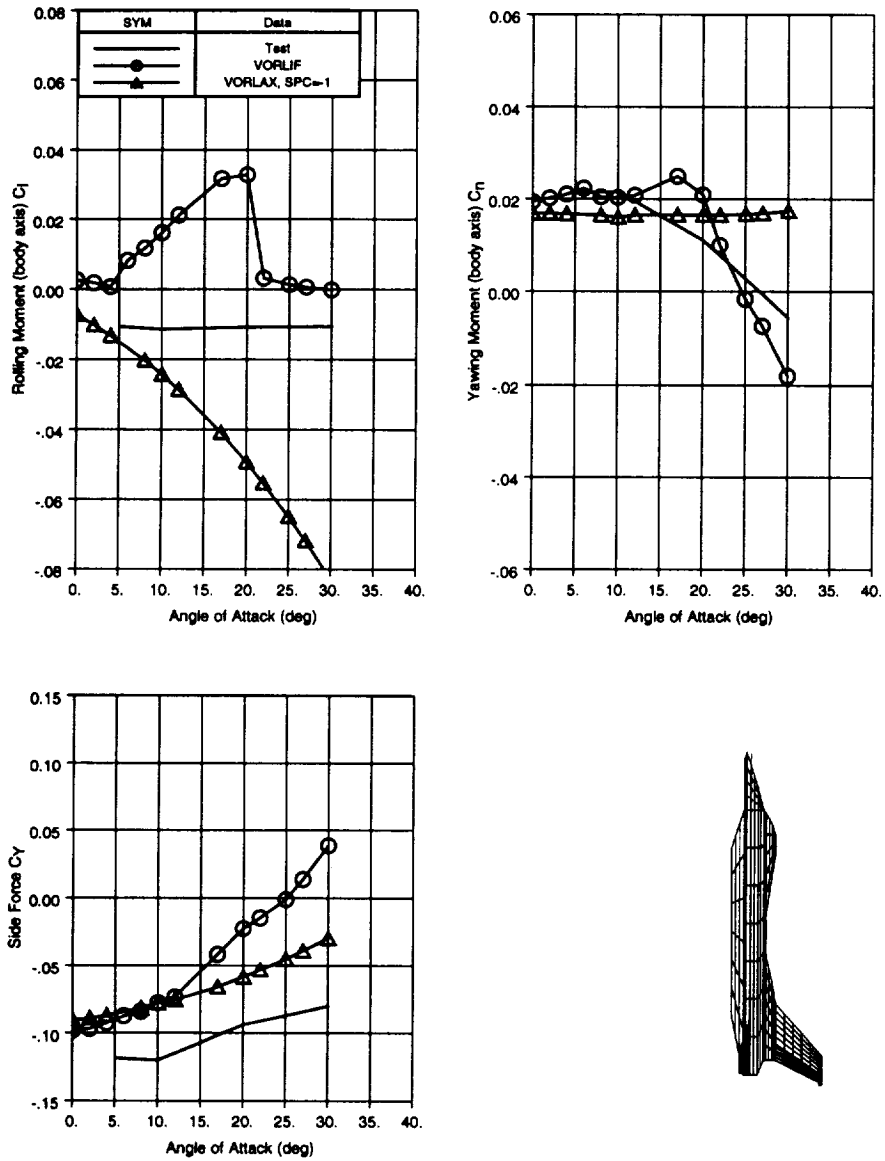


Figure 6.5-13 F-16 Comparison of VORLAX and VORLIF at 5 deg. Sideslip

### Additional Validation

The last validation plot with the F-16 configuration is a comparison of the damping derivatives. These derivatives,  $C_{mq}$ ,  $C_{nr}$ , and  $C_{lp}$ , were predicted using VORLAX analysis on all the HASC surfaces. As shown in figure 6.5-14, HASC predicted the correct sign for each derivative, but overpredicted  $C_{lp}$  and  $C_{nr}$ , and underpredicted  $C_{mq}$ . Additional validation is required using the VORLIF and VTXCHN options for predicting steady-state terms.

## Damping Derivative Comparison

Test vs HASC, VORLAX wing & HT & forebody

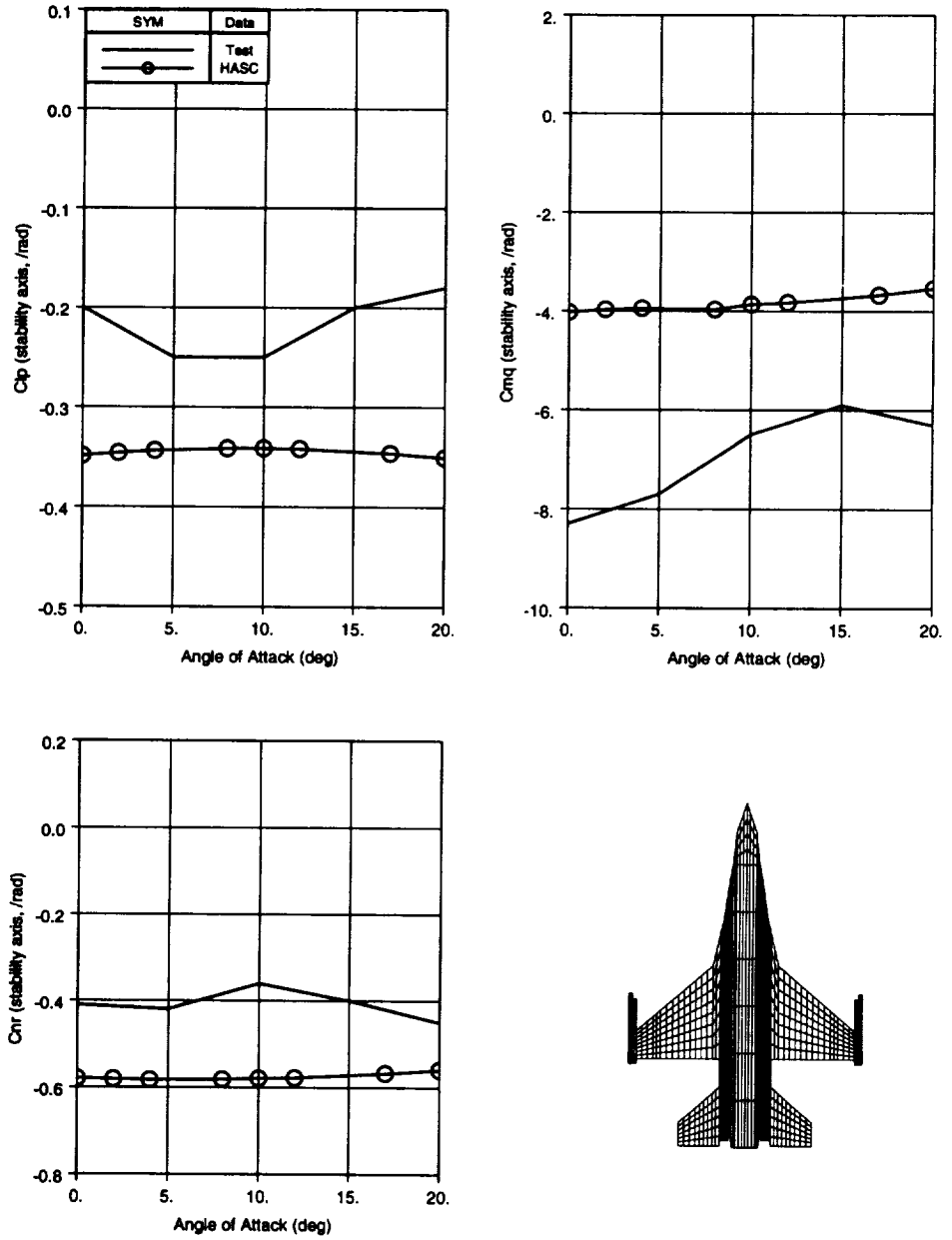


Figure 6.5-14 F-16 Steady-State Dynamic Derivatives Comparison

## 6.6 Convair Model 200 Configuration

### Background

The last configuration utilized in the HASC validation is referred to as the Convair Model 200. Low speed test data from the GDLST tunnel (reference 20) was used as the validation data. The data presented in the reference document had been adjusted to represent the study configuration. The wind tunnel model had slight variations in the wing planform and canard size compared to the baseline data. Although the data was adjusted to compensate for these differences, the data used in the HASC validation are considered adequate for comparative purposes.

### Validation

Limited geometric data was available for the Model 200. Therefore the HASC model was very basic. Camber and twist were set to zero. Default wing definitions were also used. HASC predictions were made analyzing the wing and canard both in VORLIF (ISRTYP=2 on canard and ISRTYP=1 on wing) and in VORLAX (ISRTYP=5 on the canard and wing) with SPC=-1. The comparison is presented in figure 6.6-1. The VOLIF predictions agree closer to the test lift values through 15 degrees angle of attack, while VORLAX results are closer to the test pitching moment curve.

# Baseline Comparison

Test vs HASC

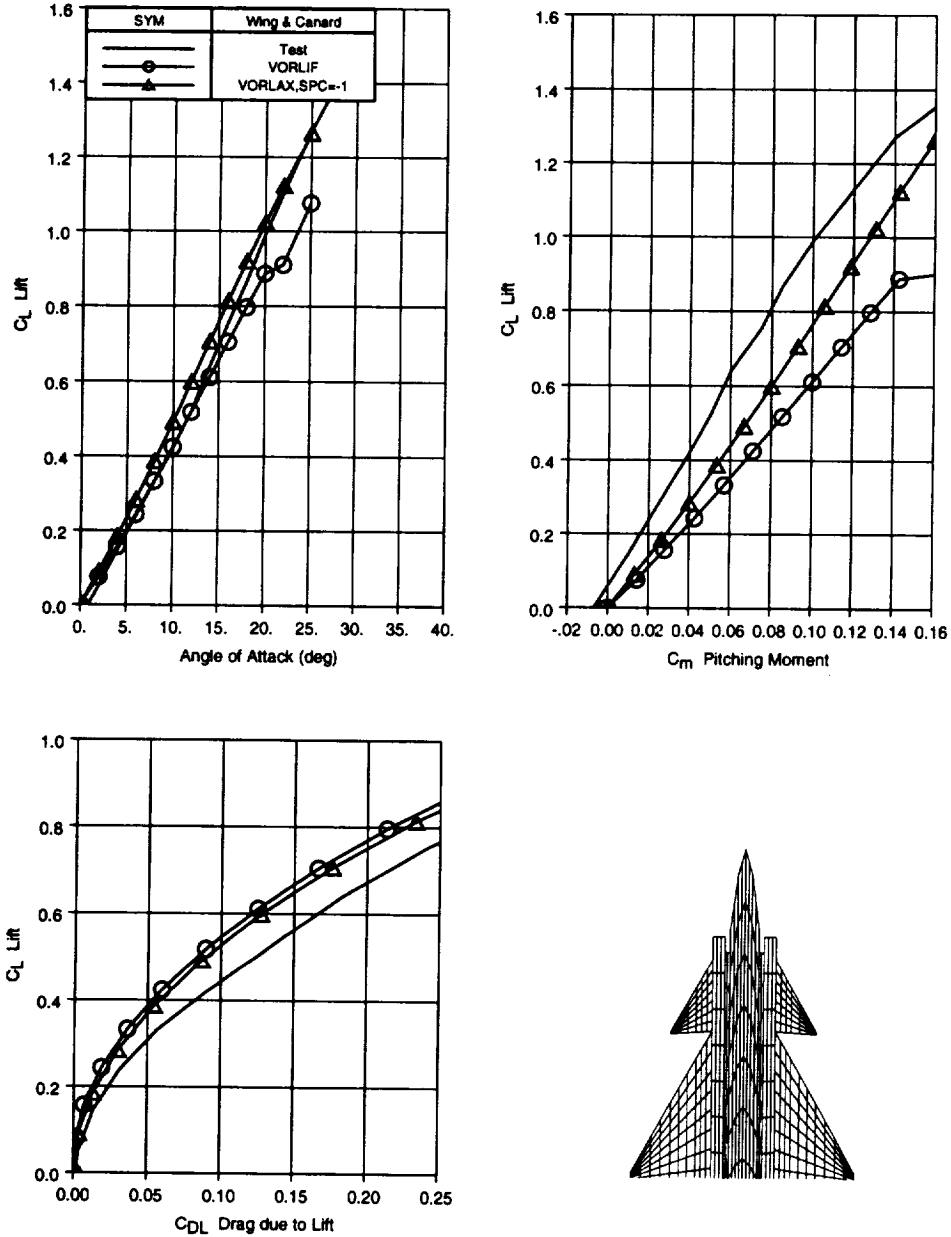


Figure 6.6-1 Convair Model 200 Baseline Comparison



## 6.7 HASC Validation Summary

Several comments relating to the HASC validation runs in this report and general limitations of HASC are listed below.

- 1) VORLIF predictions (ISRTYP = 1 or 2 on lifting surfaces) are sensitive to the input model (paneling).
- 2) VORLIF predictions often result in 'noisy' trends in the middle to high angle of attack regions.
- 3) VORLAX predictions (ISRTYP=5), often using SPC = -1, often produced good agreement with the test data.
- 4) Lateral/directional effects were poorly predicted for the F-16 configuration.
- 5) High angle of attack results (stall & post stall) will not be accurate for configurations that have trailing edge stall before the leading edge stalls; i.e., wings having airfoils with large leading-edge radius and camber.
- 6) For low angles of attack (less than 10 degrees) and thin airfoils the HASC results should be good for Mach numbers up to 0.9. For higher angles of attack and thin airfoils the results should be good for Mach numbers up to 0.5.
- 7) Camber and airfoil shape must be represented accurately because the vortex breakdown is very sensitive to these terms.
- 8) No more than two tandem lifting surfaces can be run with vortex lift and breakdown (in VORLIF).
- 9) Due the basic method being a vortex lattice approach some configurations may be difficult to represent accurately. For example any panel edge can have only one height (z) from the reference. Trailing edge and leading edge heights of this edge are represented only by incidence input.
- 10) Swept forward wings can not be analyzed in VORLIF.

11) Canards with their vertical placement below the wing level will cause abnormal effects at the angle of attack where the wake passes through the wing. This occurs in real life, but not to such adverse degree.

## **7.0 CONCLUSIONS**

Several improvements have been made to the HASC code providing an improved conceptual/preliminary design level aerodynamic prediction method. Many software errors were identified and corrected, setup requirements were simplified, enhancements were made to the methodology, validation runs were made on several aircraft configurations, and a comprehensive document has been created. This modification task has been successful in providing an improved aerodynamic prediction tool for non-linear aerodynamic predictions, however additional improvements are still required in several areas for the code to satisfy all the requirements envisioned for a non-linear aerodynamic prediction code with wide application. The development of new non-linear prediction methods must continue through small modification tasks such as reported herein, and/or larger development efforts for new state-of-the-art prediction methods.

## 8.0 RECOMMENDATIONS

Several recommendations for future improvements to HASC were identified during this modification task. The recommendations for the VTXCHN routine are listed first, followed by those for the VORLIF/VORLAX routines, and finally some general recommendations for the HASC development. Many of these recommendations when implemented will further increase the accuracy and robustness of the HASC code.

### VTXCHN Recommendations

- Investigate different methods for determining vortex separation location and strength related to separation from chines.
- Investigate methods for modeling volume effects in the physical plane.
- Improve the method for determining the mapping coefficients to prevent the body from being stretched vertically.
- For bodies with corners or chines, extend VTXCHN to determine multiple separation points depending on the flow conditions.
- Make comparisons with higher order algorithms and experimental flow visualization to determine the validity and accuracy of the vortex field calculated in VTXCHN.
- Further clean up the code, enhance maintainability, improve efficiency, and further improve the user friendliness of the code.
- VTXCHN should be further integrated into HASC by including the vortices from the forebody in the vortex tracking analysis of VORLIF.

### VORLIF Recommendations

- Include the free vortices in the flow field when calculating the boundary conditions in the vortex lattice part of the code. This change will improve the analysis of merging vortices and vortex stability analysis.
- New algorithms should be developed to include effects of trailing edge stall.
- Determine reasons for and correct discrepancy within VORLIF due to changing number of spanwise stations.
- Modify to allow analysis of swept forward wings.
- Allow panels with 90 degree sweeps anywhere along the span of a VORLIF surface.

### General Recommendations

- Continue checkout and validation of recent code modifications.
- Expand the validation of HASC using a variety of aircraft configurations.
- Continue research and development on additional empiricism.
- Automate geometry paneling.
- Include calculations for hinge moments.
- Conduct a major overhaul of the software by using modern programming languages and GUI interfaces.
- Provide continuous technical support and collect recommendations for future code enhancements.

## REFERENCES

1. Adler, C.O. and Dixon, C.J.: **High Angle of Attack Stability and Control -- Prediction Methods and Code**, Air Force Report, WL-TR-92-3050, October 1992.
2. Miranda, L.R., Elliott, R.D., and Baker, W.M.: **A Generalized Vortex Lattice Method for Subsonic and Supersonic Flow Applications**, NASA CR-2865, December 1977.
3. Dixon, D.J. and Driskill, G.T.: **A Unique Applied Computational Method for Vortex Lift Aerodynamics and Burst for Arbitrary Aircraft**, AIAA 85-4057, AIAA 3rd Applied Aerodynamic Conference, Colorado Springs, Colorado, October 14-16, 1985.
4. Mendenhall, M.R. and Lesieutre, D.J.: **Prediction of Vortex Shedding from Circular and Noncircular Bodies in Subsonic Flow**, NASA CR 4037, January 1987.
5. Lan, C.E. and Hsu, C.H.: **Effects of Vortex Breakdown on Longitudinal and Lateral-Directional Aerodynamics of Slender Wings by the Suction Analogy**, AIAA-82-1385, AIAA Atmospheric Flight Mechanics Conference, August 9-11, 1982, San Diego, California.
6. Ericsson, L.E. and Reding J.P.: **Asymmetric Vortex Shedding from Bodies of Revolution**, Chapter VII, Tactical Missile Aerodynamics, Vol. 104, Progress in Astronautics and Aeronautics Series, M. Hemsch and J.N. Nielsen editors, 1986, pp 243-296.
7. Uberoi, M.S.: **Mechanisms of Decay of Laminar and Turbulent Vortices**, Journal Fluid Mechanics, Vol. 90, part 2, pp. 241-255, 1979.
8. Dixon, C.J.: **Semi-Empirical Analysis of Vortex Breakdown with Aerodynamic and Buffet Effects**, AIAA Paper 94-3483, August 1994.
9. Hubner, J.P. and Komerath, N.M.: **Spectral Mapping of Quasi-Periodic Structures in a Vortex Flow**, Journal of Aircraft, Vol. 32, No. 3, page 493, May-June 1995.
10. Anderson, A.E.: **Chordwise and Spanwise Loading Measured at Low Speed on Large Triangular Wings**, National Advisory Committee for Aeronautics, RM No. A9B17, April 1949.

11. Hummel, I.D.: **On the Vortex Formation Over A Slender Wing at Large Angles Of Attack**, AGARD-CPP-247, High Angle of Attack Aerodynamics AGARD - FDP Symposium, Sande F' Jord 1978, pages 15-1 through 15-17.
12. Mendenhall, M.R. and Lesieutre, D.J.: **Prediction of Subsonic Vortex Shedding from Forebodies with Chines**, NASA CR 4323, September 1990.
13. Hegedus, M.C, Dillenius, M.F.E., Perkins, S.C. Jr., and Mendenhall, M.R.: **Improved Version of the VTXCHN Code**, NEAR TR 498, August 1995.
14. Guynn, M.D.: **Evaluation of Two Discrete Vortex Based Forebody Aerodynamic Prediction Codes**, Proceedings of the Non-Linear Aerodynamic Prediction Methodology Workshop (draft), October 1994.
15. Carlson, H.W., Darden, C.M., and Mann, M.J.: **Validation of a Computer Code for Analysis of Subsonic Aerodynamic Performance of Wings with Flaps in Combination with a Canard or Horizontal Tail and an Application to Optimization**, NASA TP-2961, January 1990.
16. Hsia, A.H., Myatt, H., and Jenkins, J.E.: **Nonlinear and Unsteady Aerodynamic Responses of a Rolling 65-Degree Delta Wing**, AIAA paper 93-3682, Presented at the AIAA Applied Aerodynamics Conference, August 9-11, 1993, Monterey, California.
17. Huang, X.Z., and Hanff, E.S.: **Prediction of Normal Force on a Delta Wing Rolling at High Incidence**, AIAA paper 93-3686, Presented at the AIAA Atmospheric Flight Mechanics Conference, August 9-11, 1993, Monterey, California.
18. Abbott, I.H. and Doenhoff, A.E.V.: **Theory of Wing Sections**, 1959.
19. Grafton, S.B. and Nguyen, L.T.: **Wind-Tunnel Free-Flight Investigation of a Model of a Cranked-Arrow-Wing Fighter Configuration**, NASA TP 2410, 1985.
20. **Additional Data on Convair Model 200 NAVY V/STOL Fighter-Attack, Volume V**, Report No. GDC PSA72-1004, 1972.





## **Appendix A**

### **Description of HASC Utility Program**

A HASC utility code named HASCUTIL was written to provide a method to easily create and modify HASC and VTXCHN input files. All of the subroutines required to run HASCUTIL are contained in the file hascutil.f. The following sections briefly describe the program.

### Program Options

HASCUTIL includes four basic menu options as shown in figure A-1.

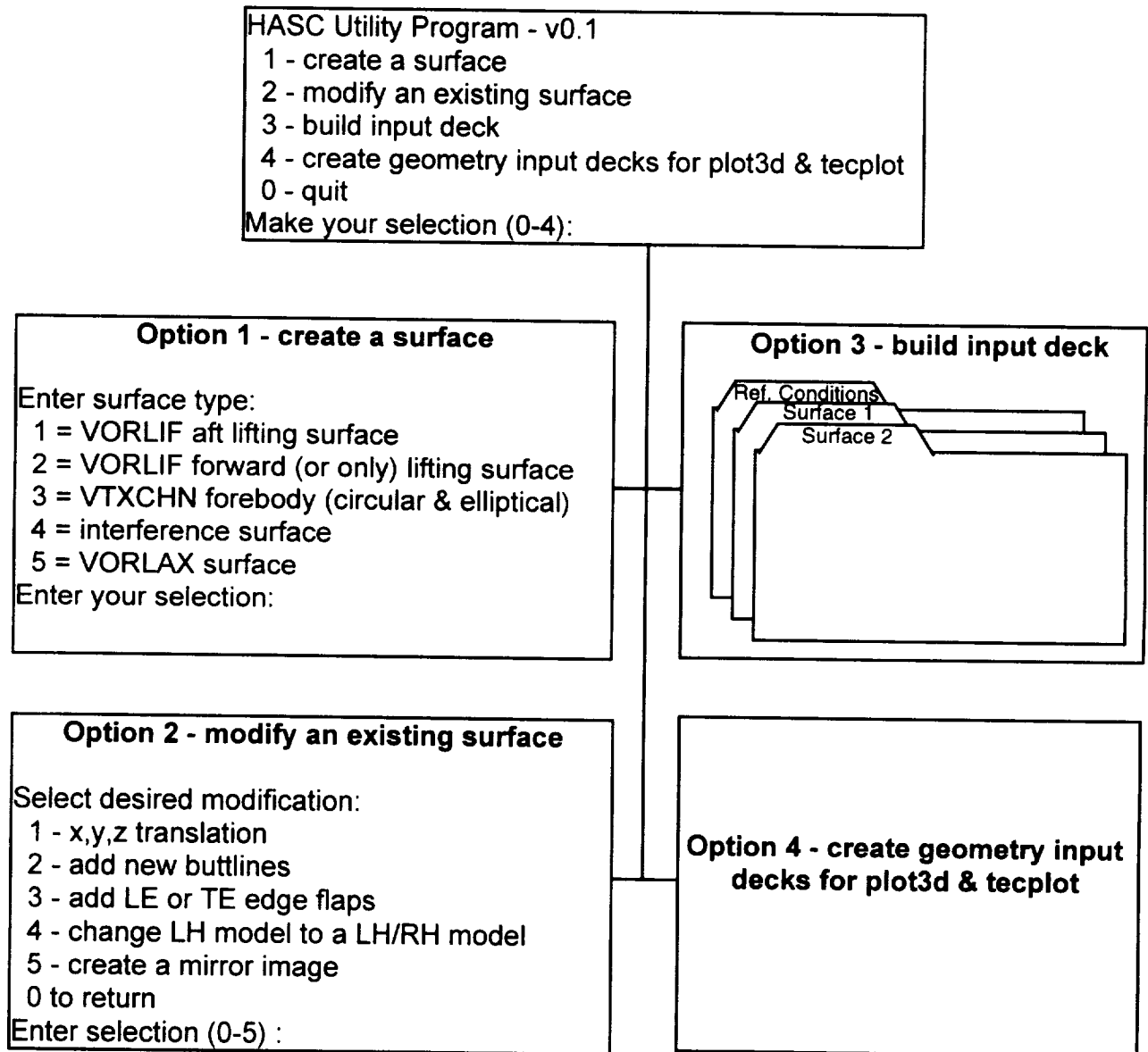


Figure A-1 Overview of HASCUTIL Program Options

The first menu option in HASCUTIL, Create a Surface, allows the user to create a surface file from a series of interactive questions. These surface files are written and stored in separate files (i.e., wing, fuselage, horizontal tail, and vertical tail surfaces would be stored in four individual files). Option 2 allows modifying an existing surface file by either adding breakpoints, translating the surface, adding leading edge and/or trailing edge flaps, change a left-hand surface to a continuous left-hand to right-hand surface (such as a fuselage), and to create a mirror image of a surface. Option 3 is used to build a complete HASC input file starting with existing files of the reference data and the surface files. Finally, option 4 reads in a complete HASC input file and writes out formatted geometry files for plot3d and Tecplot.

The following sections describe each of these options in more detail.

### **Option 1 -- Creating a New Surface**

If menu option 1 is chosen, the following menu appears:

Enter surface type:  
1 = VORLIF aft lifting surface  
2 = VORLIF forward (or only) lifting surface  
3 = VTXCHN forebody(circular & elliptical)  
4 = interference surface  
5 = VORLAX surface

Enter your selection:

HASCUTIL creates two types of surface files. The first type, from options 1-2 & 4-5, is a subset of the primary hasc input file. Items 9 through 12 as listed in table A-1 are written to this surface file. HASCUTIL asks for the number of buttock lines that define the leading and/or trailing edges. A BL should be inserted at each break in the planform shape. HASCUTIL computes the number of panels (LNPAN) that make up the surface by subtracting one from the number of BL's.

Table A-1 Summary of Parameters in HASC Input File hasc.inp

<u>Item</u>	<u>Variables</u>							
1	JOBTITL							
2	LAX	LAY	HAG	IRSTFLG	NPAN	NSURF	ALXP	
3	REY	NMACH	MACH(s)					
4	NALPHA	ALPSTB(s)						
5	NBETA	BETSTB(s)						
6	PITCHQ	ROLLQ	YAWQ	VINP				
7	SREF	CBAR	XREF	ZREF	SPAN			
8	SRFTITL							
9	<b>ISRTYP</b>	<b>LNPAN</b>	<b>ISYMFLG</b>	<b>ENETAR</b>	<b>FTAIL</b>	<b>ALZL</b>	<b>XGAP</b>	
10	<b>X1</b>	<b>Y1</b>	<b>Z1</b>	<b>CORD1</b>	<b>AINC1</b>			
11	<b>X2</b>	<b>Y2</b>	<b>Z2</b>	<b>CORD2</b>	<b>AINC2</b>			
12	<b>ISPNDIV</b>	<b>ICHRDIV</b>	<b>SPC</b>	<b>IARFYL</b>	<b>NAP</b>	<b>IVTXFLG</b>		
13	TOC1	TOC2	ROC1	ROC2	TLOC1	TLOC2	DELLE1	DELLE2
14	XAF							
15	ZC1							
16	ZC2							

At the appropriate prompt, the user supplies the X, Y, and Z coordinates along with the chord length or trailing edge values (X+chord) for each of the input BL values of the edge defining each panel that makes up the surface (i.e., X1, Y1, Z1 and CORD1 followed by X2, Y2, Z2 and CORD2). HASCUTIL will write out the Z1,Y1,Z1,CORD1 and X2,Y2,Z2,CORD2 values for the panels defined by the number of input BLs.

HASCUTIL displays a list of parameters that will be written into the surface file. All parameters are defaulted to zero except for SPC, ISPNDIV and ICHRDIV. These values are set to 1, 6 and 10, respectively. Finally, the user supplies a surface title (SRFTITL) and a filename for the newly created surface. To change any of the defaulted input parameters in the list, the user must edit the new surface file, and change the values as desired. Airfoil definition (items 13 through 16) must be added later by hand.

The second surface type, from option 3, is a complete condensed VTXCHN input file (vchn.inp) for analyzing circular and elliptical forebodies in VTXCHN (see tables 4.2-9 and 4.2-10). HASCUTIL does not provide a method for modifying this forebody file.

### Creating a Forebody Geometry File for VTXCHN

Option 3 writes the condensed VTXCHN forebody geometry file as discussed in section 4.2. Option 3 runs a routine called VXCXGEO. VXCXGEO is used to define the forebody cross sectional parameters. This option is useful when a HASC forebody analysis is desired. VXCXGEO only handles the input data requirements for circular and elliptical forebodies. Forebodies with arbitrary cross-sectional shape (including chines) can be run in HASC, but the input files must be created manually.

The prompts for VXCXGEO are self-explanatory, and are used to define basic geometric forebody parameters and the general shape. With the input parameters, the code generates two geometry files containing fuselage station (XR), radius (R), variation of the radius slope with station (DR), and for elliptical bodies, major and minor axis lengths (AE and BE) and the slopes of each axis of the ellipse with station (DAE and DBE). All of the length parameters are non-dimensionalized by total length which is recorded at the top of each output file. A mirror image of the front portion of the forebody is modeled at the rear of the body to provide a closed volume. The length of the closure is included in the total length. The file used by HASC for forebody analyses is vchn.inp. A second file, filename.tcp, contains the same data in tabular format for Tecplot.

## Option 2 -- Modifying an Existing Surface

Pre-existing surfaces can be modified by running the second option as shown below.

After selecting menu option 2, the following menu appears:

```
Select desired modification:
  1 - x,y,z translation
  2 - add new buttlines
  3 - add LE or TE edge flaps
  4 - change LH model to a LH/RH model
  5 - create a mirror image
  0 to return
Enter selection (0-5) :
```

When selecting any option one through five, HASCUTIL will first ask for the filename of the surface to modify, the output filename of the surface after modification, and a new surface title.

### Translation

The translation option is useful for moving a wing or tail surface to quickly evaluate impacts on stability. To translate a surface, select 1 and enter the appropriate increments for X, Y and Z. Default values for the increments are zero.

### Adding a New Buttock Line

When adding a new BL, the program will step through each panel in the surface file, and ask the user if a new BL is desired at that location. The user responds with a 'Y' for yes, 'N' for no, or 'E' for exit. After a 'yes' response, the program will ask for the new BL, or Y-value, and then linearly interpolates for the corresponding X, Z, and chord lengths. This option is most useful when adding a control surface such as a canard or horizontal tail. Recall that the surface breaks defining a preceding surface must line up with the breaks in all surfaces that follow it. For example, if a horizontal tail is added, the BL's that define its breakpoints must also be transferred to the wing to prevent trailing vortex filaments off of the wing from passing through a control point on the horizontal tail.

### Adding Leading or Trailing Edge Flaps

When adding a control surface (option 3), HASCUTIL will echo the existing panel geometry to the screen. Next, the user is prompted if the new panel is to be a leading edge or trailing edge flap. The program then steps through each panel and asks which panels the control surfaces should be added to. At each panel, the user responds to the prompts with a 'Y', 'N', or 'E' (yes, no or exit). When a panel is identified for modification, the program asks for the chord length of the new control surface at the BL's that define the panel. HASCUTIL will define a new panel at the LE or TE, located at the desired BL's with the appropriate chord lengths. It will also adjust the modified panel by subtracting the control surface chord lengths from the previous total chord length.

SPC is automatically set to 1.0 on leading edge panels, and 0.0 on any panels not at the leading edge. ICHRDIV is also automatically modified from 10 to 6. The user may change these values by editing the new surface file after completing the HASCUTIL session.

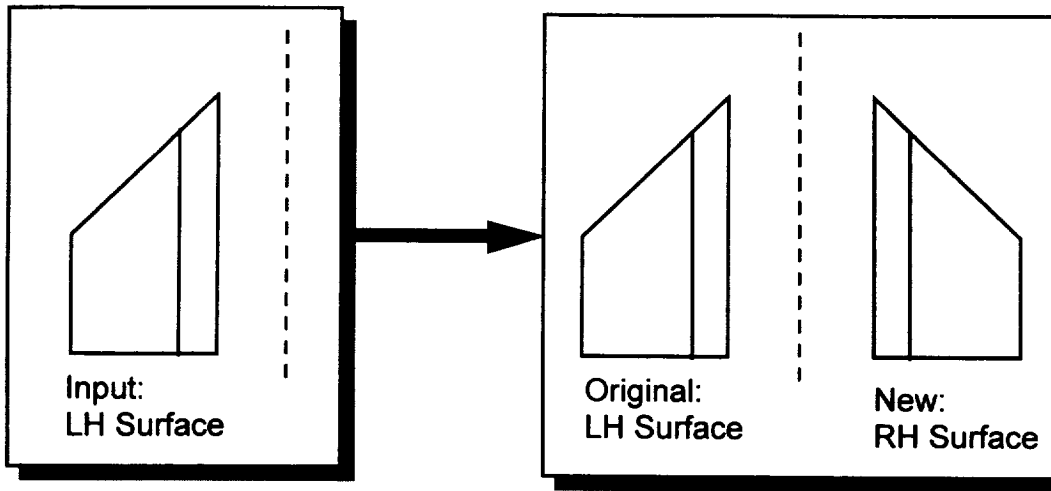
### Creating a LH and RH Surface

HASC panel geometry is entered from left to right, with left-hand surfaces defined first. Option 4 will take a left-hand surface file and write out a file containing both left-hand and right-hand surfaces combined into one continuous surface. This option is useful for creating fuselage surfaces.

### Creating a Mirror Image

Option 5 negates the BL values in a left or right hand surface file, and writes out the mirror right or left-hand file, respectively after re-ordering the spanwise paneling to be consistent with HASC input requirements. This option is useful for creating a right hand wing surface file when a left hand wing surface file has already been created. Options 4 and 5 are shown in figure A-1

Option 5 - create a mirror image



Option 4 - change LH model to a LH/RH model

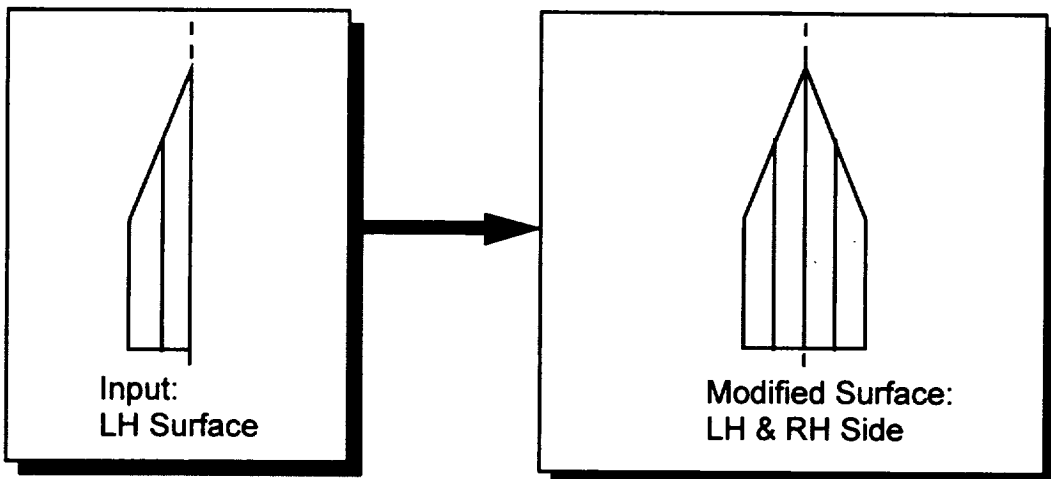


Figure A-2 HASCUTIL Options 4 and 5 for Modifying a Surface



### **Option 3 -- Building a HASC Input Deck**

Up to this point, HASCUTIL has worked with files representing individual surfaces. Option 3 can be used to stack several surface files, along with a file containing the program options, flow conditions, etc., into a complete HASC input deck. HASCUTIL simply asks the user for the filenames of the surfaces to be stacked. When finished, the user responds to the input filename prompt with 'END'. The user is responsible for entering the files that make up the input deck in the proper order (e.g., program options first, followed by the surface files).

### **Option 4 -- Creating PLOT3D and TECPLOT Input Files**

Option 4 creates geometry files for verifying desired paneling prior to running HASC. HASCUTIL asks for a HASC input file (not just a surface file), and writes out four files. Files panel.p3d and grid.p3d are written for input to plot3d. Files panel.tcp and grid.tcp are written for input to Tecplot. Linear spacing, independent of LAX and LAY, is used in computing the sub-panels as written to the two grid files. A fifth file, panel.sum, is a tabular summary of the input geometry data. This file may be useful when checking a HASC input file for geometry errors.



## **Appendix B**

### **VTXCHN Input Listings**

This appendix contains VTXCHN input files for the four forebody shapes used during the validation of VTXCHN at NEAR. Two inputs are provided for the B1 forebody, one as a smooth body and the other as a chined body. The input listings are provided in tables B-1 through B-5.

Two additional input files are provided. The first of these is a listing of a condensed VTXCHN input file vchn.inp modeling the F-16 forebody (table B-6). This file was used during the HASC validation of the F-16. The second listing (table B-7) is the complete VTXCHN input file for the same F-16 forebody as created within HASC. This complete file can be submitted in a VTXCHN ONLY execution of HASC.

Table B-1 Forebody A1 VTXCHN Input File

```

0 0 1 1 0 1 1 0 0 0 0 0 0 0
-1 0 1
1 1 1 1 3 2 0 0 1 1
MODEL A1 (from ITAR restricted NASA TP-3471) laminar separation, VRF=0.6
12.57 4.000 14.06 36.12 4.00
20.000000 0.000000 400000. 0.20
0.00 0.00 0.00 0.00 0.00 0.00
0.260 14.060 0.20 0.0 0.0 1.05 0.0 0.60
.00050 0.0 0.0 0.0 0.0 0.0 0.0 0.025
-1 2
76
0.0000000 0.0138427 0.0276855 0.0415282 0.0537099 0.0692137 0.0830565 0.0968992
0.1107420 0.1245847 0.1384275 0.1522702 0.1661130 0.1799557 0.1937985 0.2076412
0.2214839 0.2353267 0.2491694 0.2630122 0.2768549 0.2906977 0.3045404 0.3183832
0.3322259 0.3460687 0.3599114 0.3737542 0.3875969 0.3892580 0.4014396 0.4152824
0.4291251 0.4429679 0.4568106 0.4706534 0.4844961 0.4983389 0.5121816 0.5260244
0.5398671 0.5537099 0.5675526 0.5813953 0.5952381 0.6090808 0.6107420 0.6124031
0.6262458 0.6400886 0.6539313 0.6677741 0.6816168 0.6954596 0.7093023 0.7231451
0.7369878 0.7508306 0.7646733 0.7785161 0.7923588 0.8062015 0.8200443 0.8338870
0.8477298 0.8615725 0.8754153 0.8892580 0.9031008 0.9169435 0.9307863 0.9462901
0.9584718 0.9723145 0.9861573 1.0000000
0.0000000 0.0039423 0.0077309 0.0113671 0.0148523 0.0181875 0.0213738 0.0244123
0.0273040 0.0300498 0.0326505 0.0351070 0.0374201 0.0395906 0.0416190 0.0435059
0.0452520 0.0468578 0.0483239 0.0496504 0.0508381 0.0518871 0.0527979 0.0535706
0.0542054 0.0547027 0.0550625 0.0552849 0.0553699 0.0553710 0.0553710 0.0553710
0.0553710 0.0553710 0.0553710 0.0553710 0.0553710 0.0553710 0.0553710 0.0553710
0.0553710 0.0553710 0.0553710 0.0553710 0.0553710 0.0553710 0.0553710 0.0553699
0.0552849 0.0550625 0.0547027 0.0542054 0.0535706 0.0527979 0.0518871 0.0508381
0.0496504 0.0483239 0.0468578 0.0452520 0.0435059 0.0416190 0.0395906 0.0374201
0.0351070 0.0326505 0.0300498 0.0273040 0.0244123 0.0213738 0.0181875 0.0148523
0.0113671 0.0077309 0.0039423 0.0000000
0.2903705 0.2792232 0.2681717 0.2572111 0.2463368 0.2355442 0.2248291 0.2141872
0.2036144 0.1931067 0.1826604 0.1722716 0.1619367 0.1516522 0.1414144 0.1312201
0.1210659 0.1109484 0.1008644 0.0908108 0.0807845 0.0707823 0.0608012 0.0508382
0.0408902 0.0309544 0.0210277 0.0111072 0.0189992 0.0000000 0.0000000 0.0000000
0.0000000 0.0000000 0.0000000 0.0000000 0.0000000 0.0000000 0.0000000 0.0000000
0.0000000 0.0000000 0.0000000 0.0000000 0.0000000 0.0000000 0.0000000 0.0000000
-0.0111072 -0.0210277 -0.0309544 -0.0408902 -0.0508382 -0.0608012 -0.0707823 -0.0807845
-0.0908108 -0.1008644 -0.1109484 -0.1210659 -0.1312201 -0.1414144 -0.1516522 -0.1619367
-0.1722716 -0.1826604 -0.1931067 -0.2036144 -0.2141872 -0.2248291 -0.2355442 -0.2463368
-0.2572111 -0.2681717 -0.2792232 -0.2903705

```

Table B-2 Forebody A2 VTXCHN Input File

```

2      0      1      1      0      1      1      0      0      0      0      0      0      0
-1     1      1
1      1      1      1      3      2      0      0      1      1
MODEL A2 (from ITAR restricted NASA TP-3471) chine separation
12.57      4.000      14.06      36.12      4.00
20.000000  0.000000  400000.  0.20
0.00      0.00      0.00      0.00      0.00      0.00
0.260     14.060     0.20      0.0      0.0      1.05      0.0      1.00
.00050    0.0      0.0      0.0      0.0      0.0      0.0      0.025
-1      2
11
0.00000  0.13843  0.27685  0.38898  0.38953  0.50000  0.61046  0.61102
0.72314  0.86157  1.00000
0.00000  0.02060  0.04120  0.05788  0.05788  0.05788  0.05788  0.05788
0.04120  0.02060  0.00000
0.14880  0.14880  0.14880  0.14880  0.00000  0.00000  0.00000 -0.14880
-0.14880 -0.14880 -0.14880
0.00000  0.02060  0.04120  0.05788  0.05788  0.05788  0.05788  0.05788
0.04120  0.02060  0.00000
0.14880  0.14880  0.14880  0.14880  0.00000  0.00000  0.00000 -0.14880
-0.14880 -0.14880 -0.14880
30      1
18.06
5
9
0.00000E+00 6.25000E-01 1.25000E+00 1.87500E+00 2.50000E+00 1.87500E+00
1.25000E+00 6.25000E-01 0.00000E+00
-2.50000E+00 -1.87500E+00 -1.25000E+00 -6.25000E-01 0.00000E+00 6.25000E-01
1.25000E+00 1.87500E+00 2.50000E+00
1      0.5000
0.00      36.12
2      2      2
1      1
1.00      1.00

```

Table B-3 Forebody B1 (smooth body) VTXCHN Input File

2	0	1	1	0	1	1	0	0	0	0	0	0	0	0
-1	0	1												
1	1	1	1	3	2	0	0	1	1					
MODEL B1 (from ITAR restricted NASA TP-3471) chine separation														
12.57		4.000		14.06		36.12		4.00						
20.000000		0.000000		400000.		0.20								
0.00		0.00		0.00		0.00		0.00		0.00				
0.260		14.060		0.20		0.0		0.0		1.05		0.0		1.00
.00050		0.0		0.0		0.0		0.0		0.0		0.0		0.05
-1	2													
76														
0.0000000	0.0138427	0.0276855	0.0415282	0.0537099	0.0692137	0.0830565	0.0968992							
0.1107420	0.1245847	0.1384275	0.1522702	0.1661130	0.1799557	0.1937985	0.2076412							
0.2214839	0.2353267	0.2491694	0.2630122	0.2768549	0.2906977	0.3045404	0.3183832							
0.3322259	0.3460687	0.3599114	0.3737542	0.3875969	0.3892580	0.4014396	0.4152824							
0.4291251	0.4429679	0.4568106	0.4706534	0.4844961	0.4983389	0.5121816	0.5260244							
0.5398671	0.5537099	0.5675526	0.5813953	0.5952381	0.6090808	0.6107420	0.6124031							
0.6262458	0.6400886	0.6539313	0.6677741	0.6816168	0.6954596	0.7093023	0.7231451							
0.7369878	0.7508306	0.7646733	0.7785161	0.7923588	0.8062015	0.8200443	0.8338870							
0.8477298	0.8615725	0.8754153	0.8892580	0.9031008	0.9169435	0.9307863	0.9462901							
0.9584718	0.9723145	0.9861573	1.0000000											
0.0000000	0.0039800	0.0078049	0.0114759	0.0149944	0.0183615	0.0215783	0.0246459							
0.0275653	0.0303374	0.0329629	0.0354430	0.0377782	0.0399695	0.0420173	0.0439222							
0.0456850	0.0473062	0.0487863	0.0501255	0.0513246	0.0523836	0.0533032	0.0540832							
0.0547241	0.0552262	0.0555894	0.0558139	0.0558998	0.0559009	0.0559009	0.0559009							
0.0559009	0.0559009	0.0559009	0.0559009	0.0559009	0.0559009	0.0559009	0.0559009							
0.0559009	0.0559009	0.0559009	0.0559009	0.0559009	0.0559009	0.0559009	0.0559009							
0.0558139	0.0555894	0.0552262	0.0547241	0.0540832	0.0533032	0.0523836	0.0513246							
0.0501255	0.0487863	0.0473062	0.0456850	0.0439222	0.0420173	0.0399695	0.0377782							
0.0354430	0.0329629	0.0303374	0.0275653	0.0246459	0.0215783	0.0183615	0.0149944							
0.0114759	0.0078049	0.0039800	0.0000000											
0.2931492	0.2818952	0.2707380	0.2596725	0.2486941	0.2377982	0.2269806	0.2162369							
0.2055629	0.1949546	0.1844084	0.1739202	0.1634864	0.1531034	0.1427677	0.1324758							
0.1222244	0.1120101	0.1018296	0.0916798	0.0815576	0.0714597	0.0613830	0.0513247							
0.0412815	0.0312506	0.0212289	0.0112135	0.0191810	0.0000000	0.0000000	0.0000000							
0.0000000	0.0000000	0.0000000	0.0000000	0.0000000	0.0000000	0.0000000	0.0000000							
0.0000000	0.0000000	0.0000000	0.0000000	0.0000000	0.0000000	0.0000000	0.0000000							
-0.0112135	-0.0212289	-0.0312506	-0.0412815	-0.0513247	-0.0613830	-0.0714597	-0.0815576							
-0.0916798	-0.1018296	-0.1120101	-0.1222244	-0.1324758	-0.1427677	-0.1531034	-0.1634864							
-0.1739202	-0.1844084	-0.1949546	-0.2055629	-0.2162369	-0.2269806	-0.2377982	-0.2486941							
-0.2596725	-0.2707380	-0.2818952	-0.2931492											
0.0000000	0.0039800	0.0078049	0.0114759	0.0149944	0.0183615	0.0215783	0.0246459							
0.0275653	0.0303374	0.0329629	0.0354430	0.0377782	0.0399695	0.0420173	0.0439222							
0.0456850	0.0473062	0.0487863	0.0501255	0.0513246	0.0523836	0.0533032	0.0540832							
0.0547241	0.0552262	0.0555894	0.0558139	0.0558998	0.0559009	0.0559009	0.0559009							
0.0559009	0.0559009	0.0559009	0.0559009	0.0559009	0.0559009	0.0559009	0.0559009							
0.0559009	0.0559009	0.0559009	0.0559009	0.0559009	0.0559009	0.0559009	0.0559009							
0.0558139	0.0555894	0.0552262	0.0547241	0.0540832	0.0533032	0.0523836	0.0513246							
0.0501255	0.0487863	0.0473062	0.0456850	0.0439222	0.0420173	0.0399695	0.0377782							
0.0354430	0.0329629	0.0303374	0.0275653	0.0246459	0.0215783	0.0183615	0.0149944							
0.0114759	0.0078049	0.0039800	0.0000000											
0.2931492	0.2818952	0.2707380	0.2596725	0.2486941	0.2377982	0.2269806	0.2162369							
0.2055629	0.1949546	0.1844084	0.1739202	0.1634864	0.1531034	0.1427677	0.1324758							
0.1222244	0.1120101	0.1018296	0.0916798	0.0815576	0.0714597	0.0613830	0.0513247							
0.0412815	0.0312506	0.0212289	0.0112135	0.0191810	0.0000000	0.0000000	0.0000000							
0.0000000	0.0000000	0.0000000	0.0000000	0.0000000	0.0000000	0.0000000	0.0000000							

0.0000000 0.0000000 0.0000000 0.0000000 0.0000000 0.0000000 0.0000000-0.0191810  
-0.0112135-0.0212289-0.0312506-0.0412815-0.0513247-0.0613830-0.0714597-0.0815576  
-0.0916798-0.1018296-0.1120101-0.1222244-0.1324758-0.1427677-0.1531034-0.1634864  
-0.1739202-0.1844084-0.1949546-0.2055629-0.2162369-0.2269806-0.2377982-0.2486941  
-0.2596725-0.2707380-0.2818952-0.2931492

30 1

0.10

29

0.00000E+00 2.31402E-03 4.62803E-03 6.94205E-03 9.25607E-03 1.15701E-02  
1.38841E-02 1.61981E-02 1.85121E-02 2.08261E-02 2.31402E-02 2.54542E-02  
2.77682E-02 3.00822E-02 3.47102E-02 3.00822E-02 2.77682E-02 2.54542E-02  
2.31402E-02 2.08261E-02 1.85121E-02 1.61981E-02 1.38841E-02 1.15701E-02  
9.25607E-03 6.94205E-03 4.62803E-03 2.31402E-03 0.00000E+00  
-2.77682E-02-2.76638E-02-2.73452E-02-2.68041E-02-2.60326E-02-2.50224E-02  
-2.37653E-02-2.22533E-02-2.04781E-02-1.84317E-02-1.61058E-02-1.34924E-02  
-1.05832E-02-7.37022E-03 0.00000E+00 7.37022E-03 1.05832E-02 1.34924E-02  
1.61058E-02 1.84317E-02 2.04781E-02 2.22533E-02 2.37653E-02 2.50224E-02  
2.60326E-02 2.68041E-02 2.73452E-02 2.76638E-02 2.77682E-02



Table B-4 Forebody B1(chined body) VTXCHN Input File

2	0	1	1	0	1	1	0	0	0	0	0	0	0	0
-1	1	1												
1	1	1	1	3	2	0	0	1	1					
MODEL B1 (from ITAR restricted NASA TP-3471) chine separation														
12.57	4.000	14.06	36.12	4.00										
20.000000	0.000000	400000.	0.20											
0.00	0.00	0.00	0.00	0.00	0.00	0.00	0.00	0.00	0.00	0.00	0.00	0.00	0.00	0.00
0.260	14.060	0.20	0.0	0.0	0.0	1.05	0.0	0.0	0.0	0.0	0.0	0.0	1.00	0.05
.00050	0.0	0.0	0.0	0.0	0.0	0.0	0.0	0.0	0.0	0.0	0.0	0.0	0.0	0.05
-1	2													
76														
0.0000000	0.0138427	0.0276855	0.0415282	0.0537099	0.0692137	0.0830565	0.0968992							
0.1107420	0.1245847	0.1384275	0.1522702	0.1661130	0.1799557	0.1937985	0.2076412							
0.2214839	0.2353267	0.2491694	0.2630122	0.2768549	0.2906977	0.3045404	0.3183832							
0.3322259	0.3460687	0.3599114	0.3737542	0.3875969	0.3892580	0.4014396	0.4152824							
0.4291251	0.4429679	0.4568106	0.4706534	0.4844961	0.4983389	0.5121816	0.5260244							
0.5398671	0.5537099	0.5675526	0.5813953	0.5952381	0.6090808	0.6107420	0.6124031							
0.6262458	0.6400886	0.6539313	0.6677741	0.6816168	0.6954596	0.7093023	0.7231451							
0.7369878	0.7508306	0.7646733	0.7785161	0.7923588	0.8062015	0.8200443	0.8338870							
0.8477298	0.8615725	0.8754153	0.8892580	0.9031008	0.9169435	0.9307863	0.9462901							
0.9584718	0.9723145	0.9861573	1.0000000											
0.0000000	0.0039800	0.0078049	0.0114759	0.0149944	0.0183615	0.0215783	0.0246459							
0.0275653	0.0303374	0.0329629	0.0354430	0.0377782	0.0399695	0.0420173	0.0439222							
0.0456850	0.0473062	0.0487863	0.0501255	0.0513246	0.0523836	0.0533032	0.0540832							
0.0547241	0.0552262	0.0555894	0.0558139	0.0558998	0.0559009	0.0559009	0.0559009							
0.0559009	0.0559009	0.0559009	0.0559009	0.0559009	0.0559009	0.0559009	0.0559009							
0.0559009	0.0559009	0.0559009	0.0559009	0.0559009	0.0559009	0.0559009	0.0558998							
0.0558139	0.0555894	0.0552262	0.0547241	0.0540832	0.0533032	0.0523836	0.0513246							
0.0501255	0.0487863	0.0473062	0.0456850	0.0439222	0.0420173	0.0399695	0.0377782							
0.0354430	0.0329629	0.0303374	0.0275653	0.0246459	0.0215783	0.0183615	0.0149944							
0.0114759	0.0078049	0.0039800	0.0000000											
0.2931492	0.2818952	0.2707380	0.2596725	0.2486941	0.2377982	0.2269806	0.2162369							
0.2055629	0.1949546	0.1844084	0.1739202	0.1634864	0.1531034	0.1427677	0.1324758							
0.1222244	0.1120101	0.1018296	0.0916798	0.0815576	0.0714597	0.0613830	0.0513247							
0.0412815	0.0312506	0.0212289	0.0112135	0.0191810	0.0000000	0.0000000	0.0000000							
0.0000000	0.0000000	0.0000000	0.0000000	0.0000000	0.0000000	0.0000000	0.0000000							
0.0000000	0.0000000	0.0000000	0.0000000	0.0000000	0.0000000	0.0000000	0.0000000							
-0.0112135	-0.0212289	-0.0312506	-0.0412815	-0.0513247	-0.0613830	-0.0714597	-0.0815576							
-0.0916798	-0.1018296	-0.1120101	-0.1222244	-0.1324758	-0.1427677	-0.1531034	-0.1634864							
-0.1739202	-0.1844084	-0.1949546	-0.2055629	-0.2162369	-0.2269806	-0.2377982	-0.2486941							
-0.2596725	-0.2707380	-0.2818952	-0.2931492											
0.0000000	0.0039800	0.0078049	0.0114759	0.0149944	0.0183615	0.0215783	0.0246459							
0.0275653	0.0303374	0.0329629	0.0354430	0.0377782	0.0399695	0.0420173	0.0439222							
0.0456850	0.0473062	0.0487863	0.0501255	0.0513246	0.0523836	0.0533032	0.0540832							
0.0547241	0.0552262	0.0555894	0.0558139	0.0558998	0.0559009	0.0559009	0.0559009							
0.0559009	0.0559009	0.0559009	0.0559009	0.0559009	0.0559009	0.0559009	0.0559009							
0.0559009	0.0559009	0.0559009	0.0559009	0.0559009	0.0559009	0.0559009	0.0559009							
0.0559009	0.0559009	0.0559009	0.0559009	0.0559009	0.0559009	0.0559009	0.0558998							
0.0558139	0.0555894	0.0552262	0.0547241	0.0540832	0.0533032	0.0523836	0.0513246							
0.0501255	0.0487863	0.0473062	0.0456850	0.0439222	0.0420173	0.0399695	0.0377782							
0.0354430	0.0329629	0.0303374	0.0275653	0.0246459	0.0215783	0.0183615	0.0149944							
0.0114759	0.0078049	0.0039800	0.0000000											
0.2931492	0.2818952	0.2707380	0.2596725	0.2486941	0.2377982	0.2269806	0.2162369							
0.2055629	0.1949546	0.1844084	0.1739202	0.1634864	0.1531034	0.1427677	0.1324758							
0.1222244	0.1120101	0.1018296	0.0916798	0.0815576	0.0714597	0.0613830	0.0513247							
0.0412815	0.0312506	0.0212289	0.0112135	0.0191810	0.0000000	0.0000000	0.0000000							
0.0000000	0.0000000	0.0000000	0.0000000	0.0000000	0.0000000	0.0000000	0.0000000							

0.0000000 0.0000000 0.0000000 0.0000000 0.0000000 0.0000000 0.0000000-0.0191810  
 -0.0112135-0.0212289-0.0312506-0.0412815-0.0513247-0.0613830-0.0714597-0.0815576  
 -0.0916798-0.1018296-0.1120101-0.1222244-0.1324758-0.1427677-0.1531034-0.1634864  
 -0.1739202-0.1844084-0.1949546-0.2055629-0.2162369-0.2269806-0.2377982-0.2486941  
 -0.2596725-0.2707380-0.2818952-0.2931492  
 30 1  
 0.10  
 15  
 29  
 0.00000E+00 2.31402E-03 4.62803E-03 6.94205E-03 9.25607E-03 1.15701E-02  
 1.38841E-02 1.61981E-02 1.85121E-02 2.08261E-02 2.31402E-02 2.54542E-02  
 2.77682E-02 3.00822E-02 3.47102E-02 3.00822E-02 2.77682E-02 2.54542E-02  
 2.31402E-02 2.08261E-02 1.85121E-02 1.61981E-02 1.38841E-02 1.15701E-02  
 9.25607E-03 6.94205E-03 4.62803E-03 2.31402E-03 0.00000E+00  
 -2.77682E-02-2.76638E-02-2.73452E-02-2.68041E-02-2.60326E-02-2.50224E-02  
 -2.37653E-02-2.22533E-02-2.04781E-02-1.84317E-02-1.61058E-02-1.34924E-02  
 -1.05832E-02-7.37022E-03 0.00000E+00 7.37022E-03 1.05832E-02 1.34924E-02  
 1.61058E-02 1.84317E-02 2.04781E-02 2.22533E-02 2.37653E-02 2.50224E-02  
 2.60326E-02 2.68041E-02 2.73452E-02 2.76638E-02 2.77682E-02  
 1 0.5000  
 0.00 36.12  
 2 2 2  
 1 1  
 1.00 1.00



-0.0116585-0.0220714-0.0324908-0.0429198-0.0533615-0.0638190-0.0742956-0.0847942  
 -0.0953182-0.1058708-0.1164553-0.1270750-0.1377332-0.1484334-0.1591794-0.1699744  
 -0.1808222-0.1917267-0.2026915-0.2137207-0.2248183-0.2359884-0.2472353-0.2585636  
 -0.2699777-0.2814823-0.2930823-0.3047829  
 100 1  
 0.10  
 15  
 29  
 0.00000E+00 1.19970E-03 2.39939E-03 4.79878E-03 7.19818E-03 9.59757E-03  
 1.21270E-02 1.67957E-02 2.15945E-02 2.63933E-02 2.87927E-02 3.11921E-02  
 3.35915E-02 3.47912E-02 3.59909E-02 3.47912E-02 3.35915E-02 3.11921E-02  
 2.87927E-02 2.63933E-02 2.15945E-02 1.67957E-02 1.21270E-02 9.59757E-03  
 7.19818E-03 4.79878E-03 2.39939E-03 1.19970E-03 0.00000E+00  
 -3.59909E-02-3.58770E-02-3.55454E-02-3.42905E-02-3.23486E-02-2.98420E-02  
 -2.68931E-02-2.01580E-02-1.31222E-02-6.76463E-03-4.14610E-03-2.06424E-03  
 -6.41405E-04-2.15383E-04 0.00000E+00 2.15383E-04 6.41405E-04 2.06424E-03  
 4.14610E-03 6.76463E-03 1.31222E-02 2.01580E-02 2.68931E-02 2.98420E-02  
 3.23486E-02 3.42905E-02 3.55454E-02 3.58770E-02 3.59909E-02  
 1 0.5000  
 0.00 36.12  
 2 2 2  
 1 1  
 1.00 1.00

Table B-6 Condensed VTXCHN Input File (vchn.inp) for an F-16 Forebody

```

* THIS FILE WRITTEN BY HASCUTIL, F-16 FOREBODY
*   NCIR  NBLSEP  NCHINE      DROOP      DX      E5
      1      1      0  4.16000  8.82000  0.0500
*   TNOSE      ENOSE      BNOSE      FBLNTH      SL      SD
      1.00000  0.70830  0.00000 104.80000 209.60001 44.10000
* NXR
      40
* XR(s)
      0.00000  0.02500  0.05000  0.07500  0.10000  0.12500  0.15000  0.17500
      0.20000  0.22500  0.25000  0.27500  0.30000  0.32500  0.35000  0.37500
      0.40000  0.42500  0.45000  0.47500  0.52500  0.55000  0.57500  0.60000
      0.62500  0.65000  0.67500  0.70000  0.72500  0.75000  0.77500  0.80000
      0.82500  0.85000  0.87500  0.90000  0.92500  0.95000  0.97500  1.00000
* R(s)
      0.00000  0.00912  0.01770  0.02575  0.03328  0.04030  0.04682  0.05286
      0.05841  0.06350  0.06812  0.07229  0.07600  0.07926  0.08208  0.08447
      0.08641  0.08792  0.08900  0.08964  0.08964  0.08900  0.08792  0.08641
      0.08447  0.08208  0.07926  0.07600  0.07229  0.06812  0.06350  0.05841
      0.05286  0.04682  0.04030  0.03328  0.02575  0.01770  0.00912  0.00000
* DR(s)
      0.36496  0.34313  0.32186  0.30110  0.28081  0.26094  0.24144  0.22230
      0.20346  0.18489  0.16658  0.14849  0.13058  0.11284  0.09525  0.07777
      0.06039  0.04308  0.02583  0.00861  -0.00861  -0.02583  -0.04308  -0.06039
      -0.07777  -0.09525  -0.11284  -0.13058  -0.14849  -0.16658  -0.18489  -0.20346
      -0.22230  -0.24144  -0.26094  -0.28081  -0.30110  -0.32186  -0.34313  -0.36496
* AE(s)
      0.00000  0.01068  0.02072  0.03015  0.03896  0.04718  0.05481  0.06188
      0.06839  0.07434  0.07975  0.08463  0.08898  0.09280  0.09610  0.09889
      0.10116  0.10293  0.10419  0.10495  0.10495  0.10419  0.10293  0.10116
      0.09889  0.09610  0.09280  0.08898  0.08463  0.07975  0.07434  0.06839
      0.06188  0.05481  0.04718  0.03896  0.03015  0.02072  0.01068  0.00000
* BE(s)
      0.00000  0.00757  0.01468  0.02135  0.02759  0.03342  0.03883  0.04383
      0.04844  0.05266  0.05649  0.05994  0.06302  0.06573  0.06807  0.07004
      0.07165  0.07291  0.07380  0.07434  0.07434  0.07380  0.07291  0.07165
      0.07004  0.06807  0.06573  0.06302  0.05994  0.05649  0.05266  0.04844
      0.04383  0.03883  0.03342  0.02759  0.02135  0.01468  0.00757  0.00000
* DAE(s)
      0.42728  0.40172  0.37682  0.35252  0.32876  0.30550  0.28267  0.26026
      0.23820  0.21647  0.19502  0.17384  0.15287  0.13211  0.11151  0.09105
      0.07070  0.05044  0.03024  0.01008  -0.01008  -0.03024  -0.05044  -0.07070
      -0.09105  -0.11151  -0.13211  -0.15287  -0.17384  -0.19502  -0.21647  -0.23820
      -0.26026  -0.28267  -0.30550  -0.32876  -0.35252  -0.37682  -0.40172  -0.42728
* DBE(s)
      0.30264  0.28454  0.26690  0.24969  0.23286  0.21638  0.20022  0.18434
      0.16872  0.15332  0.13814  0.12313  0.10828  0.09357  0.07898  0.06449
      0.05007  0.03572  0.02142  0.00714  -0.00714  -0.02142  -0.03572  -0.05007
      -0.06449  -0.07898  -0.09357  -0.10828  -0.12313  -0.13814  -0.15332  -0.16872
      -0.18434  -0.20022  -0.21638  -0.23286  -0.24969  -0.26690  -0.28454  -0.30264
* Ro(s)
      0.00000  0.00912  0.01770  0.02575  0.03328  0.04030  0.04682  0.05286
      0.05841  0.06350  0.06812  0.07229  0.07600  0.07926  0.08208  0.08447
      0.08641  0.08792  0.08900  0.08964  0.08964  0.08900  0.08792  0.08641
      0.08447  0.08208  0.07926  0.07600  0.07229  0.06812  0.06350  0.05841
      0.05286  0.04682  0.04030  0.03328  0.02575  0.01770  0.00912  0.00000
* DRo(s)
      0.36496  0.34313  0.32186  0.30110  0.28081  0.26094  0.24144  0.22230

```

0.20346	0.18489	0.16658	0.14849	0.13058	0.11284	0.09525	0.07777
0.06039	0.04308	0.02583	0.00861	-0.00861	-0.02583	-0.04308	-0.06039
-0.07777	-0.09525	-0.11284	-0.13058	-0.14849	-0.16658	-0.18489	-0.20346
-0.22230	-0.24144	-0.26094	-0.28081	-0.30110	-0.32186	-0.34313	-0.36496

Table B-7 Complete VTXCHN Input File for an F-16 Forebody

```

1 0 0 1 0 1 1 0 1 0 0 0 0 0
-1 0 1
1 0 0 0 0 0 0 0 0 1
F-16A FOREBODY MODEL for HASC95
43200.00 360.00000 325.60000 209.60001 44.10000
36.95165 0.00000 1020990. 0.600
0.00000 0.00000 0.00000 0.00000 0.00000 0.00000
11.60000 99.80998 8.82000 999.00000 999.00000 1.05000 0.00000 0.60000
0.05000 0.00000 0.00000 0.00000 0.00000 0.00000 0.00000 0.05000
-1 0
40
0.00000 0.02500 0.05000 0.07500 0.10000 0.12500 0.15000 0.17500
0.20000 0.22500 0.25000 0.27500 0.30000 0.32500 0.35000 0.37500
0.40000 0.42500 0.45000 0.47500 0.52500 0.55000 0.57500 0.60000
0.62500 0.65000 0.67500 0.70000 0.72500 0.75000 0.77500 0.80000
0.82500 0.85000 0.87500 0.90000 0.92500 0.95000 0.97500 1.00000
0.00000 0.00912 0.01770 0.02575 0.03328 0.04030 0.04682 0.05286
0.05841 0.06350 0.06812 0.07229 0.07600 0.07926 0.08208 0.08447
0.08641 0.08792 0.08900 0.08964 0.08964 0.08900 0.08792 0.08641
0.08447 0.08208 0.07926 0.07600 0.07229 0.06812 0.06350 0.05841
0.05286 0.04682 0.04030 0.03328 0.02575 0.01770 0.00912 0.00000
0.36496 0.34313 0.32186 0.30110 0.28081 0.26094 0.24144 0.22230
0.20346 0.18489 0.16658 0.14849 0.13058 0.11284 0.09525 0.07777
0.06039 0.04308 0.02583 0.00861 -0.00861 -0.02583 -0.04308 -0.06039
-0.07777 -0.09525 -0.11284 -0.13058 -0.14849 -0.16658 -0.18489 -0.20346
-0.22230 -0.24144 -0.26094 -0.28081 -0.30110 -0.32186 -0.34313 -0.36496
0.00000 0.01068 0.02072 0.03015 0.03896 0.04718 0.05481 0.06188
0.06839 0.07434 0.07975 0.08463 0.08898 0.09280 0.09610 0.09889
0.10116 0.10293 0.10419 0.10495 0.10495 0.10419 0.10293 0.10116
0.09889 0.09610 0.09280 0.08898 0.08463 0.07975 0.07434 0.06839
0.06188 0.05481 0.04718 0.03896 0.03015 0.02072 0.01068 0.00000
0.00000 0.00757 0.01468 0.02135 0.02759 0.03342 0.03883 0.04383
0.04844 0.05266 0.05649 0.05994 0.06302 0.06573 0.06807 0.07004
0.07165 0.07291 0.07380 0.07434 0.07434 0.07380 0.07291 0.07165
0.07004 0.06807 0.06573 0.06302 0.05994 0.05649 0.05266 0.04844
0.04383 0.03883 0.03342 0.02759 0.02135 0.01468 0.00757 0.00000
0.42728 0.40172 0.37682 0.35252 0.32876 0.30550 0.28267 0.26026
0.23820 0.21647 0.19502 0.17384 0.15287 0.13211 0.11151 0.09105
0.07070 0.05044 0.03024 0.01008 -0.01008 -0.03024 -0.05044 -0.07070
-0.09105 -0.11151 -0.13211 -0.15287 -0.17384 -0.19502 -0.21647 -0.23820
-0.26026 -0.28267 -0.30550 -0.32876 -0.35252 -0.37682 -0.40172 -0.42728
0.30264 0.28454 0.26690 0.24969 0.23286 0.21638 0.20022 0.18434
0.16872 0.15332 0.13814 0.12313 0.10828 0.09357 0.07898 0.06449
0.05007 0.03572 0.02142 0.00714 -0.00714 -0.02142 -0.03572 -0.05007
-0.06449 -0.07898 -0.09357 -0.10828 -0.12313 -0.13814 -0.15332 -0.16872
-0.18434 -0.20022 -0.21638 -0.23286 -0.24969 -0.26690 -0.28454 -0.30264
0.00000 0.00912 0.01770 0.02575 0.03328 0.04030 0.04682 0.05286
0.05841 0.06350 0.06812 0.07229 0.07600 0.07926 0.08208 0.08447
0.08641 0.08792 0.08900 0.08964 0.08964 0.08900 0.08792 0.08641
0.08447 0.08208 0.07926 0.07600 0.07229 0.06812 0.06350 0.05841
0.05286 0.04682 0.04030 0.03328 0.02575 0.01770 0.00912 0.00000
0.36496 0.34313 0.32186 0.30110 0.28081 0.26094 0.24144 0.22230
0.20346 0.18489 0.16658 0.14849 0.13058 0.11284 0.09525 0.07777
0.06039 0.04308 0.02583 0.00861 -0.00861 -0.02583 -0.04308 -0.06039
-0.07777 -0.09525 -0.11284 -0.13058 -0.14849 -0.16658 -0.18489 -0.20346
-0.22230 -0.24144 -0.26094 -0.28081 -0.30110 -0.32186 -0.34313 -0.36496
99.80000

```





## **Appendix C**

### **Examples of HASC Input Files**

Several examples of HASC input files are provided in this appendix for the aircraft configurations used in validation sections 6.2 through 6.6. These examples, covering many of the HASC options as described below, should be referenced to help answer questions on preparing HASC input files.

### Tailless Fighter

Table C-1 contains an input file for the Tailless Fighter configuration. The configuration is modeled with two VORLIF surfaces (left wing and right wing). The wing camber is defined at 23 points along the chord. The airfoil input file airfoil.inp is listed in table C-2. Airfoil information must be provided for each panel side with IARFYL set to 2.

### Falcon 21

Table C -3 lists an input file for the Falcon 21 configuration analyzed with all surfaces in VORLAX. Panels representing the trailing edge flaps are included. This file is an example of an input for flap effectiveness with all surfaces, including the forebody, analyzed in VORLAX.

### F-16XL

A HASC input file for the F-16XL configuration is provided in table C-4. This file provides an example of a HASC analysis on VORLIF wing surfaces with trailing edge controls, camber, and airfoil definition.

### F-16

An F-16 HASC input file including VTXCHN analysis of the forebody, VORLIF analysis of the wings and horizontal tail, and sideview paneling is listed in table C-5. The forebody input file vchn.inp is listed in table C-6.

### Convair Model 200

The input file for the Convair Model 200 canard configuration is listed in table C-7.

Table C-1 HASC Input File hasc.inp for the Tailless Fighter Configuration

```

Tailless Fighter Configuration
*LAX      LAY      HAG      RUN      NPAN      NSURF      ALXP
0         1         0.        0.        12         2         0.0
*REY      NMACH(s)
3200000. 1         0.30
*NALPHA   ALPHA(s)
20        -4.        -2.        0.        2.        4.
6.        8.        10.       12.       14.       16.       18.       20.
22.       24.       26.       28.       30.       32.       35.
*NBETA    BETA(s)
1         0.        0.        0.
*PITCHQ   ROLLQ     YAWQ      V
0.        0.        0.        1.0
*SREF     CBAR      XREF      ZREF      WSPAN
359.377  19.1667  15.98     5.5556    25.00
*****
*****
* SURFACE 1
LEFT WING
*ISRTYP   LNPNAN   ISYMFLG   ENETAR    FTAIL     ALZL      XGAP
2         6         0         0.0       0.0       0.0       0.0
* panel 1, left wing tip
*X1        Y1         Z1         CORD1     AINC1
26.326   -12.275   4.976     0.604     -15.198
*X2        Y2         Z2         CORD2     AINC2
23.507   -10.961   5.038     4.042     -7.17
*ISPNDIV  ICHRDIV  SPC        IARFYL    NAP        IVTXFLG
2         8         1.0       2         23         0
* Panel 1, BL 12.3, -11.0
* SECTION CAMBER DEFN - X LOCATIONS (%)
  0.0000   1.0000   2.5000   5.0000   10.0000   15.0000   20.0000   25.0000
 30.0000   35.0000   40.0000   45.0000   50.0000   55.0000   60.0000   65.0000
 70.0000   75.0000   80.0000   85.0000   90.0000   95.0000  100.0000
* BL -12.3
* SECTION CAMBER DEFN - Z LOCATIONS (%)
  0.0000   0.4243   0.8507   1.4423   2.0915   2.6367   3.1063   3.3444
  3.4970   3.6496   3.6779   3.6264   3.5162   3.3270   3.1946   2.9046
  2.6919   2.3222   1.9315   1.5595   1.1056   0.5394   0.0000
* BL -11.0
* SECTION CAMBER DEFN - Z LOCATIONS (%)
  0.0000   0.4288   0.8901   1.4502   2.2706   2.8312   3.2098   3.4591
  3.5989   3.6615   3.6519   3.5657   3.4288   3.2318   3.0066   2.7341
  2.4119   2.0755   1.7032   1.3182   0.9078   0.4596   0.0000
*****
* panel 2
*X1        Y1         Z1         CORD1     AINC1
23.507   -10.961   5.038     4.042     -7.17
*X2        Y2         Z2         CORD2     AINC2
20.689   -9.647    5.100     7.462     -3.497
*ISPNDIV  ICHRDIV  SPC        IARFYL    NAP        IVTXFLG
2         8         1.0       2         23         0
* Panel 2, BL -10.96, -9.65
* SECTION CAMBER DEFN - X LOCATIONS (%)
  0.0000   1.0000   2.5000   5.0000   10.0000   15.0000   20.0000   25.0000
 30.0000   35.0000   40.0000   45.0000   50.0000   55.0000   60.0000   65.0000
 70.0000   75.0000   80.0000   85.0000   90.0000   95.0000  100.0000

```

```

* BL -11.0
* SECTION CAMBER DEFN - Z LOCATIONS (%)
  0.0000  0.4288  0.8901  1.4502  2.2706  2.8312  3.2098  3.4591
  3.5989  3.6615  3.6519  3.5657  3.4288  3.2318  3.0066  2.7341
  2.4119  2.0755  1.7032  1.3182  0.9078  0.4596  0.0000

* BL -9.6
* SECTION CAMBER DEFN - Z LOCATIONS (%)
  0.0000  0.4319  0.8793  1.4427  2.2131  2.6800  2.9583  3.1147
  3.1443  3.0935  2.9957  2.8504  2.6723  2.5132  2.3281  2.1095
  1.8765  1.5841  1.2783  0.9655  0.6389  0.3062  0.0000
*****
* panel 3
*X1      Y1      Z1      CORD1      AINC1
20.689  -9.647  5.100  7.462  -3.497
*X2      Y2      Z2      CORD2      AINC2
17.871  -8.333  5.162  10.885  -2.073
*ISPNDIV ICHRDIV  SPC      IARFYL      NAP      IVTXFLG
2        8        1.0      2          23         0
* Panel 3, BL -9.65, -8.33
* SECTION CAMBER DEFN - X LOCATIONS (%)
  0.0000  1.0000  2.5000  5.0000  10.0000  15.0000  20.0000  25.0000
  30.0000  35.0000  40.0000  45.0000  50.0000  55.0000  60.0000  65.0000
  70.0000  75.0000  80.0000  85.0000  90.0000  95.0000  100.0000

* BL -9.6
* SECTION CAMBER DEFN - Z LOCATIONS (%)
  0.0000  0.4319  0.8793  1.4427  2.2131  2.6800  2.9583  3.1147
  3.1443  3.0935  2.9957  2.8504  2.6723  2.5132  2.3281  2.1095
  1.8765  1.5841  1.2783  0.9655  0.6389  0.3062  0.0000

* BL -8.3
* SECTION CAMBER DEFN - Z LOCATIONS (%)
  0.0000  0.4112  0.8208  1.3100  1.9070  2.2509  2.4145  2.4589
  2.4204  2.3220  2.1686  1.9922  1.8111  1.6299  1.4488  1.2676
  1.0821  0.9053  0.7200  0.5432  0.3575  0.1764  0.0000
*****
* panel 4
*X1      Y1      Z1      CORD1      AINC1
17.871  -8.333  5.162  10.885  -2.073
*X2      Y2      Z2      CORD2      AINC2
15.049  -7.018  5.225  13.091  -1.448
*ISPNDIV ICHRDIV  SPC      IARFYL      NAP      IVTXFLG
2        8        1.0      2          23         0
* Panel 4, BL -8.33, -7.02
* SECTION CAMBER DEFN - X LOCATIONS (%)
  0.0000  1.0000  2.5000  5.0000  10.0000  15.0000  20.0000  25.0000
  30.0000  35.0000  40.0000  45.0000  50.0000  55.0000  60.0000  65.0000
  70.0000  75.0000  80.0000  85.0000  90.0000  95.0000  100.0000

* BL -8.3
* SECTION CAMBER DEFN - Z LOCATIONS (%)
  0.0000  0.4112  0.8208  1.3100  1.9070  2.2509  2.4145  2.4589
  2.4204  2.3220  2.1686  1.9922  1.8111  1.6299  1.4488  1.2676
  1.0821  0.9053  0.7200  0.5432  0.3575  0.1764  0.0000

* BL -7.0
* SECTION CAMBER DEFN - Z LOCATIONS (%)
  0.0000  0.3798  0.7571  1.1803  1.6486  1.8664  1.9198  1.8775
  1.7668  1.6440  1.5138  1.3873  1.2646  1.1381  1.0079  0.8813
  0.7550  0.6322  0.5021  0.3756  0.2527  0.1226  0.0000
*****
* panel 5

```

```

*X1      Y1      Z1      CORD1      AINC1
15.049  -7.018   5.225   13.091   -1.448
*X2      Y2      Z2      CORD2      AINC2
8.935   -4.167   5.359   17.872   -0.632
*ISPNDIV ICHRDIV  SPC      IARFYL     NAP      IVTXFLG
2        8        1.0      2         23       0
* Panel 5, BL -7.02, -4.2
* SECTION CAMBER DEFN - X LOCATIONS (%)
  0.0000   1.0000   2.5000   5.0000   10.0000   15.0000   20.0000   25.0000
 30.0000   35.0000   40.0000   45.0000   50.0000   55.0000   60.0000   65.0000
 70.0000   75.0000   80.0000   85.0000   90.0000   95.0000  100.0000
* BL -7.0
* SECTION CAMBER DEFN - Z LOCATIONS (%)
  0.0000   0.3798   0.7571   1.1803   1.6486   1.8664   1.9198   1.8775
 1.7668   1.6440   1.5138   1.3873   1.2646   1.1381   1.0079   0.8813
 0.7550   0.6322   0.5021   0.3756   0.2527   0.1226   0.0000
* BL -4.2
* SECTION CAMBER DEFN - Z LOCATIONS (%)
  0.0000   0.3183   0.5894   0.8241   0.9742   0.9343   0.8791   0.8240
 0.7689   0.7138   0.6586   0.6035   0.5484   0.4932   0.4381   0.3830
 0.3279   0.2756   0.2204   0.1625   0.1073   0.0523   0.0000
*****
* panel 6
*X1      Y1      Z1      CORD1      AINC1
8.935   -4.167   5.359   17.872   -0.632
*X2      Y2      Z2      CORD2      AINC2
0.0      0.0      5.383   28.794   -0.0
*ISPNDIV ICHRDIV  SPC      IARFYL     NAP      IVTXFLG
4        8        1.0      1         23       1
0.044   0.11    0.00056 0.00056   0.45     0.45     3.92     3.92
* Panel 5, BL -4.2, 0.0
* SECTION CAMBER DEFN - X LOCATIONS (%)
  0.0000   1.0000   2.5000   5.0000   10.0000   15.0000   20.0000   25.0000
 30.0000   35.0000   40.0000   45.0000   50.0000   55.0000   60.0000   65.0000
 70.0000   75.0000   80.0000   85.0000   90.0000   95.0000  100.0000
* BL -4.2
* SECTION CAMBER DEFN - Z LOCATIONS (%)
  0.0000   0.3183   0.5894   0.8241   0.9742   0.9343   0.8791   0.8240
 0.7689   0.7138   0.6586   0.6035   0.5484   0.4932   0.4381   0.3830
 0.3279   0.2756   0.2204   0.1625   0.1073   0.0523   0.0000
* BL 0.0
* SECTION CAMBER DEFINITION - Z LOCATIONS (%)
  0.0      0.0001   0.0002   0.0003   0.0004   0.0005   0.0006   0.0007
 0.0008   0.0009   0.0010   0.0011   0.0012   0.0013   0.0014   0.0015
 0.0014   0.0012   0.0010   0.0008   0.0006   0.0003   0.0000
*****
*****
* SURFACE 2
RIGHT WING
*ISRSTYP LNPNAN  ISYMFLG  ENETAR   FTAIL    ALZL     XGAP
2        6        0        0.0      0.0      0.0      0.0
* panel 1, right wing root (centerline)
*X2      Y2      Z2      CORD2      AINC2
0.0      0.0      5.383   28.794   0.0
*X1      Y1      Z1      CORD1      AINC1
8.935   4.167   5.359   17.872   -0.632
*ISPNDIV ICHRDIV  SPC      IARFYL     NAP      IVTXFLG
4        8        1.0      1         23       1

```

```

0.11      0.044    0.00056   0.00056    0.45     0.45     3.92     3.92
* Panel 5, BL 0.0, 4.2
* SECTION CAMBER DEFN - X LOCATIONS (%)
  0.0000    1.0000    2.5000    5.0000    10.0000   15.0000   20.0000   25.0000
 30.0000   35.0000   40.0000   45.0000   50.0000   55.0000   60.0000   65.0000
 70.0000   75.0000   80.0000   85.0000   90.0000   95.0000  100.0000
* BL 0.0
* SECTION CAMBER DEFINITION - Z LOCATIONS (%)
  0.0        0.0001    0.0002    0.0003    0.0004    0.0005    0.0006    0.0007
 0.0008     0.0009    0.0010    0.0011    0.0012    0.0013    0.0014    0.0015
 0.0014     0.0012    0.0010    0.0008    0.0006    0.0004    0.0003    0.0000
* BL -4.2
* SECTION CAMBER DEFN - Z LOCATIONS (%)
  0.0000    0.3183    0.5894    0.8241    0.9742    0.9343    0.8791    0.8240
 0.7689    0.7138    0.6586    0.6035    0.5484    0.4932    0.4381    0.3830
 0.3279    0.2756    0.2204    0.1625    0.1073    0.0523    0.0000
*****
* panel 3
*X2      Y2      Z2      CORD2    AINC2
8.935   4.167   5.359   17.872  -0.632
*X1      Y1      Z1      CORD1    AINC1
15.049  7.018   5.225   13.091  -1.448
*ISPNDIV ICHRDIV SPC      IARFYL    NAP      IVTXFLG
2        8        1.0      2         23       0
* Panel 2, BL 4.2, 7.02
* SECTION CAMBER DEFN - X LOCATIONS (%)
  0.0000    1.0000    2.5000    5.0000    10.0000   15.0000   20.0000   25.0000
 30.0000   35.0000   40.0000   45.0000   50.0000   55.0000   60.0000   65.0000
 70.0000   75.0000   80.0000   85.0000   90.0000   95.0000  100.0000
* BL -4.2
* SECTION CAMBER DEFN - Z LOCATIONS (%)
  0.0000    0.3183    0.5894    0.8241    0.9742    0.9343    0.8791    0.8240
 0.7689    0.7138    0.6586    0.6035    0.5484    0.4932    0.4381    0.3830
 0.3279    0.2756    0.2204    0.1625    0.1073    0.0523    0.0000
* BL -7.0
* SECTION CAMBER DEFN - Z LOCATIONS (%)
  0.0000    0.3798    0.7571    1.1803    1.6486    1.8664    1.9198    1.8775
 1.7668    1.6440    1.5138    1.3873    1.2646    1.1381    1.0079    0.8813
 0.7550    0.6322    0.5021    0.3756    0.2527    0.1226    0.0000
*****
* panel 4
*X2      Y2      Z2      CORD2    AINC2
15.049  7.018   5.225   13.091  -1.448
*X1      Y1      Z1      CORD1    AINC1
17.871  8.333   5.162   10.885  -2.073
*ISPNDIV ICHRDIV SPC      IARFYL    NAP      IVTXFLG
2        8        1.0      2         23       0
* Panel 3, BL 7.02, 8.33
* SECTION CAMBER DEFN - X LOCATIONS (%)
  0.0000    1.0000    2.5000    5.0000    10.0000   15.0000   20.0000   25.0000
 30.0000   35.0000   40.0000   45.0000   50.0000   55.0000   60.0000   65.0000
 70.0000   75.0000   80.0000   85.0000   90.0000   95.0000  100.0000
* BL -7.0
* SECTION CAMBER DEFN - Z LOCATIONS (%)
  0.0000    0.3798    0.7571    1.1803    1.6486    1.8664    1.9198    1.8775
 1.7668    1.6440    1.5138    1.3873    1.2646    1.1381    1.0079    0.8813
 0.7550    0.6322    0.5021    0.3756    0.2527    0.1226    0.0000
* BL -8.3

```

```

* SECTION CAMBER DEFN - Z LOCATIONS (%)
0.0000 0.4112 0.8208 1.3100 1.9070 2.2509 2.4145 2.4589
2.4204 2.3220 2.1686 1.9922 1.8111 1.6299 1.4488 1.2676
1.0821 0.9053 0.7200 0.5432 0.3575 0.1764 0.0000

```

\*\*\*\*\*

\* panel 5

```

*X2 Y2 Z2 CORD2 AINC2
17.871 8.333 5.162 10.885 -2.073
*X1 Y1 Z1 CORD1 AINC1
20.689 9.647 5.100 7.462 -3.497
*ISPNDIV ICHRDIV SPC IARFYL NAP IVTXFLG
2 8 1.0 2 23 0

```

\* Panel 4, BL 8.33, 9.65

```

* SECTION CAMBER DEFN - X LOCATIONS (%)
0.0000 1.0000 2.5000 5.0000 10.0000 15.0000 20.0000 25.0000
30.0000 35.0000 40.0000 45.0000 50.0000 55.0000 60.0000 65.0000
70.0000 75.0000 80.0000 85.0000 90.0000 95.0000 100.0000

```

\* BL -8.3

```

* SECTION CAMBER DEFN - Z LOCATIONS (%)
0.0000 0.4112 0.8208 1.3100 1.9070 2.2509 2.4145 2.4589
2.4204 2.3220 2.1686 1.9922 1.8111 1.6299 1.4488 1.2676
1.0821 0.9053 0.7200 0.5432 0.3575 0.1764 0.0000

```

\* BL -9.6

```

* SECTION CAMBER DEFN - Z LOCATIONS (%)
0.0000 0.4319 0.8793 1.4427 2.2131 2.6800 2.9583 3.1147
3.1443 3.0935 2.9957 2.8504 2.6723 2.5132 2.3281 2.1095
1.8765 1.5841 1.2783 0.9655 0.6389 0.3062 0.0000

```

\*\*\*\*\*

\* panel 6

```

*X2 Y2 Z2 CORD2 AINC2
20.689 9.647 5.100 7.462 -3.497
*X1 Y1 Z1 CORD1 AINC1
23.507 10.961 5.038 4.042 -7.17
*ISPNDIV ICHRDIV SPC IARFYL NAP IVTXFLG
2 8 1.0 2 23 0

```

\* Panel 5, BL 9.65, 10.96

```

* SECTION CAMBER DEFN - X LOCATIONS (%)
0.0000 1.0000 2.5000 5.0000 10.0000 15.0000 20.0000 25.0000
30.0000 35.0000 40.0000 45.0000 50.0000 55.0000 60.0000 65.0000
70.0000 75.0000 80.0000 85.0000 90.0000 95.0000 100.0000

```

\* BL -9.6

```

* SECTION CAMBER DEFN - Z LOCATIONS (%)
0.0000 0.4319 0.8793 1.4427 2.2131 2.6800 2.9583 3.1147
3.1443 3.0935 2.9957 2.8504 2.6723 2.5132 2.3281 2.1095
1.8765 1.5841 1.2783 0.9655 0.6389 0.3062 0.0000

```

\* BL -11.0

```

* SECTION CAMBER DEFN - Z LOCATIONS (%)
0.0000 0.4288 0.8901 1.4502 2.2706 2.8312 3.2098 3.4591
3.5989 3.6615 3.6519 3.5657 3.4288 3.2318 3.0066 2.7341
2.4119 2.0755 1.7032 1.3182 0.9078 0.4596 0.0000

```

\*\*\*\*\*

\* panel 7, right wing tip

```

*X2 Y2 Z2 CORD2 AINC2
23.507 10.961 5.038 4.042 -7.17
*X1 Y1 Z1 CORD1 AINC1
26.326 12.275 4.976 0.604 -15.198
*ISPNDIV ICHRDIV SPC IARFYL NAP IVTXFLG
2 8 1.0 2 23 0

```

\* Panel 6, BL 10.96, 12.28

\* SECTION CAMBER DEFN - X LOCATIONS (%)

0.0000	1.0000	2.5000	5.0000	10.0000	15.0000	20.0000	25.0000
30.0000	35.0000	40.0000	45.0000	50.0000	55.0000	60.0000	65.0000
70.0000	75.0000	80.0000	85.0000	90.0000	95.0000	100.0000	

\* BL -11.0

\* SECTION CAMBER DEFN - Z LOCATIONS (%)

0.0000	0.4288	0.8901	1.4502	2.2706	2.8312	3.2098	3.4591
3.5989	3.6615	3.6519	3.5657	3.4288	3.2318	3.0066	2.7341
2.4119	2.0755	1.7032	1.3182	0.9078	0.4596	0.0000	

\* BL -12.3

\* SECTION CAMBER DEFN - Z LOCATIONS (%)

0.0000	0.4243	0.8507	1.4423	2.0915	2.6367	3.1063	3.3444
3.4970	3.6496	3.6779	3.6264	3.5162	3.3270	3.1946	2.9046
2.6919	2.3222	1.9315	1.5595	1.1056	0.5394	0.0000	



Table C-2 HASC Input File airfoil.inp for the Tailless Fighter Configuration

```

*****
* LEFT HAND WING
*****
* Panel 1, outboard section, BL -12.275
*   LE RADIUS   XMAX(%)   YMAX(%)   NUM   TYPE
*   0.16564    42.9896   1.9152    15    1
*   X(%)       Y(%)
*   0.1289     0.1589
*   0.4079     0.2753
*   1.2897     0.4274
*   2.7370     0.6026
*   4.7009     0.8115
*   7.0910     0.9662
*   9.9184     1.1294
*   13.1640    1.3075
*   16.7768    1.4744
*   20.6967    1.5943
*   24.8378    1.6677
*   29.2044    1.7840
*   33.7236    1.8255
*   38.3462    1.8865
*   42.9896    1.9152
* Panel 1, inboard section, BL -10.961
*   LE RADIUS   XMAX(%)   YMAX(%)   NUM   TYPE
*   0.24739    40.9756   1.9707    15    1
*   X(%)       Y(%)
*   0.2767     0.2221
*   0.5484     0.3259
*   1.3561     0.4890
*   2.6689     0.6771
*   4.4616     0.8611
*   6.7092     1.0322
*   9.3839     1.2055
*   12.4453    1.3694
*   15.8548    1.5203
*   19.5710    1.6551
*   23.5412    1.7672
*   27.7209    1.8594
*   32.0574    1.9239
*   36.4913    1.9567
*   40.9756    1.9707
*****
* Panel 2, outboard section, BL -10.961
*   LE RADIUS   XMAX(%)   YMAX(%)   NUM   TYPE
*   0.24739    40.9756   1.9707    15    1
*   X(%)       Y(%)
*   0.2767     0.2221
*   0.5484     0.3259
*   1.3561     0.4890
*   2.6689     0.6771
*   4.4616     0.8611
*   6.7092     1.0322
*   9.3839     1.2055
*   12.4453    1.3694
*   15.8548    1.5203

```

19.5710	1.6551			
23.5412	1.7672			
27.7209	1.8594			
32.0574	1.9239			
36.4913	1.9567			
40.9756	1.9707			
* Panel 2, inboard section, BL -9.647				
* LE RADIUS	XMAX(%)	YMAX(%)	NUM	TYPE
0.13401	40.3644	1.9506	15	1
* X(%)	Y(%)			
0.1375	0.1124			
0.3989	0.2494			
1.1788	0.4371			
2.4507	0.6198			
4.2008	0.8037			
6.4052	0.9808			
9.0331	1.1617			
12.0485	1.3312			
15.4140	1.4849			
19.0903	1.6278			
23.0261	1.7597			
27.1745	1.8545			
31.4834	1.9072			
35.8956	1.9363			
40.3644	1.9506			
*****				
* Panel 3, outboard section, BL -9.647				
* LE RADIUS	XMAX(%)	YMAX(%)	NUM	TYPE
0.13401	40.3644	1.9506	15	1
* X(%)	Y(%)			
0.1375	0.1124			
0.3989	0.2494			
1.1788	0.4371			
2.4507	0.6198			
4.2008	0.8037			
6.4052	0.9808			
9.0331	1.1617			
12.0485	1.3312			
15.4140	1.4849			
19.0903	1.6278			
23.0261	1.7597			
27.1745	1.8545			
31.4834	1.9072			
35.8956	1.9363			
40.3644	1.9506			
nel 3, inboard section, BL -8.333				
LE RADIUS	XMAX(%)	YMAX(%)	NUM	TYPE
0.09187	40.1635	1.7487	15	1
X(%)	Y(%)			
0.0843	0.0740			
0.3456	0.2318			
1.1134	0.4301			
2.3705	0.6095			
4.1039	0.7944			
5.2909	0.9642			
6.9003	1.1268			
8.118992	1.2807			
9.152506	1.4169			

18.9144 1.5371  
 22.8385 1.6322  
 26.9792 1.7042  
 31.2849 1.7497  
 35.6954 1.7591  
 40.1635 1.7487

\*\*\*\*\*

\* Panel 4, outboard section, BL -8.333

	LE RADIUS	XMAX(%)	YMAX(%)	NUM	TYPE
*	0.09187	40.1635	1.7487	15	1
*	X(%)	Y(%)			
	0.0843	0.0740			
	0.3456	0.2318			
	1.1134	0.4301			
	2.3705	0.6095			
	4.1039	0.7944			
	6.2909	0.9642			
	8.9003	1.1268			
	11.8992	1.2807			
	15.2506	1.4169			
	18.9144	1.5371			
	22.8385	1.6322			
	26.9792	1.7042			
	31.2849	1.7497			
	35.6954	1.7591			
	40.1635	1.7487			

\* Panel 4, inboard section, BL -7.018

	LE RADIUS	XMAX(%)	YMAX(%)	NUM	TYPE
*	0.07639	40.0976	1.9357	15	1
*	X(%)	Y(%)			
	0.0666	0.0607			
	0.3239	0.2299			
	1.0868	0.4479			
	2.3381	0.6392			
	4.0647	0.8295			
	6.2454	1.0091			
	8.8486	1.1850			
	11.8417	1.3509			
	15.1880	1.4972			
	18.8477	1.6254			
	22.7691	1.7373			
	26.9084	1.8299			
	31.2139	1.8963			
	35.6262	1.9273			
	40.0976	1.9357			

\*\*\*\*\*

\* Panel 5, outboard section, BL -7.018

	LE RADIUS	XMAX(%)	YMAX(%)	NUM	TYPE
*	0.07639	40.0976	1.9357	15	1
*	X(%)	Y(%)			
	0.0666	0.0607			
	0.3239	0.2299			
	1.0868	0.4479			
	2.3381	0.6392			
	4.0647	0.8295			
	6.2454	1.0091			
	8.8486	1.1850			
	11.8417	1.3509			

15.1880 1.4972  
 18.8477 1.6254  
 22.7691 1.7373  
 26.9084 1.8299  
 31.2139 1.8963  
 35.6262 1.9273  
 40.0976 1.9357

\* Panel 5, inboard section, BL -4.167

* LE RADIUS	XMAX(%)	YMAX(%)	NUM	TYPE
0.05595	45.0321	2.1513	15	1
* X(%)	Y(%)			
0.0428	0.0423			
0.3282	0.2477			
1.1787	0.4934			
2.5775	0.7111			
4.5108	0.9263			
6.9557	1.1274			
9.8766	1.3289			
13.2369	1.5058			
16.9970	1.6717			
21.1121	1.8248			
25.5237	1.9513			
30.1822	2.0477			
35.0291	2.1121			
39.9971	2.1456			
45.0321	2.1513			

\*\*\*\*\*

\* RIGHT HAND WING

\*\*\*\*\*

\* Panel 2, outboard section, BL 4.167

* LE RADIUS	XMAX(%)	YMAX(%)	NUM	TYPE
0.05595	45.0321	2.1513	15	1
* X(%)	Y(%)			
0.0428	0.0423			
0.3282	0.2477			
1.1787	0.4934			
2.5775	0.7111			
4.5108	0.9263			
6.9557	1.1274			
9.8766	1.3289			
13.2369	1.5058			
16.9970	1.6717			
21.1121	1.8248			
25.5237	1.9513			
30.1822	2.0477			
35.0291	2.1121			
39.9971	2.1456			
45.0321	2.1513			

\* Panel 2, outboard section, BL 7.018

* LE RADIUS	XMAX(%)	YMAX(%)	NUM	TYPE
0.07639	40.0976	1.9357	15	1
* X(%)	Y(%)			
0.0666	0.0607			
0.3239	0.2299			
1.0868	0.4479			
2.3381	0.6392			
4.0647	0.8295			
6.2454	1.0091			

8.8486	1.1850				
11.8417	1.3509				
15.1880	1.4972				
18.8477	1.6254				
22.7691	1.7373				
26.9084	1.8299				
31.2139	1.8963				
35.6262	1.9273				
40.0976	1.9357				
*****					
* Panel 3, inboard section, BL 7.018					
*	LE RADIUS	XMAX(%)	YMAX(%)	NUM	TYPE
	0.07639	40.0976	1.9357	15	1
*	X(%)	Y(%)			
	0.0666	0.0607			
	0.3239	0.2299			
	1.0868	0.4479			
	2.3381	0.6392			
	4.0647	0.8295			
	6.2454	1.0091			
	8.8486	1.1850			
	11.8417	1.3509			
	15.1880	1.4972			
	18.8477	1.6254			
	22.7691	1.7373			
	26.9084	1.8299			
	31.2139	1.8963			
	35.6262	1.9273			
	40.0976	1.9357			
* Panel 3, outboard section BL 8.333					
*	LE RADIUS	XMAX(%)	YMAX(%)	NUM	TYPE
	0.09187	40.1635	1.7487	15	1
*	X(%)	Y(%)			
	0.0843	0.0740			
	0.3456	0.2318			
	1.1134	0.4301			
	2.3705	0.6095			
	4.1039	0.7944			
	6.2909	0.9642			
	8.9003	1.1268			
	11.8992	1.2807			
	15.2506	1.4169			
	18.9144	1.5371			
	22.8385	1.6322			
	26.9792	1.7042			
	31.2849	1.7497			
	35.6954	1.7591			
	40.1635	1.7487			
*****					
* Panel 4, outboard section BL 8.333					
*	LE RADIUS	XMAX(%)	YMAX(%)	NUM	TYPE
	0.09187	40.1635	1.7487	15	1
*	X(%)	Y(%)			
	0.0843	0.0740			
	0.3456	0.2318			
	1.1134	0.4301			
	2.3705	0.6095			
	4.1039	0.7944			

6.2909	0.9642
8.9003	1.1268
11.8992	1.2807
15.2506	1.4169
18.9144	1.5371
22.8385	1.6322
26.9792	1.7042
31.2849	1.7497
35.6954	1.7591
40.1635	1.7487

\* Panel 4, inboard section, BL 9.647

* LE RADIUS	XMAX(%)	YMAX(%)	NUM	TYPE
0.13401	40.3644	1.9506	15	1
* X(%)	Y(%)			
0.1375	0.1124			
0.3989	0.2494			
1.1788	0.4371			
2.4507	0.6198			
4.2008	0.8037			
6.4052	0.9808			
9.0331	1.1617			
12.0485	1.3312			
15.4140	1.4849			
19.0903	1.6278			
23.0261	1.7597			
27.1745	1.8545			
31.4834	1.9072			
35.8956	1.9363			
40.3644	1.9506			

\*\*\*\*\*

\* Panel 5, inboard section, BL 9.647

* LE RADIUS	XMAX(%)	YMAX(%)	NUM	TYPE
0.13401	40.3644	1.9506	15	1
* X(%)	Y(%)			
0.1375	0.1124			
0.3989	0.2494			
1.1788	0.4371			
2.4507	0.6198			
4.2008	0.8037			
6.4052	0.9808			
9.0331	1.1617			
12.0485	1.3312			
15.4140	1.4849			
19.0903	1.6278			
23.0261	1.7597			
27.1745	1.8545			
31.4834	1.9072			
35.8956	1.9363			
40.3644	1.9506			

\* Panel 5, outboard section, BL 10.961

* LE RADIUS	XMAX(%)	YMAX(%)	NUM	TYPE
0.24739	40.9756	1.9707	15	1
* X(%)	Y(%)			
0.2767	0.2221			
0.5484	0.3259			
1.3561	0.4890			
2.6689	0.6771			
4.4616	0.8611			

6.7092	1.0322
9.3839	1.2055
12.4453	1.3694
15.8548	1.5203
19.5710	1.6551
23.5412	1.7672
27.7209	1.8594
32.0574	1.9239
36.4913	1.9567
40.9756	1.9707

\*\*\*\*\*

\* Panel 6, inboard section, BL 10.961

* LE RADIUS	XMAX(%)	YMAX(%)	NUM	TYPE
0.24739	40.9756	1.9707	15	1
* X(%)	Y(%)			
0.2767	0.2221			
0.5484	0.3259			
1.3561	0.4890			
2.6689	0.6771			
4.4616	0.8611			
6.7092	1.0322			
9.3839	1.2055			
12.4453	1.3694			
15.8548	1.5203			
19.5710	1.6551			
23.5412	1.7672			
27.7209	1.8594			
32.0574	1.9239			
36.4913	1.9567			
40.9756	1.9707			

\* Panel 6, outboard section, BL 12.275

* LE RADIUS	XMAX(%)	YMAX(%)	NUM	TYPE
0.16564	42.9896	1.9152	15	1
* X(%)	Y(%)			
0.1289	0.1589			
0.4079	0.2753			
1.2897	0.4274			
2.7370	0.6026			
4.7009	0.8115			
7.0910	0.9662			
9.9184	1.1294			
13.1640	1.3075			
16.7768	1.4744			
20.6967	1.5943			
24.8378	1.6677			
29.2044	1.7840			
33.7236	1.8255			
38.3462	1.8865			
42.9896	1.9152			

Table C-3 HASC Input File hasc.inp for the Falcon 21 Configuration

```

Falcon 21 configuration
* with trailing edge flap
*
*LAX      LAY      HAG      IRSTFLG  NPAN      NSURF     ALXP
0         1         0.        0.        34         4         8.0
*REY      NMACH     MACH(s)
2032875. 1         0.2
*NALPHA   ALPHA(s)
20        -4.        -2.        0.        2.         4.         6.
8.        10.       12.       14.       16.        18.        20.        22.
25.       27.       30.       32.       35.        37.
*NBETA    BETSTB(s)
1         0.0
*PITCHQ   ROLLQ     YAWQ      VINF
0.0       0.0       0.0       1.
*SREF     CBAR      XREF      ZREF      WSPAN
90720.    263.325  325.163  91.0     416.26
*****
* SURFACE 1
FOREBODY
*ISRTYP   LNPAN     ISYMFLG   ENETAR    FTAIL     ALZL      XGAP
5         4         0         0.        0.        0.0       0.0
* panel 1, left outboard
*X1       Y1         Z1         CORD1     AINC1
94.5     -22.03    91.0      0.1       -4.16
*X2       Y2         Z2         CORD2     AINC2
41.60    -16.20    91.0      53.00     -4.16
*ISPNDIV  ICHRDIV   SPC        IARFYL    NAP       IVTXFLG
3         4         0.0       0         0         0
*****
* panel 2, left inboard
*X1       Y1         Z1         CORD1     AINC1
41.60    -16.20    91.0      53.00     -4.16
*X2       Y2         Z2         CORD2     AINC2
-6.0     0.0       91.0      100.6     -4.16
*ISPNDIV  ICHRDIV   SPC        IARFYL    NAP       IVTXFLG
3         4         0.0       0         0         0
*****
* panel 3, right inboard
*X1       Y1         Z1         CORD1     AINC1
-6.0     0.0       91.0      100.6     -4.16
*X2       Y2         Z2         CORD2     AINC2
41.60    16.20     91.0      53.00     -4.16
*ISPNDIV  ICHRDIV   SPC        IARFYL    NAP       IVTXFLG
3         4         0.0       0         0         0
*****
* panel 4, right outboard
*X1       Y1         Z1         CORD1     AINC1
41.60    16.20     91.0      53.00     -4.16
*X2       Y2         Z2         CORD2     AINC2
94.5     22.03     91.0      0.1       -4.16
*ISPNDIV  ICHRDIV   SPC        IARFYL    NAP       IVTXFLG
3         4         0.0       0         0         0
*****

```



```

*****
* SURFACE 2
FUSELAGE
*ISRTYP  LNPAN      ISYMFLG  ENETAR   FTAIL    ALZL     XGAP
5         4         0         0.       0.       0.0     0.0
* panel 1
*X1       Y1         Z1         CORD1    AINC1
94.6     -22.03    91.0     457.90   0.0
*X2       Y2         Z2         CORD2    AINC2
94.60    -16.20    91.0     457.90   0.0
*ISPNDIV  ICHRDIV   SPC        IARFYL   NAP      IVTXFLG
3         8         0.0       0         0         0
*****
* panel 2
*X1       Y1         Z1         CORD1    AINC1
94.60    -16.20    91.0     457.90   0.0
*X2       Y2         Z2         CORD2    AINC2
94.60    0.0      91.0     457.90   0.0
*ISPNDIV  ICHRDIV   SPC        IARFYL   NAP      IVTXFLG
3         8         0.0       0         0         0
*****
* panel 3
*X1       Y1         Z1         CORD1    AINC1
94.60    0.0      91.0     457.90   0.0
*X2       Y2         Z2         CORD2    AINC2
94.60    16.20    91.0     457.90   0.0
*ISPNDIV  ICHRDIV   SPC        IARFYL   NAP      IVTXFLG
3         8         0.0       0         0         0
*****
* panel 4
*X1       Y1         Z1         CORD1    AINC1
94.60    16.20    91.0     457.90   0.0
*X2       Y2         Z2         CORD2    AINC2
94.6     22.03    91.0     457.90   0.0
*ISPNDIV  ICHRDIV   SPC        IARFYL   NAP      IVTXFLG
3         8         0.0       0         0         0
*****
* SURFACE 3
LEFT HAND WING AND STRAKE
*ISRTYP  LNPAN      ISYMFLG  ENETAR   FTAIL    ALZL     XGAP
5         13        0         0.       0.       0.0     0.0
* panel 1, TE flap
*X1       Y1         Z1         CORD1    AINC1
440.23   -208.13  89.12    8.0      2.75
*X2       Y2         Z2         CORD2    AINC2
442.12   -195.42  89.18    11.97    3.84
*ISPNDIV  ICHRDIV   SPC        IARFYL   NAP      IVTXFLG
2         5         0.0       0         0         0
*****
* panel 2, ahead of TE flap
*X1       Y1         Z1         CORD1    AINC1
403.03   -208.13  89.12    37.20    -5.55
*X2       Y2         Z2         CORD2    AINC2
388.03   -195.42  89.18    54.09    -4.46
*ISPNDIV  ICHRDIV   SPC        IARFYL   NAP      IVTXFLG
2         8         -1.0      0         0         0
*****

```

```

* panel 3, TE flap
*X1      Y1      Z1      CORD1      AINC1
442.12  -195.42  89.18   11.97      3.84
*X2      Y2      Z2      CORD2      AINC2
446.03  -170.0    89.21   19.97      4.88
*ISPNDIV ICHRDIV  SPC      IARFYL     NAP      IVTXFLG
2        5        0.0      0           0         0
*****
* panel 4, ahead of TE flap
*X1      Y1      Z1      CORD1      AINC1
388.03  -195.42  89.18   54.09      -4.46
*X2      Y2      Z2      CORD2      AINC2
357.59  -170.0    89.21   88.44      -3.42
*ISPNDIV ICHRDIV  SPC      IARFYL     NAP      IVTXFLG
2        8        -1.0     0           0         0
*****
* panel 6, TE flap
*X1      Y1      Z1      CORD1      AINC1
446.03  -170.0    89.21   19.97      4.88
*X2      Y2      Z2      CORD2      AINC2
451.83  -132.0    89.67   31.90      5.66
*ISPNDIV ICHRDIV  SPC      IARFYL     NAP      IVTXFLG
3        5        0.0      0           0         0
*****
* panel 6, ahead of TE flap
*X1      Y1      Z1      CORD1      AINC1
357.59  -170.0    89.21   88.44      -3.42
*X2      Y2      Z2      CORD2      AINC2
312.31  -132.0    89.67   139.52     -2.64
*ISPNDIV ICHRDIV  SPC      IARFYL     NAP      IVTXFLG
3        8        -1.0     0           0         0
*****
* panel 7, TE flap
*X1      Y1      Z1      CORD1      AINC1
451.83  -132.0    89.67   31.90      5.66
*X2      Y2      Z2      CORD2      AINC2
457.68  -93.5     90.13   43.99      6.71
*ISPNDIV ICHRDIV  SPC      IARFYL     NAP      IVTXFLG
3        5        0.0      0           0         0
*****
* panel 8, ahead of TE flap
*X1      Y1      Z1      CORD1      AINC1
312.31  -132.0    89.67   139.52     -2.64
*X2      Y2      Z2      CORD2      AINC2
266.42  -93.5     90.13   191.26     -1.59
*ISPNDIV ICHRDIV  SPC      IARFYL     NAP      IVTXFLG
3        8        -1.0     0           0         0
*****
* panel 9, TE flap
*X1      Y1      Z1      CORD1      AINC1
457.68  -93.5     90.13   43.99      6.71
*X2      Y2      Z2      CORD2      AINC2
463.55  -55.0     91.14   56.08      8.42
*ISPNDIV ICHRDIV  SPC      IARFYL     NAP      IVTXFLG
3        5        0.0      0           0         0
*****
* panel 10, ahead of TE flap
*X1      Y1      Z1      CORD1      AINC1

```

```

266.42   -93.5    90.13    191.26   -1.59
*X2      Y2        Z2        CORD2    AINC2
220.54   -55.0    91.14    243.01    0.12
*ISPNDIV ICHRDIV  SPC      IARFYL   NAP      IVTXFLG
3         8        -1.0     0         0         0
*****
* panel 11
*X1      Y1        Z1        CORD1    AINC1
220.54   -55.0    91.14    299.09    0.12
*X2      Y2        Z2        CORD2    AINC2
166.37   -33.83   90.91    363.25    0.13
*ISPNDIV ICHRDIV  SPC      IARFYL   NAP      IVTXFLG
4         9        -1.0     0         0         0
*****
* panel 12
*X1      Y1        Z1        CORD1    AINC1
166.37   -33.83   90.91    363.25    0.13
*X2      Y2        Z2        CORD2    AINC2
116.20   -26.76   91.00    416.74    0.08
*ISPNDIV ICHRDIV  SPC      IARFYL   NAP      IVTXFLG
2         9        -1.0     0         0         0
*****
* panel 13
*X1      Y1        Z1        CORD1    AINC1
116.2    -26.76   91.00    416.74    0.08
*X2      Y2        Z2        CORD2    AINC2
94.6     -22.03   91.00    444.00    0.00
*ISPNDIV ICHRDIV  SPC      IARFYL   NAP      IVTXFLG
3         9        -1.0     0         0         0
*****
* SURFACE 4
RIGHT HAND STRAKE AND WING
*ISRTYP  LNPNAN  ISYMFLG  ENETAR   FTAIL    ALZL     XGAP
5         13      0         0.        0.        0.        0.
* panel 1
*X1      Y1        Z1        CORD1    AINC1
94.6     22.03    91.00    444.00    0.00
*X2      Y2        Z2        CORD2    AINC2
116.2    26.76    91.00    416.74    0.08
*ISPNDIV ICHRDIV  SPC      IARFYL   NAP      IVTXFLG
3         9        -1.0     0         0         0
*****
* panel 2
*X1      Y1        Z1        CORD1    AINC1
116.2    26.76    91.00    416.74    0.08
*X2      Y2        Z2        CORD2    AINC2
166.37   33.83    90.91    363.25    0.13
*ISPNDIV ICHRDIV  SPC      IARFYL   NAP      IVTXFLG
2         9        -1.0     0         0         0
*****
* panel 3
*X1      Y1        Z1        CORD1    AINC1
166.37   33.83    90.91    363.25    0.13
*X2      Y2        Z2        CORD2    AINC2
220.54   55.0     91.14    299.09    0.12
*ISPNDIV ICHRDIV  SPC      IARFYL   NAP      IVTXFLG
4         9        -1.0     0         0         0

```

```

*****
* panel 4, TE flap
*X1      Y1      Z1      CORD1      AINC1
463.55   55.0    91.14   56.08      8.42
*X2      Y2      Z2      CORD2      AINC2
457.68   93.5    90.13   43.99      6.71
*ISPNDIV ICHRDIV  SPC      IARFYL     NAP        IVTXFLG
3         5         0.0      0           0           0
*****
* panel 5, ahead of TE flap
*X1      Y1      Z1      CORD1      AINC1
220.54   55.0    91.14   243.01     0.12
*X2      Y2      Z2      CORD2      AINC2
266.42   93.5    90.13   191.26     -1.59
*ISPNDIV ICHRDIV  SPC      IARFYL     NAP        IVTXFLG
3         8        -1.0     0           0           0
*****
* panel 6, TE flap
*X1      Y1      Z1      CORD1      AINC1
457.68   93.5    90.13   43.99      6.71
*X2      Y2      Z2      CORD2      AINC2
451.83   132.0   89.67   31.90      5.66
*ISPNDIV ICHRDIV  SPC      IARFYL     NAP        IVTXFLG
3         5         0.0      0           0           0
*****
* panel 7, ahead of TE flap
*X1      Y1      Z1      CORD1      AINC1
266.42   93.5    90.13   191.26     -1.59
*X2      Y2      Z2      CORD2      AINC2
312.31   132.0   89.67   139.52     -2.64
*ISPNDIV ICHRDIV  SPC      IARFYL     NAP        IVTXFLG
3         8        -1.0     0           0           0
*****
* panel 8, TE flap
*X1      Y1      Z1      CORD1      AINC1
451.83   132.0   89.67   31.90      5.66
*X2      Y2      Z2      CORD2      AINC2
446.03   170.0   89.21   19.97      4.88
*ISPNDIV ICHRDIV  SPC      IARFYL     NAP        IVTXFLG
3         5         0.0      0           0           0
*****
* panel 9, ahead of TE flap
*X1      Y1      Z1      CORD1      AINC1
312.31   132.0   89.67   139.52     -2.64
*X2      Y2      Z2      CORD2      AINC2
357.59   170.0   89.21   88.44      -3.42
*ISPNDIV ICHRDIV  SPC      IARFYL     NAP        IVTXFLG
3         8        -1.0     0           0           0
*****
* panel 10, TE flap
*X1      Y1      Z1      CORD1      AINC1
446.03   170.0   89.21   19.97      4.88
*X2      Y2      Z2      CORD2      AINC2
442.12   195.42  89.18   11.97      3.84
*ISPNDIV ICHRDIV  SPC      IARFYL     NAP        IVTXFLG
2         5         0.0      0           0           0
*****
* panel 11, ahead of TE flap

```

```

*X1      Y1      Z1      CORD1     AINC1
357.59   170.0    89.21    88.44    -3.42
*X2      Y2      Z2      CORD2     AINC2
388.03   195.42    89.18    54.09    -4.46
*ISPNDIV ICHRDIV  SPC      IARFYL    NAP      IVTXFLG
2         8        -1.0     0         0         0
*****
* panel 12, TE flap
*X1      Y1      Z1      CORD1     AINC1
442.12   195.42    89.18    11.97    3.84
*X2      Y2      Z2      CORD2     AINC2
440.23   208.13    89.12    8.0      2.75
*ISPNDIV ICHRDIV  SPC      IARFYL    NAP      IVTXFLG
2         5         0.0     0         0         0
*****
* panel 13, ahead of TE flap
*X1      Y1      Z1      CORD1     AINC1
388.03   195.42    89.18    54.09    -4.46
*X2      Y2      Z2      CORD2     AINC2
403.03   208.13    89.12    37.20    -5.55
*ISPNDIV ICHRDIV  SPC      IARFYL    NAP      IVTXFLG
2         8        -1.0     0         0         0

```

Table C-4 HASC Input File hasc.inp for the F-16XL Configuration

```

F-16XL without controls, HASC95
*LAX      LAY      HAG      ISRTFLG  NPAN      NSURF     ALXP
0         1         0.       0        36        4         6.0
*REY      NMACH     MACH(s)
2150000. 1         0.20
*NALPHA   ALPHA(s)
15        -2.0      0.0      2.0      4.0      6.0      8.0      10.0
15.0     20.0     25.0     30.0     35.0     40.0     45.0     50.0
*NBETA    BETA(s)
1         0.
*PITCHQ   ROLLQ     YAWQ     V
0.        0.        0.       1.
*SREF     CBAR      XREF     ZREF     WSPAN
86400.    296.4    324.0    91.0     388.8
*****
*****
* SURFACE 1
FOREBODY
*ISRTYP   LNPAN     ISYMFLG  ENETAR   FTAIL     ALZL      XGAP
5         6         0        0.0     0.0      0.0      0.0
* panel 1
*X1        Y1         Z1        CORD1    AINC1
136.0     -27.0     91.0     0.5     0.0
*X2        Y2         Z2        CORD2    AINC2
79.5      -23.0     91.0     57.0    0.0
*ISPNDIV  ICHRDIV   SPC       IARFYL   NAP       IVTXFLG
4         4         0.        0        0         0
*****
* panel 2
*X1        Y1         Z1        CORD1    AINC1
79.5      -23.0     91.0     57.0    0.0
*X2        Y2         Z2        CORD2    AINC2
8.8       -15.0     91.0     127.7   0.0
*ISPNDIV  ICHRDIV   SPC       IARFYL   NAP       IVTXFLG
2         4         0.        0        0         0
*****
* panel 3
*X1        Y1         Z1        CORD1    AINC1
8.8       -15.0     91.0     127.7   0.0
*X2        Y2         Z2        CORD2    AINC2
-36.8     0.0       91.0     173.3   0.0
*ISPNDIV  ICHRDIV   SPC       IARFYL   NAP       IVTXFLG
2         4         0.        0        0         0
*****
* panel 4
*X1        Y1         Z1        CORD1    AINC1
-36.8     0.0       91.0     173.3   0.0
*X2        Y2         Z2        CORD2    AINC2
8.8       15.0     91.0     127.7   0.0
*ISPNDIV  ICHRDIV   SPC       IARFYL   NAP       IVTXFLG
2         4         0.        0        0         0
*****
* panel 5
*X1        Y1         Z1        CORD1    AINC1
8.8       15.0     91.0     127.7   0.0

```

```

*X2      Y2      Z2      CORD2      AINC2
79.5     23.0    91.0    57.0     0.0
*ISPNDIV ICHRDIV  SPC      IARFYL    NAP      IVTXFLG
2        4        0.       0         0         0
*****
* panel 6
*X1      Y1      Z1      CORD1      AINC1
79.5     23.0    91.0    57.0     0.0
*X2      Y2      Z2      CORD2      AINC2
136.0    27.0    91.0    0.5      0.0
*ISPNDIV ICHRDIV  SPC      IARFYL    NAP      IVTXFLG
2        4        0.       0         0         0
*****
* SURFACE 2
FUSELAGE
*ISRTYP  LNPNAN   ISYMFLG  ENETAR    FTAIL     ALZL      XGAP
4        6        0        0.0       0.0       0.0       0.0
* panel 1
*X1      Y1      Z1      CORD1      AINC1
136.5    -27.0   91.     383.3     0
*X2      Y2      Z2      CORD2      AINC2
136.5    -23.0   91.     406.7     0
*ISPNDIV ICHRDIV  SPC      IARFYL    NAP      IVTXFLG
2        8        0.       0         0         0
*****
* panel 2
*X1      Y1      Z1      CORD1      AINC1
136.5    -23.0   91.     406.7     0
*X2      Y2      Z2      CORD2      AINC2
136.5    -15.0   91.     408.0     0
*ISPNDIV ICHRDIV  SPC      IARFYL    NAP      IVTXFLG
2        8        0.       0         0         0
*****
* panel 3
*X1      Y1      Z1      CORD1      AINC1
136.5    -15.0   91.0    408.0     0
*X2      Y2      Z2      CORD2      AINC2
136.5    0.0     91.0    408.0     0
*ISPNDIV ICHRDIV  SPC      IARFYL    NAP      IVTXFLG
2        8        0.       0         0         0
*****
* panel 4
*X1      Y1      Z1      CORD1      AINC1
136.5    0.0     91.0    408.0     0
*X2      Y2      Z2      CORD2      AINC2
136.5    15.0    91.0    408.0     0
*ISPNDIV ICHRDIV  SPC      IARFYL    NAP      IVTXFLG
2        8        0.       0         0         0
*****
* panel 5
*X1      Y1      Z1      CORD1      AINC1
136.5    15.0    91.     408.0     0
*X2      Y2      Z2      CORD2      AINC2
136.5    23.0    91.     406.7     0
*ISPNDIV ICHRDIV  SPC      IARFYL    NAP      IVTXFLG
2        8        0.       0         0         0
*****

```

```

* panel 6
*X1      Y1      Z1      CORD1      AINC1
136.5    23.0    91.     406.7     0
*X2      Y2      Z2      CORD2      AINC2
136.5    27.0    91.     383.3     0
*ISPNDIV ICHRDIV  SPC      IARFYL     NAP      IVTXFLG
2        8        0.       0          0        0
*****
* SURFACE 3
LEFT HAND WING
*ISRTYP  LNPNAN    ISYMFLG  ENETAR     FTAIL     ALZL     XGAP
5        12        0        0.0        0.0        0.0     0.0
* panel 1
*X1      Y1      Z1      CORD1      AINC1
459.44  -194.42  89.75   64.91     -3.99
*X2      Y2      Z2      CORD2      AINC2
424.70  -165.25  87.65   93.21     -3.99
*ISPNDIV ICHRDIV  SPC      IARFYL     NAP      IVTXFLG
2        8        -1.      2          23       0
* SECTION CAMBER DEFN - X LOCATIONS (%)
0.0000  1.0000  2.5000  5.0000  10.0000  15.0000  20.0000  25.0000
30.0000  35.0000  40.0000  45.0000  50.0000  55.0000  60.0000  65.0000
70.0000  75.0000  80.0000  85.0000  90.0000  95.0000  100.0000
* panel 194.4
* SECTION CAMBER DEFN - Z LOCATIONS (%)
0.0000  0.1679  0.3998  0.7341  1.2015  1.3967  1.3992  1.3061
1.2042  1.1218  1.0391  0.9515  0.8644  0.7785  0.6983  0.6202
0.5386  0.4549  0.3686  0.2798  0.1886  0.0950  0.0000
* panel 165.3
* SECTION CAMBER DEFN - Z LOCATIONS (%)
0.0000  0.1681  0.4008  0.7379  1.2182  1.4322  1.4504  1.3645
1.2588  1.1734  1.0914  1.0044  0.9161  0.8299  0.7432  0.6539
0.5625  0.4688  0.3754  0.2820  0.1886  0.0953  0.0000
*****
* panel 2
*X2      Y2      Z2      CORD2      AINC2
424.70  -165.25  87.65   93.21     -3.99
*X1      Y1      Z1      CORD1      AINC1
388.38  -136.08  85.69   123.05    -3.84
*ISPNDIV ICHRDIV  SPC      IARFYL     NAP      IVTXFLG
4        8        -1.      2          23       0
* SECTION CAMBER DEFN - X LOCATIONS (%)
0.0000  1.0000  2.5000  5.0000  10.0000  15.0000  20.0000  25.0000
30.0000  35.0000  40.0000  45.0000  50.0000  55.0000  60.0000  65.0000
70.0000  75.0000  80.0000  85.0000  90.0000  95.0000  100.0000
* panel 165.3
* SECTION CAMBER DEFN - Z LOCATIONS (%)
0.0000  0.1681  0.4008  0.7379  1.2182  1.4322  1.4504  1.3645
1.2588  1.1734  1.0914  1.0044  0.9161  0.8299  0.7432  0.6539
0.5625  0.4688  0.3754  0.2820  0.1886  0.0953  0.0000
* panel 136.1
* SECTION CAMBER DEFN - Z LOCATIONS (%)
0.0000  0.1692  0.3922  0.7212  1.1968  1.4174  1.4457  1.3701
1.2702  1.1864  1.1077  1.0243  0.9399  0.8562  0.7726  0.6909
0.6040  0.4928  0.3904  0.3072  0.2046  0.1033  0.0001
*****
* panel 3

```



```

*X2      Y2      Z2      CORD2      AINC2
388.38  -136.08  85.69   123.05   -3.84
*X1      Y1      Z1      CORD1      AINC1
369.80  -128.75  86.05   139.94   -3.20
*ISPNDIV ICHRDIV  SPC      IARFYL     NAP      IVTXFLG
2        8        -1.      2         23       0
* SECTION CAMBER DEFN - X LOCATIONS (%)
  0.0000  1.0000  2.5000  5.0000  10.0000  15.0000  20.0000  25.0000
 30.0000  35.0000  40.0000  45.0000  50.0000  55.0000  60.0000  65.0000
 70.0000  75.0000  80.0000  85.0000  90.0000  95.0000 100.0000
* panel 136.1
* SECTION CAMBER DEFN - Z LOCATIONS (%)
  0.0000  0.1692  0.3922  0.7212  1.1968  1.4174  1.4457  1.3701
 1.2702  1.1864  1.1077  1.0243  0.9399  0.8562  0.7726  0.6909
 0.6040  0.4928  0.3904  0.3072  0.2046  0.1033  0.0001
* panel 128.8
* SECTION CAMBER DEFN - Z LOCATIONS (%)
  0.0000  0.1437  0.3303  0.5938  0.9863  1.1778  1.2145  1.1638
 1.0860  1.0094  0.9319  0.8473  0.7620  0.6808  0.6028  0.5294
 0.4555  0.3691  0.2987  0.2254  0.1501  0.0755  0.0000
*****
* panel 4
*X1      Y1      Z1      CORD1      AINC1
369.80  -128.75  86.05   139.94   -3.20
*X2      Y2      Z2      CORD2      AINC2
331.93  -114.98  86.99   176.50   -2.20
*ISPNDIV ICHRDIV  SPC      IARFYL     NAP      IVTXFLG
2        8        -1.      2         23       0
* SECTION CAMBER DEFN - X LOCATIONS (%)
  0.0000  1.0000  2.5000  5.0000  10.0000  15.0000  20.0000  25.0000
 30.0000  35.0000  40.0000  45.0000  50.0000  55.0000  60.0000  65.0000
 70.0000  75.0000  80.0000  85.0000  90.0000  95.0000 100.0000
* panel 128.8
* SECTION CAMBER DEFN - Z LOCATIONS (%)
  0.0000  0.1437  0.3303  0.5938  0.9863  1.1778  1.2145  1.1638
 1.0860  1.0094  0.9319  0.8473  0.7620  0.6808  0.6028  0.5294
 0.4555  0.3691  0.2987  0.2254  0.1501  0.0755  0.0000
* panel 115.0
* SECTION CAMBER DEFN - Z LOCATIONS (%)
  0.0000  0.1437  0.3303  0.5938  0.9863  1.1778  1.2145  1.1638
 1.0860  1.0094  0.9319  0.8473  0.7620  0.6808  0.6028  0.5294
 0.4555  0.3691  0.2987  0.2254  0.1501  0.0755  0.0000
*****
* panel 5, elevon
*X2      Y2      Z2      CORD2      AINC2
468.73  -114.98  86.99   39.70    06.40
*X1      Y1      Z1      CORD1      AINC1
468.58  -78.97   89.43   43.90    07.45
*ISPNDIV ICHRDIV  SPC      IARFYL     NAP      IVTXFLG
3        5        0.      0         0        0
*****
* panel 5, ahead of elevon
*X2      Y2      Z2      CORD2      AINC2
331.93  -114.98  86.99   136.80   -2.20
*X1      Y1      Z1      CORD1      AINC1
232.96  -78.97   89.43   235.62   -0.85
*ISPNDIV ICHRDIV  SPC      IARFYL     NAP      IVTXFLG
3        7        -1.      2         23       0

```

```

* SECTION CAMBER DEFN - X LOCATIONS (%)
  0.0000  1.0000  2.5000  5.0000  10.0000  15.0000  20.0000  25.0000
 30.0000  35.0000  40.0000  45.0000  50.0000  55.0000  60.0000  65.0000
 70.0000  75.0000  80.0000  85.0000  90.0000  95.0000 100.0000
* panel 115.0
* SECTION CAMBER DEFN - Z LOCATIONS (%)
  0.0000  0.1437  0.3303  0.5938  0.9863  1.1778  1.2145  1.1638
 1.0860  1.0094  0.9319  0.8473  0.7620  0.6808  0.6028  0.5294
 0.4555  0.3691  0.2987  0.2254  0.1501  0.0755  0.0000
* panel 79.0
* SECTION CAMBER DEFN - Z LOCATIONS (%)
  0.0000  0.0062  0.0652  0.1596  0.2853  0.3587  0.4031  0.4289
 0.4280  0.3983  0.3466  0.2907  0.2330  0.1747  0.1264  0.0894
 0.0543  0.0159 -0.0189 -0.0219 -0.0152 -0.0078  0.0000
*****
* panel 6, elevon
*X1      Y1      Z1      CORD1  AINC1
468.58  -78.97  89.43  43.90  07.45
*X2      Y2      Z2      CORD2  AINC2
468.53  -54.96  90.46  46.70  07.39
*ISPNDIV ICHRDIV  SPC      IARFYL  NAP      IVTXFLG
3        5        0.        0        0        0
*****
* panel 6, ahead of elevon
*X1      Y1      Z1      CORD1  AINC1
232.96  -78.97  89.43  235.62 -0.85
*X2      Y2      Z2      CORD2  AINC2
179.56  -54.96  90.46  288.97 -0.51
*ISPNDIV ICHRDIV  SPC      IARFYL  NAP      IVTXFLG
3        7        -1.       2       23       0
* SECTION CAMBER DEFN - X LOCATIONS (%)
  0.0000  1.0000  2.5000  5.0000  10.0000  15.0000  20.0000  25.0000
 30.0000  35.0000  40.0000  45.0000  50.0000  55.0000  60.0000  65.0000
 70.0000  75.0000  80.0000  85.0000  90.0000  95.0000 100.0000
* panel 79.0
* SECTION CAMBER DEFN - Z LOCATIONS (%)
  0.0000  0.0062  0.0652  0.1596  0.2853  0.3587  0.4031  0.4289
 0.4280  0.3983  0.3466  0.2907  0.2330  0.1747  0.1264  0.0894
 0.0543  0.0159 -0.0189 -0.0219 -0.0152 -0.0078  0.0000
* panel 55
* SECTION CAMBER DEFN - Z LOCATIONS (%)
  0.0000  0.0151  0.0541  0.1090  0.2164  0.3403  0.4303  0.4653
 0.4505  0.4111  0.3774  0.3085  0.2314  0.1764  0.1305  0.0932
 0.0536  0.0097 -0.0167 -0.0142 -0.0028  0.0082  0.0000
*****
* panel 7, elevon
*X1      Y1      Z1      CORD1  AINC1
468.53  -54.96  90.46  46.70  07.39
*X2      Y2      Z2      CORD2  AINC2
468.52  -42.96  90.54  48.10  07.44
*ISPNDIV ICHRDIV  SPC      IARFYL  NAP      IVTXFLG
2        5        0.        0        0        0
*****
* panel 7, ahead of elevon
*X1      Y1      Z1      CORD1  AINC1
179.56  -54.96  90.46  288.97 -0.51
*X2      Y2      Z2      CORD2  AINC2
164.99  -42.96  90.54  303.53 -0.46

```

```

*ISPNDIV  ICHRDIV  SPC      IARFYL  NAP      IVTXFLG
2          7        -1.      2        23       0
* SECTION CAMBER DEFN - X LOCATIONS (%)
  0.0000    1.0000    2.5000    5.0000    10.0000    15.0000    20.0000    25.0000
 30.0000    35.0000    40.0000    45.0000    50.0000    55.0000    60.0000    65.0000
 70.0000    75.0000    80.0000    85.0000    90.0000    95.0000    100.0000
* panel 55
* SECTION CAMBER DEFN - Z LOCATIONS (%)
  0.0000    0.0151    0.0541    0.1090    0.2164    0.3403    0.4303    0.4653
  0.4505    0.4111    0.3774    0.3085    0.2314    0.1764    0.1305    0.0932
  0.0536    0.0097   -0.0167   -0.0142   -0.0028    0.0082    0.0000
* panel 43
* SECTION CAMBER DEFN - Z LOCATIONS (%)
  0.0000    0.0195    0.0575    0.1201    0.2551    0.4070    0.5327    0.5820
  0.5456    0.4782    0.3792    0.3080    0.2845    0.2709    0.2154    0.2426
  0.2507    0.2041    0.1050   -0.0440   -0.1604   -0.0778    0.0000
*****
* panel 8
*X1      Y1      Z1      CORD1    AINC1
164.99  -42.96   90.54   351.63   -0.46
*X2      Y2      Z2      CORD2    AINC2
155.81  -34.98   90.53   361.73   -0.44
*ISPNDIV  ICHRDIV  SPC      IARFYL  NAP      IVTXFLG
2          8        -1.      2        23       0
* SECTION CAMBER DEFN - X LOCATIONS (%)
  0.0000    1.0000    2.5000    5.0000    10.0000    15.0000    20.0000    25.0000
 30.0000    35.0000    40.0000    45.0000    50.0000    55.0000    60.0000    65.0000
 70.0000    75.0000    80.0000    85.0000    90.0000    95.0000    100.0000
* panel 43
* SECTION CAMBER DEFN - Z LOCATIONS (%)
  0.0000    0.0195    0.0575    0.1201    0.2551    0.4070    0.5327    0.5820
  0.5456    0.4782    0.3792    0.3080    0.2845    0.2709    0.2154    0.2426
  0.2507    0.2041    0.1050   -0.0440   -0.1604   -0.0778    0.0000
* panel 35
* SECTION CAMBER DEFN - Z LOCATIONS (%)
  0.0000    0.0174    0.0620    0.1568    0.3496    0.5282    0.6732    0.7186
  0.6458    0.5405    0.4305    0.3442    0.3187    0.3128    0.2939    0.3114
  0.3265    0.3288    0.2982    0.2074    0.1635    0.1910    0.0000
*****
* panel 9
*X1      Y1      Z1      CORD1    AINC1
155.81  -34.98   90.53   361.73   -0.44
*X2      Y2      Z2      CORD2    AINC2
138.16  -27.00   90.44   380.30   -0.43
*ISPNDIV  ICHRDIV  SPC      IARFYL  NAP      IVTXFLG
2          8        -1.      2        23       0
* SECTION CAMBER DEFN - X LOCATIONS (%)
  0.0000    1.0000    2.5000    5.0000    10.0000    15.0000    20.0000    25.0000
 30.0000    35.0000    40.0000    45.0000    50.0000    55.0000    60.0000    65.0000
 70.0000    75.0000    80.0000    85.0000    90.0000    95.0000    100.0000
* panel 35
* SECTION CAMBER DEFN - Z LOCATIONS (%)
  0.0000    0.0174    0.0620    0.1568    0.3496    0.5282    0.6732    0.7186
  0.6458    0.5405    0.4305    0.3442    0.3187    0.3128    0.2939    0.3114
  0.3265    0.3288    0.2982    0.2074    0.1635    0.1910    0.0000
* panel 27
* SECTION CAMBER DEFN - Z LOCATIONS (%)
  0.0000    0.0444    0.1825    0.4085    0.7421    1.0080    1.1614    1.2126

```

	1.1819	1.1292	1.0633	1.0026	0.9628	0.9305	0.9114	0.9104
	0.8673	0.7540	0.5964	0.4506	0.3031	0.2231	0.0000	

\*\*\*\*\*

\* SURFACE 4

RIGHT HAND WING

*ISRTYP	LNPAN	ISYMFLG	ENETAR	FTAIL	ALZL	XGAP		
5	12	0	0.0	0.0	0.0	0.0		

\* panel 1

*X1	Y1	Z1	CORD1	AINC1				
138.16	27.00	90.44	380.30	-0.43				
*X2	Y2	Z2	CORD2	AINC2				
155.81	34.98	90.53	361.73	-0.44				

*ISPNDIV	ICHRDIV	SPC	IARFYL	NAP	IVTXFLG			
2	8	-1.	2	23	0			

\* SECTION CAMBER DEFN - X LOCATIONS (%)

0.0000	1.0000	2.5000	5.0000	10.0000	15.0000	20.0000	25.0000
30.0000	35.0000	40.0000	45.0000	50.0000	55.0000	60.0000	65.0000
70.0000	75.0000	80.0000	85.0000	90.0000	95.0000	100.0000	

\* panel 27

\* SECTION CAMBER DEFN - Z LOCATIONS (%)

0.0000	0.0444	0.1825	0.4085	0.7421	1.0080	1.1614	1.2126
1.1819	1.1292	1.0633	1.0026	0.9628	0.9305	0.9114	0.9104
0.8673	0.7540	0.5964	0.4506	0.3031	0.2231	0.0000	

\* SECTION CAMBER DEFN - Z LOCATIONS (%)

0.0000	0.0174	0.0620	0.1568	0.3496	0.5282	0.6732	0.7186
0.6458	0.5405	0.4305	0.3442	0.3187	0.3128	0.2939	0.3114
0.3265	0.3288	0.2982	0.2074	0.1635	0.1910	0.0000	

\*\*\*\*\*

\* panel 2

*X1	Y1	Z1	CORD1	AINC1				
155.81	34.98	90.53	361.73	-0.44				
*X2	Y2	Z2	CORD2	AINC2				
164.99	42.96	90.54	351.63	-0.46				

*ISPNDIV	ICHRDIV	SPC	IARFYL	NAP	IVTXFLG			
2	8	-1.	2	23	0			

\* SECTION CAMBER DEFN - X LOCATIONS (%)

0.0000	1.0000	2.5000	5.0000	10.0000	15.0000	20.0000	25.0000
30.0000	35.0000	40.0000	45.0000	50.0000	55.0000	60.0000	65.0000
70.0000	75.0000	80.0000	85.0000	90.0000	95.0000	100.0000	

\* panel 35

\* SECTION CAMBER DEFN - Z LOCATIONS (%)

0.0000	0.0174	0.0620	0.1568	0.3496	0.5282	0.6732	0.7186
0.6458	0.5405	0.4305	0.3442	0.3187	0.3128	0.2939	0.3114
0.3265	0.3288	0.2982	0.2074	0.1635	0.1910	0.0000	

\* panel 43

\* SECTION CAMBER DEFN - Z LOCATIONS (%)

0.0000	0.0195	0.0575	0.1201	0.2551	0.4070	0.5327	0.5820
0.5456	0.4782	0.3792	0.3080	0.2845	0.2709	0.2154	0.2426
0.2507	0.2041	0.1050	-0.0440	-0.1604	-0.0778	0.0000	

\*\*\*\*\*

\* panel 3, elevon

*X1	Y1	Z1	CORD1	AINC1				
468.52	42.96	90.54	48.10	06.40				
*X2	Y2	Z2	CORD2	AINC2				
468.53	54.96	90.46	46.70	07.45				

*ISPNDIV	ICHRDIV	SPC	IARFYL	NAP	IVTXFLG			
2	5	0.	0	0	0			

```

*****
* panel 3, ahead of elevon
*X1      Y1      Z1      CORD1      AINC1
164.99   42.96   90.54   303.53   -0.46
*X2      Y2      Z2      CORD2      AINC2
179.56   54.96   90.46   288.97   -0.51
*ISPNDIV ICHRDIV  SPC      IARFYL     NAP      IVTXFLG
2         7      -1.      2         23       0
* SECTION CAMBER DEFN - X LOCATIONS (%)
  0.0000   1.0000   2.5000   5.0000   10.0000   15.0000   20.0000   25.0000
 30.0000  35.0000  40.0000  45.0000  50.0000  55.0000  60.0000  65.0000
 70.0000  75.0000  80.0000  85.0000  90.0000  95.0000 100.0000
* panel 43
* SECTION CAMBER DEFN - Z LOCATIONS (%)
  0.0000   0.0195   0.0575   0.1201   0.2551   0.4070   0.5327   0.5820
  0.5456   0.4782   0.3792   0.3080   0.2845   0.2709   0.2154   0.2426
  0.2507   0.2041   0.1050  -0.0440  -0.1604  -0.0778   0.0000
* panel 55
* SECTION CAMBER DEFN - Z LOCATIONS (%)
  0.0000   0.0151   0.0541   0.1090   0.2164   0.3403   0.4303   0.4653
  0.4505   0.4111   0.3774   0.3085   0.2314   0.1764   0.1305   0.0932
  0.0536   0.0097  -0.0167  -0.0142  -0.0028   0.0082   0.0000
*****
* panel 4, elevon
*X1      Y1      Z1      CORD1      AINC1
468.53   54.96   90.46   46.70    07.45
*X2      Y2      Z2      CORD2      AINC2
468.58   78.97   89.43   43.90    07.39
*ISPNDIV ICHRDIV  SPC      IARFYL     NAP      IVTXFLG
3         5       0.      0         0         0
*****
* panel 4, ahead of elevon
*X1      Y1      Z1      CORD1      AINC1
179.56   54.96   90.46   288.97   -0.51
*X2      Y2      Z2      CORD2      AINC2
232.96   78.97   89.43   235.62   -0.85
*ISPNDIV ICHRDIV  SPC      IARFYL     NAP      IVTXFLG
3         7      -1.      2         23       0
* SECTION CAMBER DEFN - X LOCATIONS (%)
  0.0000   1.0000   2.5000   5.0000   10.0000   15.0000   20.0000   25.0000
 30.0000  35.0000  40.0000  45.0000  50.0000  55.0000  60.0000  65.0000
 70.0000  75.0000  80.0000  85.0000  90.0000  95.0000 100.0000
* panel 55
* SECTION CAMBER DEFN - Z LOCATIONS (%)
  0.0000   0.0151   0.0541   0.1090   0.2164   0.3403   0.4303   0.4653
  0.4505   0.4111   0.3774   0.3085   0.2314   0.1764   0.1305   0.0932
  0.0536   0.0097  -0.0167  -0.0142  -0.0028   0.0082   0.0000
* panel 79.0
* SECTION CAMBER DEFN - Z LOCATIONS (%)
  0.0000   0.0062   0.0652   0.1596   0.2853   0.3587   0.4031   0.4289
  0.4280   0.3983   0.3466   0.2907   0.2330   0.1747   0.1264   0.0894
  0.0543   0.0159  -0.0189  -0.0219  -0.0152  -0.0078   0.0000
*****
* panel 5, elevon
*X1      Y1      Z1      CORD1      AINC1
468.58   78.97   89.43   43.90    7.39
*X2      Y2      Z2      CORD2      AINC2
468.73   114.98  86.99   39.70    7.44

```

```

*ISPNDIV  ICHRDIV  SPC      IARFYL  NAP      IVTXFLG
3          5        0.       0        0        0
*****
* panel 5, ahead of elevon
*X1      Y1      Z1      CORD1  AINC1
232.96  78.97   89.43   235.62 -0.85
*X2      Y2      Z2      CORD2  AINC2
331.93  114.98   86.99   136.80 -2.20
*ISPNDIV  ICHRDIV  SPC      IARFYL  NAP      IVTXFLG
3          7        -1.      2        23       0
* SECTION CAMBER DEFN - X LOCATIONS (%)
  0.0000  1.0000  2.5000  5.0000  10.0000  15.0000  20.0000  25.0000
 30.0000 35.0000 40.0000 45.0000 50.0000 55.0000 60.0000 65.0000
 70.0000 75.0000 80.0000 85.0000 90.0000 95.0000 100.0000
* panel 79.0
* SECTION CAMBER DEFN - Z LOCATIONS (%)
  0.0000  0.0062  0.0652  0.1596  0.2853  0.3587  0.4031  0.4289
  0.4280  0.3983  0.3466  0.2907  0.2330  0.1747  0.1264  0.0894
  0.0543  0.0159 -0.0189 -0.0219 -0.0152 -0.0078  0.0000
* panel 115.0
* SECTION CAMBER DEFN - Z LOCATIONS (%)
  0.0000  0.1437  0.3303  0.5938  0.9863  1.1778  1.2145  1.1638
  1.0860  1.0094  0.9319  0.8473  0.7620  0.6808  0.6028  0.5294
  0.4555  0.3691  0.2987  0.2254  0.1501  0.0755  0.0000
*****
* panel 6
*X1      Y1      Z1      CORD1  AINC1
331.93  114.98   86.99   176.50 -2.20
*X2      Y2      Z2      CORD2  AINC2
369.80  128.75   86.05   139.94 -3.20
*ISPNDIV  ICHRDIV  SPC      IARFYL  NAP      IVTXFLG
2          8        -1.      2        23       0
* SECTION CAMBER DEFN - X LOCATIONS (%)
  0.0000  1.0000  2.5000  5.0000  10.0000  15.0000  20.0000  25.0000
 30.0000 35.0000 40.0000 45.0000 50.0000 55.0000 60.0000 65.0000
 70.0000 75.0000 80.0000 85.0000 90.0000 95.0000 100.0000
* panel 115.0
* SECTION CAMBER DEFN - Z LOCATIONS (%)
  0.0000  0.1437  0.3303  0.5938  0.9863  1.1778  1.2145  1.1638
  1.0860  1.0094  0.9319  0.8473  0.7620  0.6808  0.6028  0.5294
  0.4555  0.3691  0.2987  0.2254  0.1501  0.0755  0.0000
* panel 128.8
* SECTION CAMBER DEFN - Z LOCATIONS (%)
  0.0000  0.1437  0.3303  0.5938  0.9863  1.1778  1.2145  1.1638
  1.0860  1.0094  0.9319  0.8473  0.7620  0.6808  0.6028  0.5294
  0.4555  0.3691  0.2987  0.2254  0.1501  0.0755  0.0000
*****
* panel 7
*X1      Y1      Z1      CORD1  AINC1
369.80  128.75   86.05   139.94 -3.20
*X2      Y2      Z2      CORD2  AINC2
388.38  136.08   85.69   123.05 -3.84
*ISPNDIV  ICHRDIV  SPC      IARFYL  NAP      IVTXFLG
2          8        -1.      2        23       0
* SECTION CAMBER DEFN - X LOCATIONS (%)
  0.0000  1.0000  2.5000  5.0000  10.0000  15.0000  20.0000  25.0000
 30.0000 35.0000 40.0000 45.0000 50.0000 55.0000 60.0000 65.0000
 70.0000 75.0000 80.0000 85.0000 90.0000 95.0000 100.0000

```

```

* panel 128.8
* SECTION CAMBER DEFN - Z LOCATIONS (%)
0.0000 0.1437 0.3303 0.5938 0.9863 1.1778 1.2145 1.1638
1.0860 1.0094 0.9319 0.8473 0.7620 0.6808 0.6028 0.5294
0.4555 0.3691 0.2987 0.2254 0.1501 0.0755 0.0000

* panel 136.1
* SECTION CAMBER DEFN - Z LOCATIONS (%)
0.0000 0.1692 0.3922 0.7212 1.1968 1.4174 1.4457 1.3701
1.2702 1.1864 1.1077 1.0243 0.9399 0.8562 0.7726 0.6909
0.6040 0.4928 0.3904 0.3072 0.2046 0.1033 0.0001

*****
* panel 8
*X1 Y1 Z1 CORD1 AINC1
388.38 136.08 85.69 123.05 -3.84
*X2 Y2 Z2 CORD2 AINC2
424.70 165.25 87.65 93.21 -3.99
*ISPNDIV ICHRDIV SPC IARFYL NAP IVTXFLG
4 8 -1. 2 23 0
* SECTION CAMBER DEFN - X LOCATIONS (%)
0.0000 1.0000 2.5000 5.0000 10.0000 15.0000 20.0000 25.0000
30.0000 35.0000 40.0000 45.0000 50.0000 55.0000 60.0000 65.0000
70.0000 75.0000 80.0000 85.0000 90.0000 95.0000 100.0000

* panel 136.1
* SECTION CAMBER DEFN - Z LOCATIONS (%)
0.0000 0.1692 0.3922 0.7212 1.1968 1.4174 1.4457 1.3701
1.2702 1.1864 1.1077 1.0243 0.9399 0.8562 0.7726 0.6909
0.6040 0.4928 0.3904 0.3072 0.2046 0.1033 0.0001

* panel 165.3
* SECTION CAMBER DEFN - Z LOCATIONS (%)
0.0000 0.1681 0.4008 0.7379 1.2182 1.4322 1.4504 1.3645
1.2588 1.1734 1.0914 1.0044 0.9161 0.8299 0.7432 0.6539
0.5625 0.4688 0.3754 0.2820 0.1886 0.0953 0.0000

*****
* panel 9
*X1 Y1 Z1 CORD1 AINC1
424.70 165.25 87.65 93.21 -3.99
*X2 Y2 Z2 CORD2 AINC2
459.44 194.42 89.75 64.91 -3.99
*ISPNDIV ICHRDIV SPC IARFYL NAP IVTXFLG
2 8 -1. 2 23 0
* SECTION CAMBER DEFN - X LOCATIONS (%)
0.0000 1.0000 2.5000 5.0000 10.0000 15.0000 20.0000 25.0000
30.0000 35.0000 40.0000 45.0000 50.0000 55.0000 60.0000 65.0000
70.0000 75.0000 80.0000 85.0000 90.0000 95.0000 100.0000

* panel 165.3
* SECTION CAMBER DEFN - Z LOCATIONS (%)
0.0000 0.1681 0.4008 0.7379 1.2182 1.4322 1.4504 1.3645
1.2588 1.1734 1.0914 1.0044 0.9161 0.8299 0.7432 0.6539
0.5625 0.4688 0.3754 0.2820 0.1886 0.0953 0.0000

* panel 194.4
* SECTION CAMBER DEFN - Z LOCATIONS (%)
0.0000 0.1679 0.3998 0.7341 1.2015 1.3967 1.3992 1.3061
1.2042 1.1218 1.0391 0.9515 0.8644 0.7785 0.6983 0.6202
0.5386 0.4549 0.3686 0.2798 0.1886 0.0950 0.0000

```

Table C-5 HASC Input File hasc.inp for the F-16 Configuration

```

F-16A MODEL for HASC95
*LAX      LAY      HAG      RUN      NPAN      NSURF      ALXP
0         1         0.       0.       53        8          8.0
*REY      NMACH    MACH(s)
3144444. 1         0.6
*NALPHA   ALPHA(s)
14 -4.  -2.  0.0  2.  4.  8.  10.  12.
17. 20. 22. 25. 27. 30.
*NBETST   BTSTB(s)
1         5.
*PITCHQ   ROLLQ    YAWQ     VINQ
0.        0.        0.        1.
*SREF     CBAR     XREF     ZREF     WSPAN
43200.    135.84   320.65   91.0    360.0
*****
*SURFACE 1
FOREBODY
*ISRTYP   LNAPAN   ISYMFLG   ENETAR   FTAIL    ALZL      XGAP
3         7         0         0.0     0.0     0.0     0.0
* panel 1, right hand outer
*X1       Y1         Z1         CORD1    AINC1
94.7     -22.05    91.00     0.1     -4.16
*X2       Y2         Z2         CORD2    AINC2
41.6     -16.2     91.00     53.2    -4.16
*ISPNDIV  ICHRDIV   SPC        IARFYL   NAP      IVTXFLG
2         4         1.        0        0        0
*****
* panel 2, right hand inner
*X1       Y1         Z1         CORD1    AINC1
41.6     -16.2     91.00     53.2    -4.16
*X2       Y2         Z2         CORD2    AINC2
-5.0     0.0       91.00     99.8    -4.16
*ISPNDIV  ICHRDIV   SPC        IARFYL   NAP      IVTXFLG
3         4         1.        0        0        0
*****
* panel 3, left hand inner
*X1       Y1         Z1         CORD1    AINC1
-5.0     0.0       91.00     99.8    -4.16
*X2       Y2         Z2         CORD2    AINC2
41.6     16.2     91.00     53.2    -4.16
*ISPNDIV  ICHRDIV   SPC        IARFYL   NAP      IVTXFLG
3         4         1.        0        0        0
*****
* panel 4, left hand outer
*X1       Y1         Z1         CORD1    AINC1
41.6     16.2     91.00     53.2    -4.16
*X2       Y2         Z2         CORD2    AINC2
94.7     22.05    91.00     0.1     -4.16
*ISPNDIV  ICHRDIV   SPC        IARFYL   NAP      IVTXFLG
2         4         1.        0        0        0
*****
* panel 5, lower forebody
*X1       Y1         Z1         CORD1    AINC1
8.37     0.00     78.60     86.43   0.0

```



```

*X2      Y2      Z2      CORD2      AINC2
-5.00   0.00   82.92   99.80   0.0
*ISPNDIV ICHRDIV  SPC      IARFYL   NAP      IVTXFLG
2        4        1.        0        0        0

```

\*\*\*\*\*

\* panel 6, mid forebody

```

*X1      Y1      Z1      CORD1      AINC1
-5.00   0.00   82.92   99.80   0.0
*X2      Y2      Z2      CORD2      AINC2
57.91   0.00   103.43  36.89   0.0
*ISPNDIV ICHRDIV  SPC      IARFYL   NAP      IVTXFLG
3        4        1.        0        0        0

```

\*\*\*\*\*

\* panel 7, upper forebody

```

*X1      Y1      Z1      CORD1      AINC1
57.91   0.00   103.43  36.89   0.0
*X2      Y2      Z2      CORD2      AINC2
94.78   0.00   113.29  0.02    0.0
*ISPNDIV ICHRDIV  SPC      IARFYL   NAP      IVTXFLG
2        4        1.        0        0        0

```

\*\*\*\*\*

\* SURFACE 3

```

FUSELAGE
*ISRTYP  LNPAN    ISYMFLG  ENETAR    FTAIL     ALZL     XGAP
5         10      0         0.0       0.0       0.0     0.0

```

\* panel 1, outer

```

*X1      Y1      Z1      CORD1      AINC1
408.93  -42.0   91.00   131.13    0.0
*X2      Y2      Z2      CORD2      AINC2
408.93  -36.0   91.00   131.13    0.0
*ISPNDIV ICHRDIV  SPC      IARFYL   NAP      IVTXFLG
4        4        0.        0        0        0

```

\*\*\*\*\*

\* panel 2, mid

```

*X1      Y1      Z1      CORD1      AINC1
408.93  -36.0   91.00   131.13    0.0
*X2      Y2      Z2      CORD2      AINC2
408.93  -27.0   91.00   131.13    0.0
*ISPNDIV ICHRDIV  SPC      IARFYL   NAP      IVTXFLG
3        4        0.        0        0        0

```

\*\*\*\*\*

\* panel 3, inner

```

*X1      Y1      Z1      CORD1      AINC1
408.93  -27.0   91.00   70.7      0.0
*X2      Y2      Z2      CORD2      AINC2
408.93  -22.05  91.00   142.97   0.0
*ISPNDIV ICHRDIV  SPC      IARFYL   NAP      IVTXFLG
3        4        0.        0        0        0

```

\*\*\*\*\*

\* panel 4, outer forward fuselage

```

*X1      Y1      Z1      CORD1      AINC1
94.8    -22.05  91.00   457.1     0.0
*X2      Y2      Z2      CORD2      AINC2
94.8    -16.2   91.00   457.1     0.0
*ISPNDIV ICHRDIV  SPC      IARFYL   NAP      IVTXFLG
2        6        0.        0        0        0

```

\*\*\*\*\*

```

* panel 5, inner fuselage
*X1      Y1      Z1      CORD1      AINC1
94.8    -16.2    91.00    457.1      0.0
*X2      Y2      Z2      CORD2      AINC2
94.8     0.0     91.00    457.1      0.0
*ISPNDIV ICHRDIV  SPC      IARFYL     NAP        IVTXFLG
3        6        0.        0          0          0
*****
* panel 6, inner fuselage
*X1      Y1      Z1      CORD1      AINC1
94.8     0.0     91.00    457.1      0.0
*X2      Y2      Z2      CORD2      AINC2
94.8    16.2     91.00    457.1      0.0
*ISPNDIV ICHRDIV  SPC      IARFYL     NAP        IVTXFLG
3        6        0.        0          0          0
*****
* panel 7, outer forward fuselage
*X1      Y1      Z1      CORD1      AINC1
94.8    16.2     91.00    457.1      0.0
*X2      Y2      Z2      CORD2      AINC2
94.8    22.05    91.00    457.1      0.0
*ISPNDIV ICHRDIV  SPC      IARFYL     NAP        IVTXFLG
2        6        0.        0          0          0
*****
* panel 8, inner
*X1      Y1      Z1      CORD1      AINC1
408.93  22.05    91.00    142.97     0.0
*X2      Y2      Z2      CORD2      AINC2
408.93  27.0     91.00    70.7       0.0
*ISPNDIV ICHRDIV  SPC      IARFYL     NAP        IVTXFLG
3        4        0.        0          0          0
*****
* panel 9, inner
*X1      Y1      Z1      CORD1      AINC1
408.93  27.0     91.00    131.13     0.0
*X2      Y2      Z2      CORD2      AINC2
408.93  36.0     91.00    131.13     0.0
*ISPNDIV ICHRDIV  SPC      IARFYL     NAP        IVTXFLG
3        4        0.        0          0          0
*****
* panel 10, outer
*X1      Y1      Z1      CORD1      AINC1
408.93  36.0     91.00    131.13     0.0
*X2      Y2      Z2      CORD2      AINC2
408.93  42.0     91.00    131.13     0.0
*ISPNDIV ICHRDIV  SPC      IARFYL     NAP        IVTXFLG
4        4        0.        0          0          0
*****
*****
* SURFACE 5
LEFT HAND WING
*ISRTYP  LNPAN   ISYMFLG  ENETAR    FTAIL     ALZL     XGAP
2        9        0        0.0       0.0       2.0     0.0
* panel 1, outer wing
*X1      Y1      Z1      CORD1      AINC1
364.39  -180.0    91.0     44.54     -2.99
*X2      Y2      Z2      CORD2      AINC2
340.95  -151.97   91.0     67.98     -1.53

```

```

*ISPNDIV  ICHRDIV  SPC      IARFYL  NAP      IVTXFLG
3          8        1.       2        23       0
* panel 1, BL -180., -152
* SECTION CAMBER DEFN - X LOCATIONS (%)
  0.0000   1.0000   2.5000   5.0000   10.0000   15.0000   20.0000   25.0000
 30.0000  35.0000  40.0000  45.0000  50.0000  55.0000  60.0000  65.0000
 70.0000  75.0000  80.0000  85.0000  90.0000  95.0000 100.0000
* BL -179.9
* SECTION CAMBER DEFN - Z LOCATIONS (%)
  0.0000   0.1001   0.2096   0.3568   0.5937   0.7699   0.9244   1.0484
 1.1424   1.2176   1.2765   1.3150   1.3305   1.3245   1.3033   1.2573
 1.1842   1.0833   0.9341   0.7240   0.4897   0.2464   0.0000
* BL -152.0
* SECTION CAMBER DEFN - Z LOCATIONS (%)
  0.0000   0.0871   0.1827   0.3171   0.5392   0.7185   0.8701   0.9967
 1.0984   1.1811   1.2498   1.2981   1.3225   1.3233   1.3069   1.2640
 1.1926   1.0919   0.9433   0.7309   0.4959   0.2494   0.0000
*****
* panel 2, inner wing
*X1      Y1      Z1      CORD1   AINC1
340.95  -151.97  91.0    67.98   -1.53
*X2      Y2      Z2      CORD2   AINC2
330.91  -140.00  91.0    78.02   -1.17
*ISPNDIV  ICHRDIV  SPC      IARFYL  NAP      IVTXFLG
2          8        1.       2        23       0
* panel 2, BL -152, -140
* SECTION CAMBER DEFN - X LOCATIONS (%)
  0.0000   1.0000   2.5000   5.0000   10.0000   15.0000   20.0000   25.0000
 30.0000  35.0000  40.0000  45.0000  50.0000  55.0000  60.0000  65.0000
 70.0000  75.0000  80.0000  85.0000  90.0000  95.0000 100.0000
* BL -152.0
* SECTION CAMBER DEFN - Z LOCATIONS (%)
  0.0000   0.0871   0.1827   0.3171   0.5392   0.7185   0.8701   0.9967
 1.0984   1.1811   1.2498   1.2981   1.3225   1.3233   1.3069   1.2640
 1.1926   1.0919   0.9433   0.7309   0.4959   0.2494   0.0000
* BL -140
* SECTION CAMBER DEFN - Z LOCATIONS (%)
  0.0000   0.0897   0.1861   0.3203   0.5417   0.7214   0.8733   0.9987
 1.0997   1.1821   1.2504   1.2983   1.3227   1.3233   1.3067   1.2636
 1.1922   1.0912   0.9430   0.7303   0.4957   0.2493   0.0000
*****
* panel 3, outer strake
*X1      Y1      Z1      CORD1   AINC1
330.91  -140.00  91.0    78.02   -1.17
*X2      Y2      Z2      CORD2   AINC2
305.71  -109.97  91.0    103.22  -0.57
*ISPNDIV  ICHRDIV  SPC      IARFYL  NAP      IVTXFLG
3          8        1.       2        23       0
* panel 3, BL -140, -110
* SECTION CAMBER DEFN - X LOCATIONS (%)
  0.0000   1.0000   2.5000   5.0000   10.0000   15.0000   20.0000   25.0000
 30.0000  35.0000  40.0000  45.0000  50.0000  55.0000  60.0000  65.0000
 70.0000  75.0000  80.0000  85.0000  90.0000  95.0000 100.0000
* BL -140
* SECTION CAMBER DEFN - Z LOCATIONS (%)
  0.0000   0.0897   0.1861   0.3203   0.5417   0.7214   0.8733   0.9987
 1.0997   1.1821   1.2504   1.2983   1.3227   1.3233   1.3067   1.2636
 1.1922   1.0912   0.9430   0.7303   0.4957   0.2493   0.0000

```

```

* BL -110
* SECTION CAMBER DEFN - Z LOCATIONS (%)
  0.0000  0.0964  0.1974  0.3356  0.5600  0.7389  0.8921  1.0161
  1.1139  1.1934  1.2584  1.3032  1.3247  1.3234  1.3053  1.2610
  1.1895  1.0877  0.9405  0.7277  0.4941  0.2485  0.0000
*****
* panel 4, outer mid stroke
*X1      Y1      Z1      CORD1      AINC1
305.71  -109.97  91.0    103.22    -0.57
*X2      Y2      Z2      CORD2      AINC2
282.27  -82.04   91.0    126.66    -0.23
*ISPNDIV ICHRDIV  SPC      IARFYL     NAP      IVTXFLG
3        8        1.       2          23       0
* panel 4, BL -110, -82
* SECTION CAMBER DEFN - X LOCATIONS (%)
  0.0000  1.0000  2.5000  5.0000  10.0000  15.0000  20.0000  25.0000
 30.0000 35.0000 40.0000 45.0000 50.0000 55.0000 60.0000 65.0000
 70.0000 75.0000 80.0000 85.0000 90.0000 95.0000 100.0000
* BL -110
* SECTION CAMBER DEFN - Z LOCATIONS (%)
  0.0000  0.0964  0.1974  0.3356  0.5600  0.7389  0.8921  1.0161
  1.1139  1.1934  1.2584  1.3032  1.3247  1.3234  1.3053  1.2610
  1.1895  1.0877  0.9405  0.7277  0.4941  0.2485  0.0000
* BL -82
* SECTION CAMBER DEFN - Z LOCATIONS (%)
  0.0000  0.1012  0.2065  0.3492  0.5781  0.7559  0.9101  1.0340
  1.1293  1.2060  1.2673  1.3087  1.3270  1.3234  1.3038  1.2584
  1.1866  1.0845  0.9381  0.7252  0.4926  0.2477  0.0000
*****
* panel 5, inner mid stroke
*X1      Y1      Z1      CORD1      AINC1
282.27  -82.04   91.0    126.66    -0.23
*X2      Y2      Z2      CORD2      AINC2
258.74  -54.00   91.00   150.19    0.00
*ISPNDIV ICHRDIV  SPC      IARFYL     NAP      IVTXFLG
3        8        1.       2          23       1
* panel 5, BL -82, -54
* SECTION CAMBER DEFN - X LOCATIONS (%)
  0.0000  1.0000  2.5000  5.0000  10.0000  15.0000  20.0000  25.0000
 30.0000 35.0000 40.0000 45.0000 50.0000 55.0000 60.0000 65.0000
 70.0000 75.0000 80.0000 85.0000 90.0000 95.0000 100.0000
* BL -82
* SECTION CAMBER DEFN - Z LOCATIONS (%)
  0.0000  0.1012  0.2065  0.3492  0.5781  0.7559  0.9101  1.0340
  1.1293  1.2060  1.2673  1.3087  1.3270  1.3234  1.3038  1.2584
  1.1866  1.0845  0.9381  0.7252  0.4926  0.2477  0.0000
* BL -54
* SECTION CAMBER DEFN - Z LOCATIONS (%)
  0.0000  0.1048  0.2136  0.3603  0.5934  0.7704  0.9255  1.0493
  1.1432  1.2177  1.2756  1.3137  1.3290  1.3237  1.3024  1.2560
  1.1840  1.0817  0.9360  0.7232  0.4913  0.2462  0.0000
*****
* panel 6, inner stroke-shelf
*X1      Y1      Z1      CORD1      AINC1
258.74  -54.00   91.00   150.19    0.00
*X2      Y2      Z2      CORD2      AINC2
206.85  -42.00   91.00   202.08    0.05
*ISPNDIV ICHRDIV  SPC      IARFYL     NAP      IVTXFLG

```

```

2          8          1.          2          23          0
* panel 6, BL -54, -42.0
* SECTION CAMBER DEFN - X LOCATIONS (%)
  0.0000    1.0000    2.5000    5.0000    10.0000    15.0000    20.0000    25.0000
 30.0000    35.0000    40.0000    45.0000    50.0000    55.0000    60.0000    65.0000
 70.0000    75.0000    80.0000    85.0000    90.0000    95.0000    100.0000
* BL -54
* SECTION CAMBER DEFN - Z LOCATIONS (%)
  0.0000    0.1048    0.2136    0.3603    0.5934    0.7704    0.9255    1.0493
  1.1432    1.2177    1.2756    1.3137    1.3290    1.3237    1.3024    1.2560
  1.1840    1.0817    0.9360    0.7232    0.4913    0.2462    0.0000
* BL -42.0
* SECTION CAMBER DEFN - Z LOCATIONS (%)
  0.0000    0.0433    0.1040    0.1958    0.3486    0.4674    0.5584    0.6255
  0.6871    0.7824    0.8584    0.9140    0.9645    1.0109    1.0492    1.0772
  1.0778    1.0282    0.9202    0.7440    0.5071    0.2690    0.0309
*****
* panel 7, inner strake-shelf
*X1      Y1      Z1      CORD1      AINC1
206.85  -42.00   91.00   202.08    0.05
*X2      Y2      Z2      CORD2      AINC2
182.56  -36.00   91.00   226.37    0.04
*ISPNDIV ICHRDIV  SPC      IARFYL    NAP      IVTXFLG
4        8        1.        2        23        0
* panel 8, BL -42, -36
* SECTION CAMBER DEFN - X LOCATIONS (%)
  0.0000    1.0000    2.5000    5.0000    10.0000    15.0000    20.0000    25.0000
 30.0000    35.0000    40.0000    45.0000    50.0000    55.0000    60.0000    65.0000
 70.0000    75.0000    80.0000    85.0000    90.0000    95.0000    100.0000
* BL -42.0
* SECTION CAMBER DEFN - Z LOCATIONS (%)
  0.0000    0.0433    0.1040    0.1958    0.3486    0.4674    0.5584    0.6255
  0.6871    0.7824    0.8584    0.9140    0.9645    1.0109    1.0492    1.0772
  1.0778    1.0282    0.9202    0.7440    0.5071    0.2690    0.0309
* BL -36
* SECTION CAMBER DEFN - Z LOCATIONS (%)
  0.0000    0.0358    0.0952    0.2014    0.4051    0.5703    0.7025    0.8003
  0.8718    0.8966    0.9104    0.9284    0.9450    0.9570    0.9619    0.9572
  0.9396    0.9040    0.8404    0.7244    0.5053    0.2665    0.0276
*****
* panel 8, outer
*X1      Y1      Z1      CORD1      AINC1
182.56  -36.00   91.00   226.37    0.04
*X2      Y2      Z2      CORD2      AINC2
119.35  -27.00   91.00   289.58   -.14
*ISPNDIV ICHRDIV  SPC      IARFYL    NAP      IVTXFLG
3        8        1.        2        23        0
* panel 9, BL -36, -27
* SECTION CAMBER DEFN - X LOCATIONS (%)
  0.0000    1.0000    2.5000    5.0000    10.0000    15.0000    20.0000    25.0000
 30.0000    35.0000    40.0000    45.0000    50.0000    55.0000    60.0000    65.0000
 70.0000    75.0000    80.0000    85.0000    90.0000    95.0000    100.0000
* BL -36
* SECTION CAMBER DEFN - Z LOCATIONS (%)
  0.0000    0.0358    0.0952    0.2014    0.4051    0.5703    0.7025    0.8003
  0.8718    0.8966    0.9104    0.9284    0.9450    0.9570    0.9619    0.9572
  0.9396    0.9040    0.8404    0.7244    0.5053    0.2665    0.0276
* BL -27

```

```

* SECTION CAMBER DEFN - Z LOCATIONS (%)
0.0000 0.0268 0.0728 0.1669 0.4340 0.8054 1.1942 1.5029
1.6871 1.7648 1.7628 1.7364 1.7163 1.6545 1.5601 1.4415
1.3024 1.1442 0.9660 0.7648 0.5321 0.2768 0.0216

```

\*\*\*\*\*

\* panel 9, inner strake-shelf

```

*X1      Y1      Z1      CORD1      AINC1
119.35  -27.00   91.00   289.58    -.14
*X2      Y2      Z2      CORD2      AINC2
94.80   -22.05   91.00   314.13    -.20
*ISPNDIV ICHRDIV  SPC      IARFYL     NAP        IVTXFLG
3        8        1.       2          23         1

```

\* panel 10, BL -27, -22

```

* SECTION CAMBER DEFN - X LOCATIONS (%)
0.0000 1.0000 2.5000 5.0000 10.0000 15.0000 20.0000 25.0000
30.0000 35.0000 40.0000 45.0000 50.0000 55.0000 60.0000 65.0000
70.0000 75.0000 80.0000 85.0000 90.0000 95.0000 100.0000

```

\* BL -27

```

* SECTION CAMBER DEFN - Z LOCATIONS (%)
0.0000 0.0268 0.0728 0.1669 0.4340 0.8054 1.1942 1.5029
1.6871 1.7648 1.7628 1.7364 1.7163 1.6545 1.5601 1.4415
1.3024 1.1442 0.9660 0.7648 0.5321 0.2768 0.0216

```

\* BL -22

```

* SECTION CAMBER DEFN - Z LOCATIONS (%)
0.0000 0.2365 0.4119 0.6417 1.0364 1.4395 1.8276 2.1858
2.4502 2.5927 2.5735 2.4723 2.3602 2.2470 2.0760 1.8664
1.6305 1.3740 1.1005 0.8135 0.5246 0.2615 0.0000

```

\*\*\*\*\*

\*\*\*\*\*

\* SURFACE 6

RIGHT HAND WING

```

*ISRTYP  LNPNAN  ISYMFLG  ENETAR  FTAIL  ALZL  XGAP
2        9        0        0.0     0.0    2.0   0.0

```

\* panel 1, inner strake-shelf

```

*X1      Y1      Z1      CORD1      AINC1
94.80   22.05   91.00   314.13    -.20
*X2      Y2      Z2      CORD2      AINC2
119.35  27.00   91.00   289.58    -.14
*ISPNDIV ICHRDIV  SPC      IARFYL     NAP        IVTXFLG
3        8        1.       2          23         1

```

\* panel 1, BL 22, 27

```

* SECTION CAMBER DEFN - X LOCATIONS (%)
0.0000 1.0000 2.5000 5.0000 10.0000 15.0000 20.0000 25.0000
30.0000 35.0000 40.0000 45.0000 50.0000 55.0000 60.0000 65.0000
70.0000 75.0000 80.0000 85.0000 90.0000 95.0000 100.0000

```

\* BL 22

```

* SECTION CAMBER DEFN - Z LOCATIONS (%)
0.0000 0.2365 0.4119 0.6417 1.0364 1.4395 1.8276 2.1858
2.4502 2.5927 2.5735 2.4723 2.3602 2.2470 2.0760 1.8664
1.6305 1.3740 1.1005 0.8135 0.5246 0.2615 0.0000

```

\* BL 27

```

* SECTION CAMBER DEFN - Z LOCATIONS (%)
0.0000 0.0268 0.0728 0.1669 0.4340 0.8054 1.1942 1.5029
1.6871 1.7648 1.7628 1.7364 1.7163 1.6545 1.5601 1.4415
1.3024 1.1442 0.9660 0.7648 0.5321 0.2768 0.0216

```

\*\*\*\*\*

\* panel 2, inner mid strake

```

*X1      Y1      Z1      CORD1      AINC1

```

```

119.35    27.00    91.00    289.58    -.14
*X2       Y2       Z2       CORD2     AINC2
182.56    36.00    91.00    226.37    .04
*ISPNDIV  ICHRDIV  SPC      IARFYL    NAP      IVTXFLG
3         8         1.       2         23      0
* panel 2, BL 27, 36
* SECTION CAMBER DEFN - X LOCATIONS (%)
  0.0000    1.0000    2.5000    5.0000    10.0000    15.0000    20.0000    25.0000
 30.0000    35.0000    40.0000    45.0000    50.0000    55.0000    60.0000    65.0000
 70.0000    75.0000    80.0000    85.0000    90.0000    95.0000   100.0000
* BL 27
* SECTION CAMBER DEFN - Z LOCATIONS (%)
  0.0000    0.0268    0.0728    0.1669    0.4340    0.8054    1.1942    1.5029
 1.6871    1.7648    1.7628    1.7364    1.7163    1.6545    1.5601    1.4415
 1.3024    1.1442    0.9660    0.7648    0.5321    0.2768    0.0216
* BL 36
* SECTION CAMBER DEFN - Z LOCATIONS (%)
  0.0000    0.0358    0.0952    0.2014    0.4051    0.5703    0.7025    0.8003
 0.8718    0.8966    0.9104    0.9284    0.9450    0.9570    0.9619    0.9572
 0.9396    0.9040    0.8404    0.7244    0.5053    0.2665    0.0276
*****
* panel 3, outer mid stroke
*X1       Y1       Z1       CORD1     AINC1
182.56    36.00    91.00    226.37    .04
*X2       Y2       Z2       CORD2     AINC2
206.85    42.00    91.00    202.08    .05
*ISPNDIV  ICHRDIV  SPC      IARFYL    NAP      IVTXFLG
4         8         1.       2         23      0
* panel 3, BL 36, 42
* SECTION CAMBER DEFN - X LOCATIONS (%)
  0.0000    1.0000    2.5000    5.0000    10.0000    15.0000    20.0000    25.0000
 30.0000    35.0000    40.0000    45.0000    50.0000    55.0000    60.0000    65.0000
 70.0000    75.0000    80.0000    85.0000    90.0000    95.0000   100.0000
* BL 36
* SECTION CAMBER DEFN - Z LOCATIONS (%)
  0.0000    0.0358    0.0952    0.2014    0.4051    0.5703    0.7025    0.8003
 0.8718    0.8966    0.9104    0.9284    0.9450    0.9570    0.9619    0.9572
 0.9396    0.9040    0.8404    0.7244    0.5053    0.2665    0.0276
* BL 42.0
* SECTION CAMBER DEFN - Z LOCATIONS (%)
  0.0000    0.0433    0.1040    0.1958    0.3486    0.4674    0.5584    0.6255
 0.6871    0.7824    0.8584    0.9140    0.9645    1.0109    1.0492    1.0772
 1.0778    1.0282    0.9202    0.7440    0.5071    0.2690    0.0309
*****
* panel 4, outer stroke
*X1       Y1       Z1       CORD1     AINC1
206.85    42.00    91.00    202.08    .05
*X2       Y2       Z2       CORD2     AINC2
258.74    54.0     91.00    150.19    .000
*ISPNDIV  ICHRDIV  SPC      IARFYL    NAP      IVTXFLG
2         8         1.       2         23      0
* panel 4, BL 42, 52.5
* SECTION CAMBER DEFN - X LOCATIONS (%)
  0.0000    1.0000    2.5000    5.0000    10.0000    15.0000    20.0000    25.0000
 30.0000    35.0000    40.0000    45.0000    50.0000    55.0000    60.0000    65.0000
 70.0000    75.0000    80.0000    85.0000    90.0000    95.0000   100.0000
* BL 42.0
* SECTION CAMBER DEFN - Z LOCATIONS (%)

```

0.0000	0.0433	0.1040	0.1958	0.3486	0.4674	0.5584	0.6255
0.6871	0.7824	0.8584	0.9140	0.9645	1.0109	1.0492	1.0772
1.0778	1.0282	0.9202	0.7440	0.5071	0.2690	0.0309	
* BL 54							
* SECTION CAMBER DEFN - Z LOCATIONS (%)							
0.0000	0.1048	0.2136	0.3603	0.5934	0.7704	0.9255	1.0493
1.1432	1.2177	1.2756	1.3137	1.3290	1.3237	1.3024	1.2560
1.1840	1.0817	0.9360	0.7232	0.4913	0.2462	0.0000	
*****							
* panel 5, outer wing							
*X1	Y1	Z1	CORD1	AINC1			
258.74	54.0	91.00	150.19	.000			
*X2	Y2	Z2	CORD2	AINC2			
282.27	82.04	91.00	126.66	-.23			
*ISPNDIV	ICHRDIV	SPC	IARFYL	NAP	IVTXFLG		
3	8	1.	2	23	1		
* panel 6, BL 54, 82							
* SECTION CAMBER DEFN - X LOCATIONS (%)							
0.0000	1.0000	2.5000	5.0000	10.0000	15.0000	20.0000	25.0000
30.0000	35.0000	40.0000	45.0000	50.0000	55.0000	60.0000	65.0000
70.0000	75.0000	80.0000	85.0000	90.0000	95.0000	100.0000	
* BL 54							
* SECTION CAMBER DEFN - Z LOCATIONS (%)							
0.0000	0.1048	0.2136	0.3603	0.5934	0.7704	0.9255	1.0493
1.1432	1.2177	1.2756	1.3137	1.3290	1.3237	1.3024	1.2560
1.1840	1.0817	0.9360	0.7232	0.4913	0.2462	0.0000	
* BL 82.							
* SECTION CAMBER DEFN - Z LOCATIONS (%)							
0.0000	0.1012	0.2065	0.3492	0.5781	0.7559	0.9101	1.0340
1.1293	1.2060	1.2673	1.3087	1.3270	1.3234	1.3038	1.2584
1.1866	1.0845	0.9381	0.7252	0.4926	0.2477	0.0000	
*****							
* panel 6, outer wing							
*X1	Y1	Z1	CORD1	AINC1			
282.27	82.04	91.00	126.66	-.23			
*X2	Y2	Z2	CORD2	AINC2			
305.71	109.97	91.00	103.22	-.57			
*ISPNDIV	ICHRDIV	SPC	IARFYL	NAP	IVTXFLG		
3	8	1.	2	23	0		
* panel 7, BL 82, 110							
* SECTION CAMBER DEFN - X LOCATIONS (%)							
0.0000	1.0000	2.5000	5.0000	10.0000	15.0000	20.0000	25.0000
30.0000	35.0000	40.0000	45.0000	50.0000	55.0000	60.0000	65.0000
70.0000	75.0000	80.0000	85.0000	90.0000	95.0000	100.0000	
* BL 82							
* SECTION CAMBER DEFN - Z LOCATIONS (%)							
0.0000	0.1012	0.2065	0.3492	0.5781	0.7559	0.9101	1.0340
1.1293	1.2060	1.2673	1.3087	1.3270	1.3234	1.3038	1.2584
1.1866	1.0845	0.9381	0.7252	0.4926	0.2477	0.0000	
* BL 110							
* SECTION CAMBER DEFN - Z LOCATIONS (%)							
0.0000	0.0964	0.1974	0.3356	0.5600	0.7389	0.8921	1.0161
1.1139	1.1934	1.2584	1.3032	1.3247	1.3234	1.3053	1.2610
1.1895	1.0877	0.9405	0.7277	0.4941	0.2485	0.0000	
*****							
* panel 7, outer wing							
*X1	Y1	Z1	CORD1	AINC1			
305.71	109.97	91.00	103.22	-.57			



```

*X2      Y2      Z2      CORD2     AINC2
330.91  140.00   91.00   78.02    -1.17
*ISPNDIV ICHRDIV  SPC      IARFYL    NAP      IVTXFLG
3        8        1.       2        23       0
* panel 8, BL 110, 140
* SECTION CAMBER DEFN - X LOCATIONS (%)
  0.0000   1.0000   2.5000   5.0000   10.0000   15.0000   20.0000   25.0000
 30.0000  35.0000  40.0000  45.0000  50.0000  55.0000  60.0000  65.0000
 70.0000  75.0000  80.0000  85.0000  90.0000  95.0000 100.0000
* BL 110
* SECTION CAMBER DEFN - Z LOCATIONS (%)
  0.0000   0.0964   0.1974   0.3356   0.5600   0.7389   0.8921   1.0161
 1.1139   1.1934   1.2584   1.3032   1.3247   1.3234   1.3053   1.2610
 1.1895   1.0877   0.9405   0.7277   0.4941   0.2485   0.0000
* BL 140
* SECTION CAMBER DEFN - Z LOCATIONS (%)
  0.0000   0.0897   0.1861   0.3203   0.5417   0.7214   0.8733   0.9987
 1.0997   1.1821   1.2504   1.2983   1.3227   1.3233   1.3067   1.2636
 1.1922   1.0912   0.9430   0.7303   0.4957   0.2493   0.0000
*****
* panel 8, outer wing
*X1      Y1      Z1      CORD1     AINC1
330.91  140.00   91.00   78.02    -1.17
*X2      Y2      Z2      CORD2     AINC2
340.95  151.97   91.00   67.98    -1.53
*ISPNDIV ICHRDIV  SPC      IARFYL    NAP      IVTXFLG
2        8        1.       2        23       0
* panel 9, BL 140, 152
* SECTION CAMBER DEFN - X LOCATIONS (%)
  0.0000   1.0000   2.5000   5.0000   10.0000   15.0000   20.0000   25.0000
 30.0000  35.0000  40.0000  45.0000  50.0000  55.0000  60.0000  65.0000
 70.0000  75.0000  80.0000  85.0000  90.0000  95.0000 100.0000
* BL 140
* SECTION CAMBER DEFN - Z LOCATIONS (%)
  0.0000   0.0897   0.1861   0.3203   0.5417   0.7214   0.8733   0.9987
 1.0997   1.1821   1.2504   1.2983   1.3227   1.3233   1.3067   1.2636
 1.1922   1.0912   0.9430   0.7303   0.4957   0.2493   0.0000
* BL 152.0
* SECTION CAMBER DEFN - Z LOCATIONS (%)
  0.0000   0.0871   0.1827   0.3171   0.5392   0.7185   0.8701   0.9967
 1.0984   1.1811   1.2498   1.2981   1.3225   1.3233   1.3069   1.2640
 1.1926   1.0919   0.9433   0.7309   0.4959   0.2494   0.0000
*****
* panel 9, outer wing
*X1      Y1      Z1      CORD1     AINC1
340.95  151.97   91.00   67.98    -1.53
*X2      Y2      Z2      CORD2     AINC2
364.39  180.00   91.00   44.54    -2.99
*ISPNDIV ICHRDIV  SPC      IARFYL    NAP      IVTXFLG
3        8        1.       2        23       0
* panel 10, BL 152, 180
* SECTION CAMBER DEFN - X LOCATIONS (%)
  0.0000   1.0000   2.5000   5.0000   10.0000   15.0000   20.0000   25.0000
 30.0000  35.0000  40.0000  45.0000  50.0000  55.0000  60.0000  65.0000
 70.0000  75.0000  80.0000  85.0000  90.0000  95.0000 100.0000
* BL 152.0
* SECTION CAMBER DEFN - Z LOCATIONS (%)
  0.0000   0.0871   0.1827   0.3171   0.5392   0.7185   0.8701   0.9967

```

```

1.0984    1.1811    1.2498    1.2981    1.3225    1.3233    1.3069    1.2640
1.1926    1.0919    0.9433    0.7309    0.4959    0.2494    0.0000
* BL 179.9
* SECTION CAMBER DEFN - Z LOCATIONS (%)
0.0000    0.1001    0.2096    0.3568    0.5937    0.7699    0.9244    1.0484
1.1424    1.2176    1.2765    1.3150    1.3305    1.3245    1.3033    1.2573
1.1842    1.0833    0.9341    0.7240    0.4897    0.2464    0.0000
*****
* SURFACE 7
LEFT HAND HORIZONTAL TAIL
*ISRTYP  LNPAN    ISYMFLG  ENETAR    FTAIL    ALZL    XGAP
1         3         0         0.0       1.391    2.0     0.0
* panel 1, outerboard
*X1       Y1         Z1         CORD1     AINC1
511.83   -109.97   71.59     37.39     0.0
*X2       Y2         Z2         CORD2     AINC2
487.95   -82.04   79.53     61.27     0.0
*ISPNDIV  ICHRDIV   SPC        IARFYL    NAP       IVTXFLG
3         6         1.         0         0         0
*****
* panel 2, outerboard
*X1       Y1         Z1         CORD1     AINC1
487.95   -82.04   79.53     61.27     0.0
*X2       Y2         Z2         CORD2     AINC2
464.06   -54.0    87.46     85.16     0.0
*ISPNDIV  ICHRDIV   SPC        IARFYL    NAP       IVTXFLG
4         6         1.         0         0         0
*****
* panel 3, mid-section
*X1       Y1         Z1         CORD1     AINC1
464.06   -54.0    87.46     85.16     0.0
*X2       Y2         Z2         CORD2     AINC2
453.41   -42.0    89.67     95.81     0.0
*ISPNDIV  ICHRDIV   SPC        IARFYL    NAP       IVTXFLG
2         6         1.         0         0         1
*****
* SURFACE 8
RIGHT HAND HORIZONTAL TAIL
*ISRTYP  LNPAN    ISYMFLG  ENETAR    FTAIL    ALZL    XGAP
1         3         0         0.0       1.391    2.0     0.0
* panel 1, inboard
*X1       Y1         Z1         CORD1     AINC1
453.41   42.0     89.67     95.81     0.0
*X2       Y2         Z2         CORD2     AINC2
464.06   54.0     87.46     85.16     0.0
*ISPNDIV  ICHRDIV   SPC        IARFYL    NAP       IVTXFLG
2         6         1.         0         0         1
*****
* panel 3, outboard
*X1       Y1         Z1         CORD1     AINC1
464.06   54.0     87.46     85.16     0.0
*X2       Y2         Z2         CORD2     AINC2
487.95   82.04   79.53     61.27     0.0
*ISPNDIV  ICHRDIV   SPC        IARFYL    NAP       IVTXFLG
4         6         1.         0         0         0
*****

```

\* panel 3, outboard

*X1	Y1	Z1	CORD1	AINC1		
487.95	82.04	79.53	61.27	0.0		
*X2	Y2	Z2	CORD2	AINC2		
511.83	109.97	71.59	37.39	0.0		
*ISPNDIV	ICHRDIV	SPC	IARFYL	NAP	IVTXFLG	
3	6	1.	0	0	0	

\*\*\*\*\*  
\*\*\*\*\*

\* SIDEVIEW

FUSELAGE SIDE VIEW

*SRTYP	LNPAN	ISYMFLG	ENETAR	FTAIL	ALZL	XGAP
5	7	0	0.0	0.0	0.0	0.0

\* panel 1

*X1	Y1	Z1	CORD1	AINC1		
160.00	0.00	56.72	286.57	0.0		
*X2	Y2	Z2	CORD2	AINC2		
94.80	0.0	78.60	456.62	0.0		
*ISPNDIV	ICHRDIV	SPC	IARFYL	NAP	IVTXFLG	
3	6	0.	0	0	0	

\*\*\*\*\*

\* panel 2

*X1	Y1	Z1	CORD1	AINC1		
94.80	0.0	78.60	456.62	0.0		
*X2	Y2	Z2	CORD2	AINC2		
94.80	0.0	82.92	456.62	0.0		
*ISPNDIV	ICHRDIV	SPC	IARFYL	NAP	IVTXFLG	
2	7	0.	0	0	0	

\*\*\*\*\*

\* panel 3

*X1	Y1	Z1	CORD1	AINC1		
94.80	0.0	82.92	456.62	0.0		
*X2	Y2	Z2	CORD2	AINC2		
94.80	0.0	103.43	456.62	0.0		
*ISPNDIV	ICHRDIV	SPC	IARFYL	NAP	IVTXFLG	
3	7	0.	0	0	0	

\*\*\*\*\*

\* panel 5

*X1	Y1	Z1	CORD1	AINC1		
94.80	0.0	103.43	456.62	0.0		
*X2	Y2	Z2	CORD2	AINC2		
94.80	0.0	113.29	432.15	0.0		
*ISPNDIV	ICHRDIV	SPC	IARFYL	NAP	IVTXFLG	
2	7	0.	0	0	0	

\*\*\*\*\*

\* panel 6

*X1	Y1	Z1	CORD1	AINC1		
94.80	0.0	113.29	432.15	0.0		
*X2	Y2	Z2	CORD2	AINC2		
100.83	0.0	118.00	426.12	0.0		
*ISPNDIV	ICHRDIV	SPC	IARFYL	NAP	IVTXFLG	
2	7	0.	0	0	0	

\*\*\*\*\*

\* panel 7, canopy

*X1	Y1	Z1	CORD1	AINC1		
100.83	0.0	118.00	177.52	0.0		
*X2	Y2	Z2	CORD2	AINC2		
119.99	0.0	128.73	88.22	0.0		

```

*ISPNDIV  ICHRDIV  SPC      IARFYL  NAP      IVTXFLG
2          5        0.        0        0        0
*****
* panel 8, canopy
*X1        Y1        Z1        CORD1   AINC1
119.99    0.0        128.73   88.22   0.0
*X2        Y2        Z2        CORD2   AINC2
143.06    0.0        135.50   24.63   0.0
*ISPNDIV  ICHRDIV  SPC      IARFYL  NAP      IVTXFLG
2          5        0.        0        0        0
*****
* SURFACE 13
* SIDEVIEW
VERTICAL TAIL AND DORSAL
*SRTYP    LNPAN    ISYMFLG  ENETAR   FTAIL    ALZL     XGAP
5          5        0        0.0     0.0     0.0     0.0
* dorsal segment
*X1        Y1        Z1        CORD1   AINC1
344.29    0.0        118.0    182.66  0.0
*X2        Y2        Z2        CORD2   AINC2
392.25    0.0        128.73   134.70  0.0
*ISPNDIV  ICHRDIV  SPC      IARFYL  NAP      IVTXFLG
2          7        1.        0        0        0
*****
* dorsal segment
*X1        Y1        Z1        CORD1   AINC1
392.25    0.0        128.73   134.70  0.0
*X2        Y2        Z2        CORD2   AINC2
429.95    0.0        135.50   97.00   -24.6
*ISPNDIV  ICHRDIV  SPC      IARFYL  NAP      IVTXFLG
2          7        1.        0        0        0
*****
* rudder
*X1        Y1        Z1        CORD1   AINC1
497.84    0.0        135.50   29.11   0.0
*X2        Y2        Z2        CORD2   AINC2
548.54    0.0        211.88   15.54   0.0
*ISPNDIV  ICHRDIV  SPC      IARFYL  NAP      IVTXFLG
5          5        0.        0        0        0
*****
* in front of rudder
*X1        Y1        Z1        CORD1   AINC1
429.95    0.0        135.50   67.89   0.0
*X2        Y2        Z2        CORD2   AINC2
513.04    0.0        211.88   35.50   0.0
*ISPNDIV  ICHRDIV  SPC      IARFYL  NAP      IVTXFLG
5          6        1.        0        0        0
*****
* top of tail
*X1        Y1        Z1        CORD1   AINC1
513.04    0.0        211.88   56.77   0.0
*X2        Y2        Z2        CORD2   AINC2
519.26    0.0        217.44   50.55   0.0
*ISPNDIV  ICHRDIV  SPC      IARFYL  NAP      IVTXFLG
2          9        1.        0        0        0

```

Table C-6 HASC Input File vchn.inp for the F-16 Forebody

```

* F-16 Forebody file for HASC95
*   NCIR  NBLSEP  NCHINE      DROOP      DX      E5
      1      1      0  4.16000  8.82000  0.0500
*   TNOSE   ENOSE   RNOSE   FBLNTH      SL      SD
      1.00000  0.70830  0.00000 104.80000 209.60001  44.10000
* NXR
  40
* XR (s)
  0.00000  0.02500  0.05000  0.07500  0.10000  0.12500  0.15000  0.17500
  0.20000  0.22500  0.25000  0.27500  0.30000  0.32500  0.35000  0.37500
  0.40000  0.42500  0.45000  0.47500  0.52500  0.55000  0.57500  0.60000
  0.62500  0.65000  0.67500  0.70000  0.72500  0.75000  0.77500  0.80000
  0.82500  0.85000  0.87500  0.90000  0.92500  0.95000  0.97500  1.00000
* R (s)
  0.00000  0.00912  0.01770  0.02575  0.03328  0.04030  0.04682  0.05286
  0.05841  0.06350  0.06812  0.07229  0.07600  0.07926  0.08208  0.08447
  0.08641  0.08792  0.08900  0.08964  0.08964  0.08900  0.08792  0.08641
  0.08447  0.08208  0.07926  0.07600  0.07229  0.06812  0.06350  0.05841
  0.05286  0.04682  0.04030  0.03328  0.02575  0.01770  0.00912  0.00000
* DR (s)
  0.36496  0.34313  0.32186  0.30110  0.28081  0.26094  0.24144  0.22230
  0.20346  0.18489  0.16658  0.14849  0.13058  0.11284  0.09525  0.07777
  0.06039  0.04308  0.02583  0.00861 -0.00861 -0.02583 -0.04308 -0.06039
 -0.07777 -0.09525 -0.11284 -0.13058 -0.14849 -0.16658 -0.18489 -0.20346
 -0.22230 -0.24144 -0.26094 -0.28081 -0.30110 -0.32186 -0.34313 -0.36496
* AE (s)
  0.00000  0.01068  0.02072  0.03015  0.03896  0.04718  0.05481  0.06188
  0.06839  0.07434  0.07975  0.08463  0.08898  0.09280  0.09610  0.09889
  0.10116  0.10293  0.10419  0.10495  0.10495  0.10419  0.10293  0.10116
  0.09889  0.09610  0.09280  0.08898  0.08463  0.07975  0.07434  0.06839
  0.06188  0.05481  0.04718  0.03896  0.03015  0.02072  0.01068  0.00000
* BE (s)
  0.00000  0.00757  0.01468  0.02135  0.02759  0.03342  0.03883  0.04383
  0.04844  0.05266  0.05649  0.05994  0.06302  0.06573  0.06807  0.07004
  0.07165  0.07291  0.07380  0.07434  0.07434  0.07380  0.07291  0.07165
  0.07004  0.06807  0.06573  0.06302  0.05994  0.05649  0.05266  0.04844
  0.04383  0.03883  0.03342  0.02759  0.02135  0.01468  0.00757  0.00000
* DAE (s)
  0.42728  0.40172  0.37682  0.35252  0.32876  0.30550  0.28267  0.26026
  0.23820  0.21647  0.19502  0.17384  0.15287  0.13211  0.11151  0.09105
  0.07070  0.05044  0.03024  0.01008 -0.01008 -0.03024 -0.05044 -0.07070
 -0.09105 -0.11151 -0.13211 -0.15287 -0.17384 -0.19502 -0.21647 -0.23820
 -0.26026 -0.28267 -0.30550 -0.32876 -0.35252 -0.37682 -0.40172 -0.42728
* DBE (s)
  0.30264  0.28454  0.26690  0.24969  0.23286  0.21638  0.20022  0.18434
  0.16872  0.15332  0.13814  0.12313  0.10828  0.09357  0.07898  0.06449
  0.05007  0.03572  0.02142  0.00714 -0.00714 -0.02142 -0.03572 -0.05007
 -0.06449 -0.07898 -0.09357 -0.10828 -0.12313 -0.13814 -0.15332 -0.16872
 -0.18434 -0.20022 -0.21638 -0.23286 -0.24969 -0.26690 -0.28454 -0.30264
* Ro (s)
  0.00000  0.00912  0.01770  0.02575  0.03328  0.04030  0.04682  0.05286
  0.05841  0.06350  0.06812  0.07229  0.07600  0.07926  0.08208  0.08447
  0.08641  0.08792  0.08900  0.08964  0.08964  0.08900  0.08792  0.08641
  0.08447  0.08208  0.07926  0.07600  0.07229  0.06812  0.06350  0.05841
  0.05286  0.04682  0.04030  0.03328  0.02575  0.01770  0.00912  0.00000

```

\* DRo(s)

0.36496	0.34313	0.32186	0.30110	0.28081	0.26094	0.24144	0.22230
0.20346	0.18489	0.16658	0.14849	0.13058	0.11284	0.09525	0.07777
0.06039	0.04308	0.02583	0.00861	-0.00861	-0.02583	-0.04308	-0.06039
-0.07777	-0.09525	-0.11284	-0.13058	-0.14849	-0.16658	-0.18489	-0.20346
-0.22230	-0.24144	-0.26094	-0.28081	-0.30110	-0.32186	-0.34313	-0.36496

Table C-7 HASC Input File hasc.inp for the Model 200 Configuration

```

CONVAIR MODEL 200 planform only, with canard
*
*LAX      LAY      HAG      IRSTFLG  NPAN      NSURF     ALXP
0         1         0.        0.        18         7         0.0
*REY      NMACH     MACH(s)
2150000. 1         0.20
*NALPHA   ALPHA(s)
19        -6.0       -4.0      -2.0      0.0       2.0       4.0       6.0
8.0       10.0      12.0      14.0      16.0      18.0      20.0      22.0
25.0      30.0      35.0      40.0
*NBETA    BETA(s)
1         0.
*PITCHQ   ROLLQ      YAWQ      V
0.        0.         0.        1.
*SREF     CBAR      XBAR      ZBAR      WSPAN
64800.    228.95    448.8     91.0     377.5
*****
* SURFACE 1
FUSELAGE
*ISRTYP   LNPAN     ISYMFLG   ENETAR    FTAIL     ALZL      XGAP
5         6         0         0.0       0.0       0.0       0.0
* panel 1, left outboard
*X1        Y1         Z1         CORD1     AINC1
234.8     -32.2     91.0      382.4     0.0
*X2        Y2         Z2         CORD2     AINC2
234.8     -23.4     91.0      500.2     0.0
*ISPNDIV  ICHRDIV   SPC        IARFYL    NAP       IVTXFLG
2         8         0.        0         0         0
*****
* panel 2, left mid
*X1        Y1         Z1         CORD1     AINC1
197.7     -23.4     91.0      537.3     0.0
*X2        Y2         Z2         CORD2     AINC2
109.0     -11.7     91.0      626.0     0.0
*ISPNDIV  ICHRDIV   SPC        IARFYL    NAP       IVTXFLG
2         8         0.        0         0         0
*****
* panel 3, left inboard
*X1        Y1         Z1         CORD1     AINC1
109.0     -11.7     91.0      626.0     0.0
*X2        Y2         Z2         CORD2     AINC2
70.0      0.0       91.0      665.0     0.0
*ISPNDIV  ICHRDIV   SPC        IARFYL    NAP       IVTXFLG
2         8         0.        0         0         0
*****
* panel 4, right inboard
*X1        Y1         Z1         CORD1     AINC1
70.0      0.0       91.0      665.0     0.0
*X2        Y2         Z2         CORD2     AINC2
109.0     11.7      91.0      626.0     0.0
*ISPNDIV  ICHRDIV   SPC        IARFYL    NAP       IVTXFLG
2         8         0.        0         0         0
*****
* panel 5, right mid

```

```

*X1      Y1      Z1      CORD1      AINC1
109.0   11.7   91.0   626.0     0.0
*X2      Y2      Z2      CORD2      AINC2
197.7   23.4   91.0   537.3     0.0
*ISPNDIV ICHRDIV  SPC      IARFYL     NAP      IVTXFLG
2        8        0.        0          0          0
*****
* panel 6, right outboard
*X1      Y1      Z1      CORD1      AINC1
234.8   23.4   91.0   500.2     0.0
*X2      Y2      Z2      CORD2      AINC2
234.8   32.2   91.0   382.4     0.0
*ISPNDIV ICHRDIV  SPC      IARFYL     NAP      IVTXFLG
2        8        0.        0          0          0
*****
* SURFACE 2
LEFT HAND SHELF
*ISRTYP  LNPNAN  ISYMFLG  ENETAR    FTAIL     ALZL     XGAP
5        1        0        0.0       0.0       0.0     0.0
* panel 1
*X1      Y1      Z1      CORD1      AINC1
210.4   -52.2   91.0   404.8     0.0
*X2      Y2      Z2      CORD2      AINC2
210.4   -32.2   91.0   406.8     0.0
*ISPNDIV ICHRDIV  SPC      IARFYL     NAP      IVTXFLG
3        7        0.        0          0          0.0
*****
* SURFACE 3
RIGHT HAND SHELF
*ISRTYP  LNPNAN  ISYMFLG  ENETAR    FTAIL     ALZL     XGAP
5        1        0        0.0       0.0       0.0     0.0
* panel 1
*X1      Y1      Z1      CORD1      AINC1
210.4   32.2   91.0   406.8     0.0
*X2      Y2      Z2      CORD2      AINC2
210.4   52.2   91.0   404.8     0.0
*ISPNDIV ICHRDIV  SPC      IARFYL     NAP      IVTXFLG
3        7        0.        0          0          0.0
*****
* SURFACE 4
LEFT HAND CANARD
*SRTYP   LNPNAN   ISYMFLG  ENETAR    FTAIL     ALZL     XGAP
2        2        0        0.0       0.0       0.0     0.0
* panel 1, outboard
*X1      Y1      Z1      CORD1      AINC1
362.5   -119.5  91.0   4.0       0.0
*X2      Y2      Z2      CORD2      AINC2
291.2   -78.0   91.0   72.5     0.0
*ISPNDIV ICHRDIV  SPC      IARFYL     NAP      IVTXFLG
3        7        1.        0          0          0
*****
* panel 2, inboard
*X1      Y1      Z1      CORD1      AINC1
291.2   -78.0   91.0   72.5     0.0
*X2      Y2      Z2      CORD2      AINC2

```



```

246.9   -52.2   91.0   115.1   0.0
*ISPNDIV ICHRDIV SPC      IARFYL   NAP      IVTXFLG
3       7       1.       0         0         1
*****
*****
* SURFACE 5
RIGHT HAND CANARD
*SRTYP   LNPAN     ISYMFLG   ENETAR   FTAIL    ALZL     XGAP
2       2         0         0.0     0.0     0.0     0.0
* panel 1, inboard
*X1      Y1        Z1         CORD1    AINC1
246.9   52.2     91.0     115.1   0.0
*X2      Y2        Z2         CORD2    AINC2
291.2   78.0     91.0     72.5    0.0
*ISPNDIV ICHRDIV SPC      IARFYL   NAP      IVTXFLG
3       7       1.       0         0         1
*****
*****
* panel 2, outboard
*X1      Y1        Z1         CORD1    AINC1
291.2   78.0     91.0     72.5    0.0
*X2      Y2        Z2         CORD2    AINC2
362.5   119.5    91.0     4.0     0.0
*ISPNDIV ICHRDIV SPC      IARFYL   NAP      IVTXFLG
3       7       1.       0         0         0
*****
*****
* SURFACE 6
LEFT HAND WING
*ISRTYP  LNPAN     ISYMFLG   ENETAR   FTAIL    ALZL     XGAP
1       3         0         0.0     0.68    0.0     0.0
* panel 1, wing tip
*X1      Y1        Z1         CORD1    AINC1
591.6   -184.0    91.0     11.9    0
*X2      Y2        Z2         CORD2    AINC2
477.6   -119.5    91.0     131.8   0
*ISPNDIV ICHRDIV SPC      IARFYL   NAP      IVTXFLG
4       8       1.       0         0         0
*****
*****
* panel 2
*X1      Y1        Z1         CORD1    AINC1
477.6   -119.5    91.0     131.8   0
*X2      Y2        Z2         CORD2    AINC2
406.4   -78.0     91.0     206.9   0
*ISPNDIV ICHRDIV SPC      IARFYL   NAP      IVTXFLG
3       8       1.       0         0         0
*****
*****
* panel 3
*X1      Y1        Z1         CORD1    AINC1
406.4   -78.0     91.0     206.9   0
*X2      Y2        Z2         CORD2    AINC2
362.5   -52.2     91.0     252.7   0
*ISPNDIV ICHRDIV SPC      IARFYL   NAP      IVTXFLG
3       8       1.       0         0         1
*****
*****
* SURFACE 7
RIGHT HAND WING
*ISRTYP  LNPAN     ISYMFLG   ENETAR   FTAIL    ALZL     XGAP

```

1	3	0	0.0	0.68	0.0	0.0
* panel 1						
*X1	Y1	Z1	CORD1	AINC1		
362.5	52.2	91.0	252.7	0.0		
*X2	Y2	Z2	CORD2	AINC2		
406.4	78.0	91.0	206.9	0.0		
*ISPNDIV	ICHRDIV	SPC	IARFYL	NAP		IVTXFLG
3	8	1.	0	0		1
*****						
* panel 2						
*X1	Y1	Z1	CORD1	AINC1		
406.4	78.0	91.0	206.9	0.0		
*X2	Y2	Z2	CORD2	AINC2		
477.6	119.5	91.0	131.8	0.0		
*ISPNDIV	ICHRDIV	SPC	IARFYL	NAP		IVTXFLG
3	8	1.	0	0		0
*****						
* panel 3, wing tip						
*X1	Y1	Z1	CORD1	AINC1		
477.6	119.5	91.0	131.8	0.0		
*X2	Y2	Z2	CORD2	AINC2		
591.6	184.0	91.0	11.9	0.0		
*ISPNDIV	ICHRDIV	SPC	IARFYL	NAP		IVTXFLG
4	8	1.	0	0		0

## **Appendix D**

### **Examples of HASC Output Files**

Three examples of HASC output files are provided in this appendix. Table D-1 is a listing of the information written to the screen (unit 6) during a run. The primary force and moment hasc output file (hasc.out) is listed in table D-2. The input file used to generate these files represents a simplified F-16 model. The missiles, launchers, and wing camber have been removed. Default airfoil parameters and a reduced set of angles of attack were also used. The input file does contain both foreword and aft VORLIF lifting surfaces, and a forebody surface analyzed in VTXCHN. Figure D-1 contains plots of the geometry coordinates written to output file grid\_.p3d (grid1.p3d, grid2.p3d, grid3.p3d). This figure illustrates the three runs made by HASC when analyzing a configuration with a forebody surface analyzed in VTXCHN, plus a wing and horizontal tail (or canard and wing) analyzed in VORLIF.

Table D-1 Sample of Output Information Written to Screen (unit 6)

Running \*\* HASC95, Release 10/23/95 \*\*

INPUT LISTING from file hasc.inp  
F-16A MODEL for HASC95

isolv	lax	lay	hag	irstflg	npan	nsurf	alxp
0	0	1	0.0	0	38	6	8.00

rey = 3144444.00  
nmach = 1, mach(s) = 0.600  
nalpna = 7

angles of attack:

-4.00	-2.00	0.00	2.00	4.00	8.00	10.00
-------	-------	------	------	------	------	-------

nbeta = 1, angles of sideslip = 0.00

pitchq	rollq	yawq	vinf	
0.000	0.000	0.000	1.000	
sref	cbar	xref	zref	wspan
43200.00	135.84	320.65	91.00	360.00

Surface 1: FUSELAGE

isrtyp	lnpan	isymflg	enetar	ftail	alz1	xcgap
5	10	0	0.000	0.000	0.000	0.000
Panel Side	Y	Xle	Xte	Chord	Z	Ainc
1	1	-42.000	408.930	540.060	131.130	91.000
1	2	-36.000	408.930	540.060	131.130	91.000
	isrndiv	ichrdiv	spc	iarfyl	nap	ivtxflg
	4	4	0.00	0	0	0
Panel Side	Y	Xle	Xte	Chord	Z	Ainc
2	1	-36.000	408.930	540.060	131.130	91.000
2	2	-27.000	408.930	540.060	131.130	91.000
	isrndiv	ichrdiv	spc	iarfyl	nap	ivtxflg
	3	4	0.00	0	0	0
Panel Side	Y	Xle	Xte	Chord	Z	Ainc
3	1	-27.000	408.930	479.630	70.700	91.000
3	2	-22.050	408.930	551.900	142.970	91.000
	isrndiv	ichrdiv	spc	iarfyl	nap	ivtxflg
	3	4	0.00	0	0	0
Panel Side	Y	Xle	Xte	Chord	Z	Ainc
4	1	-22.050	94.800	551.900	457.100	91.000
4	2	-16.200	94.800	551.900	457.100	91.000
	isrndiv	ichrdiv	spc	iarfyl	nap	ivtxflg
	2	6	0.00	0	0	0
Panel Side	Y	Xle	Xte	Chord	Z	Ainc
5	1	-16.200	94.800	551.900	457.100	91.000
5	2	0.000	94.800	551.900	457.100	91.000
	isrndiv	ichrdiv	spc	iarfyl	nap	ivtxflg
	3	6	0.00	0	0	0
Panel Side	Y	Xle	Xte	Chord	Z	Ainc
6	1	0.000	94.800	551.900	457.100	91.000
6	2	16.200	94.800	551.900	457.100	91.000
	isrndiv	ichrdiv	spc	iarfyl	nap	ivtxflg
	3	6	0.00	0	0	0
Panel Side	Y	Xle	Xte	Chord	Z	Ainc
7	1	16.200	94.800	551.900	457.100	91.000
7	2	22.050	94.800	551.900	457.100	91.000
	isrndiv	ichrdiv	spc	iarfyl	nap	ivtxflg
	2	6	0.00	0	0	0

Panel	Side	Y	Xle	Xte	Chord	Z	Ainc
8	1	22.050	408.930	551.900	142.970	91.000	0.00
8	2	27.000	408.930	479.630	70.700	91.000	0.00
		ispndiv	ichrdiv	spc	iarfyl	nap	ivtxflg
		3	4	0.00	0	0	0
Panel	Side	Y	Xle	Xte	Chord	Z	Ainc
9	1	27.000	408.930	540.060	131.130	91.000	0.00
9	2	36.000	408.930	540.060	131.130	91.000	0.00
		ispndiv	ichrdiv	spc	iarfyl	nap	ivtxflg
		3	4	0.00	0	0	0
Panel	Side	Y	Xle	Xte	Chord	Z	Ainc
10	1	36.000	408.930	540.060	131.130	91.000	0.00
10	2	42.000	408.930	540.060	131.130	91.000	0.00
		ispndiv	ichrdiv	spc	iarfyl	nap	ivtxflg
		4	4	0.00	0	0	0

Surface 2: LEFT HAND WING

isrtyp	lnpan	isymflg	enetar	ftail	alzl	xgap	
2	9	0	0.000	0.000	2.000	0.000	
Panel	Side	Y	Xle	Xte	Chord	Z	Ainc
1	1	-180.000	364.390	408.930	44.540	91.000	-2.99
1	2	-151.970	340.950	408.930	67.980	91.000	-1.53
		ispndiv	ichrdiv	spc	iarfyl	nap	ivtxflg
		3	8	1.00	0	0	0
Panel	Side	Y	Xle	Xte	Chord	Z	Ainc
2	1	-151.970	340.950	408.930	67.980	91.000	-1.53
2	2	-140.000	330.910	408.930	78.020	91.000	-1.17
		ispndiv	ichrdiv	spc	iarfyl	nap	ivtxflg
		2	8	1.00	0	0	0
Panel	Side	Y	Xle	Xte	Chord	Z	Ainc
3	1	-140.000	330.910	408.930	78.020	91.000	-1.17
3	2	-109.970	305.710	408.930	103.220	91.000	-0.57
		ispndiv	ichrdiv	spc	iarfyl	nap	ivtxflg
		3	8	1.00	0	0	0
Panel	Side	Y	Xle	Xte	Chord	Z	Ainc
4	1	-109.970	305.710	408.930	103.220	91.000	-0.57
4	2	-82.040	282.270	408.930	126.660	91.000	-0.23
		ispndiv	ichrdiv	spc	iarfyl	nap	ivtxflg
		3	8	1.00	0	0	0
Panel	Side	Y	Xle	Xte	Chord	Z	Ainc
5	1	-82.040	282.270	408.930	126.660	91.000	-0.23
5	2	-54.000	258.740	408.930	150.190	91.000	0.00
		ispndiv	ichrdiv	spc	iarfyl	nap	ivtxflg
		3	8	1.00	0	0	1
Panel	Side	Y	Xle	Xte	Chord	Z	Ainc
6	1	-54.000	258.740	408.930	150.190	91.000	0.00
6	2	-42.000	206.850	408.930	202.080	91.000	0.05
		ispndiv	ichrdiv	spc	iarfyl	nap	ivtxflg
		2	8	1.00	0	0	0
Panel	Side	Y	Xle	Xte	Chord	Z	Ainc
7	1	-42.000	206.850	408.930	202.080	91.000	0.05
7	2	-36.000	182.560	408.930	226.370	91.000	0.04
		ispndiv	ichrdiv	spc	iarfyl	nap	ivtxflg
		4	8	1.00	0	0	0
Panel	Side	Y	Xle	Xte	Chord	Z	Ainc
8	1	-36.000	182.560	408.930	226.370	91.000	0.04
8	2	-27.000	119.350	408.930	289.580	91.000	-0.14
		ispndiv	ichrdiv	spc	iarfyl	nap	ivtxflg

Panel Side	Y	Xle	Xte	Chord	Z	Ainc
9 1	-27.000	119.350	408.930	289.580	91.000	-0.14
9 2	-22.050	94.800	408.930	314.130	91.000	-0.20
	ispndiv	ichrdiv	spc	iarfyl	nap	ivtxflg
	3	8	1.00	0	0	1

Surface 3: RIGHT HAND WING

isrtyp	lnpan	isymflg	enetar	ftail	alz1	xgap
2	9	0	0.000	0.000	2.000	0.000
Panel Side	Y	Xle	Xte	Chord	Z	Ainc
1 1	22.050	94.800	408.930	314.130	91.000	-0.20
1 2	27.000	119.350	408.930	289.580	91.000	-0.14
	ispndiv	ichrdiv	spc	iarfyl	nap	ivtxflg
	3	8	1.00	0	0	1
Panel Side	Y	Xle	Xte	Chord	Z	Ainc
2 1	27.000	119.350	408.930	289.580	91.000	-0.14
2 2	36.000	182.560	408.930	226.370	91.000	0.04
	ispndiv	ichrdiv	spc	iarfyl	nap	ivtxflg
	3	8	1.00	0	0	0
Panel Side	Y	Xle	Xte	Chord	Z	Ainc
3 1	36.000	182.560	408.930	226.370	91.000	0.04
3 2	42.000	206.850	408.930	202.080	91.000	0.05
	ispndiv	ichrdiv	spc	iarfyl	nap	ivtxflg
	4	8	1.00	0	0	0
Panel Side	Y	Xle	Xte	Chord	Z	Ainc
4 1	42.000	206.850	408.930	202.080	91.000	0.05
4 2	54.000	258.740	408.930	150.190	91.000	0.00
	ispndiv	ichrdiv	spc	iarfyl	nap	ivtxflg
	2	8	1.00	0	0	0
Panel Side	Y	Xle	Xte	Chord	Z	Ainc
5 1	54.000	258.740	408.930	150.190	91.000	0.00
5 2	82.040	282.270	408.930	126.660	91.000	-0.23
	ispndiv	ichrdiv	spc	iarfyl	nap	ivtxflg
	3	8	1.00	0	0	1
Panel Side	Y	Xle	Xte	Chord	Z	Ainc
6 1	82.040	282.270	408.930	126.660	91.000	-0.23
6 2	109.970	305.710	408.930	103.220	91.000	-0.57
	ispndiv	ichrdiv	spc	iarfyl	nap	ivtxflg
	3	8	1.00	0	0	0
Panel Side	Y	Xle	Xte	Chord	Z	Ainc
7 1	109.970	305.710	408.930	103.220	91.000	-0.57
7 2	140.000	330.910	408.930	78.020	91.000	-1.17
	ispndiv	ichrdiv	spc	iarfyl	nap	ivtxflg
	3	8	1.00	0	0	0
Panel Side	Y	Xle	Xte	Chord	Z	Ainc
8 1	140.000	330.910	408.930	78.020	91.000	-1.17
8 2	151.970	340.950	408.930	67.980	91.000	-1.53
	ispndiv	ichrdiv	spc	iarfyl	nap	ivtxflg
	2	8	1.00	0	0	0
Panel Side	Y	Xle	Xte	Chord	Z	Ainc
9 1	151.970	340.950	408.930	67.980	91.000	-1.53
9 2	180.000	364.390	408.930	44.540	91.000	-2.99
	ispndiv	ichrdiv	spc	iarfyl	nap	ivtxflg
	3	8	1.00	0	0	0

Surface 4: LEFT HAND HORIZONTAL TAIL

isrtyp	lnpan	isymflg	enetar	ftail	alz1	xgap
--------	-------	---------	--------	-------	------	------

Panel	Side	1	3	0	0.000	1.391	2.000	0.000
		Y	Xle	Xte	Chord	Z	Ainc	
1	1	-109.970	511.830	549.220	37.390	71.590	0.00	
1	2	-82.040	487.950	549.220	61.270	79.530	0.00	
		ispndiv	ichrdiv	spc	iarfyl	nap	ivtxflg	
		3	6	1.00	0	0	0	
Panel	Side	Y	Xle	Xte	Chord	Z	Ainc	
2	1	-82.040	487.950	549.220	61.270	79.530	0.00	
2	2	-54.000	464.060	549.220	85.160	87.460	0.00	
		ispndiv	ichrdiv	spc	iarfyl	nap	ivtxflg	
		4	6	1.00	0	0	0	
Panel	Side	Y	Xle	Xte	Chord	Z	Ainc	
3	1	-54.000	464.060	549.220	85.160	87.460	0.00	
3	2	-42.000	453.410	549.220	95.810	89.670	0.00	
		ispndiv	ichrdiv	spc	iarfyl	nap	ivtxflg	
		2	6	1.00	0	0	1	

Surface 5: RIGHT HAND HORIZONTAL TAIL

isrtyp	lnpan	isymflg	enetar	ftail	alz1	xgap	
1	3	0	0.000	1.391	2.000	0.000	
Panel	Side	Y	Xle	Xte	Chord	Z	Ainc
1	1	42.000	453.410	549.220	95.810	89.670	0.00
1	2	54.000	464.060	549.220	85.160	87.460	0.00
		ispndiv	ichrdiv	spc	iarfyl	nap	ivtxflg
		2	6	1.00	0	0	1
Panel	Side	Y	Xle	Xte	Chord	Z	Ainc
2	1	54.000	464.060	549.220	85.160	87.460	0.00
2	2	82.040	487.950	549.220	61.270	79.530	0.00
		ispndiv	ichrdiv	spc	iarfyl	nap	ivtxflg
		4	6	1.00	0	0	0
Panel	Side	Y	Xle	Xte	Chord	Z	Ainc
3	1	82.040	487.950	549.220	61.270	79.530	0.00
3	2	109.970	511.830	549.220	37.390	71.590	0.00
		ispndiv	ichrdiv	spc	iarfyl	nap	ivtxflg
		3	6	1.00	0	0	0

Surface 6: FOREBODY

isrtyp	lnpan	isymflg	enetar	ftail	alz1	xgap	
3	4	0	0.000	0.000	0.000	0.000	
Panel	Side	Y	Xle	Xte	Chord	Z	Ainc
1	1	-22.050	94.700	94.800	0.100	91.000	-4.16
1	2	-16.200	41.600	94.800	53.200	91.000	-4.16
		ispndiv	ichrdiv	spc	iarfyl	nap	ivtxflg
		2	4	1.00	0	0	0
Panel	Side	Y	Xle	Xte	Chord	Z	Ainc
2	1	-16.200	41.600	94.800	53.200	91.000	-4.16
2	2	0.000	-5.000	94.800	99.800	91.000	-4.16
		ispndiv	ichrdiv	spc	iarfyl	nap	ivtxflg
		3	4	1.00	0	0	0
Panel	Side	Y	Xle	Xte	Chord	Z	Ainc
3	1	0.000	-5.000	94.800	99.800	91.000	-4.16
3	2	16.200	41.600	94.800	53.200	91.000	-4.16
		ispndiv	ichrdiv	spc	iarfyl	nap	ivtxflg
		3	4	1.00	0	0	0
Panel	Side	Y	Xle	Xte	Chord	Z	Ainc
4	1	16.200	41.600	94.800	53.200	91.000	-4.16
4	2	22.050	94.700	94.800	0.100	91.000	-4.16
		ispndiv	ichrdiv	spc	iarfyl	nap	ivtxflg



2 4 1.00 0 0 0

Restart = 0 Run no. = 1  
Number of horseshoe vortices = 288

Reynolds number = 3144000. Mach = 0.600 Beta = 0.00

Stability Axis Data (from VORLAX)

Alpha	Beta	CL	CD	Cm	Cy	Cl	Cn
-4.000	0.000	-0.0675	0.0025	0.0561	0.0000	0.0000	0.0000
-2.000	0.000	-0.0344	0.0007	0.0277	0.0000	0.0000	0.0000
0.000	0.000	-0.0001	0.0001	-0.0019	0.0000	0.0000	0.0000
2.000	0.000	0.0336	0.0007	-0.0308	0.0000	0.0000	0.0000
4.000	0.000	0.0680	0.0025	-0.0603	0.0000	0.0000	0.0000
6.000	0.000	0.1011	0.0055	-0.0884	0.0000	0.0000	0.0000
8.000	0.000	0.1334	0.0095	-0.1156	0.0000	0.0000	0.0000
10.000	0.000	0.1648	0.0145	-0.1419	0.0000	0.0000	0.0000

Restart = 0 Run no. = 2  
Number of horseshoe vortices = 664

Reynolds number = 3144000. Mach = 0.600 Beta = 0.00

Stability Axis Data (from VORLAX)

Alpha	Beta	CL	CD	Cm	Cy	Cl	Cn
-4.000	0.000	-0.2859	0.0094	-0.0059	0.0000	0.0001	0.0000
-2.000	0.000	-0.1550	0.0028	-0.0026	0.0000	0.0001	0.0000
0.000	0.000	-0.0237	0.0002	0.0017	0.0000	0.0000	0.0000
2.000	0.000	0.1077	0.0015	0.0055	0.0000	0.0000	0.0000
4.000	0.000	0.2391	0.0068	0.0102	0.0000	0.0000	0.0000
6.000	0.000	0.3705	0.0160	0.0147	0.0000	-0.0001	0.0000
8.000	0.000	0.5001	0.0290	0.0193	0.0000	-0.0001	0.0000
10.000	0.000	0.6276	0.0457	0.0239	0.0000	-0.0001	0.0000

Restart = 0 Run no. = 3  
Number of horseshoe vortices = 704

Reynolds number = 3144000. Mach = 0.600 Beta = 0.00

Stability Axis Data (from VORLAX)

Alpha	Beta	CL	CD	Cm	Cy	Cl	Cn
-4.000	0.000	-0.2922	0.0093	-0.0128	-0.0001	0.0000	0.0000
-2.000	0.000	-0.1579	0.0028	-0.0068	0.0000	0.0000	0.0000
0.000	0.000	-0.0245	0.0003	-0.0008	0.0000	0.0000	0.0000
2.000	0.000	0.1078	0.0016	0.0046	0.0000	0.0000	0.0000
4.000	0.000	0.2411	0.0067	0.0108	0.0000	0.0000	0.0000
6.000	0.000	0.3745	0.0157	0.0169	-0.0001	0.0000	0.0000
8.000	0.000	0.5040	0.0283	0.0229	-0.0001	0.0000	0.0000
10.000	0.000	0.6316	0.0444	0.0287	-0.0001	0.0000	0.0000

Starting VORLIF cycle # 1 on surface 2  
Starting VORLIF cycle # 2 on surface 2  
At alpha = 6.00 vortex burst at 0.10256 surface y/b  
At alpha = 8.00 vortex burst at 0.10256 surface y/b  
At alpha = 10.00 vortex burst at 0.09307 surface y/b  
Starting VORLIF cycle # 3 on surface 2  
Starting VORLIF cycle # 1 on surface 3  
Starting VORLIF cycle # 2 on surface 3  
At alpha = 6.00 vortex burst at 0.10256 surface y/b

At alpha = 8.00 vortex burst at 0.10256 surface y/b  
 At alpha = 10.00 vortex burst at 0.09307 surface y/b  
 Starting VORLIF cycle # 3 on surface 3  
 Starting VORLIF cycle # 1 on surface 4  
 Starting VORLIF cycle # 2 on surface 4  
 Starting VORLIF cycle # 3 on surface 4  
 Starting VORLIF cycle # 1 on surface 5  
 Starting VORLIF cycle # 2 on surface 5  
 Starting VORLIF cycle # 3 on surface 5  
 Forebody calculation for alpha = -4.00  
 Forebody calculation for alpha = -2.00  
 Forebody calculation for alpha = 0.00  
 Forebody calculation for alpha = 2.00  
 Forebody calculation for alpha = 4.00  
 Forebody calculation for alpha = 6.00  
 Forebody calculation for alpha = 8.00  
 Forebody calculation for alpha = 10.00

Coefficients prior to VTXCHN forebody contribution

Alpha	Beta	CL	CD	Cm	Cy	Cl	Cn
-4.000	0.000	-0.2800	0.0114	0.0272	-0.0001	-0.0002	0.0000
-2.000	0.000	-0.1492	0.0027	0.0294	0.0000	0.0000	0.0000
0.000	0.000	-0.0203	0.0002	0.0323	0.0000	0.0000	0.0000
2.000	0.000	0.1082	0.0016	0.0350	0.0000	0.0000	0.0000
4.000	0.000	0.2368	0.0072	0.0382	0.0000	0.0000	0.0000
6.000	0.000	0.3519	0.0218	0.0237	-0.0001	0.0000	0.0000
8.000	0.000	0.4773	0.0450	0.0226	-0.0001	0.0000	0.0000
10.000	0.000	0.6019	0.0761	0.0171	-0.0002	0.0000	0.0000

Forebody contribution from VTXCHN execution

Alpha	Beta	CL	CD	Cm	Cy	Cl	Cn
-4.000	0.000	-0.0094	-0.0003	-0.0194	0.0000	0.0000	0.0000
-2.000	0.000	-0.0069	-0.0005	-0.0141	0.0000	0.0000	0.0000
0.000	0.000	-0.0047	-0.0004	-0.0095	0.0000	0.0000	0.0000
2.000	0.000	-0.0023	-0.0003	-0.0048	0.0000	0.0000	0.0000
4.000	0.000	0.0000	-0.0002	0.0000	0.0000	0.0000	0.0000
6.000	0.000	0.0024	0.0001	0.0048	0.0000	0.0000	0.0000
8.000	0.000	0.0048	0.0003	0.0098	0.0000	0.0000	0.0000
10.000	0.000	0.0071	0.0006	0.0146	0.0000	0.0000	0.0000

Total Stability Axis Data

Alpha	Beta	CL	CD	Cm	Cy	Cl	Cn
-4.000	0.000	-0.2895	0.0111	0.0078	-0.0001	-0.0002	0.0000
-2.000	0.000	-0.1561	0.0023	0.0154	0.0000	0.0000	0.0000
0.000	0.000	-0.0250	-0.0002	0.0228	0.0000	0.0000	0.0000
2.000	0.000	0.1059	0.0013	0.0302	0.0000	0.0000	0.0000
4.000	0.000	0.2368	0.0070	0.0382	0.0000	0.0000	0.0000
6.000	0.000	0.3543	0.0219	0.0284	-0.0001	0.0000	0.0000
8.000	0.000	0.4821	0.0453	0.0324	-0.0001	0.0000	0.0000
10.000	0.000	0.6090	0.0768	0.0317	-0.0002	0.0000	0.0000

End of configuration

Execution of HASC is complete.

Table D-2 Sample of Primary HASC Output File (hasc.out)

\*\* HASC95, Release 10/23/95 \*\*

\*\* Total Force and Moments \*\*

F-16A MODEL for HASC95

Mach = 0.60

Beta = 0.00

Pitch rate(/sec) = 0.00

Roll rate(/sec) = 0.00

Yaw rate(/sec) = 0.00

Vinf = 1.00

Sref = 43200.000 Wspan = 360.000 Cbar = 135.800

Xbar = 320.600 Zbar = 91.000

\*\*\*\*\* BODY AXIS SYSTEM \*\*\*\*\*

All Surfaces Body Axis

Alpha	Beta	CNtot	CAtot	Cmtot	CYtot	Cltot	Cntot
-4.000	0.000	-0.2895	-0.0091	0.0078	-0.0001	-0.0002	0.0000
-2.000	0.000	-0.1561	-0.0032	0.0154	0.0000	0.0000	0.0000
0.000	0.000	-0.0250	-0.0002	0.0228	0.0000	0.0000	0.0000
2.000	0.000	0.1059	-0.0024	0.0302	0.0000	0.0000	0.0000
4.000	0.000	0.2367	-0.0095	0.0382	0.0000	0.0000	0.0000
6.000	0.000	0.3546	-0.0153	0.0284	-0.0001	0.0000	0.0000
8.000	0.000	0.4837	-0.0223	0.0324	-0.0001	0.0000	0.0000
10.000	0.000	0.6131	-0.0301	0.0317	-0.0002	0.0000	0.0000

\*\*\*\*\* WIND AXIS SYSTEM \*\*\*\*\*

All Surfaces Wind Axis

Alpha	Beta	CLtot	CDtot	Cmtot	CYtot	Crtot	Cntot
-4.000	0.000	-0.2895	0.0111	0.0078	-0.0001	-0.0002	0.0000
-2.000	0.000	-0.1561	0.0023	0.0154	0.0000	0.0000	0.0000
0.000	0.000	-0.0250	-0.0002	0.0228	0.0000	0.0000	0.0000
2.000	0.000	0.1059	0.0013	0.0302	0.0000	0.0000	0.0000
4.000	0.000	0.2368	0.0070	0.0382	0.0000	0.0000	0.0000
6.000	0.000	0.3543	0.0219	0.0284	-0.0001	0.0000	0.0000
8.000	0.000	0.4821	0.0453	0.0324	-0.0001	0.0000	0.0000
10.000	0.000	0.6090	0.0768	0.0317	-0.0002	0.0000	0.0000

\*\*\*\*\* STABILITY AXIS SYSTEM \*\*\*\*\*

All Surfaces Stab Axis

Alpha	Beta	CLtot	CDtot	Cmtot	CYtot	Cltot	Cntot
-4.000	0.000	-0.2895	0.0111	0.0078	-0.0001	-0.0002	0.0000
-2.000	0.000	-0.1561	0.0023	0.0154	0.0000	0.0000	0.0000
0.000	0.000	-0.0250	-0.0002	0.0228	0.0000	0.0000	0.0000
2.000	0.000	0.1059	0.0013	0.0302	0.0000	0.0000	0.0000
4.000	0.000	0.2368	0.0070	0.0382	0.0000	0.0000	0.0000
6.000	0.000	0.3543	0.0219	0.0284	-0.0001	0.0000	0.0000
8.000	0.000	0.4821	0.0453	0.0324	-0.0001	0.0000	0.0000
10.000	0.000	0.6090	0.0768	0.0317	-0.0002	0.0000	0.0000

\*\* HASC95, Release 10/23/95 \*\*

\*\* Surface Force and Moments \*\*

F-16A MODEL for HASC95

Mach = 0.60 beta = 0.00

Pitch rate = 0.00/sec

Roll rate = 0.00/sec  
 Yaw rate = 0.00/sec  
 Vinf = 1.00

Sref = 43200.000 Wspan = 360.000 Cbar = 135.800  
 Xbar = 320.600 Zbar = 91.000

\*\*\*\*\* BODY AXIS SYSTEM \*\*\*\*\*

Surface	1	FUSELAGE	Body Axis				
Alpha	Beta	CNsrf	CAsrf	Cmsrf	CYsrf	Crsrf	Cnsrf
-4.000	0.000	-0.0368	0.0000	-0.0026	0.0000	0.0000	0.0000
-2.000	0.000	-0.0172	0.0000	0.0019	0.0000	0.0000	0.0000
0.000	0.000	0.0021	0.0000	0.0064	0.0000	0.0000	0.0000
2.000	0.000	0.0213	0.0000	0.0105	0.0000	0.0000	0.0000
4.000	0.000	0.0407	0.0000	0.0149	0.0000	0.0000	0.0000
6.000	0.000	0.0600	0.0000	0.0194	0.0000	0.0000	0.0000
8.000	0.000	0.0784	0.0000	0.0236	0.0000	0.0000	0.0000
10.000	0.000	0.0966	0.0000	0.0278	0.0000	0.0000	0.0000

Surface	2	LEFT HAND WING	Body Axis				
Alpha	Beta	CNsrf	CAsrf	Cmsrf	CYsrf	Crsrf	Cnsrf
-4.000	0.000	-0.1171	-0.0040	0.0084	-0.0155	-0.0302	-0.0003
-2.000	0.000	-0.0638	-0.0012	0.0108	-0.0050	-0.0167	-0.0001
0.000	0.000	-0.0116	0.0001	0.0136	-0.0002	-0.0037	-0.0001
2.000	0.000	0.0404	-0.0011	0.0164	-0.0028	0.0092	0.0000
4.000	0.000	0.0924	-0.0046	0.0193	-0.0122	0.0221	0.0002
6.000	0.000	0.1353	-0.0072	0.0165	-0.0224	0.0343	0.0009
8.000	0.000	0.1859	-0.0104	0.0186	-0.0381	0.0477	0.0012
10.000	0.000	0.2363	-0.0139	0.0191	-0.0575	0.0616	0.0018

Surface	3	RIGHT HAND WING	Body Axis				
Alpha	Beta	CNsrf	CAsrf	Cmsrf	CYsrf	Crsrf	Cnsrf
-4.000	0.000	-0.1166	-0.0040	0.0083	0.0153	0.0300	0.0003
-2.000	0.000	-0.0637	-0.0012	0.0107	0.0050	0.0166	0.0001
0.000	0.000	-0.0116	0.0001	0.0135	0.0002	0.0037	0.0001
2.000	0.000	0.0404	-0.0011	0.0164	0.0028	-0.0092	0.0000
4.000	0.000	0.0923	-0.0046	0.0193	0.0121	-0.0221	-0.0002
6.000	0.000	0.1353	-0.0072	0.0165	0.0224	-0.0343	-0.0009
8.000	0.000	0.1859	-0.0104	0.0185	0.0380	-0.0477	-0.0012
10.000	0.000	0.2362	-0.0138	0.0191	0.0573	-0.0615	-0.0019

Surface	4	LEFT HAND HORIZONTAL TAIL	Body Axis				
Alpha	Beta	CNsrf	CAsrf	Cmsrf	CYsrf	Crsrf	Cnsrf
-4.000	0.000	-0.0048	-0.0001	0.0065	0.0028	-0.0011	-0.0014
-2.000	0.000	-0.0022	0.0000	0.0030	0.0013	-0.0005	-0.0007
0.000	0.000	0.0004	0.0000	-0.0005	-0.0002	0.0001	0.0001
2.000	0.000	0.0030	0.0000	-0.0041	-0.0019	0.0007	0.0010
4.000	0.000	0.0056	-0.0001	-0.0077	-0.0036	0.0013	0.0019
6.000	0.000	0.0108	-0.0003	-0.0144	-0.0061	0.0023	0.0032
8.000	0.000	0.0144	-0.0006	-0.0191	-0.0083	0.0031	0.0043
10.000	0.000	0.0185	-0.0009	-0.0245	-0.0106	0.0039	0.0056

Surface	5	RIGHT HAND HORIZONTAL TAIL	Body Axis				
Alpha	Beta	CNsrf	CAsrf	Cmsrf	CYsrf	Crsrf	Cnsrf
-4.000	0.000	-0.0049	-0.0001	0.0066	-0.0028	0.0011	0.0014
-2.000	0.000	-0.0023	0.0000	0.0030	-0.0013	0.0005	0.0007
0.000	0.000	0.0004	0.0000	-0.0005	0.0002	-0.0001	-0.0001

2.000	0.000	0.0031	0.0000	-0.0042	0.0019	-0.0007	-0.0010
4.000	0.000	0.0057	-0.0001	-0.0077	0.0036	-0.0013	-0.0019
6.000	0.000	0.0108	-0.0003	-0.0144	0.0061	-0.0023	-0.0032
8.000	0.000	0.0144	-0.0006	-0.0191	0.0082	-0.0031	-0.0043
10.000	0.000	0.0184	-0.0009	-0.0244	0.0106	-0.0039	-0.0056

Surface	6	FOREBODY	Body Axis					
Alpha	Beta	CNsrfr	CAsrfr	Cmsrfr	CYsrfr	Crsrfr	Cnsrfr	
-4.000	0.000	-0.0094	-0.0010	-0.0194	0.0000	0.0000	0.0000	
-2.000	0.000	-0.0069	-0.0007	-0.0141	0.0000	0.0000	0.0000	
0.000	0.000	-0.0047	-0.0004	-0.0095	0.0000	0.0000	0.0000	
2.000	0.000	-0.0023	-0.0002	-0.0048	0.0000	0.0000	0.0000	
4.000	0.000	0.0000	-0.0002	0.0000	0.0000	0.0000	0.0000	
6.000	0.000	0.0024	-0.0002	0.0048	0.0000	0.0000	0.0000	
8.000	0.000	0.0048	-0.0004	0.0098	0.0000	0.0000	0.0000	
10.000	0.000	0.0071	-0.0006	0.0146	0.0000	0.0000	0.0000	

\*\*\*\*\* WIND AXIS SYSTEM \*\*\*\*\*

Surface	1	FUSELAGE	Wind Axis					
Alpha	Beta	CLsrfr	CDsrfr	Cmsrfr	CYsrfr	Crsrfr	Cnsrfr	
-4.000	0.000	-0.0367	0.0026	-0.0026	0.0000	0.0000	0.0000	
-2.000	0.000	-0.0172	0.0006	0.0019	0.0000	0.0000	0.0000	
0.000	0.000	0.0021	0.0000	0.0064	0.0000	0.0000	0.0000	
2.000	0.000	0.0213	0.0007	0.0105	0.0000	0.0000	0.0000	
4.000	0.000	0.0406	0.0028	0.0149	0.0000	0.0000	0.0000	
6.000	0.000	0.0597	0.0063	0.0194	0.0000	0.0000	0.0000	
8.000	0.000	0.0776	0.0109	0.0236	0.0000	0.0000	0.0000	
10.000	0.000	0.0951	0.0168	0.0278	0.0000	0.0000	0.0000	

Surface	2	LEFT HAND WING	Wind Axis					
Alpha	Beta	CLsrfr	CDsrfr	Cmsrfr	CYsrfr	Crsrfr	Cnsrfr	
-4.000	0.000	-0.1170	0.0042	0.0084	-0.0155	-0.0301	-0.0024	
-2.000	0.000	-0.0638	0.0010	0.0108	-0.0050	-0.0166	-0.0007	
0.000	0.000	-0.0116	0.0001	0.0136	-0.0002	-0.0037	-0.0001	
2.000	0.000	0.0404	0.0004	0.0164	-0.0028	0.0092	-0.0004	
4.000	0.000	0.0925	0.0019	0.0193	-0.0122	0.0221	-0.0013	
6.000	0.000	0.1353	0.0070	0.0165	-0.0224	0.0342	-0.0027	
8.000	0.000	0.1856	0.0156	0.0186	-0.0381	0.0474	-0.0054	
10.000	0.000	0.2351	0.0274	0.0191	-0.0575	0.0609	-0.0089	

Surface	3	RIGHT HAND WING	Wind Axis					
Alpha	Beta	CLsrfr	CDsrfr	Cmsrfr	CYsrfr	Crsrfr	Cnsrfr	
-4.000	0.000	-0.1166	0.0042	0.0083	0.0153	0.0299	0.0024	
-2.000	0.000	-0.0637	0.0010	0.0107	0.0050	0.0166	0.0007	
0.000	0.000	-0.0116	0.0001	0.0135	0.0002	0.0037	0.0001	
2.000	0.000	0.0404	0.0004	0.0164	0.0028	-0.0092	0.0004	
4.000	0.000	0.0924	0.0019	0.0193	0.0121	-0.0221	0.0013	
6.000	0.000	0.1354	0.0070	0.0165	0.0224	-0.0342	0.0027	
8.000	0.000	0.1855	0.0156	0.0185	0.0380	-0.0474	0.0054	
10.000	0.000	0.2351	0.0274	0.0191	0.0573	-0.0609	0.0089	

Surface	4	LEFT HAND HORIZONTAL TAIL	Wind Axis					
Alpha	Beta	CLsrfr	CDsrfr	Cmsrfr	CYsrfr	Crsrfr	Cnsrfr	
-4.000	0.000	-0.0048	0.0003	0.0065	0.0028	-0.0010	-0.0014	
-2.000	0.000	-0.0022	0.0001	0.0030	0.0013	-0.0005	-0.0007	
0.000	0.000	0.0004	0.0000	-0.0005	-0.0002	0.0001	0.0001	
2.000	0.000	0.0030	0.0001	-0.0041	-0.0019	0.0007	0.0010	

4.000	0.000	0.0056	0.0003	-0.0077	-0.0036	0.0014	0.0018
6.000	0.000	0.0108	0.0008	-0.0144	-0.0061	0.0026	0.0029
8.000	0.000	0.0143	0.0014	-0.0191	-0.0083	0.0036	0.0039
10.000	0.000	0.0183	0.0023	-0.0245	-0.0106	0.0048	0.0049

Surface	5	RIGHT HAND HORIZONTAL TAIL				Wind Axis		
Alpha	Beta	CLsrf	CDsrf	Cmsrf	CYsrf	Crsrcf	Cnsrf	
-4.000	0.000	-0.0049	0.0003	0.0066	-0.0028	0.0010	0.0014	
-2.000	0.000	-0.0023	0.0001	0.0030	-0.0013	0.0005	0.0007	
0.000	0.000	0.0004	0.0000	-0.0005	0.0002	-0.0001	-0.0001	
2.000	0.000	0.0031	0.0001	-0.0042	0.0019	-0.0007	-0.0010	
4.000	0.000	0.0057	0.0003	-0.0077	0.0036	-0.0014	-0.0018	
6.000	0.000	0.0108	0.0008	-0.0144	0.0061	-0.0026	-0.0029	
8.000	0.000	0.0143	0.0014	-0.0191	0.0082	-0.0036	-0.0038	
10.000	0.000	0.0183	0.0023	-0.0244	0.0106	-0.0048	-0.0048	

Surface	6	FOREBODY				Wind Axis		
Alpha	Beta	CLsrf	CDsrf	Cmsrf	CYsrf	Crsrcf	Cnsrf	
-4.000	0.000	-0.0094	-0.0003	-0.0194	0.0000	0.0000	0.0000	
-2.000	0.000	-0.0069	-0.0005	-0.0141	0.0000	0.0000	0.0000	
0.000	0.000	-0.0047	-0.0004	-0.0095	0.0000	0.0000	0.0000	
2.000	0.000	-0.0023	-0.0003	-0.0048	0.0000	0.0000	0.0000	
4.000	0.000	0.0000	-0.0002	0.0000	0.0000	0.0000	0.0000	
6.000	0.000	0.0024	0.0001	0.0048	0.0000	0.0000	0.0000	
8.000	0.000	0.0048	0.0003	0.0098	0.0000	0.0000	0.0000	
10.000	0.000	0.0071	0.0006	0.0146	0.0000	0.0000	0.0000	

\*\*\*\*\* STABILITY AXIS SYSTEM \*\*\*\*\*

Surface	1	FUSELAGE				Stab Axis		
Alpha	Beta	CLsrf	CDsrf	Cmsrf	CYsrf	Crsrcf	Cnsrf	
-4.000	0.000	-0.0367	0.0026	-0.0026	0.0000	0.0000	0.0000	
-2.000	0.000	-0.0172	0.0006	0.0019	0.0000	0.0000	0.0000	
0.000	0.000	0.0021	0.0000	0.0064	0.0000	0.0000	0.0000	
2.000	0.000	0.0213	0.0007	0.0105	0.0000	0.0000	0.0000	
4.000	0.000	0.0406	0.0028	0.0149	0.0000	0.0000	0.0000	
6.000	0.000	0.0597	0.0063	0.0194	0.0000	0.0000	0.0000	
8.000	0.000	0.0776	0.0109	0.0236	0.0000	0.0000	0.0000	
10.000	0.000	0.0951	0.0168	0.0278	0.0000	0.0000	0.0000	

Surface	2	LEFT HAND WING				Stab Axis		
Alpha	Beta	CLsrf	CDsrf	Cmsrf	CYsrf	Crsrcf	Cnsrf	
-4.000	0.000	-0.1170	0.0042	0.0084	-0.0155	-0.0301	-0.0024	
-2.000	0.000	-0.0638	0.0010	0.0108	-0.0050	-0.0166	-0.0007	
0.000	0.000	-0.0116	0.0001	0.0136	-0.0002	-0.0037	-0.0001	
2.000	0.000	0.0404	0.0004	0.0164	-0.0028	0.0092	-0.0004	
4.000	0.000	0.0925	0.0019	0.0193	-0.0122	0.0221	-0.0013	
6.000	0.000	0.1353	0.0070	0.0165	-0.0224	0.0342	-0.0027	
8.000	0.000	0.1856	0.0156	0.0186	-0.0381	0.0474	-0.0054	
10.000	0.000	0.2351	0.0274	0.0191	-0.0575	0.0609	-0.0089	

Surface	3	RIGHT HAND WING				Stab Axis		
Alpha	Beta	CLsrf	CDsrf	Cmsrf	CYsrf	Crsrcf	Cnsrf	
-4.000	0.000	-0.1166	0.0042	0.0083	0.0153	0.0299	0.0024	
-2.000	0.000	-0.0637	0.0010	0.0107	0.0050	0.0166	0.0007	
0.000	0.000	-0.0116	0.0001	0.0135	0.0002	0.0037	0.0001	
2.000	0.000	0.0404	0.0004	0.0164	0.0028	-0.0092	0.0004	
4.000	0.000	0.0924	0.0019	0.0193	0.0121	-0.0221	0.0013	

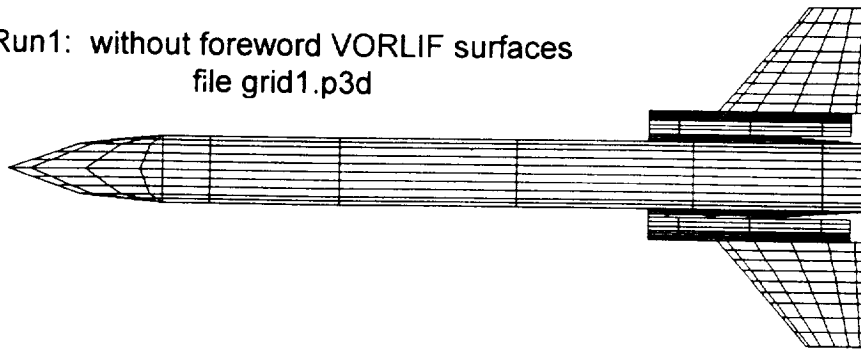
6.000	0.000	0.1354	0.0070	0.0165	0.0224	-0.0342	0.0027
8.000	0.000	0.1855	0.0156	0.0185	0.0380	-0.0474	0.0054
10.000	0.000	0.2351	0.0274	0.0191	0.0573	-0.0609	0.0089

Surface	4	LEFT HAND HORIZONTAL TAIL			Stab Axis		
Alpha	Beta	CLsrf	CDsrf	Cmsrf	CYsrf	Crsrf	Cnsrf
-4.000	0.000	-0.0048	0.0003	0.0065	0.0028	-0.0010	-0.0014
-2.000	0.000	-0.0022	0.0001	0.0030	0.0013	-0.0005	-0.0007
0.000	0.000	0.0004	0.0000	-0.0005	-0.0002	0.0001	0.0001
2.000	0.000	0.0030	0.0001	-0.0041	-0.0019	0.0007	0.0010
4.000	0.000	0.0056	0.0003	-0.0077	-0.0036	0.0014	0.0018
6.000	0.000	0.0108	0.0008	-0.0144	-0.0061	0.0026	0.0029
8.000	0.000	0.0143	0.0014	-0.0191	-0.0083	0.0036	0.0039
10.000	0.000	0.0183	0.0023	-0.0245	-0.0106	0.0048	0.0049

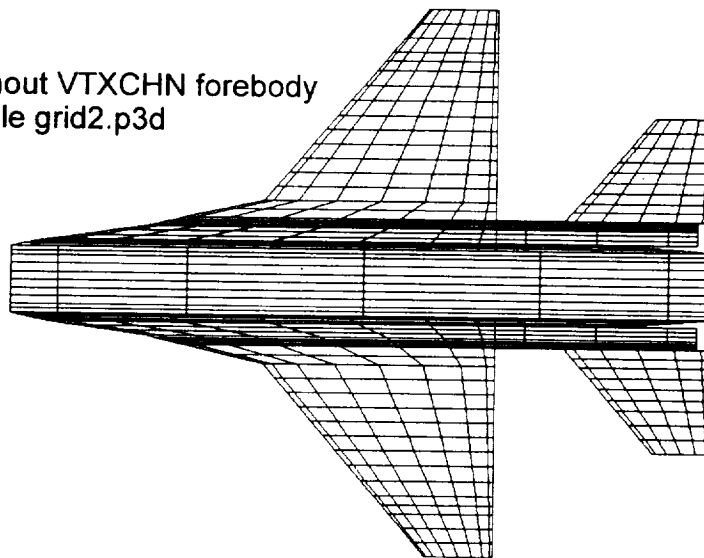
Surface	5	RIGHT HAND HORIZONTAL TAIL			Stab Axis		
Alpha	Beta	CLsrf	CDsrf	Cmsrf	CYsrf	Crsrf	Cnsrf
-4.000	0.000	-0.0049	0.0003	0.0066	-0.0028	0.0010	0.0014
-2.000	0.000	-0.0023	0.0001	0.0030	-0.0013	0.0005	0.0007
0.000	0.000	0.0004	0.0000	-0.0005	0.0002	-0.0001	-0.0001
2.000	0.000	0.0031	0.0001	-0.0042	0.0019	-0.0007	-0.0010
4.000	0.000	0.0057	0.0003	-0.0077	0.0036	-0.0014	-0.0018
6.000	0.000	0.0108	0.0008	-0.0144	0.0061	-0.0026	-0.0029
8.000	0.000	0.0143	0.0014	-0.0191	0.0082	-0.0036	-0.0038
10.000	0.000	0.0183	0.0023	-0.0244	0.0106	-0.0048	-0.0048

Surface	6	FOREBODY			Stab Axis		
Alpha	Beta	CLsrf	CDsrf	Cmsrf	CYsrf	Crsrf	Cnsrf
-4.000	0.000	-0.0094	-0.0003	-0.0194	0.0000	0.0000	0.0000
-2.000	0.000	-0.0069	-0.0005	-0.0141	0.0000	0.0000	0.0000
0.000	0.000	-0.0047	-0.0004	-0.0095	0.0000	0.0000	0.0000
2.000	0.000	-0.0023	-0.0003	-0.0048	0.0000	0.0000	0.0000
4.000	0.000	0.0000	-0.0002	0.0000	0.0000	0.0000	0.0000
6.000	0.000	0.0024	0.0001	0.0048	0.0000	0.0000	0.0000
8.000	0.000	0.0048	0.0003	0.0098	0.0000	0.0000	0.0000
10.000	0.000	0.0071	0.0006	0.0146	0.0000	0.0000	0.0000

Run1: without foreword VORLIF surfaces  
file grid1.p3d



Run 2: without VTXCHN forebody  
file grid2.p3d



Run 3: all surfaces  
file grid3.p3d

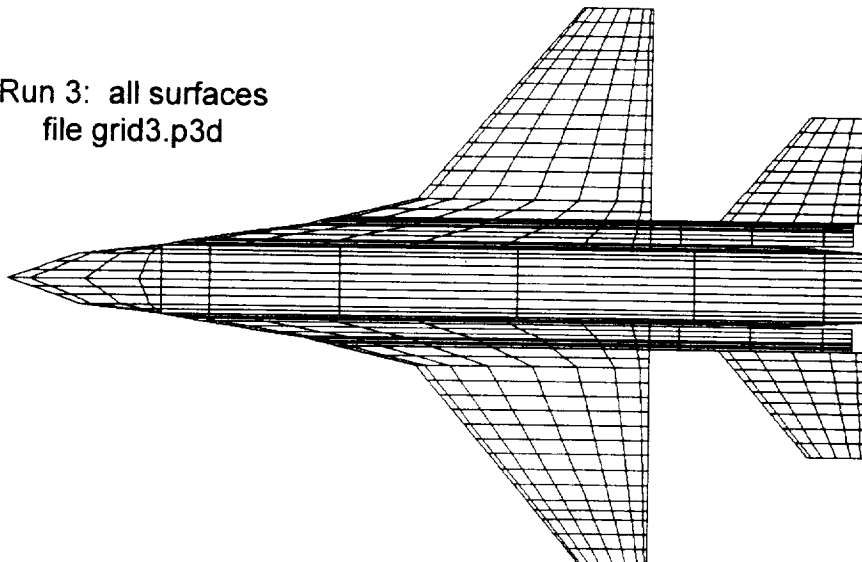


Figure D-1 Geometry Written to Output Files grid\_.p3d for the F-16



**Appendix E**

**Application of the HASC Code to Buffet Analysis**

by

Charles J. Dixon

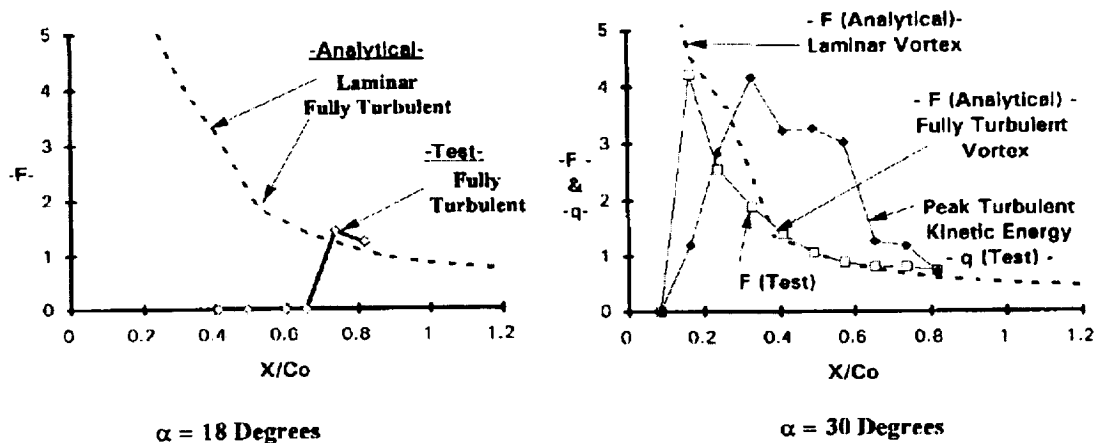
Consulting Aviation Services

## Introduction

The information presented in this appendix, although not funded by the NASA LaRC HASC modification contract, presents discussion on a unique research application of HASC for buffet analysis. Additional research and development in this area is required prior to recommending HASC as a production tool for buffet analysis.

## Research

The quasi-periodic forcing function (buffet) was a major concern of a recent effort with Georgia Tech. During this effort it was noted that the rate of rotation of the spiraling core corresponded to the frequency of the quasi-periodic forcing function. This phenomenon was expected when it was discovered that the reduced frequency of this quasi-periodic forcing function could be defined using the turbulent vortex diameter as  $fD_V / V_\infty = 0.5$ . The turbulent vortex diameter ( $D_V$ ) is computed by the HASC code. Combining that with the experimental frequency,  $f$ , and the free stream velocity,  $V_\infty$ , the reduced frequency was equal to the constant of 0.5. These results are shown in figure E-1 for the 59.3 degree delta wing. The results are for angles of attack of 18 and 30 degrees.



$$\text{Reduced Frequency} \quad F = f C_{\text{avg}} / V_\infty$$

$$\text{Peak Power} \quad q = (\text{rms} / 10 V_\infty)^2$$

Figure E-1 Analytical and Test Buffet Reduced Frequency

The experimental data were obtained with a hot wire probe at stations along and just above the delta wing's leading edge. These are plotted as a function of the longitudinal body axis,  $X$ , normalized by the root chord,  $C_o$  in figure E-1. The analytical results were obtained at  $X/C_o$  of the outer edge of the vortex core, which is very close to the leading edge.

At both angles of attack on the figure an arrow points to the position where the HASC code has predicted transition of the vortex. The arrow noted as laminar is the last position for which the code showed the vortex as laminar. The lower arrow points to where the code first predicts fully turbulent vortex. There is no experimental quasi-periodic function until after the vortex transitions to turbulence; i.e., the laminar core begins to spiral. This spiral rotates within the envelope of the predicted turbulent core; so, the rate of rotation or the frequency scales with the vortex diameter. Note: in the figure the reduced frequency is scaled by the mean chord as normally done for most test data.

The  $X$  distance between the arrows of the laminar and fully turbulent vortex is not necessarily the transition distance, but appears to be that for the 30 degree results. The experimental quasi-periodic frequency begins at the last predicted laminar vortex position. Also, the peak power that corresponds to the quasi-period frequency begins to rise at this position. The power then starts to drop near the predicted position of fully turbulent vortex. This seems very logical that the power would increase as the vortex transitions to the fully turbulent position; i.e., the vortex core size is growing and the turbulence is increasing very rapidly during the transition. Then the vortex grows at a much slower rate, and the strength of the spiral is probably decaying.

The HASC code does not gradually increase the vortex core size between the last laminar and the fully turbulent positions. If it did, the hump in the analytical curve between these positions would be smoothed. There is a hump in the analytical curve for the 18 degree alpha case also. Unfortunately, the transition for the latter is well ahead of that for the experimental results. Also, this early prediction causes the turbulent vortex diameter to be larger than it would be for a delayed prediction. A delayed prediction would raise the reduced frequency, and probably produce better agreement with the experimental frequency.

## Conclusions

In summary, the main discovery is that for the 18 or 30 degree case the predicted reduced frequencies agree well with the experimental values once the vortex has become fully turbulent. Any surface downstream of the origin of the turbulent vortex will experience severe buffet at frequencies predicted by the code. Additional research is required on a variety of configurations to further investigate this possible application of HASC.



REPORT DOCUMENTATION PAGE			Form Approved OMB No. 0704-0188	
Public reporting burden for this collection of information is estimated to average 1 hour per response, including the time for reviewing instructions, searching existing data sources, gathering and maintaining the data needed, and completing and reviewing the collection of information. Send comments regarding this burden estimate or any other aspect of this collection of information, including suggestions for reducing this burden, to Washington Headquarters Services, Directorate for Information Operations and Reports, 1215 Jefferson Davis Highway, Suite 1204, Arlington, VA 22202-4302, and to the Office of Management and Budget, Paperwork Reduction Project (0704-0188), Washington, DC 20503.				
1. AGENCY USE ONLY (Leave blank)		2. REPORT DATE March 1996	3. REPORT TYPE AND DATES COVERED Contractor Report (April-November 1995)	
4. TITLE AND SUBTITLE Modification and Validation of Conceptual Design Aerodynamic Prediction Method HASC95 with VTXCHN			5. FUNDING NUMBERS NAS1-19000	
6. AUTHOR(S) Alan E. Albright, Charles J. Dixon, and Martin C. Hegedus			505-68-70-09	
7. PERFORMING ORGANIZATION NAME(S) AND ADDRESS(ES) Lockheed Martin Tactical Aircraft Systems Fort Worth, TX 76101			8. PERFORMING ORGANIZATION REPORT NUMBER	
9. SPONSORING / MONITORING AGENCY NAME(S) AND ADDRESS(ES) National Aeronautics and Space Administration Langley Research Center Hampton, Virginia 23681-0001			10. SPONSORING / MONITORING AGENCY REPORT NUMBER NASA CR-4712	
11. SUPPLEMENTARY NOTES Langley Technical Monitor: Michael J. Logan Final Report				
12a. DISTRIBUTION / AVAILABILITY STATEMENT  Unclassified-Unlimited  Subject Category 02			12b. DISTRIBUTION CODE	
13. ABSTRACT (Maximum 200 words)  A conceptual/preliminary design level subsonic aerodynamic prediction code HASC (High Angle of Attack Stability and Control) has been improved in several areas, validated, and documented. The improved code includes improved methodologies for increased accuracy and robustness, and simplified input/output files. An engineering method called VTXCHN (Vortex Chine) for predicting nose vortex shedding from circular and non-circular forebodies with sharp chine edges has been improved and integrated into the HASC code.  This report contains a summary of modifications, description of the code, user's guide, and validation of HASC. Appendices include discussion of a new HASC utility code, listings of sample input and output files, and a discussion of the application of HASC to buffet analysis.				
14. SUBJECT TERMS aerodynamics prediction high angle of attack stability and control			15. NUMBER OF PAGES 302	
			16. PRICE CODE A14	
17. SECURITY CLASSIFICATION OF REPORT UNCLASSIFIED	18. SECURITY CLASSIFICATION OF THIS PAGE UNCLASSIFIED	19. SECURITY CLASSIFICATION OF ABSTRACT UNCLASSIFIED	20. LIMITATION OF ABSTRACT	



